Wissenschaftszentrum Weihenstephan für
Ernährung, Landnutzung und Umwelt
Lehrstuhl für Systembiologie der Pflanzen

Trafficking and polarity control of the D6 PROTEIN KINASE from *Arabidopsis thaliana*

Inês Catarina Ramos Barbosa

Vollständiger Abdruck der von der Fakultät Wissenschaftszentrum Weihenstephan für Ernährung, Landnutzung und Umwelt der Technischen Universität München zur Erlangung des akademischen Grades eines

Doktors der Naturwissenschaften

genehmigten Dissertation.

Vorsitzender:	Univ.- Prof. Dr. J. Schnyder
Prüfer der Dissertation:	1. Univ.- Prof. Dr. C. Schwechheimer
	2. Univ.- Prof. Dr. K. Schneitz
	3. Univ.- Prof. Dr. I. Heilmann (Martin-Luther-Universität Halle-Wittenberg)

Die Dissertation wurde am 23.07.2015 bei der Technischen Universität München eingereicht und durch die Fakultät Wissenschaftszentrum Weihenstephan für Ernährung, Landnutzung und Umwelt am 22.09.2015 angenommen.

Abstract

The polar transport of the phytohormone auxin is essential to the spatio-temporal control of plant development. Major players in this process are the PIN-FORMED (PINs) auxin efflux carriers, as they are polarly localized in many cells and thereby contribute to the directed cell-to-cell transport of auxin. The AGCVIII kinases, D6 PROTEIN KINASE (D6PK) and its paralogs D6PK-LIKE1 to D6PK-LIKE3, are required for auxin transport as well as for auxin-transport dependent processes, such as tropisms. At the start of this thesis, it had been shown that D6PK directly phosphorylates and co-localizes with PINs at the basal membrane of many cells, but the exact mechanism by which D6PK phosphorylation regulated PIN function was not known. It was then proposed that D6PK-dependent phosphorylation promotes PIN-mediated auxin efflux activity and, hence, that the polar co-localization of D6PK and PINs would be required for active auxin transport.

The aim of my thesis was to identify the cellular and biochemical requirements for D6PK trafficking and polarity and their impact on PIN-mediated auxin transport. As a first approach, I compared the very well described trafficking of PINs to that of D6PK and found that the two proteins traffic differently. As the PINs, D6PK undergoes GNOM-dependent constitutive recycling but with much faster kinetics. In contrast to the PINs, D6PK internalization is clathrin-independent and promoted, rather than inhibited, by auxin. This indicated that the two proteins only colocalize at the plasma membrane but are targeted to the plasma membrane independently. In support of this, conditions that specifically internalized D6PK but not the PINs led to defects on PIN phosphorylation, auxin distribution, and tropism responses similar to those observed in *d6pk* mutants. Thus, I concluded D6PK is required for the activation of PIN-mediated auxin transport at the plasma membrane. Subsequently, I discussed and reviewed these findings, together with other recent work from my group, in the context of the published role of other AGCVIII kinases, mainly PINOID and phototropins, on polar auxin transport. Finally, through biochemical and cell biological analysis I discovered that D6PK binds specific phospholipids and that phospholipid composition critically determines D6PK localization. Dissection of the D6PK protein requirements for membrane anchoring led to the identification of a lysine-rich motif and of two putatively phosphorylated serines required for D6PK-membrane interaction, polarity, and function. In summary, I identified key cellular and biochemical mechanisms determining D6PK localization, PIN function, and auxin transport in plants, thus contributing to a better understanding of the complex molecular framework governing plant development.

Zusammenfassung

Der polare Transport des Pflanzenhormons Auxin ist essentiell für die räumliche und zeitliche Kontrolle der Pflanzenentwicklung. Wichtige Komponenten in diesem Prozess sind die PIN-FORMED (PIN) Auxin-Exporter, da sie in vielen Zellen polar lokalisiert sind und dadurch zum gerichteten Transport von Auxin von Zelle zu Zelle beitragen. Die AGCVIII Kinase D6 PROTEIN KINASE (D6PK) und ihre Paraloge D6PK-LIKE1 bis D6PK-LIKE3 werden sowohl für den Auxintransport als auch für Auxintransport-abhängige Prozesse wie Tropismen benötigt. Zu Beginn dieser Arbeit war bereits gezeigt worden, dass D6PK mit den polar lokalisierten PIN Proteinen kolokalisiert und diese direkt phosphorylieren kann, jedoch war der genaue Mechanismus nicht bekannt, durch den die D6PK über Phosphorylierung die PIN Proteine reguliert. Es wurde postuliert, dass die D6PK-abhängige Phosphorylierung der PINs deren Auxintransport-Aktivität steigert und folglich, dass die polare Kolokalisierung von D6PK und den PIN Proteinen eine Voraussetzung für den aktiven Auxinransport wäre.

Ziel meiner Arbeit war, die zellulären und biochemischen Voraussetzungen des D6PK Transports und der D6PK Polarität zu identifizieren und deren Auswirkungen auf den PIN-vermittelten Auxintransport zu untersuchen. Als erstes verglich ich den sehr gut beschriebenen intrazellulären PIN Transport mit dem von D6PK und fand heraus, dass die beiden Proteine auf unterschiedliche Weise transportiert werden. Ähnlich wie die PIN Proteine unterläuft auch der Transport von D6PK einem konstitutiven GNOM-abhängigen Recycling, allerdings mit einer viel schnelleren Kinetik. Im Gegensatz zu den PINs ist die D6PK Internalisierung jedoch Clathrin-unabhängig und wird durch Auxin verstärkt und nicht inhibiert. Dies deutete darauf hin, dass diese beiden Proteine ausschließlich an der Plasmamembran kolokalisieren, aber dorthin auf unterschiedliche Weise transportiert werden. Unterstützend kam hinzu, dass Bedingungen, unter welchen D6PK nicht aber die PIN Proteine spezifisch internalisiert wird, Defekte in der PIN Phosphorylierung, der Auxinverteilung und den tropischen Reaktionen verursachen, ähnlich denen, die in den *d6pk* Mutanten beobachtet werden. Somit ist die Präsenz der D6PK an der Plasmamembran für den PIN-vermittelten Auxintransport notwendig. Anschließend fasste ich diese Ergebnisse, einschließlich anderer aktueller Arbeiten meiner Arbeitsgruppe, zusammen und diskutierte diese mit Bezug auf die bekannte Rolle weiterer AGCVIII Kinasen, hauptsächlich PINOID und Phototropine, im gerichteten Auxintransport. Durch biochemische und zellbiologische Untersuchungen entdeckte ich dann, dass D6PK an spezifische Phospholipide bindet und dass die Phospholipidzusammensetzung die D6PK Lokalisierung entscheidend beeinflusst. Durch weiterführende Analysen konnte ich die Anforderungen von D6PK für die Membranverankerung über ein Lysin-reiches Motif und zwei vermeintlich phosphorylierte Serine aufdecken, die für die D6PK-Membranwechselwirkung, Polarität und Funktion notwendig sind. Zusammengenommen habe ich wichtige zelluläre und biochemische Mechanismen aufgedeckt, die die D6PK-Lokalisierung, die PIN-Funktion und den Auxintransport in Pflanzen vermitteln und habe somit zu einem besseren Verständnis der komplexen molekularen Netzwerke beigetragen, die die Pflanzenentwicklung steuern.

List of publications

The following publications, two peer-reviewed and one manuscript draft, are included in this thesis:

Barbosa ICR, Schwechheimer C (2014) Dynamic control of auxin transport-dependent growth by AGCVIII protein kinases. *Curr Opin Plant Biol* 22: 108-115

Barbosa ICR, Zourelidou M, Willige BC, Weller B, Schwechheimer C (2014) D6 PROTEIN KINASE activates auxin transport-dependent growth and PIN-FORMED phosphorylation at the plasma membrane. *Dev Cell* 29: 674-685.

Barbosa ICR, Zourelidou M, Heilmann I, Schwechheimer C (in preparation) A phospholipid-binding K-rich motif and phosphorylation control plasma membrane localization and polarity of D6 PROTEIN KINASE.

Further publications from the doctoral work not included in this thesis:

Willige BC, Ahlers S, Zourelidou M, Barbosa ICR, Demarsy E, Trevisan M, Davis PA, Roelfsema MRG, Hangarter R, Fankhauser C, Schwechheimer C (2013) D6PK AGCVIII kinases are required for auxin transport and phototropic hypocotyl bending in Arabidopsis. *Plant Cell*, 25:1674-1688.

Zourelidou M, Absmanner B, Weller B, Barbosa ICR, Willige BC, Fastner A, Streit V, Port S, Colcombet J, van Bentem S, Hirt H, Kuster B, Schulze W, Hammes U, Schwechheimer C (2014) Auxin efflux by PIN-FORMED proteins is activated by two different protein kinases, D6 PROTEIN KINASE and PINOID. *Elife*, 2014; 3: e02860.

Stanislas T, Hüser A, Barbosa ICR, Kiefer CS, Brackmann K, Pietra S, Gustavsson A, Zourelidou M, Schwechheimer C, Grebe M D6 PROTEIN KINASE is a lipid domain-dependent mediator of Arabidopsis planar polarity. *Nature Plants* (accepted September 2015)

Abbreviations

1-NAA	1-Naphthaleneacetic acid
5-FIAA	5-Fluoroindole-3-acetic acid
ABCB	ATP-BINDING CASSETTE OF B-TYPE
ABP1	AUXIN BINDING PROTEIN 1
ADI3	AvrPto-DEPENDENT Pto-INTERACTING PROTEIN 3
AFB	AUXIN SIGNALING F-BOX
AGC	cAMP-DEPENDENT PROTEIN KINASE A, cGMP-DEPENDENT PROTEIN KINASE G AND PHOSPHOLIPID-DEPENDENT PROTEIN KINASE C
AP-2	ADAPTOR PROTEIN 2
ARA7	ARABIDOPSIS RAB GTPase HOMOLOG F2B
ARF	AUXIN RESPONSE FACTOR
ARF-GTPase	ADP-RIBOSYLATION FACTOR GUANOSINE TRIPHOSPHATASE
ARF-GEF	ARF GTPase - GUANINE NUCLEOTIDE EXCHANGE FACTOR
ATP	Adenosine triphosphate
AUX1	AUXIN RESISTANT1
AUX/IAA	AUXIN/INDOLE-3-ACETIC ACID PROTEIN
BFA	Brefeldin A
BKI1	BRI1 KINASE INHIBITOR 1
BRI1	BRASSINOSTEROID INSENSITIVE1
CDC42	CELL DIVISION CONTROL PROTEIN42
CBB	Coomassie-Brilliant-Blue
D6PK	D6 PROTEIN KINASE
D6PKL	D6PK-LIKE
DAG	Diacylglycerol
DGK	DAG Kinase
ER	Endoplasmic reticulum
FAPP1	FOUR PHOSPHATE ADAPTOR PROTEIN1
FLS2	FLAGELLIN SENSING2
FM4-64	N-(3-triethylammoniumpropyl)-4-(6-(4(diethylamino)phenyl)hexatrienyl) pyridinium dibromide
FRAP	Fluorescence recovery after photobleaching
FYVE	FAB 1, YOTB, VAC 1, AND EEA1
GFP	GREEN FLUORESCENT PROTEIN
GNL1	GNOM-LIKE1
GTP	Guanosine triphosphate
GTPase	GUANOSINE TRIPHOSPHATASES
GST	GLUTATHIONE S-TRANSFERASE
IAA	Indole-3-acetic acid
$Ins(1,4,5)P_3$	Inositol 1,4,5-triphosphate
K-rich	Lysine-rich
K-RAS	K-RAS GTPases

KIPK	KCBP-INTERACTING PROTEIN KINASE
LAX	LIKE AUX1
LPP	LIPID PHOSPHATE PHOSPHATASE
MAPK	MITOGEN-ACTIVATED PROTEIN KINASE
MARCKS	MYRISTOYLATED ALANINE-RICH PROTEIN KINASE C SUBSTRATE
NPA	1-N-Naphthylphthalamic acid
OXI1	OXIDATIVE STRESS-RESPONSE PROTEIN KINASE
PA	Phosphatidic acid
PAR	PARTITIONING-DEFECTIVE PROTEIN
PC	Phosphatidylcholine
PE	Phosphatidylethanolamine
PEN1	PENETRATION1
PEO-IAA	α-(phenylethyl-2-oxo)-indole-3-acetic acid
PH	Pleckstrin Homology domain
phot	Phototropin
PI	Phosphatidylinositol
PI3K	PI 3-KINASE
PI4K	PI 4-KINASE
PI5K	PI 5-KINASE
PID	PINOID
PIN	PIN-FORMED
PIP	Phosphoinositide
PIP5K	PI(4)P 5-KINASE
PI-PLC	PHOSPHOINOSITIDE PHOSPHOLIPASE C
PI(x)P	Phosphatidylinositol mono-/bi-/tri-phosphates or phosphoinositides
PKC	PROTEIN KINASE C
PLD	Phospholipase D
PP2A	PROTEIN PHOSPHATASE2A
PP6	PROTEIN PHOSPHATASE6
PS	Phosphatidylserine
PX	Phox homology
RDI	RHO-GDP DISSOCIATION INHIBITOR
ROP-GAP	RHO-GTPase ACTIVATING PROTEIN
ROP-GEF	ROP GTPase-GUANINE NUCLEOTIDE EXCHANGE FACTOR
ROP-GTPase	RHO-LIKE GUANOSINE TRIPHOSPHATASES FROM PLANTS
S1P	Sphingosine-1-phosphate;
SCF	SKP-CULLIN-F-BOX
SKP2a	S-PHASE KINASE-ASSOCIATED PROTEIN2a
TGN	Trans-Golgi network
TIR1	TRANSPORT INHIBITOR RESPONSE1
TMK	TRANSMEMBRANE KINASE
UCN	UNICORN
UCNL	UCN-LIKE
UGP	UDP-GLUCOSE PYROPHOSPHORYLASE
WM	Wortmannin
YFP	YELLOW FLUORESCENT PROTEIN

List of Figures

List of Tables

Contents

1 Introduction

1.1 Auxin and plant development

1.1.1 Tropisms and the discovery of auxin

Already in ancient Greece, the philosophers Aristotle and Theofrastus were fascinated by the ability of plants to direct their growth towards light (phototropism) or gravity (gravitropism)(Whippo & Hangarter, 2009). In the following centuries, numerous studies of plant tropisms paved the way to the discovery of auxin as the first hormone from plants (Whippo & Hangarter, 2006). Observations by Charles Darwin and his son Francis Darwin on the phototropism and gravitropism of grass seedlings, summarized in the seminal work *The Power of Movement in Plants*, have led to the postulation of three founding principles about tropisms as early as in 1880 (Darwin & Darwin, 1880): First, that tropisms result from the unequal growth in response to light or gravity; second, that the part of the plant that perceives the stimulus, root or coleoptile tips, is different from the part that responds to it, and finally that an 'influence' moves from the site of perception to the zone of bending (Darwin & Darwin, 1880; Holland et al, 2009). Others – like Hans Fitting, Peter Boysen-Jensen and Arpad Paál – followed up on this work using refined and more quantitative phototropism experiments and provided strong evidence for the downward as well as lateral transmission of a tip-produced substance that results in coleoptile bending (Boysen-Jensen 1911; Fitting, 1907; Paál, 1918). Phototropism was also successfully used as a bioassay to identify this coleoptile bending 'influence' as indole-3-acetic acid, which was then named auxin from the Greek verb '*auxein*' (to grow) (Kogl F, 1931; Thimann & Went, 1934). These studies culminated by 1928 in the Cholodny-Went hypothesis, which stated that asymmetric growth during tropism responses is a result of the unequal distribution of auxin between two sides of the bending organ, brought by the transverse polarization of the cells and consequent lateral auxin transport (Abel & Theologis, 2010; Moore, 2002; Whippo & Hangarter, 2006).

It soon became evident that auxin affects many other aspects of plant development such as vascular differentiation, root growth, shoot differentiation, apical dominance, and leaf as well as fruit abscission (Abel & Theologis, 2010). Currently, it is believed that the complexity of auxin effects in plant development relies in the combination of auxin distribution patterns, as a result of auxin metabolism and polar auxin transport, as well as of auxin signaling mechanisms that take place at the cellular level. In the forthcoming paragraphs, I will briefly summarize the current knowledge on the molecular players and mechanisms involved in auxin transport and auxin signaling. Though auxin-dependent plant development is studied since centuries, the molecular dissection of auxin action, as exemplified with work in this thesis, still leads to the identification of unforeseen and intriguing mechanisms that will surely occupy scientists for a longer time.

1.1.2 Auxin distribution, signaling and development

Virtually all embryonic and post-embryonic developmental processes in plants are accompanied and controlled by differential auxin distribution patterns. These patterns determine cell fate, cell elongation, cell division, morphogenesis and ultimately organ development (Teale et al, 2006). Besides the already mentioned auxin asymmetric distribution during tropism responses, the formation of auxin maxima, auxin gradients, and auxin minima is a recurrent theme throughout plant development. Local auxin maxima, defining founder cell populations, specify the early embryo apical-basal axis or the positioning of *de novo* organ primordia at the shoot apical meristem. Auxin gradients determine root meristem patterning and leaf primordia development and, finally, auxin minima are required for seed dispersal and the formation of axillary meristems, to mention just a few **(Figure 1.1.1)** (Hofmann, 2014; Sorefan et al, 2009; Tanaka et al, 2006; Vanneste & Friml, 2009).

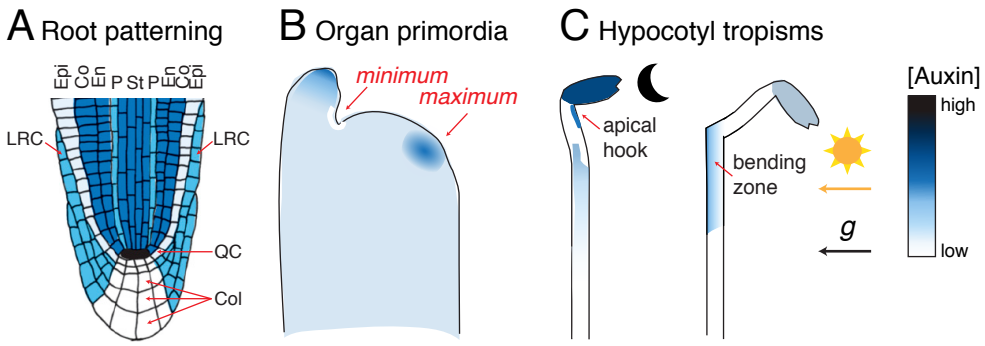

Figure 1.1.1 Auxin distribution patterns in different organs and developmental processes.
(A) An auxin gradient is required for stem-cell maintenance and tissue differentiation in the root meristem. LRC, lateral root cap; Epi, epidermis; Co, cortex; En, endodermis; P, pericycle; St, stele; QC, quiescent centre; Col, columella. Root scheme adapted from (Petersson et al, 2009). **(B)** The formation of leaf and floral organ primordia in the shoot apical meristem is preceded by the formation of local auxin maxima whereas auxin minima define axillary meristems. **(C)** Auxin distribution changes in etiolated seedlings during phototropic or negatively gravitropic hypocotyl bending. In the dark, auxin accumulates in the cotyledons and in the apical hook. Upon light exposure or following changes in the gravity vector, auxin is redistributed to the shaded side of the bending zone or the side, which is distant from the gravity vector. *g,* gravity. Representative auxin intensities are explained by the blue gradient on the right. Relative intensities are only qualitative and rely on estimates from indirect auxin sensors, such as the DR5:GUS, DR5:GFP or DII:Venus.

Within the cell, auxin is perceived by at least three different signaling modules: Two modules mediate auxin-dependent transcriptional changes via auxin binding to SCF E3 ubiquitin ligase (SKP-Cullin-F-box) complexes that promote the degradation of transcription regulators. Of these two, the best studied auxin-regulatory SCF is the $SCF^{TIR1/AFB}$ module with the F-box protein TIR1 (TRANSPORT INHIBITOR RESPONSE 1) or its AFB (AUXIN SIGNALING F-BOX)

paralogs, which serve at the same time as auxin receptors. Auxin binding to TIR1/AFB triggers the degradation of the AUX/IAA (AUXIN/INDOLE-3-ACETIC ACID) repressor proteins, thereby releasing ARF (AUXIN RESPONSE FACTOR) transcription factors, which can then mediate transcriptional auxin responses (Dharmasiri et al, 2005; Gray et al, 2001; Kepinski & Leyser, 2005; Tan et al, 2007). SCF^{SKP2A} with the F-box protein SKP2a (S-PHASE KINASE-ASSOCIATED PROTEIN 2a) is comparatively little understood but also here auxin binding seemingly leads to the degradation of transcription repressors (Jurado et al, 2010).

Besides TIR1/AFB and SKP2a, ABP1 (AUXIN BINDING PROTEIN 1), which localizes to the ER (endoplasmic reticulum) and to the extracellular space, represents a biochemically different type of auxin receptor that controls non-transcriptional auxin responses (Robert et al, 2010; Xu et al, 2011b). Current models suggest that ABP1 interacts with the plasma membrane receptor-like kinases TMKs (TRANSMEMBRANE KINASES) and controls the intracellular activity of ROPs (RHO-LIKE GTPase FROM PLANTS), which leads to the downstream regulation of the cytoskeleton and endocytosis (Robert et al, 2010; Xu et al, 2014; Xu et al, 2011b). While the auxin binding ability of ABP1 is firmly established, recent findings obtained with novel *abp1* alleles challenge the current model and ask for a reevaluation of essentially all genetic and cell biological studies that have as yet been conducted with older *abp1* mutants (Enders et al, 2015; Gao et al, 2015; Grones et al, 2015; Liu, 2015).

The identification of the auxin signaling modules and their requirements allowed developing *in vivo* auxin sensors. DR5:GUS and DR5:GFP are the two most prominently used reporters that are based on an auxin-responsive promoter with ARF binding sites and a GUS or GFP reporter; also very popular is DII:Venus (and its mutant variant mDII:Venus), an auxin-labile reporter composed of the fluorescent protein Venus fused to the AUX/IAA protein domain (DII) required for auxin and TIR1/AFB interaction and subsequent degradation (Brunoud et al, 2012; Sabatini et al, 1999; Ulmasov et al, 1997). With these valuable tools at hand, it is possible to infer auxin response and auxin distribution in intact plants, under different conditions and with *in vivo* dynamics **(Figure 1.1.1)**.

Understanding the function of the diverse auxin signaling modules should help explaining how auxin, as a single signaling molecule, can control such a diverse set of developmental processes. For instance, considering only the signaling module $SCF^{TIR1/AFB}$ in *Arabidopsis*, the specificity and diversity of auxin signal outputs in individual cells could rely on the cell-specific differential expression of signaling molecules but also on the vast range of interactions and differential affinities that can be predicted to exist between the numerous isoforms of $SCF^{TIR1/AFB}$ – AUX/IAA – ARF proteins, encoded in Arabidopsis by six, 29 and 23 members, respectively (Bargmann et al, 2013; Korasick et al, 2014). Recent studies testing only a subset (36 and 48) among the hundreds of possible interactions between TIR1/AFB and AUX/IAAs using the yeast two-hybrid system revealed that each TIR1/AFB – AUX/IAA co-receptor pair has differential affinities for auxin and different AUX/IAA degradation kinetics (Calderon Villalobos et al, 2012; Havens et al, 2012). At the same time, AUX/IAAs and ARFs engage both in homo-, hetero- and multimerization events that, in the few cases analyzed, influenced the final ARF-mediated

transcriptional events (Korasick et al, 2014; Vernoux et al, 2011; Wang & Estelle, 2014). Since the mechanisms of cellular auxin responses will not be of fundamental importance for the present thesis, they will not be explained in greater detail here. However, the mentioned complexities should be kept in mind when interpreting auxin-mediated growth and cellular responses as studied here.

1.2 Polar auxin transport

1.2.1 The chemiosmotic model and auxin transporters

The spatial and temporal auxin distribution patterns within the plant are determined by local auxin metabolism and polar auxin transport (Petrasek & Friml, 2009; Robert et al, 2015). Auxin is transported within the plant via two major routes: the rapid long-distance transport via the phloem, driven by passive loading in the source tissue and unloading in the sink tissue, and the slower, highly regulated, and polarized cell-to-cell transport (Robert & Friml, 2009; Vanneste & Friml, 2009).

The most abundant auxin, IAA (indole-3-acetic acid), is a lipophilic weak acid (pKa 4.7) that can enter the cells rapidly as an undissociated acid (IAAH) when compared to the anion (IAA^-) (Rubery & Sheldrake, 1973). Based on these properties, Rubery and Sheldrake (1975) and Raven (1975) independently proposed the chemiosmotic model for polar auxin transport, which is still valid today (Raven, 1975; Rubery & Sheldrake, 1974). The model states that auxin, at the acidic pH (pH 5.5) outside of the cell (apoplast), is mostly protonotated (IAAH) and can freely diffuse through cell membranes. Inside the cell, auxin dissociates into the less permeable anion IAA^- due to the higher cytosolic pH (pH 7.0) leading to a concentration gradient that favors further IAAH influx and IAA^- accumulation in the cells. In order to achieve polar transport, the chemiosmotic model predicts the existence of polarly localized transporters that promote IAA^- membrane permeability, which, when repeated in nearby cells, could lead to a directional cell-to-cell auxin flow (Goldsmith, 1977; Raven, 1975; Rubery & Sheldrake, 1974).

With the advent of molecular genetics, three types of plasma membrane auxin transporters were identified: AUX1 (AUXIN RESISTANT1) and LAX (LIKE AUX1) as H^+-driven IAA^- influx carriers; a sub-set of the ATP-dependent ABCB/MDR/PGP (ATP-BINDING CASSETTE OF B-TYPE/MULTIDRUG RESISTANCE/P-GLYCOPROTEIN) transporters as efflux and influx carriers; PIN (PIN-FORMED) proteins as auxin efflux carriers (Adamowski & Friml, 2015; Zazimalova et al, 2010). The discovery that PINs, in contrast to the other transporters, are polarly distributed within the cell provided molecular support for the chemiosmotic model (Gälweiler et al, 1998; Muller et al, 1998). Since the polar distribution of PIN proteins within the plant seemingly allowed predicting auxin flow, it appeared possible to disentangle the complex molecular mechanisms regulating polar auxin transport simply based on the analysis of PIN distribution.

1.2.2 Predicting auxin transport using PIN polarity

Arabidopsis contains eight PIN proteins, the five *long* plasma membrane-localized PINs, PIN1 to PIN4 and PIN7 that have a long cytoplasmic loop, and three seemingly ER-localized *short* PINs, PIN5, PIN6, and PIN8 (Krecek et al, 2009). The plasma membrane-localized long PINs, from here on olnly PINs, have redundant functions, differential expression domains, and are in most cells polarly localized (Blilou et al, 2005; Friml et al, 2003).

As would be predicted based on the dynamic formation of auxin maxima, auxin gradients, and auxin minima, PIN polarity is context-specific and dynamically regulated. PIN polarities and PIN polarity changes allow explaining auxin distribution patterns at the organ level, e.g. in the root or shoot apical meristem, and in a stimulus-dependent manner, e.g. after a gravity or light stimulus (Benkova et al, 2003; Friml et al, 2003; Heisler et al, 2005; Kleine-Vehn et al, 2010; Rakusova et al, 2015) **(Figure 1.2.1)**.

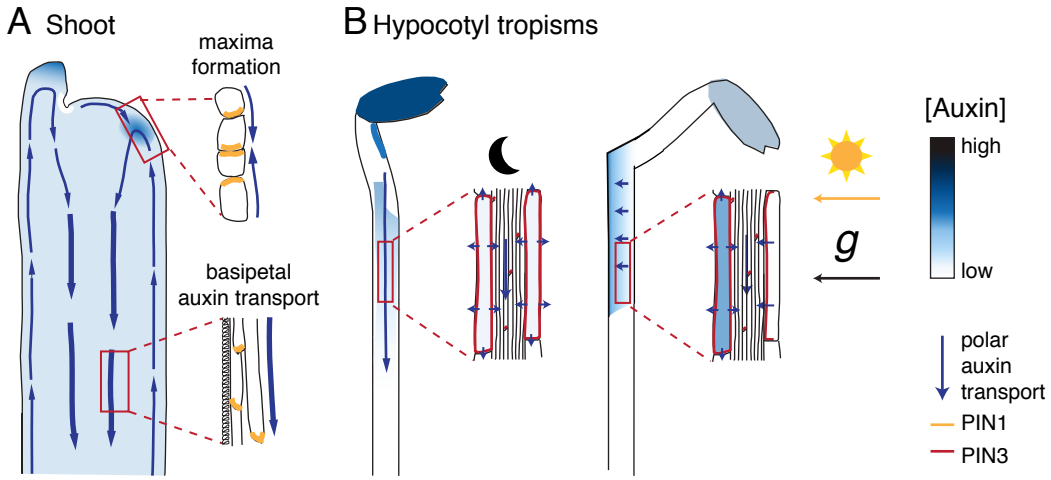

Figure 1.2.1 Cell-type and context-specific PIN polarities allow predicting auxin distribution patterns. **(A)** In the epidermis of the shoot apical meristem (inset above), PIN1 polarity orients to and predicts auxin maxima formation required for the development of organ primordia; while in the xylem parenchyma cells (inset below) PIN1 is basally localized and is required for the basipetal auxin transport in the shoots. **(B)** In the dark, PIN3 is apolar in the endodermis and basal in the vasculature of hypocotyls from etiolated seedlings (left seedling and inset); and upon unilateral light or gravity stimulus PIN3 re-polarizes in the endodermis to the shaded side or towards the gravity vector, presumably controlling the lateral auxin transport flux required for the bending response. Representative auxin intensities are depicted by the blue gradient on the right. Relative intensities are only qualitative and rely on estimates from indirect auxin sensors such as the DR5:GUS, DR5:GFP or DII:Venus (see main text).

Besides the correlation of PIN polarities with auxin distribution, at least three more lines of evidence support that PIN polarity determines the direction of auxin transport. First, the manipulation of PIN polarities by ectopic PIN expression or disruption of polarity signals encrypted in the cytoplasmic loop leads to defects in auxin distribution and development (Wisniewska et al, 2006; Zhang et al, 2010). Second, shifting of PIN polarity by the antagonistic

activities of the kinase PID (PINOID) and the PP2A phosphatase (PROTEIN PHOSPHATASE 2A) through PIN phosphorylation and dephosphorylation – discussed in greater detail below – leads to auxin transport-related phenotypes (Friml et al, 2004; Michniewicz et al, 2007). Third, organ level models taking only into account PIN polarities and a limited number of regulatory mechanisms, e.g. the auxin-controlled feedback regulation in the control of PIN abundance, are seemingly sufficient to explain and predict auxin distribution patterns at the level of the whole root or shoot meristem (Grieneisen et al, 2007; Jönsson et al, 2006). Together, these findings led to the widely accepted model that PIN polarity allows predicting auxin transport and auxin-transport dependent growth. During the work for my dissertation, together with additional work from my host laboratory, I have accumulated ample evidence that PIN distribution alone is not sufficient to explain auxin transport and, hence, that this model is inadequate.

1.3 Regulation of PIN-mediated auxin transport

1.3.1 Control of PIN polarity and abundance by membrane trafficking

Due to its importance for the understanding of auxin transport, much effort has been made in the identification of the mechanisms controlling the plasma membrane abundance and polarity of long PINs (Adamowski & Friml, 2015; Baster et al, 2013). Long PINs, from here on only PINs, are plasma membrane integral proteins, thus the establishment and maintenance of PIN polarity require membrane trafficking. Although it is still unclear whether *de novo* targeting of PINs is polar or apolar (retracted Dhonukshe et al, 2008; Kania et al, 2014), it is well established that PIN polarity maintenance is achieved through the constitutive recycling between the plasma membrane and endosomes, as well as by reduced membrane lateral diffusion (Feraru et al, 2011; Kleine-Vehn et al, 2011). Several trafficking regulators responsible for PIN exocytosis, endocytosis, recycling and also protein degradation in the vacuole have by now been identified (Grunewald & Friml, 2010; Luschnig & Vert, 2014). Only a few specific regulators will be listed and explained here, since they are used for further analysis in the context of this thesis.

GNOM

GNOM was the first identified trafficking regulator of PIN proteins, and it is probably the major PIN polarity regulator, as judged by the severe growth and PIN polarity defects of its mutants (Busch et al, 1996; Geldner et al, 2003; Geldner et al, 2004; Kleine-Vehn et al, 2008; Mayer et al, 1993; Shevell et al, 1994; Steinmann et al, 1999; Wolters et al, 2011). GNOM is an ARF-GEF (ADP-RIBOSYLATION FACTOR GTPase-GTP EXCHANGE FACTOR) involved in ARF-GTPase-dependent vesicle budding and coating, presumably at the Golgi and plasma membrane (Anders & Jürgens, 2008; D'Souza-Schorey & Chavrier, 2006; Naramoto et al, 2010; Naramoto et al, 2014). Treatments with the ARF-GEF-inhibitory toxin BFA (Brefeldin A) and mutant analyses enabled to show that GNOM is required for PIN recycling and, together with the BFA-insensitive GNL1 (GNOM LIKE 1), also for PIN endocytosis (Geldner et al, 2003; Naramoto et al, 2010; Naramoto et al, 2014). Some studies point to a preferential function of

GNOM in the sorting of basally rather than apically-localized PINs in roots and embryos, while other studies show the involvement of GNOM on PIN re-polarization after light and gravity stimuli, or during stomata development (Dhonukshe, 2011; Ding et al, 2011; Kleine-Vehn et al, 2008; Kleine-Vehn et al, 2010; Le et al, 2014). GNOM is probably involved in the targeting of multiple and also non-polar cargos, as predicted based on the essential function of ARF-GEF proteins in membrane trafficking and also by the reduced number of protein family members in *Arabidopsis* (3 members of the GBF (GOLGI-SPECIFIC BFA RESISTANCE FACTOR)-clade and 5 members of the BIG (BFA INHIBITED GEF)-clade), (Richter et al, 2007). This hypothesis is also supported by the fact that several PIN-unrelated and apolar plasma membrane proteins also recycle in a GNOM-dependent manner, such as PEN1 (PENETRATION 1), BRI1 (BRASSINOSTEROID INSENSITIVE 1) or FLS2 (FLAGELLIN SENSING 2) (Beck et al, 2012; Irani et al, 2012; Nielsen et al, 2012).

Auxin

As a result of a series of physiologic experiments examining the role of auxin in the context of vasculature development, Tsvi Sachs and co-workers proposed a model about how auxin positively feeds back on its own transport (Sachs, 1969; Sachs, 1981). According to this *canalization hypothesis,* auxin self-enhances its own transport leading to vasculature differentiation, in a similar manner as water streams generate water canals that ultimately lead to the formation of river systems.

Several molecular and cellular feedback mechanisms between auxin and its PIN transporters are in support of this canalization hypothesis. Short-term auxin treatments (≤ 2 h) promote the transcription of *PIN* genes through $SCF^{TIR1/AFB}$-signaling and inhibit clathrin-mediated endocytosis of PIN proteins through ABP1-signaling, thus resulting in the cellular accumulation of PINs (Benjamins & Scheres, 2008; Robert et al, 2010). In turn, long-term auxin treatments (> 2 h) promote internalization, vacuolar targeting, and degradation of PINs through $SCF^{TIR1/AFB}$-signaling resulting in a reduction of PIN levels (Abas et al, 2006; Baster et al, 2013; Benjamins & Scheres, 2008; Paciorek et al, 2005). These complex auxin-feedback regulatory effects on PIN trafficking and abundance are dependent on auxin levels. During the dynamic gravitropism response, differential auxin levels due to auxin redistribution lead to dynamic changes on PIN2 levels, i.e. from protein stabilization to degradation, that are proposed to ensure the fine-tuning of auxin fluxes to maintain and terminate asymmetric growth responses (Baster et al, 2013).

The dissection of auxin action in PIN trafficking led to the discovery that auxin binding to ABP1 in the extracellular space triggers, via the plasma membrane localized TMK, the ROP-GEF-dependent activation of ROPs and downstream effectors leading to reduced clathrin-mediated endocytosis of PINs (but also of other unrelated cargoes) and cytoskeleton rearrangements (Chen et al, 2012; Dhonukshe et al, 2007; Kitakura et al, 2011; Robert et al, 2010; Xu et al, 2014; Xu et al, 2011b). Furthermore, presumably higher and suboptimal concentrations of auxin can as well control PIN abundance by promoting endocytosis, vacuolar targeting, and degradation of the PINs, via $SCF^{TIR1/AFB}$ signaling (Baster et al, 2013).

PI(4,5)P_2

Recent studies have also implicated the plasma membrane composition on the phospholipid species PI(4,5)P_2 (phosphoinositide-4,5-bi-phosphate) in PIN polarity control (Ischebeck et al, 2013; Tejos et al, 2014).

PIPs (phosphoinositides) are low abundant signaling phospholipids derived from the phosphorylation of the inositol ring at three free hydroxyl positions 3, 4 and 5 from PI (phosphatidylinositol) (Balla, 2013; Thole & Nielsen, 2008). They are produced at specific cellular compartments or membrane domains and, thus, together with other effectors, such as small GTPases, serve as organelle and domain identity landmarks that recruit peripheral membrane proteins important for membrane trafficking (Behnia & Munro, 2005). PIPs also define the identity of plasma membrane polarity domains in different eukaryotic organisms and cell types: PI(4,5)P_2 defines the bud scar of *Saccharomyces cerevisiae* and the leading pseudopods of *Dictyostelium discoideum*; PI(4,5)P_2- and PI(3,4,5)P_3-rich domains determine apical and basolateral identity, respectively, of *Drosophila* and mammalian epithelia; and finally PI(4,5)P_2 defines an apical domain in pollen tube and root hair cells in plants (Ischebeck et al, 2010; Krahn et al, 2010; McCaffrey & Macara, 2009; Orlando & Guo, 2009; Santiago-Tirado & Bretscher, 2011). PIPs recruit proteins to the membranes which bind to them either through specific PIP-binding domains (e.g. FYVE-, PH- or PX-domains) or through the electrostatic interactions between polybasic amino acid stretches within the proteins and the acidic PIP-headgroups. Membranes differential composition on PIPs and its recruited proteins contributes to the determination of organelle/membrane domain identity and function (Heo et al, 2006; Li et al, 2014).

Arabidopsis mutants lacking *PIP5K1* (*PI(4)P 5-kinase*) and *PIP5K2* have reduced PI(4,5)P_2 content and display defects in PIN polarity and trafficking but also in plasma membrane clathrin dynamics. Curiously, PI(4,5)P_2 is polarly localized in different cell types throughout plant development (Tejos et al, 2014). Since PI(4,5)P_2 is a known regulator of clathrin-mediated endocytosis in other organisms, it was proposed that PI(4,5)P_2 has a similar role in plants in determining PIN endocytosis and PIN polarity maintenance (Ischebeck et al, 2013; Sun et al, 2007).

The few PIN trafficking and polarity regulators described above are only a subset of a bigger and growing list that, as an initial matrix of molecular players and mechanisms, played a critical role in hypothesis generation and work performed in this thesis **(Figure 1.3.1)**.

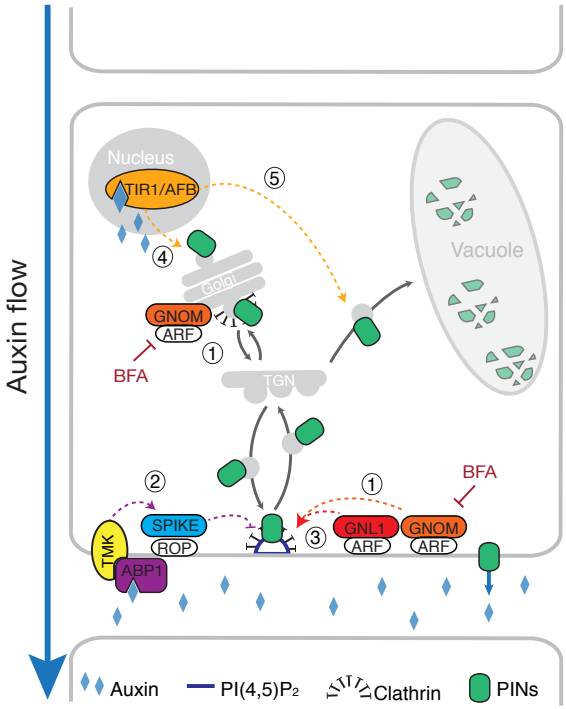

Figure 1.3.1 Cellular routes for the control of PIN polarity and abundance at the plasma membrane.
(1) PINs are constitutively recycling between the plasma membrane and endosomes in a process that requires the ARF-GEF GNOM and GNL1. GNOM is localized in the Golgi as well as at the plasma membrane and has been implicated in endocytosis and exocytosis during PIN recycling. **(2)** Extracellular auxin controls PIN endocytosis by binding to the extracellular auxin receptor ABP1, which together with the receptor-like kinase TMK mediates the downstream activation of ROP signaling. **(3)** PINs are internalized via clathrin-mediated endocytosis whose dynamics depends on the $PI(4,5)P_2$ composition. **(4)** and **(5)** Auxin signaling in the nucleus via $SCF^{TIR1/AFB}$ regulates PIN abundance by controlling both the transcription (4) or the vacuolar targeting and degradation of PINs (5).

1.3.2 PIN polarity control and the AGCVIII Kinases PID and WAGs

Another regulator of PIN polarity, the serine/threonine kinase PID, was isolated in a mutant screen for floral development defects (Bennett et al, 1995; Christensen et al, 2000). PID belongs to the plant-specific family of AGCVIII protein kinases, which have been named based on their homology to AGC (cAMP-DEPENDENT PROTEIN KINASE A, cGMP-DEPENDENT PROTEIN KINASE G, and the PHOSPHOLIPID-DEPENDENT PROTEIN KINASE C) kinases. *Arabidopsis* has 23 AGCVIII kinases with unique and distinctive features including an amino acid substitution in the Mg^{2+}-binding loop (DFG to DFD) and an 36-109 amino acid insertion in the activation segment or T-loop between the subdomains VII and VIII (Rademacher & Offringa, 2012).

Characterization of PID loss- and gain-of-function alleles revealed PIN1 polarity defects in shoot epidermis cells (apical-to-basal shift) and in root stele cells (basal-to-apical shift), respectively, that correlated with defects in auxin distribution and development (Friml et al, 2004). PID-mediated PIN1 polarity defects depend on the early endosome trafficking regulator, ARA7 (ARABIDOPSIS RAB GTPase HOMOLOG F2B), and on PID phosphorylation at three conserved serine residues in the cytoplasmic loop of PIN proteins, leading to the model that PID-mediated phosphorylation controls PIN trafficking and sorting to either apical or basal polarity domains (Dhonukshe et al, 2010; Huang et al, 2010). Additionally, PID-mediated changes in PIN polarity are independent from the GNOM sorting pathway. And PID as well as GNOM were proposed to act antagonisically in the control of PIN polarity (Kleine-Vehn et al, 2009). PID-mediated phosphorylation seems also to be required for other PIN polarity-dependent

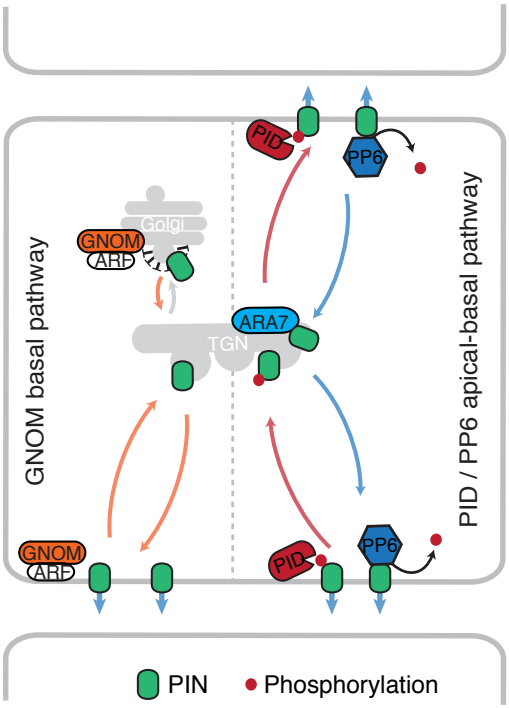

Figure 1.3.2 PIN polarity control by the antagonistic action of GNOM, PID, and PP6. Unphosphorylated PINs traffic through the GNOM-dependent recycling pathway to the basal polar domain, e.g. in roots and embryos. Current data also suggest that PID-phosphorylated PINs traffic through a GNOM-independent but ARA7-dependent pathway that leads to the apical localization of PINs. The PP6 phosphatase holoenzyme complex de-phosphorylates PINs and antagonizes the effects of PID on PIN polarity.

processes besides apico-basal polarity control. In the lobes of pavement cells, PID is required for PIN1 distribution in lobe versus indent plasma membrane, and also the tropism-induced PIN3 polarity switch between outer and inner lateral plasma membranes of hypocotyl endodermis (Ding et al, 2011; Li et al, 2011; Rakusová et al, 2011).

Interestingly, overexpression of the PID homologues WAG1 and WAG2 leads to similar basal-to-apical shifts of PIN1 polarity as overexpression of PID. *pid wag1 wag2* mutants display apical-to-basal shifts of PIN2 in the root epidermis, which is not observed in any of the single mutants, thus pointing to functional redundancy of these kinases (Dhonukshe et al, 2010). In support of a role for the phosphorylation-control of PIN polarity is also the finding that mutants of the catalytic and regulatory subunits of the heterotrimeric phosphatase PP6 (PROTEIN PHOSPHATASE6) display PIN polarity defects similar to PID overexpressors (Ballesteros et al, 2013; Dai et al, 2012; Michniewicz et al, 2007).

The mechanisms of PIN polarity control by PID/WAGs- and PP6-mediated phosphorylation and desphosphorylation, as summarized above, are widely accepted in the plant community **(Figure 1.3.2)**. However, the exact mechanism by which phosphorylation promotes the differential sorting of PINs to different polar domains needs to be identified (Offringa & Huang, 2013). In addition, other findings, which will be discussed in more detail later in this thesis, make other missing links of this model apparent: the facts that PID cannot explain all PIN polarity defects observed and that PID-phosphorylation also regulates PIN auxin efflux activity. This opens the possibility that the regulation of PIN activity may precede changes in polarity control and even directly impact on it.

1.3.3 PIN activity control by AGCVIII protein kinases

Besides PID, WAG1, and WAG2, also other members of the AGCVIII kinase family have been identified in my host laboratory as regulators of PIN-mediated auxin transport, namely D6PK (D6 PROTEIN KINASE) and its homologues D6PK-LIKE1 to D6PKL3 (Zourelidou et al, 2009). Loss-of-function mutations of these kinases leads to phenotypes that are typical for auxin transport defects such as lateral root formation, cotyledon formation, and gravitropism defects. These phenotypes correlated well with reduced basipetal auxin transport and defects in auxin distribution as inferred from the activity of the auxin sensor DR5:GUS. D6PK, like PID, is able to directly phosphorylate the cytosolic loop of the long PINs. However, D6PK, unlike PID, does not control PIN polarity or PIN abundance, which are not obviously altered in complex *d6pk* mutants or in *D6PK* overexpressors (Zourelidou et al, 2009). These results led to the hypothesis, which was postulated at the beginning of my thesis work, that D6PK-dependent PIN phosphorylation could control PIN auxin efflux activity and that PIN activity regulation is an additional layer of auxin transport regulation. This hypothesis found substantial support in subsequent years through work from our group and these findings have also had an important impact on the work described in this thesis (Barbosa & Schwechheimer, 2014; Barbosa et al, 2014; Willige et al, 2013; Zourelidou et al, 2014).

2 Aims of this thesis

The work summarized in this thesis describes cell biological and biochemical studies that aimed at understanding the mechanisms controlling D6PK polar targeting and D6PK regulation of PIN activity through phosphorylation.

At the beginning of my thesis project, the understanding of D6PK had been rather limited: D6PK had been identified as a polarly localized protein kinase, essential for auxin transport, that colocalized with and phosphorylated PINs but that did not influence PIN abundance or localization (Zourelidou et al, 2009). D6PK had been proposed to regulate PIN-mediated auxin efflux by direct PIN phosphorylation. The colocalization of D6PK and PIN had also raised the questions whether the trafficking of the kinase and its substrates to the plasma membrane was co-regulated and whether the two proteins functionally interacted at different cellular compartments than the plasma membrane. Importantly, the plasma membrane-associated (peripheral) D6PK lacks protein domains or motifs that would explain or allow predicting its membrane anchoring or intracellular transport. In the studies for this thesis, I aimed at identifying the molecular and cellular mechanisms that control the polarity establishment and maintenance and also the membrane anchoring of D6PK.

My studies on the intracellular trafficking of D6PK gave rise to **Publication 1** published in *Developmental Cell* (Barbosa et al, 2014). There, I examined whether D6PK localization required polar PIN localization and whether D6PK behavior is dependent on known regulators of PIN trafficking and polarity. To this end, I determined D6PK localization under genetic and pharmacologic conditions that affect PIN polarity and trafficking. Gathering some mechanistic information on the control of D6PK localization, it was then possible to test the hypothesis that the presence of D6PK at the plasma membrane is a requirement for PIN-mediated auxin transport *in planta*. To this end, I differentially manipulated D6PK and PIN localization using pharmacological and genetic means and determined the consequences on PIN phosphorylation and auxin transport-dependent growth. The findings in this work supported a critical role for D6PK localization in the control of PIN-mediated auxin transport and demonstrate that D6PK and PINs are targeted to the plasma membrane via independent trafficking pathways.

The emerging picture of PIN activation by protein kinases such as D6PK, which was based on work exclusively produced in my host laboratory (Barbosa et al, 2014; Willige et al, 2013; Zourelidou et al, 2014; Zourelidou et al, 2009), was then discussed in **Publication 2**, a review article published in *Current Opinion in Plant Biology* on the role of D6PK and the AGCVIII kinases phot1 (phototropin1) and PID/WAGs in auxin transport control (Barbosa & Schwechheimer, 2014). There, we describe auxin transport regulation by these protein kinases at three different levels: First, we compared the mechanisms of D6PK subcellular localization control as described in my own work (Barbosa et al, 2014) in comparison to the scarce reports of subcellular localization of the plasma membrane localized phots and PID/WAGs kinases

(Dhonukshe et al, 2010; Kaiserli et al, 2009). Second, we comparatively discussed the role of D6PK in hypocotyl tropism responses, PIN3 phosphorylation, and basipetal auxin transport as published by our group and with my contribution (Willige et al 2013; not part of this thesis) with the proposed roles of phot1 in the inhibition of the ABCB19 auxin transporter in phototropism response; and of PID/WAGs in the control of PIN3 re-polarization in photo- and gravitropic responses as proposed by others (Christie et al, 2011; Ding et al, 2011; Rakusová et al, 2011). Third, we discussed the overlapping but differential affinities of D6PK and PID kinases towards the same residues in the PIN cytosolic loop reported described by our group and with my contribution (Zourelidou et al 2014; not part of this thesis) in the context of the known differential biological roles of these kinases in the regulation of auxin transport.

Finally, in **Publication draft 3** (Barbosa et al, in preparation), I describe my results from biochemical and cell biology studies aiming at the identification of the domain and motif required for D6PK anchoring to the plasma membrane and D6PK polarity control. I tested the possibility of D6PK to directly bind phospholipids and ultimately identified a motif required for the phospholipid binding and anchoring of D6PK to membranes. I furthermore explored the possible role of phosphorylation in the control of D6PK membrane localization. As a consequence of my studies, a clearer picture of D6PK plasma membrane localization and polarity control has emerged, which likely represents a novel molecular determinant of PIN-mediated auxin transport.

3 Embedded Publications

3.1 Publication 1 D6 PROTEIN KINASE activates auxin transport-dependent growth and PIN-FORMED phosphorylation at the plasma membrane (2014) *Developmental Cell*

Inês C.R. Barbosa[1], Melina Zourelidou[1], Björn C. Willige[1,2], Benjamin Weller[1] and Claus Schwechheimer[1]

3.1.1 Summary

The first publication of this thesis, *D6 PROTEIN KINASE activates auxin transport-dependent growth and PIN-FORMED phosphorylation at the plasma membrane*, was published in June 2014 in the peer-reviewed journal *Developmental Cell*.

Prior to this work, my host laboratory had shown that D6PK was a key regulator of PIN-mediated auxin transport and that D6PK phosphorylated and colocalized with the polarly-distributed PIN proteins at the plasma membrane (Zourelidou et al, 2009). We hypothesized that D6PK localization was not coincidental and may be required for the activation of PIN-mediated auxin transport. Meanwhile, we identified that complex mutants of *D6PK*, *D6PKL1*, *D6PKL2* and *D6PKL3* were impaired in the negative gravitropism and phototropism of etiolated seedlings, which correlated with reduced PIN3 phosphorylation, reduced basipetal auxin transport and defective auxin distribution (Willige et al, 2013). These phenotypes were crucial for testing our hypothesis and biological validation of a model proposed in the here summarized publication.

In this publication, we aimed at understanding the cellular mechanisms underlying D6PK polarity and at determining whether its membrane localization is required for PIN phosphorylation and auxin transport-dependent growth. For this, I conducted a comparative analysis of the subcellular trafficking of the PINs and D6PK, based on the current knowledge on PIN polarity control, to identify the major commonalities and differences between the polarity control of the kinase and its PIN substrates. I showed that YFP:D6PK, as the PINs, undergoes BFA-sensitive constitutive recycling between the plasma membrane and endosomes. However, the fast kinetics of YFP:D6PK suggested a more rapid turnover than that of the PINs, which were only partially internalized after BFA treatment. As for the PINs, YFP:D6PK recycling requires the ARF-GEF protein GNOM. However, while PINs were still at the plasma membrane but had polar defects in the *gnom*$^{B/E}$ mutant (Ikeda et al, 2009), YFP:D6PK was almost completely internalized, found in FM4-64 labeled endosomes but polarly distributed whenever present at the plasma membrane. Thus, GNOM was required for the targeting of YFP:D6PK from endosomes to the plasma membrane, whereas GNOM mediated the recycling of PINs but was not requiredfor plasma membrane targeting *per se*. Also, differently from the PINs, YFP:D6PK internalization was independent from clathrin-mediated endocytosis and this

could not be inhibited by auxin. On the contrary, auxin treatments promoted the transient as well as long-term internalization of YFP:D6PK. Besides these differences in the trafficking kinetics and requirements, determination of YFP:D6PK polarity seemed to be independent from PIN polarity in the same cell: inspection of YFP:D6PK polarities in different tissues and organs suggested that it was basal in most cells and did not follow PIN polarity patterns. Furthermore, the manipulation of PIN1 polarities in the shoot and root by *PID* loss- or gain-of-function did not affect the basal localization of D6PK.

Subsequently, I used this knowledge to explore conditions where YFP:D6PK, but not the PINs, was displaced from the plasma membrane to test D6PK function in the tropism responses, PIN3 phosphorylation, and auxin distribution. Etiolated seedlings grown on low BFA concentrations, where YFP:D6PK but not the PINs were internalized, phenocopied *D6PK* loss-of-function mutants, displaying typical tropism, PIN3 phosphorylation, and auxin distribution defects. In further support of a critical role of D6PK in these processes, I found that the phenotype of *D6PK* overexpressors was normalized after BFA treatment and resembled that of untreated wild-type seedlings. Accordingly, also $gnom^{B/E}$ mutants phenocopied the agravitropism of complex *d6pk* mutants and shared their PIN3 phosphorylation defects.

I could further establish a similar correlation between YFP:D6PK plasma membrane abundance and PIN1 phosphorylation in the root. In this tissue, short term BFA-treatments or treatments with low concentrations of BFA sufficiently affected YFP:D6PK localization but had minimal or no detectable effects on PIN1:GFP internalization. This led to a dramatic reduction of PIN1:GFP phosphorylation, which could be reversed by BFA-washout treatments where the recovery of the YFP:D6PK plasma membrane localization correlated well with an increase in PIN phosphorylation. The same BFA-treatments seemingly led to an accumulation of auxin in the stele cells, as monitored by the disappearance of the DII:Venus reporter. Altogether, this suggested that reduced PIN phosphorylation impacts on auxin fluxes in this tissue by YFP:D6PK internalization and possibly also other BFA-sensitive kinases.

Taken together, I could show that YFP:D6PK is a peripheral membrane protein, that is polarly localized at the plasma membrane and which traffics through a different pathway than its also polarly localized PIN substrates. In support of our initial hypothesis, D6PK localization at the plasma membrane and co-localization with the PINs were strictly required for PIN phosphorylation and auxin-transport dependent growth (tropisms). This indicates that D6PK and PINs only colocalized at the plasma membrane and that unphosphorylated PINs were inactive *in vivo*. The fact that the PINs were quickly dephosphorylated upon D6PK removal from the plasma membrane suggested that PIN phosphorylation was readily antagonized by phosphatases.

With this work, I firmly established D6PK-dependent PIN phosphorylation as a novel requirement for auxin transport. In addition, D6PK subcellular trafficking and polarity kinetics revealed novel routes for cell polarity control in plants, which are worth further investigations.

3.1.2 Contributions

I contributed all experiments and data analysis to this publication with the exception of the kinase assays presented in Supplementary Figure S3 and S7 (i.e. confocal imaging and immunoblots and respective signal intensity quantification; histochemical and phenotypical analysis). All experiments were designed by myself and Claus Schwechheimer. Kinase assays were carried out by Melina Zourelidou[1], immunostaining was performed with the help of Benjamin Weller, and PIN western blots were performed with the help of Björn Willige[1,2]. Benjamin Weller[1] and Björn Willige[1,2] had established the respective techniques and materials in the context of their research projects and are therefore coauthors of this publication. Mutants and reporter lines were generated with the technical assistance of Jutta Elgner and Deborah Schnell who are acknowledged in the paper. The manuscript concept, manuscript writing as well as all figures were performed and prepared by myself together with Claus Schwechheimer.

[1]Plant Systems Biology, Center of Life and Food Sciences Weihenstephan, Technische Universität München, 85354 Freising, Germany

[2]Present address: Salk Institute for Biological Studies, 10010 North Torrey Pines Road, La Jolla, CA 92037, USA

Please cite this article in press as: Barbosa et al., D6 PROTEIN KINASE Activates Auxin Transport-Dependent Growth and PIN-FORMED Phosphorylation at the Plasma Membrane, Developmental Cell (2014), http://dx.doi.org/10.1016/j.devcel.2014.05.006

Developmental Cell
Article

CellPress

D6 PROTEIN KINASE Activates Auxin Transport-Dependent Growth and PIN-FORMED Phosphorylation at the Plasma Membrane

Inês C.R. Barbosa,[1] Melina Zourelidou,[1] Björn C. Willige,[1,2] Benjamin Weller,[1] and Claus Schwechheimer[1,*]
[1]Department of Plant Systems Biology, Center of Life and Food Sciences Weihenstephan, Technische Universität München, 85354 Freising, Germany
[2]Present address: Salk Institute for Biological Studies, 10010 North Torrey Pines Road, La Jolla, CA 92037, USA
*Correspondence: claus.schwechheimer@wzw.tum.de
http://dx.doi.org/10.1016/j.devcel.2014.05.006

SUMMARY

The directed cell-to-cell transport of the phytohormone auxin by efflux and influx transporters is essential for proper plant growth and development. Like auxin efflux facilitators of the PIN-FORMED (PIN) family, D6 PROTEIN KINASE (D6PK) from *Arabidopsis thaliana* localizes to the basal plasma membrane of many cells, and evidence exists that D6PK may directly phosphorylate PINs. We find that D6PK is a membrane-bound protein that is associated with either the basal domain of the plasma membrane or endomembranes. Inhibition of the trafficking regulator GNOM leads to a rapid internalization of D6PK to endomembranes. Interestingly, the dissociation of D6PK from the plasma membrane is also promoted by auxin. Surprisingly, we find that auxin transport-dependent tropic responses are critically and reversibly controlled by D6PK and D6PK-dependent PIN phosphorylation at the plasma membrane. We conclude that D6PK abundance at the plasma membrane and likely D6PK-dependent PIN phosphorylation are prerequisites for PIN-mediated auxin transport.

INTRODUCTION

The phytohormone auxin controls virtually all aspects of plant growth and development. Auxin is transported from cell to cell from sites of synthesis to sites of action via a system of auxin influx and efflux carriers (Kleine-Vehn and Friml, 2008; Teale et al., 2006). A subset of the PIN-formed (PIN) proteins, namely PIN1-PIN4 and PIN7, are the proposed plasma membrane auxin efflux facilitators in *Arabidopsis thaliana* (Friml et al., 2002; Gälweiler et al., 1998; Müller et al., 1998; Wisniewska et al., 2006). PINs are asymmetrically distributed in the plasma membrane of many cells and they constantly traffic to and from the plasma membrane. This exocytosis and endocytosis can be visualized using Brefeldin A (BFA), which reversibly inhibits a subset of ADP RIBOSYLATION FACTOR-GUANINE NUCLEOTIDE EXCHANGE FACTORS (ARF-GEFs) including GNOM (GN; Geldner et al., 2001, 2003). Following BFA treatment, endocytosed PINs accumulate in artificial vesicular aggregates referred to as BFA compartments (Geldner et al., 2001; Robinson et al., 2008). Whether auxin transporters are constitutively active or require additional factors is not fully understood.

The *Arabidopsis* genome encodes 23 so-called AGCVIII kinases (Galván-Ampudia and Offringa, 2007), serine/threonine kinases related to mammalian protein kinase A, protein kinase G, and protein kinase C (Pearce et al., 2010). Several *Arabidopsis* AGCVIII kinases function in the regulation of auxin transport or auxin transport-dependent growth (Rademacher and Offringa, 2012): phototropin1 (phot1) and phot2 are the blue light receptors essential for phototropic hypocotyl bending (Briggs and Huala, 1999). PINOID (PID), WAG1, and WAG2 control PIN polarity by direct PIN phosphorylation (Dhonukshe et al., 2010; Huang et al., 2010; Kleine-Vehn et al., 2009; Michniewicz et al., 2007)—loss of *PID* function results in shoot differentiation defects that correlate with a defect in targeting PIN1 to the apical plasma membrane in shoot epidermis cells (Friml et al., 2004), and inversely, *PID*, *WAG1*, or *WAG2* overexpression promotes the apicalization of PINs in the root (Dhonukshe et al., 2010). We have previously characterized mutants of four AGCVIII kinases that we collectively refer to as D6 PROTEIN KINASES (D6PKs), namely D6PK and D6PK-LIKE1 through D6PK-LIKE3 (D6PKL1–D6PKL3; Zourelidou et al., 2009). Higher order *d6pk* mutants have a number of phenotypes that suggest a role for D6PKs in the control of auxin transport (Zourelidou et al., 2009). These phenotypes include defects in phototropic and negatively gravitropic hypocotyl bending that correlate directly with reduced basipetal auxin transport in etiolated seedlings (Willige et al., 2013). Intriguingly, D6PK, which does not have any sequence features indicative for a membrane association, colocalizes with PINs at the basal plasma membrane and D6PK can directly phosphorylate PINs in vitro and seemingly also in vivo (Willige et al., 2013; Zourelidou et al., 2009).

Here, we examine the cell biological behavior of D6PK in the context of its physiological role in controlling tropic responses. We find that D6PK is highly sensitive to BFA treatment and subject to an active removal from the plasma membrane that is much faster than can be measured for PIN proteins. We further demonstrate that D6PK promotes PIN phosphorylation and auxin transport-dependent growth, but only when present at the plasma membrane. Our study suggests that D6PK abundance at the plasma membrane and likely D6PK-dependent

Please cite this article in press as: Barbosa et al., D6 PROTEIN KINASE Activates Auxin Transport-Dependent Growth and PIN-FORMED Phosphorylation at the Plasma Membrane, Developmental Cell (2014), http://dx.doi.org/10.1016/j.devcel.2014.05.006

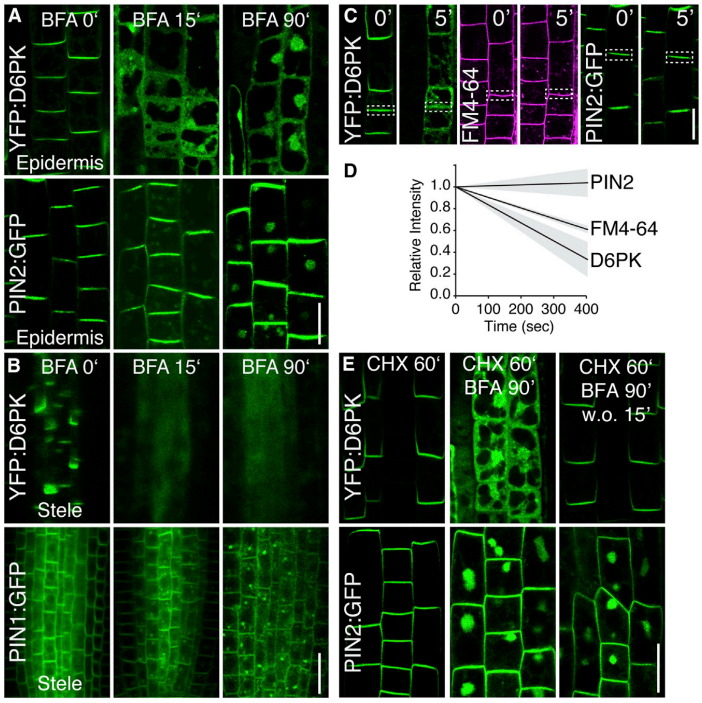

Figure 1. D6PK Is Cycling in a BFA-Dependent Manner

(A and B) Confocal images revealing the differential sensitivities of YFP:D6PK and PIN2:GFP in the root epidermis (A) or PIN1:GFP in the stele (B) to the trafficking inhibitor BFA (50 μM) after treatment for 0, 15, and 90 min.

(C and D) Confocal images (C) and (D) quantitative kinetic analyses of YFP:D6PK, FM4-64, and PIN2:GFP abundance (signal intensity) at the plasma membrane. FM4-64 stained seedlings were pulse-stained with 2 μM FM4-64 for 5 min before the BFA treatment. Shown are representative confocal images taken at 0 and 5 min after BFA treatment, signal intensities were quantified every 40 s from plasma membrane regions as highlighted by a white frame in (C). All data were normalized to the signal intensity at time point 0 min for each set of measurements obtained from a single cell. The average slope of at least 24 cells from at least three roots is represented (thick line) together with the respective SD (shaded area).

(E) Confocal images of YFP:D6PK and PIN2:GFP distribution on root epidermis from seedlings pretreated with 50 μM cycloheximide (CHX) for 60 min, followed by 90 min BFA-treatment and subsequent washout of the BFA for 15 min (w.o.). CHX was included in all treatments.

Scale bars represent 20 μm. See also Figures S1 and S2.

PIN phosphorylation are prerequisites for active PIN-mediated auxin transport.

RESULTS

D6PK Localizes to the Basal Plasma Membrane

D6PK is a polarly distributed protein kinase that localizes to the basal (rootward) plasma membrane in root cells of *Arabidopsis thaliana* seedlings (Zourelidou et al., 2009). To gain an insight into the subcellular localization of D6PK in a diverse set of cell types, we examined the distribution of a fully functional YFP-tagged D6PK variant expressing YFP:D6PK from a *D6PK* promoter fragment or from the constitutive 35S CaMV promoter (Willige et al., 2013; Figure S1 available online). We found that D6PK localizes to the basal membrane in all cells that expressed the protein including epidermal cells of the shoot apical meristem (Figure S1A), endodermis cells of hypocotyls (Figure S1C), xylem parenchymatous cells of the stem (Figure S1E), as well as various cell types of the root (Figure S1G). Whereas D6PK, in most cell types, shared the basal plasma membrane localization with its proposed phosphorylation substrates PIN1, PIN2, or PIN3 (Abas et al., 2006; Benková et al., 2003; Willige et al., 2013; Zádníková et al., 2010; Zourelidou et al., 2009), we identified at least two cases in which D6PK and PINs did not colocalize (Figure S1). First, whereas PIN1 was apical in epidermal cells of the shoot apical meristem (Friml et al., 2004), D6PK localized to the basal plasma membrane (Figures S1A and S1B). Second, whereas PIN2 was apical in root epidermis cells and basal in cortex cells, D6PK was basally localized in both cell types (Figures S1G and S1I). We thus concluded that D6PK is a basally localized protein and that D6PK polarity is independent from that of the PINs, at least in some cell types.

D6PK Is a Rapidly Cycling Protein

We had previously reported that D6PK is a BFA-sensitive protein (Zourelidou et al., 2009). Importantly, our kinetic analysis now revealed that D6PK is internalized much more rapidly than PIN2 or PIN1 (Figures 1A and 1B). In contrast to the PINs, D6PK was completely depleted from the plasma membrane already within minutes after the onset of BFA treatment (Figures 1A–1D). Over this period of time, D6PK became visible in the cytosol and in intracellular compartments that stained positive for FM4-64, a fluorescent general endocytosis tracer (Figure S2A). After 60 min, D6PK accumulated at even larger intracellular structures, which we identified as BFA compartments (Robinson et al., 2008; Figures 1A and 1B; Figure S2A). At least during the first 5 min of BFA treatment, the rate of D6PK internalization was a constant linear process that was faster than the endocytosis of FM4-64, which we considered as a reporter for the average endocytosis rate (Figures 1C and 1D). Importantly according to our quantitative analysis, PIN2 showed no detectable changes in its abundance in the plasma membrane over this period of time (Figures 1C and 1D) although it had previously been reported that PIN2 can be detected intracellularly already

Please cite this article in press as: Barbosa et al., D6 PROTEIN KINASE Activates Auxin Transport-Dependent Growth and PIN-FORMED Phosphorylation at the Plasma Membrane, Developmental Cell (2014), http://dx.doi.org/10.1016/j.devcel.2014.05.006

Developmental Cell

D6PK Activates PINs at the Plasma Membrane

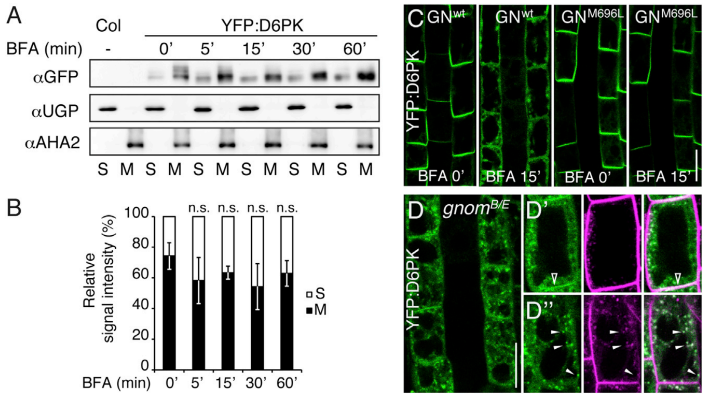

Figure 2. D6PK Is Mainly Associated with Membranes, Also When Internalized

(A) Representative immunoblots of the soluble fraction (S) and microsomal fraction (M) obtained by subcellular fractionation of roots from seven-day old light-grown seedlings that had been treated with BFA (50 μM). αGFP detects YFP:D6PK; αUGP, anti-UDP-glucose pyrophosphorylase, S marker; αAHA2 (*Arabidopsis* H^+-ATPASE 2), M marker. The experiment was repeated four times with similar results.

(B) Densitometric quantification of the relative signal intensities of S and M fraction signals obtained with YFP:D6PK. Signal intensities were normalized to the respective UGP and AHA2 loading control. The normalized signal intensities of each S and M fractionation sample were added and set to 100%. The relative S and M fraction, average and standard error, from three experiments is plotted. Student's t test, not significant (n.s.) $p > 0.05$.

(C) Representative frames taken at 0 min and 15 min after BFA treatment from a time course experiment imaging YFP:D6PK in the root epidermis in a background containing wild-type GN^{wt} or BFA-resistant GN^{M696L} transgenes.

(D) Representative confocal images of YFP:D6PK localization in $gnom^{B/E}$. Staining with FM4-64 reveals the localization of a fraction of YFP:D6PK at the basal plasma membrane (D′, open white arrowhead) or in FM4-64-labeled intracellular aggregates (D′′, closed white arrowhead).

Scale bars represent 20 μm. See also Figure S3.

after 5 min of BFA treatment (Robert et al., 2010). To further characterize the BFA-sensitivity of D6PK, we analyzed D6PK and PIN localization over increasing BFA concentrations. We noticed that D6PK was efficiently internalized with 5 μM BFA when expressed from a *D6PK* promoter fragment whereas the internalization of overexpressed D6PK required higher BFA dosage (10 μM). Notably, neither PIN1 nor PIN2 were detectable in endosomes in these conditions (Figure S2B). Because a kinase-dead version of D6PK was rapidly internalized after BFA treatment, we concluded that this process is independent from its kinase activity (Figure S2C).

Similarly to what had been reported for PINs, the effects of BFA on D6PK could be reversed by washout treatments. After a 15 min washout treatment, the complete pool of D6PK was rapidly redirected to the basal plasma membrane, whereas PIN2 (Figure 1E) or FM4-64 (Figure S2A) could still be detected in BFA compartments. Because this behavior was observed in the presence of the protein biosynthesis inhibitor cycloheximide (CHX), which efficiently inhibited YFP:D6PK de novo synthesis (Figure S2D), we concluded that D6PK rapidly cycles between the basal plasma membrane and the cytoplasm or cytoplasmic compartments.

D6PK Recycling Is GN Dependent

Already shortly after BFA treatment, D6PK was completely dissociated from the plasma membrane. The confocal analysis suggested that the plasma membrane-dissociated D6PK in the cytoplasm was largely soluble and that only a minor fraction was associated with intracellular vesicles (Figures 1A–1C and Figure S2). Interestingly, our analyses with immunoblots after the subcellular fractionation of root extracts revealed that D6PK is a predominantly membrane-associated protein (M), before and after BFA treatment (Figures 2A and 2B). At the same time, we observed a slight increase in soluble D6PK (S) shortly after BFA treatment (5 min), suggesting that a small fraction of D6PK may become soluble after BFA treatment (Figure 2B). This increase was, however, not significant when averaged over independent experiments.

Because BFA targets the ARF-GEF GN, we examined whether D6PK recycling is GN-dependent in the background of the GN^{M696L} transgene, which encodes a BFA-insensitive but fully functional GN variant (Geldner et al., 2003). Interestingly, we found D6PK to be BFA-insensitive in GN^{M696L} suggesting that the recycling of D6PK requires GN function (Figure 2C). We further examined D6PK in the weak $gnom^{B/E}$ mutant (Anders et al., 2008; Geldner et al., 2004). In $gnom^{B/E}$, D6PK accumulated mainly in intracellular FM4-64 labeled structures, possibly endosomes (Figure 2D′′) and in some cells D6PK was detected at the basal plasma membrane (Figure 2D′), indicating that efficient D6PK targeting from endosomes to the basal plasma membrane requires fully functional GNOM (Figure 2D). Thus, D6PK is a mainly membrane-associated protein that requires GN ARF-GEF function for its efficient targeting to and from the plasma membrane.

D6PK Polarity Is Independent from PID

PID controls the polarity of PINs by direct phosphorylation (Friml et al., 2004). We tested whether PID may also control D6PK polarity, directly or indirectly, in the shoots of a *pid* loss-of-function mutant and roots of a *PID* overexpression line (Friml et al., 2004). Because the apical meristem of *pid* mutants is undifferentiated, YFP:D6PK localization in the wild-type could best be compared with *pid* mutants when shoot differentiation in the wild-type was inhibited with the auxin transport inhibitor 1-N-naphthylphthalamic acid (NPA; Friml et al., 2004). Whereas PIN1 in *pid* mutant inflorescences showed the previously reported apical-to-basal shift, we detected an exclusively basal localization of D6PK in undifferentiated *pid* and NPA-treated wild-type inflorescences (Figure S3A). Also in roots, where *PID* overexpression resulted in the previously reported PIN1

Please cite this article in press as: Barbosa et al., D6 PROTEIN KINASE Activates Auxin Transport-Dependent Growth and PIN-FORMED Phosphorylation at the Plasma Membrane, Developmental Cell (2014), http://dx.doi.org/10.1016/j.devcel.2014.05.006

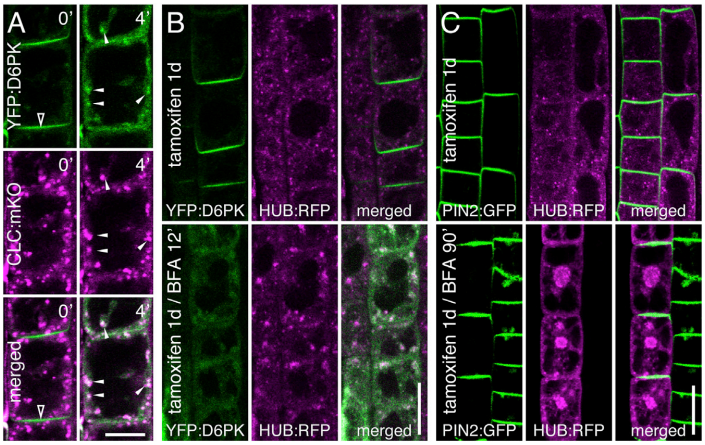

Figure 3. D6PK Internalization Cannot Be Inhibited by Expression of a Dominant-Negative Clathrin Variant

(A) Confocal images of root epidermal cells before and after a 4 min treatment with BFA (50 μM) of a transgenic line expressing YFP:D6PK and CLC:mKO. Open white arrowheads mark the initial plasma membrane-localized YFP:D6PK, white arrowheads mark the intracellular compartments that are positive for YFP:D6PK and CLC:mKO after BFA treatment.

(B and C) Confocal images of root epidermal cells from 6-day-old seedlings expressing YFP:D6PK (B) and PIN2:GFP (C) and the tamoxifen-inducible construct pINTAM > HUB:RFP (1 day induction with tamoxifen, 2 μM) before and after treatment with BFA (50 μM) for 12 min (B) and 90 min (C). Note that intracellular HUB:RFP compartments aggregate after BFA treatment. The different size of these aggregates in (B) and (C) is explained by the different length of the BFA treatment. Also note that PIN2:GFP endocytosis is blocked only in the HUB-expressing cell file (C).

Scale bars represent 10 μm (A), 20 μm (B and C). See also Figure S4.

basal-to-apical polarity shift, D6PK maintained its basal polarity in all cells examined (Figures S3B–S3D). In in vitro phosphorylation experiments, we found that PID cannot phosphorylate D6PK, thus further substantiating the conclusion that D6PK and PID are functionally unrelated (Figures S3E and S3F).

D6PK Internalization Is Independent from Clathrin-Mediated Endocytosis

Clathrin-dependent endocytosis is the best-characterized endocytosis pathway (Brodsky et al., 2001; Ito et al., 2012). Clathrin-coated vesicles sort cargo proteins at the plasma membrane and at the *trans*-Golgi network (TGN; Brodsky et al., 2001; Ito et al., 2012). Because, already 4 min after BFA treatment, we observed a colocalization of D6PK with the intracellular pool of a clathrin light chain marker (35S:CLC:mKO), we speculated that the internalization of D6PK was clathrin-mediated (Figure 3A and Figure S4A). However, we found no effect on D6PK internalization when we inhibited clathrin cage formation by overexpression of HUB, a dominant-negative variant of the clathrin heavy chain (Dhonukshe et al., 2007; Kitakura et al., 2011; Liu et al., 1998; Figure 3B and Figure S4B). At the same time, the effectiveness of HUB overexpression could be verified because the formation of PIN2-containing BFA compartments was efficiently blocked in HUB-expressing cells while the previously reported BFA-induced aggregation of endomembrane-localized HUB was visible (Kitakura et al., 2011; Figures 3B and 3C). We thus concluded that the internalization of D6PK is independent from the clathrin-dependent endocytosis pathway, although internalized D6PK colocalized with endosomal clathrin, presumably at the TGN.

Auxin Promotes D6PK Internalization

Auxin was previously found to inhibit the endocytosis of PINs and other plasma membrane proteins (Paciorek et al., 2005; Robert et al., 2010). We tested whether D6PK internalization is also blocked by auxin using the synthetic auxin 1-naphthaleneacetic acid (1-NAA). Interestingly, while PIN2 endocytosis and FM4-64 uptake were inhibited by 1-NAA treatment as suggested by the absence of BFA compartments containing PIN2 or FM4-64, we could not inhibit BFA-induced D6PK internalization with 1-NAA (Figure 4A). On the contrary, we observed that D6PK became rapidly internalized into FM4-64-labeled endosomes within minutes after 1-NAA treatment (Figure 4B and Figure S5). After a delay of approximately 30 min, D6PK was then efficiently retargeted to the plasma membrane (Figure 4B and Figure S5). Following longer auxin treatments (e.g., 4 hr), we also noted a pronounced intracellular accumulation of D6PK; in some cells, even a complete depletion of the protein from the plasma membrane (Figure 4C). For each of these behaviors, we noted with interest that the kinetics and effects of the respective auxin-dependent dissociation and reassociation responses were not uniform when compared between different auxin-treated seedlings. These findings suggest that auxin levels control the distribution of D6PK either by promoting D6PK internalization or by inhibiting its retargeting to the plasma membrane.

D6PK Activity Is Critical at the Plasma Membrane

We next examined whether the physiological activity of D6PK correlates with its localization at the plasma membrane. We exploited the differential BFA sensitivity of D6PK and PINs and correlated D6PK and PIN3 protein abundance at the plasma membrane of hypocotyl endodermis cells with defects in negative gravitropism of etiolated seedlings, which can be explained by defects in PIN-mediated auxin transport (Willige et al., 2013). We found that D6PK could be partially and strongly depleted from the plasma membrane when seedlings were grown on 3 μM and 5 μM BFA, respectively (Figures 5A and 5B). At the same time, we could only detect significant PIN3 internalization in seedlings grown on 5 μM BFA but not on 3 μM BFA (Figures 5A and 5B). At the physiological level, we found that dark-grown wild-type seedlings, when grown on 3 μM or 5 μM BFA, displayed a strong negative gravitropism defect similar to the

Please cite this article in press as: Barbosa et al., D6 PROTEIN KINASE Activates Auxin Transport-Dependent Growth and PIN-FORMED Phosphorylation at the Plasma Membrane, Developmental Cell (2014), http://dx.doi.org/10.1016/j.devcel.2014.05.006

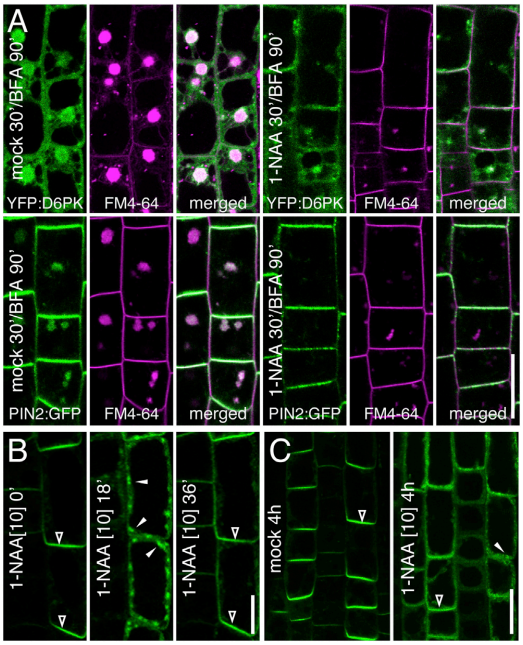

Figure 4. Auxin Does Not Inhibit YFP:D6PK Endocytosis but Induces Its Transient Relocalization

(A) Confocal images of root epidermal cells of 6-day-old seedlings expressing YFP:D6PK or PIN2:GFP after a 30 min mock or 1-NAA (10 μM) pretreatment followed by a 90 min BFA (50 μM) treatment in the presence of FM4-64 (2 μM).

(B) Representative frames from a time series experiment after 1-NAA treatment (10 μM) of YFP:D6PK seedlings.

(C) Representative confocal images of YFP:D6PK in root cells treated for 4 hr with 1-NAA (10 μM) or a mock solution. Note that intracellular YFP:D6PK signals are increased and plasma membrane signals are decreased in 1-NAA-treated cells when compared to the mock control. Open white arrowheads mark the plasma membrane-localized YFP:D6PK, white arrowheads mark the transient intracellular accumulation of the protein.

Scale bars represent 20 μm (A and C), 10 μm (B). See also Figure S5.

defects observed in *d6pk d6pkl1 d6pkl2* (*d6pk012*) or *pin3 pin4 pin7* (*pin347*) triple mutants or in seedlings grown in the presence of the auxin transport inhibitor NPA (Willige et al., 2013; Figures 5C–5E). Interestingly, this BFA-induced phenotype was not observed in BFA-resistant GN^{M696L} seedlings, suggesting that it was caused by a functional impairment of GN (Figures 5C and 5D). Furthermore, we found that the growth of etiolated D6PK overexpressor seedlings, which is characterized by the absence of an apical hook and an irregularly growing hypocotyl with gravitropism defects, was largely normalized after BFA treatment (Figures 5C, 5D, and 5F). In line with a role of GN in this BFA-triggered D6PK-dependent response, this was only observed in the presence of the BFA sensitive wild-type GN protein but not in the GN^{M696L} background (Figures 5C, 5D, and 5F). Furthermore, the D6PK overexpression phenotype was dependent on D6PK kinase activity because the overexpression of a kinase-dead D6PK (D6PKin) did not display this phenotype but behaved in a similar manner as the wild-type (Figures 5C and 5D). Because D6PK abundance was not altered after BFA treatments (Figure S6A) and the D6PK overexpressor phenotypes could also be largely normalized by NPA treatment (Figures 5C, 5D, and 5F), we argue that the observed growth defects of the D6PK overexpressors are a consequence of increased or aberrant auxin transport. Additionally, we also measured phototropism and negative gravitropism responses in the D6PK overexpressors and in *d6pk* single and double mutants where auxin transport and tropic responses are partially impaired (Willige et al., 2013; Figures S6B and S6C). Whereas we found *d6pk* mutants to be hypersensitive to the effects of BFA treatments in both tropic responses, the D6PK overexpressors as well as GN^{M696L} seedlings were partially or fully BFA-insensitive (Figures S6B and S6C). Because the BFA sensitivity in these assays was dependent on *D6PK* gene dosage and kinase activity, we propose that D6PK or one of its orthologs is the BFA-sensitive protein that controls these tropisms.

PIN Phosphorylation and Auxin Distribution Correlate with the Abundance of D6PK at the Plasma Membrane

We next tried to link the observed effects of BFA treatment on the intracellular distribution of D6PK with changes in auxin distribution and PIN phosphorylation. To this end, we examined auxin distribution using the auxin response reporter DR5:GUS (Sabatini et al., 1999). We found that dark-grown wild-type seedlings, when grown on medium containing 3 μM BFA, had a reduced auxin response in the hypocotyl and failed to establish an apical hook as well as a DR5:GUS auxin response maximum that typically forms in the concave side of the hook (Figures 5C and 6A). Instead, BFA-treated wild-type seedlings had a DR5:GUS auxin response maximum in the cotyledons, the proposed sites of auxin biosynthesis. In all these regards, BFA-treated wild-type seedlings phenocopied *d6pk012* triple mutants (Figures 5C, 5E, and 6A). Interestingly, when we examined D6PK overexpressing seedlings, which we propose to have increased and possibly aberrant auxin transport also due to the fact that NPA treatments could normalize their phenotype (Figure 5C), BFA treatment did not only lead to a normalization of their growth phenotype but also largely normalized the auxin response pattern of dark-grown seedlings (Figure 6A). Thus, manipulation of D6PK abundance at the plasma membrane by BFA treatment results in predictable D6PK-dependent changes in auxin distribution and auxin-dependent plant growth.

Because loss of *D6PK* function correlates with decreased PIN3 phosphorylation (Willige et al., 2013), we also examined the effects of the BFA-induced D6PK depletion from the plasma membrane on PIN3 phosphorylation. Indeed, we observed reduced PIN3 phosphorylation in seedlings grown on increasing concentrations of BFA, in the strongest case reminiscent of the PIN3 phosphorylation defect observed in *d6pk012* triple mutants (Figures 6B–6D): Whereas, the relative intensity of the upper (phosphorylated PIN3) band when compared to the lower (un- or dephosphorylated PIN3) band was high in untreated wild-type seedlings (87%), this intensity was reduced (58%) when wild-type seedlings were grown on 3 μM BFA and thereby displayed an intensity of the phosphorylated band that was similar to the intensity measured in untreated *d6pk012* triple mutants (53%; Figures 6B–6D). In turn, the D6PK overexpressors

Please cite this article in press as: Barbosa et al., D6 PROTEIN KINASE Activates Auxin Transport-Dependent Growth and PIN-FORMED Phosphorylation at the Plasma Membrane, Developmental Cell (2014), http://dx.doi.org/10.1016/j.devcel.2014.05.006

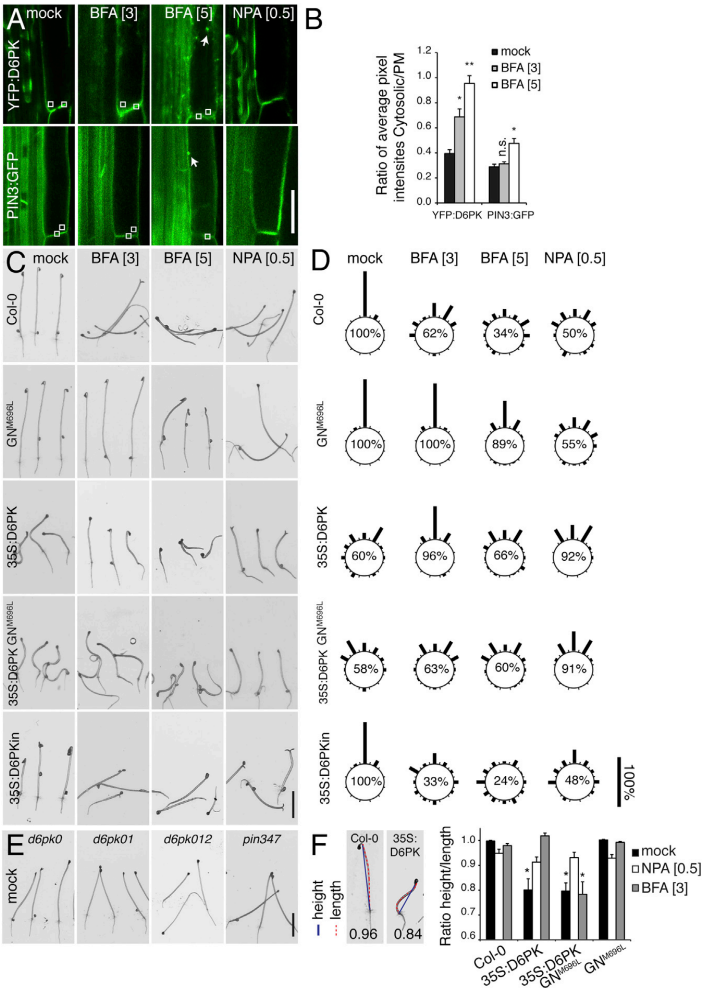

Figure 5. D6PK Critically Determines D6PK-Dependent Growth at the Plasma Membrane

(A) Confocal images of hypocotyl endodermis cells from 3-day-old etiolated YFP:D6PK and PIN3:GFP seedlings grown in the absence (mock) and presence of BFA (3 μM; 5 μM) or NPA (0.5 μM). Open white squares mark the regions of interest (ROIs) used for measurements in (B); white arrows mark YFP:D6PK signal in cytosolic strands; arrowheads mark PIN3:GFP and YFP:D6PK-positive BFA-compartments. Scale bar represents 20 μm.

(B) Ratio of average pixel intensities quantified at the cytosol and the plasma mebrane (cytosol/PM) in selected ROIs as in (A). A reduced size of the ROIs was selected due to the restricted cytosolic area of endodermal cells. Due to the absence of fluorescence in the cytosol of PIN3:GFP expressing lines, ROIs were placed either adjacent to the plasma membrane or, whenever present, at the BFA compartments (arrowhead, BFA 5 μM). Shown is the mean and standard error of at least ten cells from at least four hypocotyls. Student's t test in comparison to the respective mock, $^{*}p < 0.01$.

(C and D) Photographs of 3-day-old etiolated seedlings grown in the absence (mock) and presence of BFA (3 μM; 5 μM) or NPA (0.5 μM). Scale bar represents 5 mm. (D) Quantification of the negative hypocotyl gravitropism; $n \geq 50$, 3 biological replicates. Values were binned in 30° angle classes and the relative frequency distribution is presented in the circular graphs. The percentage of seedlings corresponding to the phenotype classes (hypocotyl angle) 315°–345°, 345°–15°, and 15°–45° is indicated in each circular graph as a comparative measure for the different phenotypes.

(E) Photographs of 3-day-old etiolated seedlings showing negative gravitropism defects from single (*d6pk0*), double (*d6pk01*), and triple mutants (*d6pk012*) as well as that of the *pin3 pin4 pin7* (*pin347*) triple mutant.

(F) Representative images of seedlings with their respective length (red line) and height (blue) and their height/length ratio, and quantification of hypocotyl growth defects expressed as height/length ratios (average and standard error); $n \geq 20$; three biological replicates. A Student's t test was performed in comparison to the respective wild-type (Col-0), $^{*}p < 0.001$. See also Figure S6.

displayed a slightly stronger phosphorylation than the wild-type (98% compared to 87% in untreated wild-type seedlings), its PIN3 phosphorylation was largely unaffected at 3 μM (95%) and required higher BFA concentrations (5 μM) than the wild-type before an effect on PIN3 phosphorylation was observable (76%; Figures 6B–6D). Importantly, the overexpression of the kinase-dead version (35S:D6PKin) behaved as the wild-type (Figures 6B–6D). Furthermore and as could be expected based on the BFA-insensitive phenotype, PIN3 phosphorylation remained unaffected by BFA treatments in the GN^{M696L} background (Figures 6B–6D). When interpreted in the context of our previous observations that the overexpressed D6PK is less sensitive to BFA than D6PK expressed from a *D6PK* promoter fragment (Figure S2B), these results reveal that the manipulation of D6PK levels at the plasma membrane by BFA or by altering gene dosage lead to predictable changes in PIN3 phosphorylation.

Interestingly, PIN3 phosphorylation as observed in *d6pk012* triple mutants was further decreased from 54% in untreated seedlings to 32% in BFA (5 μM)-treated *d6pk012* mutants, suggesting that other BFA-sensitive kinases might control PIN3 phosphorylation in addition to the three D6PKs defective in *d6pk012* (Figures 6B–6D).

To evaluate the dependence of PIN3 phosphorylation on D6PK abundance at the plasma membrane in experimental conditions that would not require BFA application, we examined PIN3 phosphorylation in the $gnom^{B/E}$ background where D6PK accumulates largely intracellularly in roots (Figure 2D) as well as in hypocotyls of etiolated seedlings (Figure 6E). Also in protein

Please cite this article in press as: Barbosa et al., D6 PROTEIN KINASE Activates Auxin Transport-Dependent Growth and PIN-FORMED Phosphorylation at the Plasma Membrane, Developmental Cell (2014), http://dx.doi.org/10.1016/j.devcel.2014.05.006

Developmental Cell

D6PK Activates PINs at the Plasma Membrane

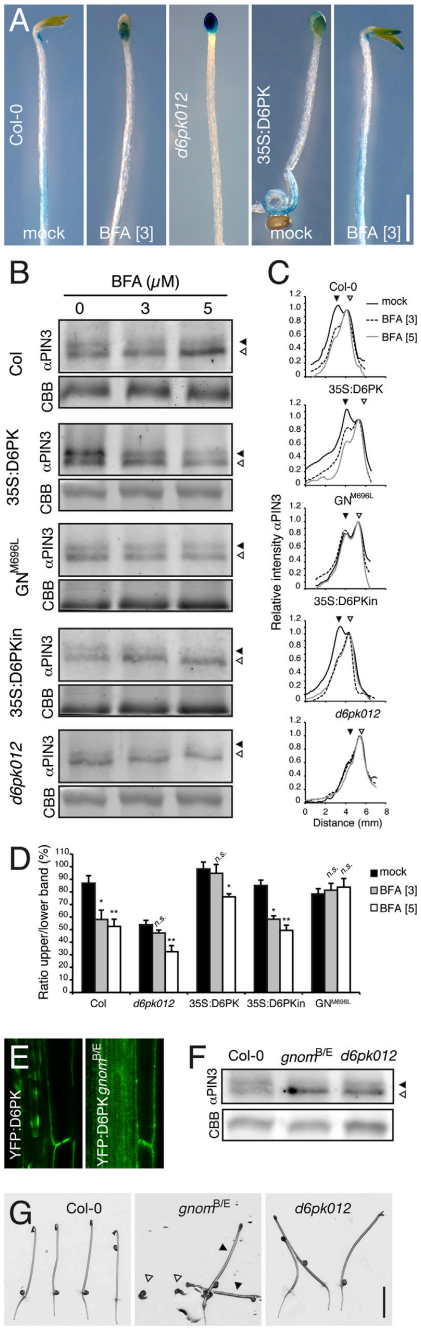

Figure 6. D6PK Abundance at the Plasma Membrane Determines Auxin Distribution and PIN3 Phosphorylation in Dark-Grown Seedlings

(A) Photographs of GUS-stained 4-day-old dark-grown seedlings grown in the absence and presence of BFA (3 μM) expressing the auxin (response) reporter DR5:GUS. Scale bar represents 1 mm.

(B) Representative immunoblots with αPIN3 of membrane protein extracts obtained from 4 day-old etiolated seedlings grown in the absence and presence of BFA (3 μM and 5 μM). CBB, Coomassie Brilliant Blue-stained gel, loading control.

(C) Representative densitometric profiles of immunoblots as shown in (B). The positions of the upper and lower bands are marked with filled and open arrowheads, respectively. To correct for positioning differences between samples, signal intensities were normalized and aligned to the maximum intensity of the lower band. Background was substracted for each genotype using the line method.

(D) Ratio between the intensities of the upper and lower band of PIN3 immunoblots were determined by densitometric analyses of at least three independent replicate experiments. The graphs show averages and SE. Student's t test, $^{*}p < 0.05$, $^{**}p < 0.01$, n.s. $p > 0.05$.

(E) Confocal images of hypocotyl endodermal cells from 4d old seedlings expressing YFP:D6PK in wild-type and *gnom*$^{B/E}$ mutant background.

(F) Representative αPIN3 immunoblot of membrane protein extracts obtained from 4 day-old etiolated Col-0 wild-type as well as *gnom*$^{B/E}$ and *d6pk012* triple mutants. CBB, Coomassie brilliant blue-stained gel, loading control.

(G) Photographs of 3- day-old etiolated seedlings with the genotypes indicated in the figure. The transheterozygous *gnom*$^{B/E}$ partial loss-of-function (filled arrowheads) and the severe *gnom*$^{B/B}$ or *gnom*$^{E/E}$ homozygous loss-of-function segregants (open arrowheads) are indicated. For the western blot analysis in (F), protein extracts were prepared from seedlings with a *gnom*$^{B/E}$ phenotype. Scale bar represents 5 mm.

extracts of the *gnom*$^{B/E}$ mutants, we found PIN3 phosphorylation to be strongly decreased (Figure 6F). In line with a biological role of this reduced PIN3 phosphorylation on auxin transport-dependent growth in *gnom*$^{B/E}$, we found that these mutants displayed a strong negative gravitropism defect further supporting our conclusion that PIN phosphorylation and tropic responses are dependent on the presence of D6PK at the plasma membrane (Figure 6G).

We also examined PIN1 phosphorylation and auxin distribution in the root after short-term BFA treatments. In anti-GFP immunoblots testing for PIN1:GFP expression, we noticed the presence of high molecular weight bands above the major PIN1:GFP band, which could correspond to phosphorylated forms of PIN1:GFP (Figures 7A–7E). Indeed, treatments with an active but not with a heat-inactived phosphatase resulted in a reduction of the high molecular weight PIN1:GFP forms (Figure 7C). We then tested whether PIN1 phosphorylation was altered after BFA treatment using the initially established conditions that lead to a depletion of D6PK but not of PIN1:GFP from the plasma membrane (Figure 1). Interestingly, a rapid decrease in PIN1 phosphorylation was observed already 15 min after BFA treatment (Figure 7A). Conversely, PIN1 phosphorylation was readily reestablished 30 min after a BFA washout treatment (Figure 7B). The fast kinetics of this response would thereby follow the initially described kinetics for the depletion of D6PK from and its reassociation with the plasma membrane (Figure 1). Furthermore, we could detect a reduction of PIN1:GFP phosphorylation levels with low concentrations of BFA (Figure 7D), which were sufficient to trigger D6PK but not PIN1 internalization (Figure S2B).

Please cite this article in press as: Barbosa et al., D6 PROTEIN KINASE Activates Auxin Transport-Dependent Growth and PIN-FORMED Phosphorylation at the Plasma Membrane, Developmental Cell (2014), http://dx.doi.org/10.1016/j.devcel.2014.05.006

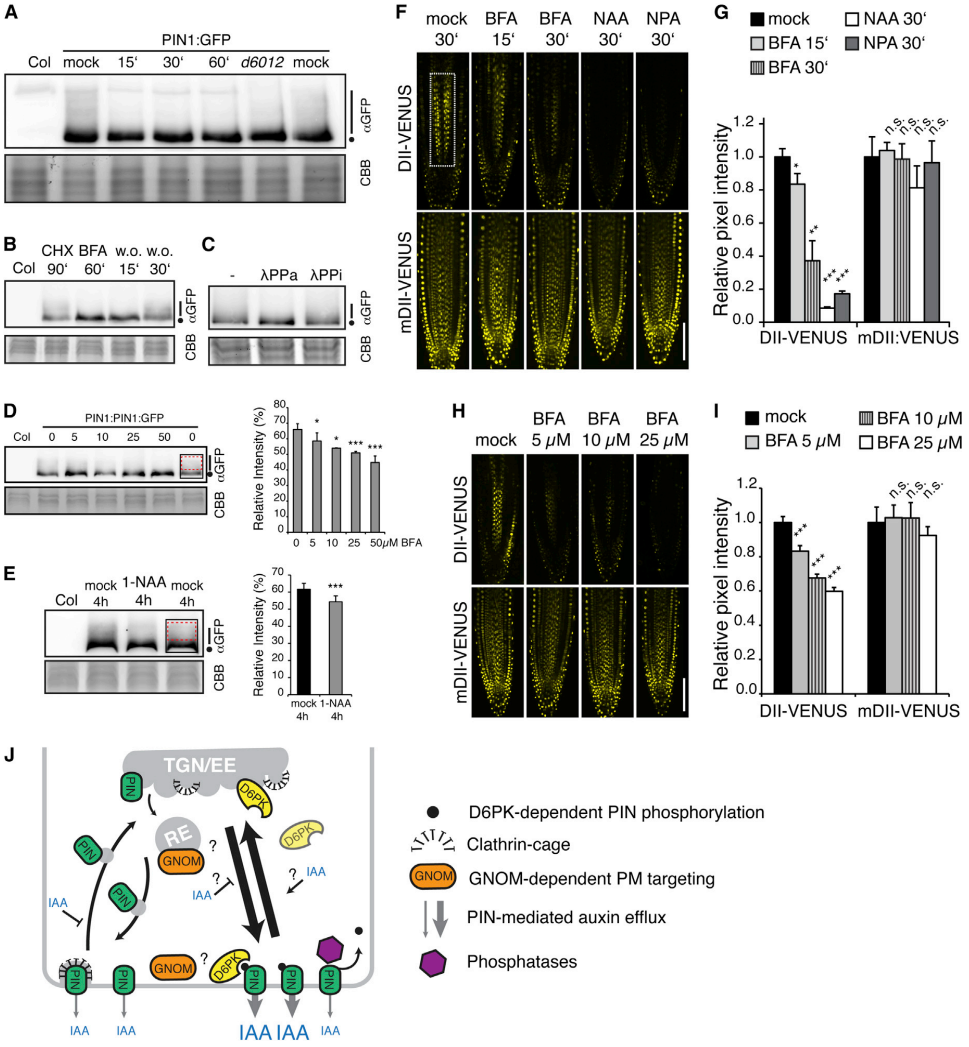

Figure 7. Dynamic Control of PIN1 Phosphorylation in *Arabidopsis* Roots by D6PK at the Plasma Membrane

(A–E) Representative immunoblots of PIN1:GFP as detected with αGFP of total protein extracts obtained from roots of 8-day-old light-grown seedlings. Results with extracts obtained from seedlings after mock-, BFA (50 μM)-, or BFA washout (w.o.)-treatment, performed in the presence of CHX (50 μM) for the periods of time specified in the figure (A and B). In (C), extracts were treated for 15 min with active (λPPa) or heat-inactivated λ-phosphatase (λPPi). CBB, Coomassie Brilliant Blue, loading control. Seedlings were treated with mock solution and 5 - 50 μM BFA for 60 min (D) or with mock solution and 10 μM 1-NAA of 4 hr (E). The relative PIN1 phosphorylation was determined as the ratio of total pixel intensities from the lower mobility forms (red dotted square) to the total PIN1:GFP (black square) from at least three independent replicate experiments (left images in D and E). The averages and standard deviations are presented (right panels in D and E). Student's t test *0.01 < p < 0.05; ** 0.01 ≥ p. The closed dot marks the lower band, presumably de- or unphosphorylated form(s) of PIN1:GFP, the line marks phosphorylated PIN1:GFP.

(F–I) Representative confocal images of root meristems of 6 day-old seedlings expressing the auxin-sensitive reporter DII-VENUS or its auxin-insensitive counterpart mDII-VENUS, treated for 30 min with mock, 1-NAA (10 μM), and NPA (50 μM) or for 15 min or 30 min with BFA (50 μM) as specified in the figure (F); and treated for 60 min with mock, 5–50 μM BFA (H). Scale bar represents 100 μm. (G and I) Relative signal intensities in the stele region of seedlings after the experiments shown in (F) and (H), respectively, and as marked by a rectangle in the first image in (F). The experiments were repeated three times, shown are the averages and standard errors of one replicate measurement (n ≥ 6; G) and of three replicate measurements (n ≥ 16; I). Student's t test *0.05 > p > 0.01; **0.01 > p > 0.001; ***p < 0.001; n.s., not significant.

(legend continued on next page)

Please cite this article in press as: Barbosa et al., D6 PROTEIN KINASE Activates Auxin Transport-Dependent Growth and PIN-FORMED Phosphorylation at the Plasma Membrane, Developmental Cell (2014), http://dx.doi.org/10.1016/j.devcel.2014.05.006

Developmental Cell

D6PK Activates PINs at the Plasma Membrane

CellPress

Because these findings could potentially also be explained by an inactivation of D6PK kinase function after BFA treatment, we tested the activity of immunoprecipitated YFP:D6PK before and after BFA treatment using recombinant PIN1 as a substrate. However, this experiment indicated that D6PK remains an active protein kinase after BFA treatment, at least when examined in vitro (Figure S7).

To further confirm the dependency of PIN1 phosphorylation on D6PK abundance at the plasma membrane in experimental conditions that avoided the use of BFA, we also tested whether prolonged 1-NAA treatment (4 hr), which leads to partial internalization of D6PK (Figure 4), would affect PIN phosphorylation. Interestingly, also auxin treatments negatively affected PIN1:GFP phosphorylation, thus providing another piece of evidence that the phosphorylation of PIN1:GFP in planta correlates with the abundance of D6PK at the plasma membrane (Figure 7E).

To understand whether the rapid changes in PIN1 phosphorylation also affect the cellular distribution and accumulation of auxin within the root, we followed the abundance of the dynamic auxin-sensitive reporter DII-VENUS and its auxin-insensitive counterpart mDII-VENUS (Brunoud et al., 2012). Interestingly, DII-VENUS abundance in the root decreased over time after BFA treatment (Figures 7F and 7G). Similar responses were obtained after auxin (1-NAA) treatment but also after NPA treatment, suggesting that the inhibition of auxin transport by NPA may lead to a cellular accumulation of auxin that is sufficient to trigger DII-VENUS degradation (Figures 7F and 7G). Surprisingly, we could detect a significant reduction of DII-VENUS in stele cells with BFA concentrations as low as 5 μM (Figures 7H and 7I), concentrations at which we could not detect any effects on PIN1:GFP localization (Figure S2B). Although we cannot rule out that BFA-induced internalization of PINs or other relevant proteins contribute to the observed effects on DII-VENUS abundance, the fast kinetics and high sensitivity of this response can best be explained by an accumulation of auxin as a consequence of the dissociation of D6PK from the plasma membrane followed by a reduction of PIN phosphorylation and consequently auxin export.

DISCUSSION

Our study identifies the AGCVIII protein kinase D6PK as a basal polarity marker that rapidly cycles to and from the plasma membrane. The respective targeting mechanisms are largely distinct from the mechanisms that control polar targeting of PINs, the proposed D6PK phosphorylation substrates. Furthermore, we can show that D6PK plasma membrane localization is essential to establish and maintain PIN phosphorylation and auxin transport-dependent plant growth.

We had previously found that *d6pk* mutants are defective in negative gravitropism and phototropism and that these defects correlate with reductions in PIN3 phosphorylation and basipetal auxin transport (Willige et al., 2013; Zourelidou et al., 2009). Based on the differential BFA-sensitivities of D6PK and PINs, we could now differentially manipulate the abundance of D6PK and PINs at the plasma membrane. Using selected genetic backgrounds, we show that the presence and absence of D6PK at the plasma membrane directly correlates with changes in PIN protein phosphorylation and auxin distribution that may reflect changes in PIN-dependent auxin efflux. Importantly, because we could predictably manipulate plant growth with BFA in a D6PK- and GN-dependent manner and it has previously been shown that the PIN phosphorylating kinase PID is BFA-insensitive (Kleine-Vehn et al., 2009), we propose that one or more D6PK family members control these processes. Because D6PK phosphorylates PINs only when at the plasma membrane, PIN phosphorylation is only transient and most likely antagonized by phosphatases, and PIN phosphorylation levels correlate with auxin distribution and auxin transport-dependent processes, we predict that PINs are only active when phosphorylated by D6PKs or related kinases at the plasma membrane.

D6PK polar targeting to the plasma membrane differs from the targeting of its proposed PIN substrates in a number of ways. First, D6PK is more sensitive to the trafficking inhibitor BFA than the three PIN proteins tested. Second, in comparison to the PINs, D6PK also showed a faster retargeting to the plasma membrane after BFA washout treatments. Third, while it had previously been shown that the polar targeting of de novo synthesized PINs to the plasma membrane is preceded by their initial nonpolar targeting (Dhonukshe et al., 2008, 2010), we found that the polar targeting of D6PK to the basal plasma membrane is immediate and direct. Fourth, whereas PIN polarity shifts had previously been reported in weak *gnom* mutants (Ikeda et al., 2009; Kleine-Vehn and Friml, 2008; Kleine-Vehn et al., 2009), the partial loss-of-function mutation $gnom^{B/E}$ leads to partial internalization and partial but basal plasma membrane-targeted localization of D6PK. Finally, whereas PINs are mainly plasma membrane-localized also in weak *gnom* mutants, a large fraction of D6PK remained associated with apparent endosomes in $gnom^{B/E}$. This suggests that the targeting of D6PK from endosomes to the plasma membrane is more sensitive to GN function than that of the PINs. Thus, D6PK plasma membrane polar targeting differs from PIN trafficking regarding its kinetics, its trafficking, and its GN-dependency.

(J) Model for the plasma membrane polar targeting and role of D6PK in the context of PIN-mediated auxin transport regulation. D6PK is a mostly membrane-associated protein localizing to the basal plasma membrane where it activates PIN auxin-efflux carriers. D6PK promotes PIN activity and auxin transport-dependent growth presumably by direct PIN phosphorylation and most likely antagonized by phosphatases. The plasma membrane localization of both, D6PKs and PINs, is controlled by the trafficking regulator GN and both proteins constitutively recycle between the plasma membrane and endosomes. D6PK recycling has much faster kinetics than the PINs and is independent from PIN trafficking, as indicated by the differential width of the arrows. Whereas clathrin-mediated endocytosis controls PIN internalization and GN controls PIN targeting from recycling endosomes to the plasma membrane, the exact molecular mechanisms for the control of the clathrin-independent internalization of D6PK and GN-dependent D6PK plasma membrane targeting remains to be elucidated. Auxin alters the intracellular D6PK distribution, either by inducing D6PK internalization or by blocking D6PK targeting to the plasma membrane. The dynamics of D6PK recycling and its susceptibility to auxin suggests that this process is highly regulated and essential for the control of PIN-mediated auxin transport between cells and tissues.

See also Figure S7.

Please cite this article in press as: Barbosa et al., D6 PROTEIN KINASE Activates Auxin Transport-Dependent Growth and PIN-FORMED Phosphorylation at the Plasma Membrane, Developmental Cell (2014), http://dx.doi.org/10.1016/j.devcel.2014.05.006

GN is thought to act as an activator of ARF-GTPases at early endosomes or recycling endosomes where GN mediates budding events for the targeting and recycling of plasma membrane proteins (Anders and Jürgens, 2008; D'Souza-Schorey and Chavrier, 2006; Geldner et al., 2003; Nielsen et al., 2012; Tanaka et al., 2009). Our observation that BFA promotes a rapid and complete dissociation of D6PK from the plasma membrane to the cytoplasm and to endomembrane compartments suggests a very direct effect of GN on D6PK localization. This effect is certainly faster than the known BFA-imposed inhibition of GN for the recycling of plasma membrane proteins. Along the same lines, the accumulation of D6PK in endosomal compartments in *gnom*$^{B/E}$ could be either explained by a reduced but not fully impaired GN function leading to an alternative targeting of D6PK to endomembranes or by partial blockage of D6PK transport from the TGN to the plasma membrane. In both cases, we hypothesize that the impaired GN function would result in the lack of a D6PK-recruiting factor at the plasma membrane. Whereas additional evidence points to a role for GN in the control of endocytosis at the plasma membrane (Irani et al., 2012; Naramoto et al., 2010), our findings do not support such a role for GN in the case of D6PK because we do not observe a stabilization of D6PK at the plasma membrane when inhibiting GN by BFA or in *gnom*$^{B/E}$. Our data, however, suggest that GN can act in the targeting of plasma membrane-associated proteins in a manner that is much faster and sensitive than what has previously been reported for integral plasma membrane proteins. The elucidation of the exact molecular mechanism underlying such targeting might unravel yet-unknown ARF-GEF-dependent targeting mechanisms.

We found no evidence for D6PK being endocytosed by clathrin-mediated pathways. However, the rapid appearance of D6PK at CLC-labeled endosomes, presumably at the TGN (Ito et al., 2012), and our biochemical fractionation experiments suggest that D6PK resides constitutively on membranes. These observations indicate that D6PK is rapidly recruited from the plasma membrane to endosomes through an as-yet-unknown mechanism. We hypothesize that D6PK is either transported via a vesicle-mediated process or recruited by as-yet-unknown but GN-regulated factors to endomembranes or the plasma membrane (Figure 7J).

As part of our attempts to inhibit D6PK endocytosis by 1-NAA, we noted with interest that auxin might have an effect on the distribution of D6PK within the cell. Here, we could distinguish short-term and long-term effects, which, intriguingly, were not uniform between different seedlings examined. Based on these observations, we speculate that auxin may be part of a feedback mechanism that controls D6PK distribution within the cell, e.g., to control auxin fluxes within the plant. This finding may thus add a role for auxin in the control of PIN regulatory kinases and it thereby expands the previously known repertoire of auxin effects on controlling PIN trafficking (Robert et al., 2010), PIN degradation (Abas et al., 2006; Baster et al., 2013), and PIN polarity (Sauer et al., 2006).

In addition, the AGCVIII kinases phot1 and phot2 as well as the PID/WAGs reside at the plasma membrane and were previously observed in endomembrane compartments, suggesting that these structurally related kinases traffic via vesicular transport pathways (Dhonukshe et al., 2010; Kaiserli et al., 2009). Interestingly, the mechanisms for the regulation and the trafficking of these kinases are distinct: First, D6PK is not trafficking by clathrin-mediated endocytosis as reported for phot1 (Kaiserli et al., 2009; Kong et al., 2006). Second, in contrast to D6PK, PID trafficking was reported to be BFA insensitive (Kleine-Vehn et al., 2009). Additionally, we show that there is also no evidence for an interdependency of the respective kinases because PID, as a regulator of PIN polarity (Dhonukshe et al., 2010; Friml et al., 2004; Huang et al., 2010; Li et al., 2011), does not affect D6PK polarity and because PID cannot phosphorylate D6PK. Furthermore, we previously showed that phot kinase signaling is independent from D6PK (Ding et al., 2011; Willige et al., 2013). We thus suggest that the plasma membrane abundance of the different AGCVIII kinases is controlled by independent transport mechanisms and that their functions are not interrelated.

In summary, we propose that the abundance of the fast cycling D6PK critically determines PIN phosphorylation, PIN activity, and auxin transport at the plasma membrane (Figure 7J). Accordingly, D6PK and functionally homologous kinases such as D6PKL1 - D6PK3 are key regulators of PIN-mediated auxin efflux. Additionally, auxin may have an effect on the distribution of D6PK and related kinases and this may represent a sensitive way to reversibly control the activity of PIN-mediated auxin efflux. Previous studies have described the modeling of auxin- and auxin transport-dependent plant growth based on the knowledge of the asymmetric distribution of PINs and the regulatory mechanisms controlling their asymmetric distribution (Band et al., 2012; Bayer et al., 2009; Grieneisen et al., 2007; Hosek et al., 2012; Jönsson et al., 2006; Laskowski et al., 2008; van Berkel et al., 2013). Based on our findings, future models have to take into account the presence of regulatory AGCVIII kinases at the plasma membrane, not only as regulators of PIN polarity but also as critical regulators of PIN activity.

EXPERIMENTAL PROCEDURES

Confocal Microscopy

Confocal microscopy was performed using an Olympus FV1000/IX81 laser scanning confocal microscope (Olympus, Hamburg, Germany). For FM4-64 staining, seedlings were stained in liquid media with 2 μM FM4-64. The respective staining regimes are specified in the figure legends. To follow the short-term response to BFA and to minimize movement of the sample, the seedlings were mounted on slides between two strips of double-sided Scotch tape containing the respective media. The root was covered with a coverslip and a drop of media was applied to the cotyledons to avoid drying-out. After focusing, the BFA responses were recorded in a movie with a scanning frequency of 30–60 s per frame. Frame 1 of each movie was considered as the beginning of the treatment (t = 0), which corresponded to a technical delay of approximately 1 min after placing the seedling on the slide immersed in the respective media. Signal quantifications were performed using the Olympus FV1000 software and Fiji (Schindelin et al., 2012) as specified in the respective figure legends.

Immunostaining was performed with an InsituPro Vsi (Intavis) robot as previously described (Sauer et al., 2006) using roots of 6-day-old 35S:YFP:D6PK or 35S:YFP:D6PK 35S:PID seedlings and the following antibody dilutions: mouse anti-GFP (1:300; Roche), rabbit anti-PIN1 (1:500; Paciorek et al., 2005), anti-rabbit Cy3 (1:500; Dianova), and anti-mouse Alexa 488 (1:500; Dianova).

Immunoblot Analyses

For the subcellular fractionation after BFA treatment, roots of 7-day-old seedlings were treated with 50 μM BFA in liquid media or the correspondent amount

Please cite this article in press as: Barbosa et al., D6 PROTEIN KINASE Activates Auxin Transport-Dependent Growth and PIN-FORMED Phosphorylation at the Plasma Membrane, Developmental Cell (2014), http://dx.doi.org/10.1016/j.devcel.2014.05.006

Developmental Cell

D6PK Activates PINs at the Plasma Membrane

CellPress

of solvent and then dissected and frozen. Subsequently, roots were homogenized with PEB (50 mM Tris-HCl, pH 7.5, 150 mM NaCl, 0.1 mM MG132, 0.1 mM PMSF, 1% (v/v) Protease inhibitor cocktail; Sigma; and PhosStop phosphatase inhibitor cocktail; Roche). After homogenization, extracts were centrifuged at 10,000 × *g* and the supernatant was subsequently ultracentrifuged at 100,000 × *g*. The resulting supernatant (soluble fraction) was collected and the pellet (membrane fraction) was resuspended in the same volume of PEB supplemented with 1% Triton X-100 and dissolved by shaking on an orbital shaker at 4°C. After heat denaturation at 42°C in 1× Laemmli Buffer, the equivalent of 10 μg total protein was separated on 10% SDS-PAGE gels and transferred onto nitrocellulose. The blots were probed with anti-GFP (1:3,000; LifeTechnologies) for YFP:D6PK, anti-UGPase (1:3,000; Agrisera) as a soluble protein control and plasma membrane H^+-ATPase (AHA2) as membrane protein control (1:4,000; a gift from Toshinori Kinoshita, Nagoya University, Japan).

For PIN3 immunoblots, membrane protein extracts were prepared as previously described (Willige et al., 2013). The equivalent of 10 μg total protein was separated on 10% SDS-PAGE gels and transferred to nitrocellulose. The blots were probed with anti-PIN3 (1:3,000; Nottingham *Arabidopsis* Stock Centre). Coomassie brilliant blue staining was used to control for equal loading.

All treatments for the detection of phosphorylated forms of PIN1:GFP after BFA and after BFA washout were performed in the presence of CHX (50 μM). The equivalent of 10 μg total protein was separated on 10% SDS-PAGE gels and transferred to nitrocellulose. The blots were probed with anti-GFP (1:3,000; Life Technologies). Dephosphorylation of PIN1:GFP was performed with λ phosphatase (λPP; New England Biolabs) by incubating 350 U λPPase with 30 μg total protein extract for 15 min at room temperature. Heat inactivated (98°C for 5 min) λPPase was used as a negative control. The dephosphorylation reaction was stopped by the addition of 5× Laemmli buffer. Coomassie brilliant blue staining was used to control for equal loading. Chemiluminescence detection was performed with a Fujifil LAS 4000 mini (Fuji) and signal quantifications were performed as specified in the respective figure legends using the Fujifilm Multi Gauge v3.0 software.

Additional information is available in the Supplemental Experimental Procedures.

SUPPLEMENTAL INFORMATION

Supplemental Information includes Supplemental Experimental Procedures and seven figures and can be found with this article online at http://dx.doi.org/10.1016/j.devcel.2014.05.006.

ACKNOWLEDGMENTS

We thank Markus Grebe (University of Potsdam, Germany) and Erika Isono (Technische Universität München, Germany) for critical reading of the manuscript and Markus Grebe, Erika Isono, Jürgen Kleine-Vehn (Vienna, Austria), and Niko Geldner (Lausanne, Switzerland) for providing important comments throughout this project. Jutta Elgner and Deborah Schnell are thanked for their technical support. This work was supported by a fellowship from the Fundação para a Ciência e a Tecnologia (FCT) to I.C.R.B. (SFRH/BD/73187/2010) and a grant from the Deutsche Forschungsgemeinschaft (SCHW751/8-1) to C.S.

Received: November 11, 2013
Revised: March 20, 2014
Accepted: May 9, 2014
Published: June 12, 2014

REFERENCES

Abas, L., Benjamins, R., Malenica, N., Paciorek, T., Wiśniewska, J., Moulinier-Anzola, J.C., Sieberer, T., Friml, J., and Luschnig, C. (2006). Intracellular trafficking and proteolysis of the Arabidopsis auxin-efflux facilitator PIN2 are involved in root gravitropism. Nat. Cell Biol. *8*, 249–256.

Anders, N., and Jürgens, G. (2008). Large ARF guanine nucleotide exchange factors in membrane trafficking. Cell. Mol. Life Sci. *65*, 3433–3445.

Anders, N., Nielsen, M., Keicher, J., Stierhof, Y.D., Furutani, M., Tasaka, M., Skriver, K., and Jürgens, G. (2008). Membrane association of the Arabidopsis ARF exchange factor GNOM involves interaction of conserved domains. Plant Cell *20*, 142–151.

Band, L.R., Wells, D.M., Larrieu, A., Sun, J., Middleton, A.M., French, A.P., Brunoud, G., Sato, E.M., Wilson, M.H., Péret, B., et al. (2012). Root gravitropism is regulated by a transient lateral auxin gradient controlled by a tipping-point mechanism. Proc. Natl. Acad. Sci. USA *109*, 4668–4673.

Baster, P., Robert, S., Kleine-Vehn, J., Vanneste, S., Kania, U., Grunewald, W., De Rybel, B., Beeckman, T., and Friml, J. (2013). SCF(TIR1/AFB)-auxin signalling regulates PIN vacuolar trafficking and auxin fluxes during root gravitropism. EMBO J. *32*, 260–274.

Bayer, E.M., Smith, R.S., Mandel, T., Nakayama, N., Sauer, M., Prusinkiewicz, P., and Kuhlemeier, C. (2009). Integration of transport-based models for phyllotaxis and midvein formation. Genes Dev. *23*, 373–384.

Benková, E., Michniewicz, M., Sauer, M., Teichmann, T., Seifertová, D., Jürgens, G., and Friml, J. (2003). Local, efflux-dependent auxin gradients as a common module for plant organ formation. Cell *115*, 591–602.

Briggs, W.R., and Huala, E. (1999). Blue-light photoreceptors in higher plants. Annu. Rev. Cell Dev. Biol. *15*, 33–62.

Brodsky, F.M., Chen, C.Y., Knuehl, C., Towler, M.C., and Wakeham, D.E. (2001). Biological basket weaving: formation and function of clathrin-coated vesicles. Annu. Rev. Cell Dev. Biol. *17*, 517–568.

Brunoud, G., Wells, D.M., Oliva, M., Larrieu, A., Mirabet, V., Burrow, A.H., Beeckman, T., Kepinski, S., Traas, J., Bennett, M.J., and Vernoux, T. (2012). A novel sensor to map auxin response and distribution at high spatio-temporal resolution. Nature *482*, 103–106.

D'Souza-Schorey, C., and Chavrier, P. (2006). ARF proteins: roles in membrane traffic and beyond. Nat. Rev. Mol. Cell Biol. *7*, 347–358.

Dhonukshe, P., Aniento, F., Hwang, I., Robinson, D.G., Mravec, J., Stierhof, Y.D., and Friml, J. (2007). Clathrin-mediated constitutive endocytosis of PIN auxin efflux carriers in Arabidopsis. Curr. Biol. *17*, 520–527.

Dhonukshe, P., Grigoriev, I., Fischer, R., Tominaga, M., Robinson, D.G., Hasek, J., Paciorek, T., Petrásek, J., Seifertová, D., Tejos, R., et al. (2008). Auxin transport inhibitors impair vesicle motility and actin cytoskeleton dynamics in diverse eukaryotes. Proc. Natl. Acad. Sci. USA *105*, 4489–4494.

Dhonukshe, P., Huang, F., Galvan-Ampudia, C.S., Mähönen, A.P., Kleine-Vehn, J., Xu, J., Quint, A., Prasad, K., Friml, J., Scheres, B., and Offringa, R. (2010). Plasma membrane-bound AGC3 kinases phosphorylate PIN auxin carriers at TPRXS(N/S) motifs to direct apical PIN recycling. Development *137*, 3245–3255.

Ding, Z., Galván-Ampudia, C.S., Demarsy, E., Łangowski, Ł., Kleine-Vehn, J., Fan, Y., Morita, M.T., Tasaka, M., Fankhauser, C., Offringa, R., and Friml, J. (2011). Light-mediated polarization of the PIN3 auxin transporter for the phototropic response in Arabidopsis. Nat. Cell Biol. *13*, 447–452.

Friml, J., Wiśniewska, J., Benková, E., Mendgen, K., and Palme, K. (2002). Lateral relocation of auxin efflux regulator PIN3 mediates tropism in Arabidopsis. Nature *415*, 806–809.

Friml, J., Yang, X., Michniewicz, M., Weijers, D., Quint, A., Tietz, O., Benjamins, R., Ouwerkerk, P.B., Ljung, K., Sandberg, G., et al. (2004). A PINOID-dependent binary switch in apical-basal PIN polar targeting directs auxin efflux. Science *306*, 862–865.

Galván-Ampudia, C.S., and Offringa, R. (2007). Plant evolution: AGC kinases tell the auxin tale. Trends Plant Sci. *12*, 541–547.

Gälweiler, L., Guan, C., Müller, A., Wisman, E., Mendgen, K., Yephremov, A., and Palme, K. (1998). Regulation of polar auxin transport by AtPIN1 in Arabidopsis vascular tissue. Science *282*, 2226–2230.

Geldner, N., Friml, J., Stierhof, Y.D., Jürgens, G., and Palme, K. (2001). Auxin transport inhibitors block PIN1 cycling and vesicle trafficking. Nature *413*, 425–428.

Geldner, N., Anders, N., Wolters, H., Keicher, J., Kornberger, W., Müller, P., Delbarre, A., Ueda, T., Nakano, A., and Jürgens, G. (2003). The Arabidopsis GNOM ARF-GEF mediates endosomal recycling, auxin transport, and auxin-dependent plant growth. Cell *112*, 219–230.

Please cite this article in press as: Barbosa et al., D6 PROTEIN KINASE Activates Auxin Transport-Dependent Growth and PIN-FORMED Phosphorylation at the Plasma Membrane, Developmental Cell (2014), http://dx.doi.org/10.1016/j.devcel.2014.05.006

Geldner, N., Richter, S., Vieten, A., Marquardt, S., Torres-Ruiz, R.A., Mayer, U., and Jürgens, G. (2004). Partial loss-of-function alleles reveal a role for GNOM in auxin transport-related, post-embryonic development of Arabidopsis. Development *131*, 389–400.

Grieneisen, V.A., Xu, J., Marée, A.F., Hogeweg, P., and Scheres, B. (2007). Auxin transport is sufficient to generate a maximum and gradient guiding root growth. Nature *449*, 1008–1013.

Hosek, P., Kubes, M., Lanková, M., Dobrev, P.I., Klíma, P., Kohoutová, M., Petrásek, J., Hoyerová, K., Jirina, M., and Zazímalová, E. (2012). Auxin transport at cellular level: new insights supported by mathematical modelling. J. Exp. Bot. *63*, 3815–3827.

Huang, F., Zago, M.K., Abas, L., van Marion, A., Galván-Ampudia, C.S., and Offringa, R. (2010). Phosphorylation of conserved PIN motifs directs Arabidopsis PIN1 polarity and auxin transport. Plant Cell *22*, 1129–1142.

Ikeda, Y., Men, S., Fischer, U., Stepanova, A.N., Alonso, J.M., Ljung, K., and Grebe, M. (2009). Local auxin biosynthesis modulates gradient-directed planar polarity in Arabidopsis. Nat. Cell Biol. *11*, 731–738.

Irani, N.G., Di Rubbo, S., Mylle, E., Van den Begin, J., Schneider-Pizoń, J., Hniliková, J., Šíša, M., Buyst, D., Vilarrasa-Blasi, J., Szatmári, A.M., et al. (2012). Fluorescent castasterone reveals BRI1 signaling from the plasma membrane. Nat. Chem. Biol. *8*, 583–589.

Ito, E., Fujimoto, M., Ebine, K., Uemura, T., Ueda, T., and Nakano, A. (2012). Dynamic behavior of clathrin in Arabidopsis thaliana unveiled by live imaging. Plant J. *69*, 204–216.

Jönsson, H., Heisler, M.G., Shapiro, B.E., Meyerowitz, E.M., and Mjolsness, E. (2006). An auxin-driven polarized transport model for phyllotaxis. Proc. Natl. Acad. Sci. USA *103*, 1633–1638.

Kaiserli, E., Sullivan, S., Jones, M.A., Feeney, K.A., and Christie, J.M. (2009). Domain swapping to assess the mechanistic basis of Arabidopsis phototropin 1 receptor kinase activation and endocytosis by blue light. Plant Cell *21*, 3226–3244.

Kitakura, S., Vanneste, S., Robert, S., Löfke, C., Teichmann, T., Tanaka, H., and Friml, J. (2011). Clathrin mediates endocytosis and polar distribution of PIN auxin transporters in Arabidopsis. Plant Cell *23*, 1920–1931.

Kleine-Vehn, J., and Friml, J. (2008). Polar targeting and endocytic recycling in auxin-dependent plant development. Annu. Rev. Cell Dev. Biol. *24*, 447–473.

Kleine-Vehn, J., Huang, F., Naramoto, S., Zhang, J., Michniewicz, M., Offringa, R., and Friml, J. (2009). PIN auxin efflux carrier polarity is regulated by PINOID kinase-mediated recruitment into GNOM-independent trafficking in Arabidopsis. Plant Cell *21*, 3839–3849.

Kong, S.G., Suzuki, T., Tamura, K., Mochizuki, N., Hara-Nishimura, I., and Nagatani, A. (2006). Blue light-induced association of phototropin 2 with the Golgi apparatus. Plant J. *45*, 994–1005.

Laskowski, M., Grieneisen, V.A., Hofhuis, H., Hove, C.A., Hogeweg, P., Marée, A.F., and Scheres, B. (2008). Root system architecture from coupling cell shape to auxin transport. PLoS Biol. *6*, e307.

Li, Y., Dai, X., Cheng, Y., and Zhao, Y. (2011). NPY genes play an essential role in root gravitropic responses in Arabidopsis. Mol. Plant *4*, 171–179.

Liu, S.H., Marks, M.S., and Brodsky, F.M. (1998). A dominant-negative clathrin mutant differentially affects trafficking of molecules with distinct sorting motifs in the class II major histocompatibility complex (MHC) pathway. J. Cell Biol. *140*, 1023–1037.

Michniewicz, M., Zago, M.K., Abas, L., Weijers, D., Schweighofer, A., Meskiene, I., Heisler, M.G., Ohno, C., Zhang, J., Huang, F., et al. (2007). Antagonistic regulation of PIN phosphorylation by PP2A and PINOID directs auxin flux. Cell *130*, 1044–1056.

Müller, A., Guan, C., Gälweiler, L., Tänzler, P., Huijser, P., Marchant, A., Parry, G., Bennett, M., Wisman, E., and Palme, K. (1998). AtPIN2 defines a locus of Arabidopsis for root gravitropism control. EMBO J. *17*, 6903–6911.

Naramoto, S., Kleine-Vehn, J., Robert, S., Fujimoto, M., Dainobu, T., Paciorek, T., Ueda, T., Nakano, A., Van Montagu, M.C., Fukuda, H., and Friml, J. (2010). ADP-ribosylation factor machinery mediates endocytosis in plant cells. Proc. Natl. Acad. Sci. USA *107*, 21890–21895.

Nielsen, M.E., Feechan, A., Böhlenius, H., Ueda, T., and Thordal-Christensen, H. (2012). Arabidopsis ARF-GTP exchange factor, GNOM, mediates transport required for innate immunity and focal accumulation of syntaxin PEN1. Proc. Natl. Acad. Sci. USA *109*, 11443–11448.

Paciorek, T., Zazímalová, E., Ruthardt, N., Petrásek, J., Stierhof, Y.D., Kleine-Vehn, J., Morris, D.A., Emans, N., Jürgens, G., Geldner, N., and Friml, J. (2005). Auxin inhibits endocytosis and promotes its own efflux from cells. Nature *435*, 1251–1256.

Pearce, L.R., Komander, D., and Alessi, D.R. (2010). The nuts and bolts of AGC protein kinases. Nat. Rev. Mol. Cell Biol. *11*, 9–22.

Rademacher, E.H., and Offringa, R. (2012). Evolutionary Adaptations of Plant AGC Kinases: From Light Signaling to Cell Polarity Regulation. Front. Plant Sci. *3*, 250.

Robert, S., Kleine-Vehn, J., Barbez, E., Sauer, M., Paciorek, T., Baster, P., Vanneste, S., Zhang, J., Simon, S., Čovanová, M., et al. (2010). ABP1 mediates auxin inhibition of clathrin-dependent endocytosis in Arabidopsis. Cell *143*, 111–121.

Robinson, D.G., Langhans, M., Saint-Jore-Dupas, C., and Hawes, C. (2008). BFA effects are tissue and not just plant specific. Trends Plant Sci. *13*, 405–408.

Sabatini, S., Beis, D., Wolkenfelt, H., Murfett, J., Guilfoyle, T., Malamy, J., Benfey, P., Leyser, O., Bechtold, N., Weisbeek, P., and Scheres, B. (1999). An auxin-dependent distal organizer of pattern and polarity in the Arabidopsis root. Cell *99*, 463–472.

Sauer, M., Balla, J., Luschnig, C., Wisniewska, J., Reinöhl, V., Friml, J., and Benková, E. (2006). Canalization of auxin flow by Aux/IAA-ARF-dependent feedback regulation of PIN polarity. Genes Dev. *20*, 2902–2911.

Schindelin, J., Arganda-Carreras, I., Frise, E., Kaynig, V., Longair, M., Pietzsch, T., Preibisch, S., Rueden, C., Saalfeld, S., Schmid, B., et al. (2012). Fiji: an open-source platform for biological-image analysis. Nat. Methods *9*, 676–682.

Tanaka, H., Kitakura, S., De Rycke, R., De Groodt, R., and Friml, J. (2009). Fluorescence imaging-based screen identifies ARF GEF component of early endosomal trafficking. Curr. Biol. *19*, 391–397.

Teale, W.D., Paponov, I.A., and Palme, K. (2006). Auxin in action: signalling, transport and the control of plant growth and development. Nat. Rev. Mol. Cell Biol. *7*, 847–859.

van Berkel, K., de Boer, R.J., Scheres, B., and ten Tusscher, K. (2013). Polar auxin transport: models and mechanisms. Development *140*, 2253–2268.

Willige, B.C., Ahlers, S., Zourelidou, M., Barbosa, I.C., Demarsy, E., Trevisan, M., Davis, P.A., Roelfsema, M.R., Hangarter, R., Fankhauser, C., and Schwechheimer, C. (2013). D6PK AGCVIII kinases are required for auxin transport and phototropic hypocotyl bending in Arabidopsis. Plant Cell *25*, 1674–1688.

Wisniewska, J., Xu, J., Seifertová, D., Brewer, P.B., Ruzicka, K., Blilou, I., Rouquié, D., Benková, E., Scheres, B., and Friml, J. (2006). Polar PIN localization directs auxin flow in plants. Science *312*, 883.

Zádníková, P., Petrásek, J., Marhavy, P., Raz, V., Vandenbussche, F., Ding, Z., Schwarzerová, K., Morita, M.T., Tasaka, M., Hejátko, J., et al. (2010). Role of PIN-mediated auxin efflux in apical hook development of Arabidopsis thaliana. Development *137*, 607–617.

Zourelidou, M., Müller, I., Willige, B.C., Nill, C., Jikumaru, Y., Li, H., and Schwechheimer, C. (2009). The polarly localized D6 PROTEIN KINASE is required for efficient auxin transport in Arabidopsis thaliana. Development *136*, 627–636.

Developmental Cell, Volume *29*
Supplemental Information

D6 PROTEIN KINASE Activates Auxin Transport-Dependent Growth and PIN-FORMED Phosphorylation at the Plasma Membrane

Inês C.R. Barbosa, Melina Zourelidou, Björn C. Willige, Benjamin Weller, and Claus Schwechheimer

Supplemental Information

Supplemental Figure Legends

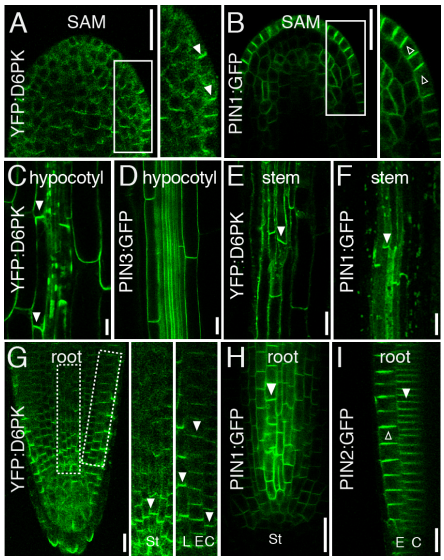

Supplemental Figure S1: D6PK is polarly localized in many tissues and cell types. (A) and **(B)** Confocal images of shoot apical meristems (SAM) from 4 week-old wild type plants grown on NPA [50 μM] to prevent floral meristem differentiation. **(C)** and **(D)** Confocal images of hypocotyl cells of 4 day-old dark-grown seedlings. PIN3:GFP is not polarly distributed in this tissue. **(E)** and **(F)** Confocal images of longitudinal sections of primary inflorescence stems from 4 week-old plants revealing the basal localization of YFP:D6PK (E) and PIN1:GFP (F) in xylem parenchyma cells. **(G)** - **(I)** Confocal optical median sections of 6 day-old primary roots expressing YFP:D6PK (G), PIN1:GFP (H) and PIN2:GFP (I). Smaller panels show magnifications of YFP:D6PK localization in specific cell types: L, lateral root cap; E, epidermis; C, cortex; St, stele. Filled white arrowheads mark the basal,

open white arrowheads mark the apical localization of YFP:D6PK and PIN:GFP proteins. YFP:D6PK localization was analysed in a D6PK:YFP:D6PK *d6pk012* complementation line, with exception of the analyses in hypocotyls (C) and stems (E) where 35S:YFP:D6PK was used due to the very low expression of the D6PK:YFP:D6PK in these tissues. *PIN:GFP* expression is under control of the respective endogenous *PIN* promoters. Scale bars = 20 μm.

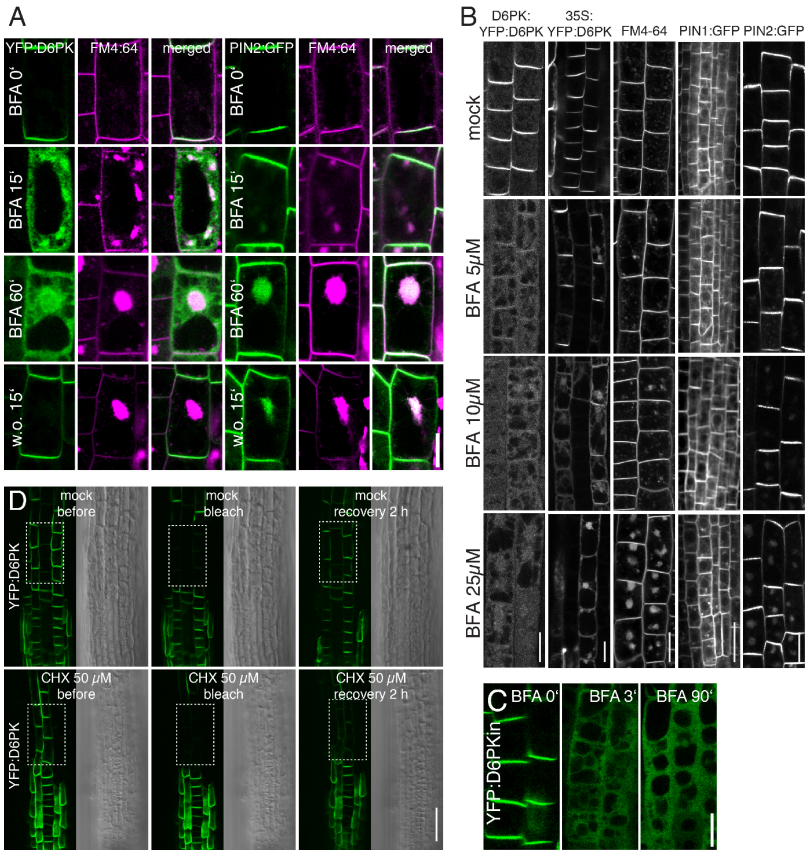

Supplemental Figure S2, related to Figure 1: D6PK accumulates in FM4-64-labeled BFA compartments after BFA treatment. (A) Confocal images from a time course experiment examining the co-localization of YFP:D6PK or PIN2:GFP with FM4-64 before (0 min), after BFA [50µM] treatment (15 and 60 min) and after BFA treatment (60 min) followed by a washout treatment (15 min). Seedlings had been pretreated for 1 hr with CHX [50 μM] and CHX was included in all treatments, seedlings were stained with FM4-64 [2 μM] 15 min

prior to the BFA treatment (BFA 0') and FM4-64 [2 μM] was included in all subsequent treatments. Scale bar = 10 μm. **(B)** The effects of BFA on D6PK are *D6PK* gene-dosage dependent. Confocal images of root epidermis (D6PK:YFP:D6PK, 35S::YFP:D6PK, FM4-64 and PIN2:GFP) and stele cells (PIN1:GFP) of 5-day-old seedlings treated for 60 min with mock and BFA [5 - 25 μM]. FM4-64 [2 μM] was included througout the 60 min treatments. Please note that YFP:D6PK expressed from a D6PK promoter fragment (D6PK:YFP:D6PK) is readily internalized at 5 μM BFA whereas overexpressed YFP:D6PK (35S:YFP:D6PK) is only efficiently internalized at 10 μM BFA. At the same time, the intracellular accumulation of PINs is only discernably at 10 μM BFA in the case of PIN2 and at 25 μM BFA in the case of PIN1. Scale bar = 20 μm. **(C)** YFP:D6PKin, a kinase-dead version of YFP:D6PK, is BFA-sensitive. Confocal images of a kinase-dead YFP:D6PKin in root epidermis cells before and after (3 min, 90 min) BFA [50 μM]-treatment. Scale bar = 20 μm. **(D)** Cycloheximide treatment efficiently blocks *de novo* protein synthesis. Confocal images of 6-day-old seedlings before, after photobleaching and after a 2 hr recovery phase in mock and cycloheximide [50 μM] containning media. Bleaching was performed using the 515 nm laser beam with laser power adjusted ten-fold higher than used for scanning, scanning the ROI area (94 x 55 pixels) in 30 frames with 12.5 μs/pixel speed. Scale bar = 50 μm.

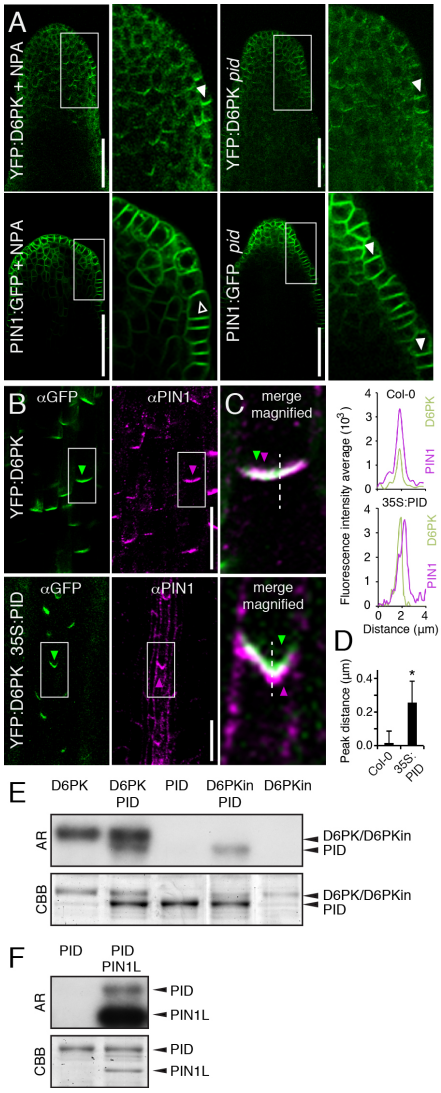

Supplemental Figure S3. D6PK polarity is independent from PID and PID-induced PIN polarity changes. (A) Representative confocal images of shoot apical meristems of 3-week old wild type (Col-0) plants grown in the presence of NPA [50 μM] or *pid* mutants expressing YFP:D6PK (upper panel) or PIN1:GFP (lower panel). Shown is the full view of the meristem and a

magnified view of the framed area from the full view image. Filled white arrowheads mark the basal localization of YFP:D6PK and PIN1:GFP in epidermal cells, open white arrowheads mark the apical localization of PIN1:GFP in epidermal cells of the wild type. Scale bar = 10 μm. **(B)** Results of immunostaining experiments with anti-GFP (YFP:D6PK) and anti-PIN1 of root meristems of 6 day-old 35S:YFP:D6PK (upper panel) and 35S:YFP:D6PK 35S:PID (lower panel) seedlings. Scale bar = 20 μm. **(C)** Merged overlay image of the framed areas from the αGFP and αPIN1 immunostainings shown in (B) and their fluorescence intensity profiles across the distance represented by the dashed white line in the left panels. The colored arrowheads mark the deducted polar distribution of YFP:D6PK (green) and PIN1 (magenta) in the two genetic backgrounds. **(D)** Quantification of the peak distances from fluorescence intensity profiles as shown in (C). Average and standard error; n $\geq$ 52 cells from a total of 9 roots per genotype. Student's t-test, * p = 0.015. 0.2 μm is a distance expected for the distance between two adjacent plasma membranes. **(E)** and **(F)** Representative autoradiographs (AR) and Coomassie Brilliant Blue (CBB)-stained gels (loading controls) from *in vitro* kinase assays with recombinant GST:D6PK, kinase-dead GST:D6PKin and GST:PID. PID autophosphorylation is stimulated in the presence of active or inactive GST:D6PK in the experiments shown in (E), but PID autophosphorylation can also be activated by other proteins such as PIN1 cytoplasmic loop (PIN1L; F).

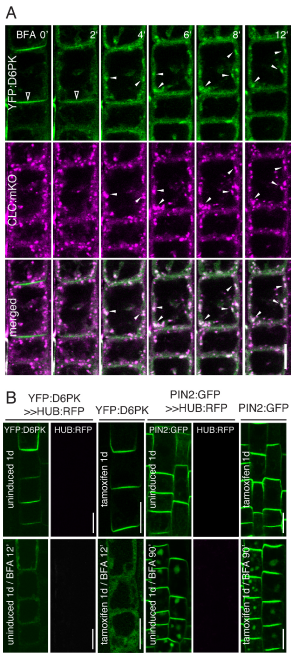

Supplemental Figure S4, related to Figure 3. D6PK colocalizes with clathrin light chain in intracellular compartments. (A) Representative frames from the time series experiment shown in Figure 3 with a transgenic line expressing YFP:D6PK and CLC:mKO after BFA [50 μM]-treatment. Open white arrowheads mark the initial plasma membrane-localized YFP:D6PK, white arrowheads mark the intracellular compartments after BFA treatment that are positive for YFP:D6PK and CLC:mKO. Scale bar = 10 μm. **(B)** Negative control experiments for the experiment shown in Figure 3 (B) and (C), proving that the mock-treated YFP:D6PK>>HUB:RFP and PIN2:GFP>>HUB:RFP are BFA-responsive and that tamoxifen-treatment does not inhibit the response of YFP:D6PK and PIN2:GFP to BFA. Acquisition settings used for RFP channel were the same as in Fig. 3. Scale bar = 20 μm.

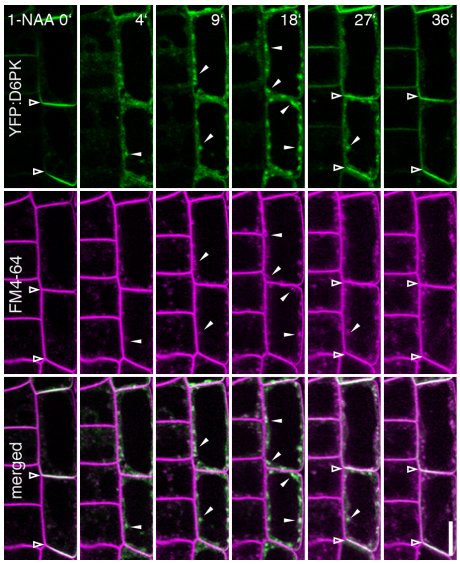

Supplemental Figure S5, related to Figure 4. Auxin modulates the intracellular distribution of D6PK. Representative frames from the time series experiment of Figure 4 of YFP:D6PK seedling roots treated with auxin treatment 1-NAA [10 μM]. The roots were prestained for 15 min with FM4-64 [2 μM]. Open white arrowheads mark the plasma membrane-localized YFP:D6PK, white arrowheads mark the transient intracellular accumulation of the protein, which colocalizes with intracellular FM4-64-labeled compartments. Scale bar = 10 μm.

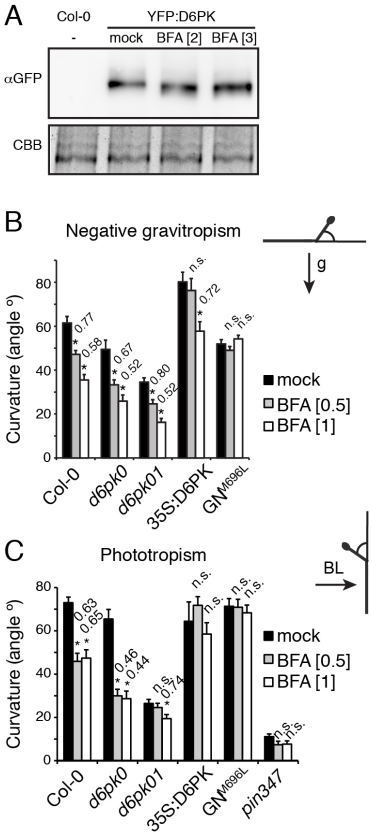

Supplemental Figure S6, related to Figure 5. D6PK abundance is not affected by BFA-treatment. (A) Immunoblot with αGFP to monitor YFP:D6PK abundance in etiolated seedlings grown in the absence (mock) or presence of BFA [2 *μ*M; 3μM]. **(B)** and **(C)** *D6PK* gene dosage affects BFA-sensitivity of tropic responses. Negative gravitropic hypocotyl bending after reorientation by 90º for 20 hrs (B) and hypocotyl phototropic response after 4 hrs of 5 μmol m^{-2} s^{-1} blue light (C) of 3 day-old etiolated seedlings grown on 0.5 μM and 1 μM BFA. Average and standard error; n ≥ 50 seedlings, 3 biological replicates. Student's t-test, * $p < 0.05$, n.s., not significant. Where significant, the effect of the treatment is indicated above the bar as the ratio of

the angles between the BFA-grown seedlings and mock-treated seedlings. Please note that *d6pk* single mutants are hypersensitive to BFA in both assays whereas 35S:D6PK (35S:YFP:D6PK) is insensitive compared to the wild type (Col-0).

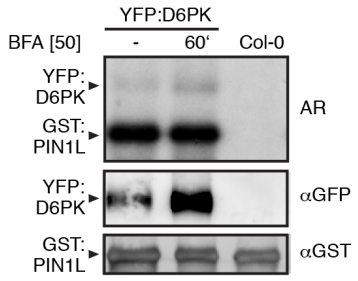

Supplemental Figure S7, related to Figure 7. D6PK activity is not influenced by BFA. Representative autoradiograph (AR), anti-GST and anti-GFP immunoblots (loading controls) from *in vitro* kinase assays with YFP:D6PK immunoprecipitated from 10 day-old seedlings, mock-treated or treated with BFA [50 μM] for 1 hr using recombinant PIN1 cytosolic loop (GST:PIN1L) as a substrate.

was extracted using a protein extraction buffer (PEB) [50 mM Tris-HCl, pH 7.5, 150 mM NaCl, 0.1 mM MG132, 0.1 mM PMSF, 1 % (v/v) Protease inhibitor cocktail (Sigma, Germany), PhosStop phosphatase inhibitor cocktail (Roche, Penzberg, Germany), 0.5% Triton X-100]. 500 µg of protein extract was incubated on ice for 30 min, then the Triton X-100 concentration was diluted to 0.2 %, and 20 µL GFP-Trap beads (ChromoTek, Martinsried, Gemany) were added for 1 hr at 4°C to precipitate YFP:D6PK. After three rounds of washing with extraction buffer containing 0.1 % Triton X-100, the beads with immunoprecipitated YFP:D6PK were resuspended in 20 μl PEB buffer and after quantification of the different samples, 4-7 µl bead suspension was used for phosphorylation experiments as described above.

Supplemental Experimental Procedures

Biological material: The following previously published *Arabidopsis thaliana* mutants and transgenic lines were used: single (*d6pk0*), double (*d6pk01*), and triple (*d6pk012*) mutants of the alleles *d6pk*-1 (*d6pk0*; SALK_061847), *d6pkl1*-1 (*d6pk1*; SALK_056618) and *d6pkl2*-2 (*d6pk2*; SALK_086127) (Zourelidou et al., 2009); 35S:YFP:D6PK and D6PK:YFP:D6PK transgenic lines (Willige et al., 2013; Zourelidou et al., 2009); DR5:GUS, DR5:GUS *d6pk012*; DR5:GUS YFP:D6PK (Sabatini et al., 1999; Zourelidou et al., 2009); DII-VENUS and mDII-VENUS (Brunoud et al., 2012); $gnom^{B/E}$ transheterozygotes of the *gnom* alleles *emb30-1* and *b4049* (Geldner et al., 2004); GN^{wt} and GN^{M696L} transgenic lines expressing BFA-sensitive GNOM-myc and BFA-resistant GNOM M696L-myc, respectively (Geldner et al., 2003); INTAM:HUB (a gift from Jiri Friml) (Dhonukshe et al., 2007; Kitakura et al., 2011); *pinoid* (*pid*) (SALK_049736) (Dhonukshe et al., 2010); *pin3-3, pin4-101*, *pin7-102* triple mutants (*pin347*) (Willige et al., 2013); PIN1:PIN1:GFP (Benkova et al., 2003); PIN2:PIN2:GFP (Abas et al., 2006); PIN3:PIN3:GFP (Zadnikova et al., 2011); 35S:CLC:mKO (mKusabira-Orange; a gift from Jiri Friml) (Naramoto et al., 2010).

35S:PID was obtained by PCR-amplification of the *PID* coding sequence with the primers PID-GW-FW (attB1-TCATGTTACGAGAATCAGACGGT) and PID-GW-RV (attB2-CTC AAAAGTAATCGAACGCCGCTG) followed by cloning into the destination vector p35SGW-MYC using Gateway technology (LifeTechnologies, Carlsbad, CA). *PID* overexpressing lines were obtained by floral dip transformation, selected based on root meristem collapse, a

previously described phenotype of PID overexpressors (Friml et al., 2004), and subsequently crossed with 35S:YFP:D6PK for further studies.

Physiological assays: Unless otherwise stated, seedlings were grown in continuous light (110 μmol m^{-2} s^{-1}) at 21 ºC for 6-7 days on ½ MS [2.15 g/l Murashige and Skoog salts, 0.5 g/l 2- (N-morpholino)ethanesulfonic acid, 8 g/l agar, pH 5.8]. Brefeldin A, cycloheximide and 1-naphthaleneacetic acid (1-NAA) (Sigma, Germany) were dissolved in DMSO to 50 mM, 50 mM and 100 mM stock concentrations and added to the growth media in the indicated concentrations. For mock controls, the same amount of solvent was added to the media. For the 1-NAA endocytosis inhibition experiment, seedlings were grown at 18 ºC because the inhibitory effect of 1-NAA on PIN endocytosis was more stable at this temperature.

For the analysis of phototropism and negative gravitropism, dark-grown seedlings were grown for 3 days on ½ MS containing either BFA [0.5 μM, 1 μM, 2 μM, 3 μM and 5 μM], 1-N-Naphthylphthalamic acid (NPA) [0.5 μM] or the corresponding volume of solvent (mock). For the analysis of negative gravitropism, hypocotyl angles from the vertical axis were measured using the NIH ImageJ software. For phototropism and hypocotyl negative gravitropism response experiments, agravitropically growing seedlings were straightened under safe green light 2 hrs prior to the experiment. For phototropism response experiments, etiolated seedlings were transferred to a FloraLED chamber (CLF Plant Climatics, Wertingen, Germany) and illuminated for 4 hrs with 5 µmol m^{-2} s^{-1} unilateral blue light before plates were scanned for quantification using ImageJ. For the hypocotyl negative gravitropism response

experiments, plates were reoriented by 90º and hypocotyl angles were determined after 20 hrs from scanned plates. For quantification of the wavy hypocotyl growth phenotype of dark-grown 35S:D6PK seedlings, the ratio between the heigth of the hypocotyl, as defined by the distance between the root-hypocotyl junction and the apical hook, and its actual length was calculated.

GUS staining procedures were previously reported (Willige et al., 2013).

Phosphorylation experiments: *In vitro* phosphorylation experiments were carried out using purified recombinant GST:D6PK, GST:PID, kinase-dead GST:D6PKin (K236E) and kinase-dead GST:PIDin (K207E) in combination with purified recombinant protein for the GST:PIN1 cytosolic loop (Zourelidou et al., 2009). GST:PIDin was generated by mutation PCR of GST:PID with the primer [Phos-]GAGATCTGGAGCCTGAAAATATC. The phosphorylation reactions were performed for 60 min at 28°C with recombinant proteins in phosphorylation buffer [25 mM Tris-HCl pH 7.5, 5 mM $MgCl_2$, 0.2 mM EDTA, 50 µM ATP, 1x Complete protease inhibitor cocktail (Roche, Penzberg, Gernany)] supplemented with 10 µCi [γ-^{32}P]ATP (370 MBq, specific activity 185 TBq; Hartmann Analytic, Braunschweig, Germany). The reaction was stopped by adding 5X Laemmli buffer and then separated on a 10% SDS-PAGE. Auto- and trans-phosphorylation were detected by autoradiography, equal protein loading was verified by Coomassie Brilliant Blue-staining.

For kinase assays with immunoprecipitated YFP:D6PK, 10 day-old light-grown 35S:YFP:D6PK seedlings were treated for 1 hr in liquid growth media with BFA [50 µM] or an equivalent volume of DMSO (mock) and total protein

was extracted using a protein extraction buffer (PEB) [50 mM Tris-HCl, pH 7.5, 150 mM NaCl, 0.1 mM MG132, 0.1 mM PMSF, 1 % (v/v) Protease inhibitor cocktail (Sigma, Germany), PhosStop phosphatase inhibitor cocktail (Roche, Penzberg, Germany), 0.5% Triton X-100]. 500 µg of protein extract was incubated on ice for 30 min, then the Triton X-100 concentration was diluted to 0.2 %, and 20 µL GFP-Trap beads (ChromoTek, Martinsried, Gemany) were added for 1 hr at 4°C to precipitate YFP:D6PK. After three rounds of washing with extraction buffer containing 0.1 % Triton X-100, the beads with immunoprecipitated YFP:D6PK were resuspended in 20 *µ*l PEB buffer and after quantification of the different samples, 4-7 µl bead suspension was used for phosphorylation experiments as described above.

3.2 Publication 2 Dynamic control of auxin transport-dependent growth by AGCVIII protein kinases (2014) Current Opinion Plant Biology

Inês C.R. Barbosa[1] and Claus Schwechheimer[1]

3.2.1 Summary

The second publication summarized in this dissertation is an invited review, published in October 2014 and entitled *Dynamic control of auxin transport-dependent growth by AGCVIII protein kinases*. This manuscript was written by myself and Claus Schwechheimer for the peer-reviewed journal *Current Opinion in Plant Biology*.

This review presents the most recent findings on the phosphorylation control of auxin efflux carriers by AGCVIII kinases. We were invited to write this review due to the recent contributions of our group on D6PK-mediated PIN phosphorylation and activation (Barbosa et al, 2014; Zourelidou et al, 2014). In this review, we discuss the function of three AGCVIII kinase subgroups: the D6PKs (D6PK, D6PKL1 to D6PKL3), the PID/WAGs (PID, WAG1, and WAG2), and the phots (phot1 and phot2) in the control of auxin transport-dependent growth via phosphorylation of PINs or ABCBs. The requirement of these three subgroups for the control of different aspects of the phototropism response is discussed and used to illustrate the different levels at which these kinases control auxin transport.

D6PK-mediated phosphorylation had been shown to regulate PIN activity both in heterologous systems as well as *in planta*, but did not affect PIN polarity *in planta*. Accordingly, complex *d6pk* mutants display reduced auxin transport and phenotypes, which resemble those of complex *pin* mutants. The requirement of D6PK for the phototropism response is independent of the light stimulus, and does not affect PIN3 repolarization during phototropic responses. We propose that reduced basipetal auxin transport through the hypocotyl limits auxin availability in the hypocotyl and prevents the formation of auxin maxima in the hypocotyl and consequent hypocotyl bending.

PID-mediated phosphorylation was until recently believed to impact only PIN polarity. In our recent work, we show that PID also promotes PIN auxin efflux activity, at least in *Xenopus* oocytes (Zourelidou et al, 2014). The fact that the same phosphorylation target residues, which were previously proposed to allow PIN polarity switching are also required for PID-mediated PIN activation is puzzling and could indicate that both processes are linked, i.e. that PIN activation precedes and leads to PIN repolarization. We also discuss how the differential affinities of D6PK and PID for the same PIN phosphorylation sites might explain the differential *in vivo* functions of these kinases. The involvement of PID/WAGs in the phototropism response also differs from that of D6PK. While *PID/WAGs* mutants and *PID* overexpression lines are impaired in light-induced PIN3 repolarization *D6PK* mutants and overexpressors are not. The exact mechanism how PID/WAGs controls PIN3 repolarization process is still unclear: while some studies report phot-mediated and light-induced *PID* repression, others reject it. Thus, additional work is required to clarify the role of PID/WAGs in phototropism.

phots are blue light-receptors and protein kinases that determine all phototropism responses. Besides the regulation of downstream transcripitional programs, a direct link between blue light-signaling and auxin transport was revealed by phot-mediated phosphorylation and inactivation of the auxin efflux carrier ABCB19. This event was proposed as a mechanism to block basipetal auxin transport necessary for auxin accumulation in the hypocotyls prior to phototropic hypocotyl bending. Additionally, while PID/WAGs and D6PKs can phosphorylate and activate PINs, phots seem unable to do so.

Finally, we also discuss how AGCVIII kinase localization and its regulation at the plasma membrane might have an impact on these kinases functions. In all cases, these kinases are not only present at the plasma membrane but are also internalized in the cytosol or in endomembranes. In the case of D6PK and phot, this dual localization might have a function in the control of the kinase activities, because auxin and blue-light determine D6PK and phot plasma membrane abundance, respectively. In summary, we portrayed the field of phosphorylation regulation by AGCVIII kinases in the control of PINs and ABC transporters as an active and highly dynamic field of plant cell biology and biochemistry.

3.2.2 Contributions

The review was outlined and written by myself and Claus Schwechheimer. The figures were conceptualized by myself and, after discussion with Claus Schwechheimer, designed and finalized by myself.

[1]Plant Systems Biology, Center of Life and Food Sciences Weihenstephan, Technische Universität München, 85354 Freising, Germany

Available online at www.sciencedirect.com

ScienceDirect

Current Opinion in Plant Biology

Dynamic control of auxin transport-dependent growth by AGCVIII protein kinases

Inês CR Barbosa and Claus Schwechheimer

Recent years have seen important advances in understanding the *Arabidopsis thaliana* AGCVIII protein kinases D6 PROTEIN KINASE, PINOID/WAGs, and the phototropins. It has become apparent that these kinases control the distribution of the phytohormone auxin within the plant through phosphorylation of PIN-FORMED efflux carriers or of ABC transporters. Strikingly, D6PK and PID share the same phosphosites in PIN-FORMED proteins but have differential phosphosite preferences, which appear to control the activity and polar distribution of PIN-FORMED transporters. All three AGCVIII kinases are membrane-associated proteins that are dynamically transported to and from the plasma membrane. The implications of this dynamic transport for the activity and cell biological behavior of their phosphorylation substrates are just now starting to be understood.

Addresses
Plant Systems Biology, Technische Universität München, Emil-Ramann-Strasse 4, 85354 Freising Germany

Corresponding author: Schwechheimer, Claus (ines.barbosa@wzw.tum.de, claus.schwechheimer@wzw.tum.de)

Current Opinion in Plant Biology 2014, **22**:108–115

This review comes from a themed issue on **Cell biology**

Edited by **Shaul Yalovsky** and **Viktor Žárský**

For a complete overview see the Issue and the Editorial

Available online 8th October 2014

http://dx.doi.org/10.1016/j.pbi.2014.09.010

AGCVIII kinases: regulators of auxin-dependent growth

AGC protein kinases are evolutionarily conserved serine/threonine kinases related to the mammalian cAMP-dependent, cGMP-dependent and Ca^{2+}-dependent protein kinases [1]. D6 PROTEIN KINASES (D6PK and D6PK-LIKE1–D6PKL3) [2], PINOID (PID) and the related WAG1 and WAG2 (PID/WAGs) [3,4,5], as well as the two blue light receptor kinases phototropin1 (phot1) and phot2 (phots)[1] [6] are members of the structurally distinct AGCVIII family from *Arabidopsis thaliana* [7]. All three kinases are associated with the plasma membrane and have been implicated in the control of auxin transport-dependent growth. Here, we discuss the control of auxin transporters by these kinases and highlight common and distinct mechanisms in the regulation of their transport to and from the plasma membrane.

PIN and ABC transporters promote auxin transport through the plant

Auxin and its distribution within the plant and within individual cells determine basic cellular processes such as cell elongation and cell division. Thereby, auxin controls almost all aspects of plant growth, tropic responses, cell differentiation and ultimately determines plant morphology [8]. For example, phototropic and gravitropic bending are controlled by the lateral distribution of auxin whereas the initiation of shoot and root lateral organs requires the formation of local auxin maxima through local redistribution of the hormone. Auxin export from the cell is controlled at the plasma membrane by the so-called 'long' PIN-FORMED efflux carriers PIN1–PIN4 and PIN7 and ATP-BINDING CASSETTE (ABC) transporters such as ABCB19 [8,9,10••]. Particularly, the — in many cells — polar distribution of PINs seemingly allows predicting auxin fluxes through the plant [11–13]. The major contributions of individual PINs or ABC transporters to the control of auxin transport-dependent processes are revealed by their mutant phenotypes: *pin1* mutants are defective in shoot differentiation [14], *pin2* mutants are agravitropic [15], *pin3 pin4 pin7* mutants are non-phototropic [16••] whereas *abcb19* mutants are hyperphototropic [9]. Corresponding AGCVIII kinase mutant phenotypes have provided the first indication for a direct interplay between the protein kinases and the auxin transporters: *pid* mutants are defective in shoot differentiation [4,5], *d6pk* mutants are slightly agravitropic [2,16••], and *d6pk*, *pid/wag*, and *phot* mutants are defective in phototropic hypocotyl bending [6,16••,17••,18].

D6PK — an activator of PINs

d6pk loss-of-function mutants have strong defects in basipetal auxin transport and, as PINs, D6PK localizes to the basal (rootward) plasma membrane in many cells [2,16••]. This co-localization is not coincidental because D6PK phosphorylates PINs and D6PK-dependent PIN phosphorylation at the plasma membrane is required for basipetal auxin transport [16••,19••,20••]. In *Xenopus* oocytes, PIN1 and PIN3 are inactive in the absence of an

[1] The nomenclature for phototropins (phots) differs from the standard nomenclature for proteins in *Arabidopsis*. Whereas the biologically inactive apoprotein is written in capital letters, the biologically active holoprotein bound to the flavin chromophore is written in lower case letters.

activating kinase but can be activated by D6PK [19••,20••]. Since this shows that kinases critically regulate PIN activity, the hitherto predominant concept that the knowledge about PIN distribution is sufficient to predict auxin transport has to be revised [11–13].

D6PK activates PINs preferentially at two phosphosites, S4 and S5, that are conserved in the intracellular cytoplasmic loops of PIN1 (S4 only), PIN3, PIN4 and PIN7 (Figure 1a,b) [19••]. *pin1* expressing PIN1 where S4 is replaced by alanine (S4A) is defective in auxin transport (Figure 2). S5, interestingly, corresponds to aspartic acid (D215) in PIN1 and may represent a natural phosphomimic variant of this phosphosite (Figure 1b). Remarkably, PIN2, which is apical (shootward) in root epidermis cells where it does not co-localize with basally localized D6PK, diverges from the other PINs precisely at S4 and S5 (Figure 1b). However, genetic analysis and transport assays conducted in oocytes suggest that the phosphosites S1–S3, originally identified as PID phosphosites but also targeted by D6PK, also contribute to D6PK-dependent PIN activation, although to a minor extent (Figure 1a and b) [19••].

D6PK phosphorylates PINs at the plasma membrane

D6PK is membrane-associated and traffics to and from the plasma membrane with the help of the ARF-GEF GNOM (GN) (Figure 3) [20••]. PIN trafficking requires GN, too, but there are substantial differences between the trafficking of D6PK and PINs: D6PK trafficking is faster than that of PINs, D6PK internalization is independent from clathrin (unlike PIN endocytosis), and D6PK polarity is independent from PID (unlike PIN polarity) (Figure 3) [20••,24]. As a consequence, D6PK encounters its PIN substrates only at the plasma membrane and PINs are only phosphorylated and active in the presence of the kinase [20••]. Inversely, PIN phosphorylation must be antagonized by phosphatases since the removal of D6PK from the plasma membrane is followed by the rapid decrease of PIN phosphorylation and concomitant changes in auxin distribution (Figure 3) [19••,20••].

PID/WAGs control PIN polarity and activity

The shoot differentiation phenotype of *pid* and *pin1* mutants is explained by the inability of these mutants to form auxin maxima in the shoot epidermis required for lateral organ initiation (Figure 3) [4,5,14]. In wild-type shoots, the formation of such maxima correlates with the polar distribution of PIN1, which is apical on the periphery and convergent in the primordium, such that convergent auxin flows result in local auxin accumulations (Figure 2c) [11]. PIN1 apicalization is impaired in *pid* mutants and basal PINs are apical in *PID* overexpressors (Figure 2) [25]. These observations gave rise to the

Figure 1

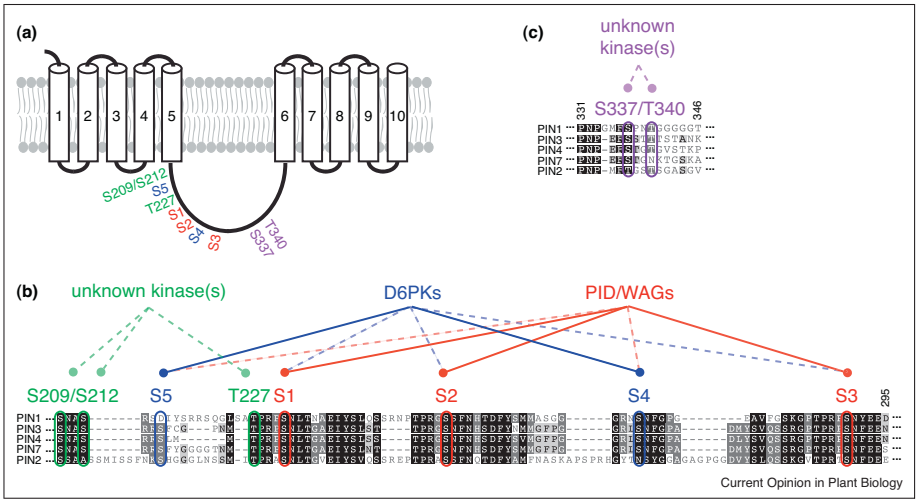

Topology and annotated partial sequence alignment of the 'long' PINs. **(a)** Schematic representation of the 'long' PINs with the predicted transmembrane-spanning domains and the cytoplasmic hydrophilic loop (CL) with identified phosphosites. **(b)** Sequence alignment of the N-terminal part of the CL with the five D6PK and PID/WAG phosphosites and their respective phosphosite preferences indicated by the blue/red color code and continuous or dashed lines [19••,29••,30••]. Additional phosphosites that are unlikely targets of D6PK or PID are shown in green [19••,21,22]. **(c)** Alignment of the C-terminal part of the CL with two potential phosphosites that are likely not phosphorylated by PID or by D6PK [19••,36••]. Amino acid references are for PIN1.

Figure 2

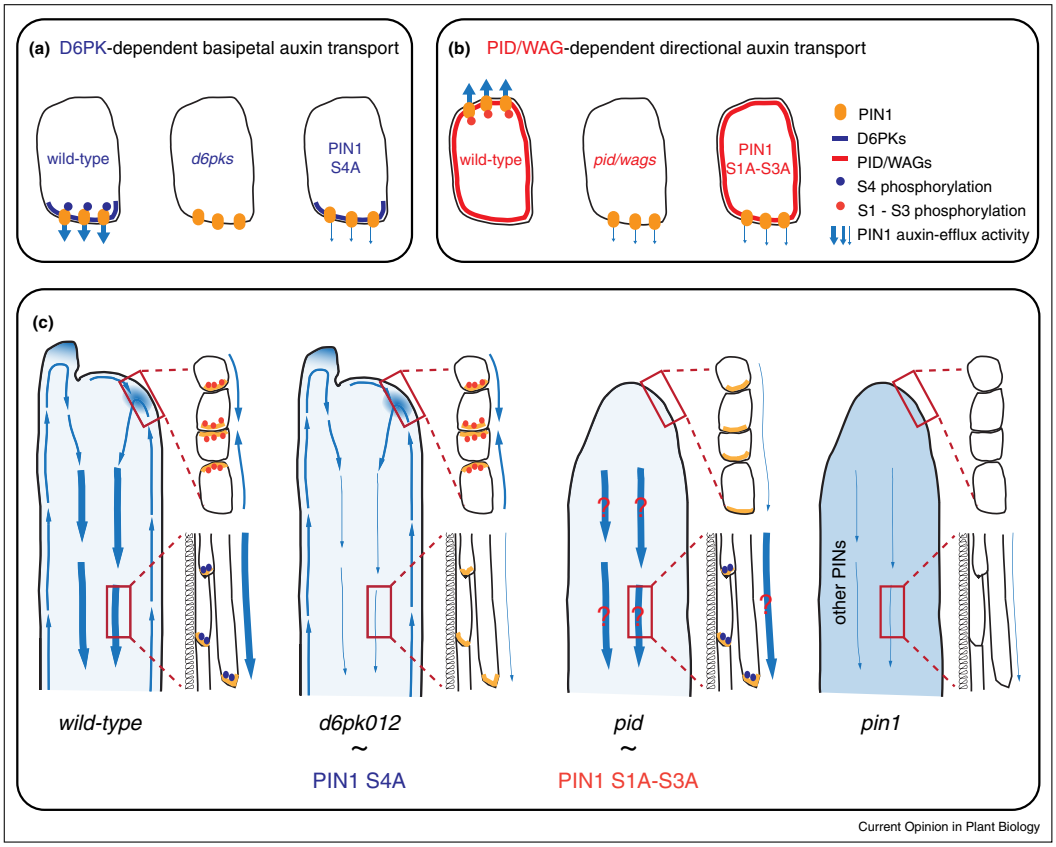

Model of PIN1 activity and polarity control by D6PKs and PID/WAGs in the shoot apex. **(a)** Schematic representation of the control of basipetal auxin transport in xylem parenchyma cells by PIN1 through D6PK-dependent phosphorylation at PIN1 S4 in the specified genotypes [19••]. **(b)** Schematic representation of the control of PIN polarity and activity by PID/WAGs in epidermal cells [19••,29••,30••]. **(c)** Model of shoot apices with different auxin streams as indicated by arrows of different width and auxin maxima formed at the sites of lateral organ initiation (blue shading). Magnifications of cells from the epidermis (upper inset) and the xylem parenchyma (lower inset) with the respective PIN1 polarities, their predicted phosphorylations, and auxin transport activities as inferred from direct measurements of basipetal auxin transport, auxin efflux activities determined in *Xenopus* oocytes or organ primordia formation and shoot differentiation — whenever such data were available [19••,29••,30••].

current model where PID-dependent PIN phosphorylations at the plasma membrane directly promote PIN apicalization whereas unphosphorylated PINs are basal (Figure 2b,c) [25–27]. Additionally, the establishment of the PIN polarity could be promoted by the inhibitory effect of auxin on PIN endocytosis [12,28].

The non-polar plasma membrane-associated PID phosphorylates PINs preferentially at the phosphosites S1–S3 [29••,30••]. These three sites are strongly related to each other and conserved in all 'long' PINs (Figure 1). S1–S3 phosphorylations are required and also sufficient to promote PIN apicalization whereas phosphatases antagonistically regulate PIN phosphorylation (Figure 3) [26,31,32].

Also WAGs, but interestingly not D6PK or related AGC-VIII kinases, promote PIN apicalization when overexpressed [29••]. Thus, PID and WAGs may have redundant biochemical functions and this is also suggested by the stronger phenotypes of *pid wag* mutants [29••]. *wag* mutant phenotypes suggest that WAGs function primarily

Figure 3

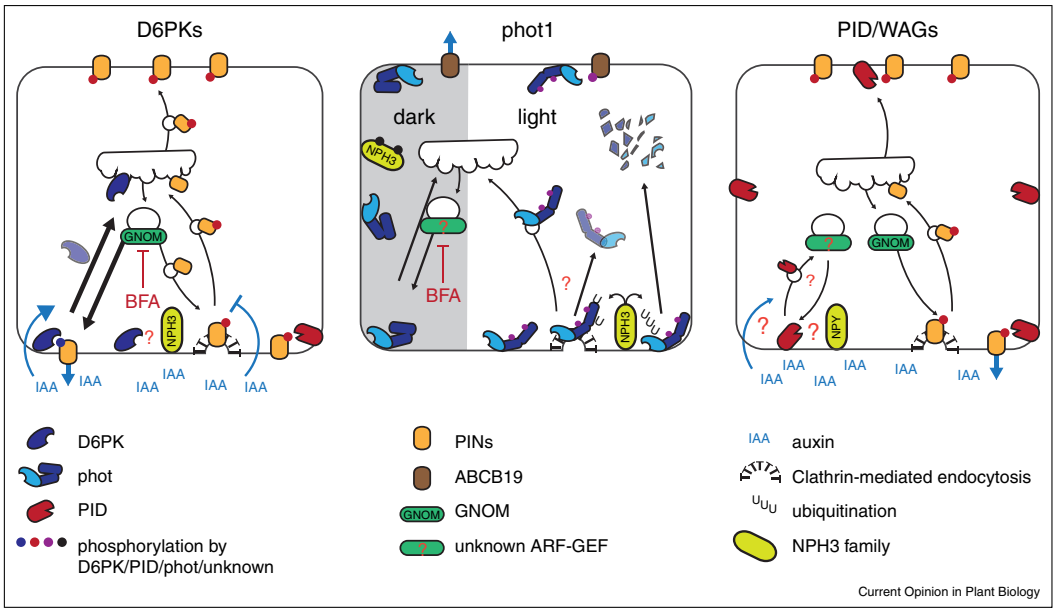

Intracellular trafficking of D6PK, phots, and PID. Schematic overview of the current knowledge about the intracellular localization and trafficking of the three kinase types and the known mechanisms involved in controlling their abundance and activity. The different phosphorylation events for the different kinases are marked with different colors as explained in the figure.

in the control of auxin fluxes during directional root growth or in the maintenance of the apical hook [3,29••,33]. The predicted increase of basally localized PINs in the *pid wag* mutants could result in increased basipetal auxin transport and this was indeed measured in *wag* mutant hypocotyls [16••]. The increased acropetal auxin transport that would inversely be predicted for the *PID/WAG* overexpressors should result in a depletion of auxin from the root meristem, which may explain the root meristem collapse observed in such lines [26,29••].

PID targets PINs to a GN-insensitive apical pathway

PIN polarity is not only controlled by PID but also by the trafficking regulator GN [27]. PIN polarity is altered in *gn* mutants and these observations gave rise to a model according to which PID-dependent PIN phosphorylations target PINs to an (apical) GN-independent pathway whereas unphosphorylated PINs traffic preferentially in a (basal) GN-dependent pathway (Figure 3). Indeed, *PID* overexpression or PIN1 phosphomimic mutations prevent PIN1 recruitment into BFA-sensitive GN-recycling pathways [27]. This model of PIN polarity control by PID/WAGs and GN, established in root cells, seemingly holds true for other cell types [17••,34,35]. In several cases, however, PIN polarities do not change between the apical and basal domains but between other membrane domains, and it has thus to be asked, which cues instruct these different polarity readouts in different contexts.

PID/WAG-dependent polarity control — is the model sufficient?

Besides promoting changes in PIN polarity, PID-dependent PIN phosphorylations, predominantly at S1–S3, also activate PIN-mediated auxin efflux at least in *Xenopus* oocytes [19••]. Because PID-dependent PIN activation also alters auxin distribution, PIN polarity could also be regulated indirectly. In this context, it is important to note that PID/WAG function and PIN phosphorylation cannot explain PIN polarity control in all cases: First, PID-independent PIN1 phosphorylations at S337 or T340 also promote PIN1 apicalization (Figure 1c) [36••]. This suggests that other kinases can control PIN polarity. Second, whereas PIN2 is apical in the root epidermis, PIN1 is basal when expressed in this cell type [37]. Since S1–S3 are conserved between PIN1 and PIN2, other differences must govern their differential polarities. Third, PIN1 is targeted in root epidermis cells to the basal or the apical plasma membrane depending on the

position of an internal GFP-tag [37]. Thus, the disruption of an as yet unknown PIN1 protein motif could control PIN1 polarity. Fourth, S1 phosphorylated PIN1 resides longer at the plasma membrane than unphosphorylated PIN1 after cytokinin treatment [38]. Thus, phosphorylations at this site are transport-inhibitory rather than transport-promoting. Finally, an insertion of the PIN2 cytoplasmic loop into the short PIN5 is sufficient for the plasma membrane targeting of PIN5 but this PIN5–PIN2 chimera, although phosphorylated, is not polarly localized [23]. Thus, there must be other regulatory mechanisms for PIN polarity control besides phosphorylation.

Differential control of PIN activity and polarity by D6PK and PID/WAGs

The biological relevance of the differential phosphosite preferences of D6PK for S4 and S5 as well as PID for S1–S3 find support in complementation experiments of *pin1* and *pin3 pin4 pin7* mutants [19••]: First, a *pin1* mutant expressing a PIN1 S4A is defective in basipetal auxin transport but has no shoot differentiation phenotype (Figure 2). Whereas the rescue of the shoot differentiation phenotype could be explained by the fact that phosphorylations at S1–S3, critical for PIN1 polarity control, can still take place in the PIN1 S4A variant, the defect in basipetal auxin transport should be a result of impaired D6PK activation in the absence of S4, the major phosphosite for D6PK. Second, whereas the strong phototropism defect of *pin3 pin4 pin7* is complemented with a wild-type *PIN3* transgene, the mutants expressing a PIN3 S4A S5A transgene are only partially phototropic [16••,19••]. This suggests that other phosphosites in addition to S4 and S5, possibly S1–S3, contribute to the activation by D6PK. Interestingly, *pin3 pin4 pin7* expressing PIN3 S1A–S3A remained non-phototropic. The role of S1–S3 phosphorylations in this case could be two-fold: contributing to the full activation of PIN3 by D6PK, thereby activating auxin efflux *per se*, or contributing to the lateralization of PIN3 by PID, thereby promoting the lateral auxin distribution essential for hypocotyl bending. Importantly, the lateralization of PIN3 in the hypocotyl is independent from D6PK and PIN-mediated basipetal auxin transport is not inhibited in *pid/wag* mutants, thus D6PK and PID have differential functions in the control of PIN3-mediated phototropic bending (Figure 4) [16••]. In analogy to the control of PIN1 polarity and activity in the shoot (Figure 2), there might thus also be a differential contribution of the different phosphosites to the control of PIN3 polarity and activity during phototropism, which still requires further investigation.

Phototropins: blue light receptors and auxin transport regulation

The two N-terminal blue light receptor domains distinguish phots from other AGCVIII kinases [7]. Phototropic hypocotyl bending is a prominent auxin transport-dependent response among several blue light and phot-regulated responses. During phototropism, phot1 is rapidly autophosphorylated and phosphorylation of PHYTOCHROME SUBSTRATE4 (PKS4) as well as dephosphorylation of NON-PHOTOTROPIC HYPOCOTYL3 (NPH3) take place shortly after light stimulation (Figure 3) [39–42]. The contribution of phot1 to hypocotyl bending and auxin transport appears to be two-fold. On the one side, phot1 mediates light-regulated phosphorylation of ABCB19, which seemingly inhibits its auxin efflux activity, at least in HeLa cells [10••], on the other side one study reports that phot1 activation results in a transcriptional downregulation of *PID* thereby preventing PIN3 lateralization [17••]. This latter finding is controversial since a second report reports no evidence for a transcriptional regulation of *PID* by blue light [43]. Thus, phot1 activation could result in the local accumulation of auxin, which may then be available for redistribution to the shaded side of the hypocotyl through PINs (Figure 4). The interaction between phot1 and ABCB19 is ameliorated by light and, at the same time, light induces the rapid internalization of phot1 after light stimulation (Figure 3) [44]. This is suggestive for a transient inactivating interaction between phot1 and ABCB19 at the plasma membrane, which should thus also result in an only transient inhibition of ABC transporter-mediated auxin transport. At the same time, phot1 does not appear to phosphorylate PINs or activate PIN1-mediated auxin efflux [17••,19••]. Thus, the regulation of auxin transport by phot1 is mediated by ABC transporters rather than by PINs. The fact that both types of transporters may physically interact suggests an even more complex molecular crosstalk between the transporters and their regulatory kinases [45–48].

phots are dynamically transported regulators

In the dark, phots presumably recycle constitutively between the plasma membrane and endosomes [49,50]. Upon blue light stimulation, phot1 and possibly also phot2 are partially internalized in a kinase activity-dependent manner (Figure 3) [49,50]. The destination of blue-light internalized phots is still unclear. Whereas phot2 accumulates at the Golgi apparatus [50], phot1 may become soluble [44] or may be subject to clathrin-mediated endocytosis [49]. Prolonged blue light exposure leads to the degradation of phot1, possibly to attenuate signaling [44]. Indeed, the phot interactor NPH3 is part of an E3 ubiquitin ligase and seemingly required for poly-ubiquitination and degradation of phot1 in high light conditions as well as for phot1 mono/multi-ubiquitination in low light conditions, possibly to promote phot1 endocytosis [51]. This complex regulation of phot1 stability and localization by NPH3 is very exciting since genes closely related to *NPH3* genetically interact with *PID* [52] indicating that PID/WAGs and possibly also D6PKs may be the subject of a similar ubiquitin-dependent regulation (Figure 3).

Figure 4

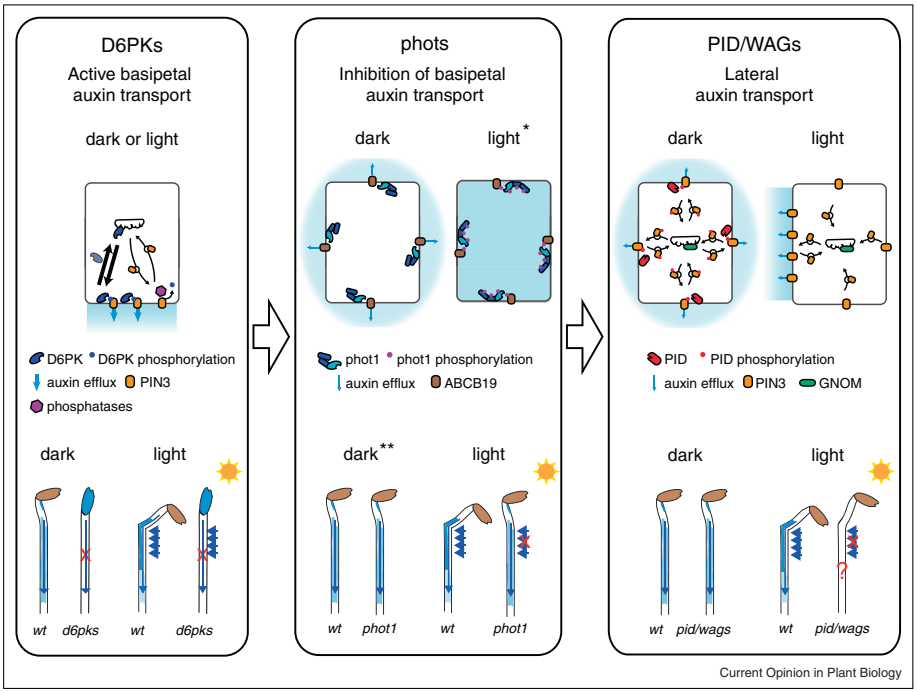

Different auxin transport-dependent processes during phototropic hypocotyl bending are controlled by D6PKs, phots, and PID/WAGs. Upper panels: Models for the mode of action of the kinases in the control of auxin transport activity and auxin distribution in dark-stimulated and light-stimulated hypocotyl cells. * Although phot1 and ABCB19 are thought to be apolarly localized, light-mediated phot1 inhibition of auxin efflux activity via ABCB19 seems to have only an effect on the basipetal transport of auxin at the tissue level [10••]. Lower panels: Phenotypes of wild-type and protein kinase mutant seedlings after growth in the dark and following light-stimulation. Whenever such data were available, depicted auxin distribution and transport activities are based on direct measurements of basipetal auxin transport in hypocotyls [10••,16••], inferred from the distribution of the DR5 auxin reporters [10••,16••,17••], and inferred from the observed light-dependent PIN3 lateralization in the hypocotyl endodermis in the different genotypes [16••,17••]. Arrows indicate direction and activity of auxin efflux; blue shading shows auxin distribution. ** This scheme is an abstraction since the corresponding experiment was performed with light-grown seedlings after dark-acclimation [10••].

Conclusions

D6PKs, PID/WAGs and phots are critical regulators of auxin transport-dependent developmental processes, and interestingly all three kinase types directly regulate the functions of auxin efflux transporters. Biochemical analyses revealed that D6PK and PID/WAGs share several phosphosites in PINs but that their differential phosphosite preferences may govern their differential effects on controlling PIN activity and polarity. Further biochemical analyses of these and other PIN phosphorylation events will allow researchers to obtain a comprehensive understanding of PIN function during polar auxin transport. In addition, resolving the interplay between phot-controlled ABCB19-mediated auxin transport and D6PK-controlled and PID-controlled PIN-mediated auxin transport at the temporal and spatial level has the potential to disentangle the complexity of the molecular as well as physiological mechanisms that govern phototropic responses and possibly also other auxin transport-dependent processes. In this context, understanding the regulation of the trafficking not only of the auxin transporters but also of their regulatory kinases emerges as another interesting level of auxin transport regulation. Since it is apparent that the subcellular localization of the kinases is subject to dynamic regulation, this should become an exciting field for future research.

Acknowledgements

We thank John Christie (University of Glasgow), Erika Isono (Technische Universität München, Germany), Tobias Preuten (Université de Lausanne), and Björn C. Willige (Salk Institute, San Diego, CA) for their helpful comments on the manuscript. This work was supported by a fellowship from the Fundação para a Ciência e a Tecnologia (FCT) to Inês C.R. Barbosa (SFRH/BD/73187/2010) and grants from the Deutsche Forschungsgemeinschaft (SCHW751/8-1 and SCHW751/12-1) to Claus Schwechheimer.

References and recommended reading

Papers of particular interest, published within the period of review, have been highlighted as:

- • of special interest
- •• of outstanding interest

1. Pearce LR, Komander D, Alessi DR: **The nuts and bolts of AGC protein kinases**. *Nat Rev Mol Cell Biol* 2010, **11**:9-22.

2. Zourelidou M, Muller I, Willige BC, Nill C, Jikumaru Y, Li H, Schwechheimer C: **The polarly localized D6 PROTEIN KINASE is required for efficient auxin transport in *Arabidopsis thaliana***. *Development* 2009, **136**:627-636.

3. Santner AA, Watson JC: **The WAG1 and WAG2 protein kinases negatively regulate root waving in *Arabidopsis***. *Plant J* 2006, **45**:752-764.

4. Benjamins R, Quint A, Weijers D, Hooykaas P, Offringa R: **The PINOID protein kinase regulates organ development in *Arabidopsis* by enhancing polar auxin transport**. *Development* 2001, **128**:4057-4067.

5. Christensen SK, Dagenais N, Chory J, Weigel D: **Regulation of auxin response by the protein kinase PINOID**. *Cell* 2000, **100**:469-478.

6. Briggs WR, Christie JM: **Phototropins 1 and 2: versatile plant blue-light receptors**. *Trends Plant Sci* 2002, **7**:204-210.

7. Galvan-Ampudia CS, Offringa R: **Plant evolution: AGC kinases tell the auxin tale**. *Trends Plant Sci* 2007, **12**:541-547.

8. Teale WD, Paponov IA, Palme K: **Auxin in action: signalling, transport and the control of plant growth and development**. *Nat Rev Mol Cell Biol* 2006, **7**:847-859.

9. Noh B, Bandyopadhyay A, Peer WA, Spalding EP, Murphy AS: **Enhanced gravi- and phototropism in plant mdr mutants mislocalizing the auxin efflux protein PIN1**. *Nature* 2003, **423**:999-1002.

10. •• Christie JM, Yang H, Richter GL, Sullivan S, Thomson CE, Lin J, Titapiwatanakun B, Ennis M, Kaiserli E, Lee OR *et al.*: **phot1 inhibition of ABCB19 primes lateral auxin fluxes in the shoot apex required for phototropism**. *PLoS Biol* 2011, **9**:e1001076.
This article describes a plausible mechanism for the control of ABC transporters by phot1

11. Smith RS, Guyomarc'h S, Mandel T, Reinhardt D, Kuhlemeier C, Prusinkiewicz P: **A plausible model of phyllotaxis**. *Proc Natl Acad Sci USA* 2006, **103**:1301-1306.

12. Jonsson H, Heisler MG, Shapiro BE, Meyerowitz EM, Mjolsness E: **An auxin-driven polarized transport model for phyllotaxis**. *Proc Natl Acad Sci USA* 2006, **103**:1633-1638.

13. Grieneisen VA, Xu J, Maree AF, Hogeweg P, Scheres B: **Auxin transport is sufficient to generate a maximum and gradient guiding root growth**. *Nature* 2007, **449**:1008-1013.

14. Galweiler L, Guan C, Muller A, Wisman E, Mendgen K, Yephremov A, Palme K: **Regulation of polar auxin transport by AtPIN1 in *Arabidopsis* vascular tissue**. *Science* 1998, **282**:2226-2230.

15. Luschnig C, Gaxiola RA, Grisafi P, Fink GR: **EIR1, a root-specific protein involved in auxin transport, is required for gravitropism in *Arabidopsis thaliana***. *Genes Dev* 1998, **12**:2175-2187.

16. •• Willige BC, Ahlers S, Zourelidou M, Barbosa IC, Demarsy E, Trevisan M, Davis PA, Roelfsema MR, Hangarter R, Fankhauser C *et al.*: **D6PK.AGCVIII kinases are required for auxin transport and phototropic hypocotyl bending in *Arabidopsis***. *Plant Cell* 2013, **25**:1674-1688.
The paper emphasizes the importance of the three PINs, PIN3, PIN4 and PIN7, as well as D6PK-dependent basipetal auxin transport for the formation of essential auxin distribution patterns required for phototropic hypocotyl bending

17. •• Ding Z, Galvan-Ampudia CS, Demarsy E, Langowski L, Kleine-Vehn J, Fan Y, Morita MT, Tasaka M, Fankhauser C, Offringa R *et al.*: **Light-mediated polarization of the PIN3 auxin transporter for the phototropic response in *Arabidopsis***. *Nat Cell Biol* 2011, **13**:447-452.
The PIN3 polarity changes described in this paper allow explaining the formation of lateral auxin maxima during phototropic hypocotyl bending

18. Preuten T, Hohm T, Bergmann S, Fankhauser C: **Defining the site of light perception and initiation of phototropism in *Arabidopsis***. *Curr Biol* 2013, **23**:1934-1938.

19. •• Zourelidou M, Absmanner B, Weller B, Barbosa IC, Willige BC, Fastner A, Streit V, Port SA, Colcombet J, de la Fuente van Bentem S *et al.*: **Auxin efflux by PIN-FORMED proteins is activated by two different protein kinases, D6 PROTEIN KINASE and PINOID**. *Elife* 2014, **3** http://dx.doi.org/10.7554/eLife.02860.
The paper presents a comprehensive phosphosite analysis of PIN phosphorylation that allows proposing a model for the differential regulation of PINs by activating phosphorylations through D6PK and PID

20. •• Barbosa IC, Zourelidou M, Willige BC, Weller B, Schwechheimer C: **D6 PROTEIN KINASE activates auxin transport-dependent growth and PIN-FORMED phosphorylation at the plasma membrane**. *Dev Cell* 2014, **29**:674-685.
This study reveals that D6PK and their PIN substrates traffic independently within the cell and suggests that activating PIN phosphorylations by D6PK take place only at the plasma membrane

21. Sasayama D, Ganguly A, Park M, Cho HT: **The M3 phosphorylation motif has been functionally conserved for intracellular trafficking of long-looped PIN-FORMEDs in the *Arabidopsis* root hair cell**. *BMC Plant Biol* 2013, **13**:189.

22. Ganguly A, Cho HT: **The phosphorylation code is implicated in cell type-specific trafficking of PIN-FORMEDs**. *Plant Signal Behav* 2012, **7**:1215-1218.

23. Ganguly A, Park M, Kesawat MS, Cho HT: **Functional analysis of the hydrophilic loop in intracellular trafficking of *Arabidopsis* PIN-FORMED proteins**. *Plant Cell* 2014, **26**:1570-1585.

24. Geldner N, Anders N, Wolters H, Keicher J, Kornberger W, Muller P, Delbarre A, Ueda T, Nakano A, Jurgens G: **The *Arabidopsis* GNOM ARF-GEF mediates endosomal recycling, auxin transport, and auxin-dependent plant growth**. *Cell* 2003, **112**:219-230.

25. Friml J, Yang X, Michniewicz M, Weijers D, Quint A, Tietz O, Benjamins R, Ouwerkerk PB, Ljung K, Sandberg G *et al.*: **A PINOID-dependent binary switch in apical-basal PIN polar targeting directs auxin efflux**. *Science* 2004, **306**:862-865.

26. Michniewicz M, Zago MK, Abas L, Weijers D, Schweighofer A, Meskiene I, Heisler MG, Ohno C, Zhang J, Huang F *et al.*: **Antagonistic regulation of PIN phosphorylation by PP2A and PINOID directs auxin flux**. *Cell* 2007, **130**:1044-1056.

27. Kleine-Vehn J, Huang F, Naramoto S, Zhang J, Michniewicz M, Offringa R, Friml J: **PIN auxin efflux carrier polarity is regulated by PINOID kinase-mediated recruitment into GNOM-independent trafficking in *Arabidopsis***. *Plant Cell* 2009, **21**:3839-3849.

28. Paciorek T, Zazimalova E, Ruthardt N, Petrasek J, Stierhof YD, Kleine-Vehn J, Morris DA, Emans N, Jurgens G, Geldner N *et al.*: **Auxin inhibits endocytosis and promotes its own efflux from cells**. *Nature* 2005, **435**:1251-1256.

29. •• Dhonukshe P, Huang F, Galvan-Ampudia CS, Mahonen AP, Kleine-Vehn J, Xu J, Quint A, Prasad K, Friml J, Scheres B *et al.*: **Plasma membrane-bound AGC3 kinases phosphorylate PIN auxin carriers at TPRXS(N/S) motifs to direct apical PIN recycling**. *Development* 2010, **137**:3245-3255.

30. •• Huang F, Zago MK, Abas L, van Marion A, Galvan-Ampudia CS, Offringa R: **Phosphorylation of conserved PIN motifs directs *Arabidopsis* PIN1 polarity and auxin transport**. *Plant Cell* 2010, **22**:1129-1142.
These two studies show that S1–S3 phosphorylations are required and sufficient to promote PIN apicalization and provide evidence for a differential activity of different AGCVIII kinase family members on PINs

31. Ballesteros I, Dominguez T, Sauer M, Paredes P, Duprat A, Rojo E, Sanmartin M, Sanchez-Serrano JJ: **Specialized functions of the PP2A subfamily II catalytic subunits PP2A-C3 and PP2A-C4 in the distribution of auxin fluxes and development in *Arabidopsis***. *Plant J* 2013, **73**:862-872.

32. Dai M, Zhang C, Kania U, Chen F, Xue Q, McCray T, Li G, Qin G, Wakeley M, Terzaghi W *et al.*: **A PP6-type phosphatase holoenzyme directly regulates PIN phosphorylation and auxin efflux in *Arabidopsis***. *Plant Cell* 2012, **24**:2497-2514.

33. Willige BC, Ogiso-Tanaka E, Zourelidou M, Schwechheimer C: **WAG2 represses apical hook opening downstream from gibberellin and PHYTOCHROME INTERACTING FACTOR 5**. *Development* 2012, **139**:4020-4028.

34. Kleine-Vehn J, Ding Z, Jones AR, Tasaka M, Morita MT, Friml J: **Gravity-induced PIN transcytosis for polarization of auxin fluxes in gravity-sensing root cells**. *Proc Natl Acad Sci USA* 2010, **107**:22344-22349.

35. Li H, Lin D, Dhonukshe P, Nagawa S, Chen D, Friml J, Scheres B, Guo H, Yang Z: **Phosphorylation switch modulates the interdigitated pattern of PIN1 localization and cell expansion in *Arabidopsis* leaf epidermis**. *Cell Res* 2011, **21**:970-978.

36. •• Zhang J, Nodzynski T, Pencik A, Rolcik J, Friml J: **PIN phosphorylation is sufficient to mediate PIN polarity direct auxin transport**. *Proc Natl Acad Sci USA* 2010, **107**:918-922.
The paper presents the functional characterization of two PIN1 phosphosites that may control PIN polarity in a PID-independent manner

37. Wisniewska J, Xu J, Seifertova D, Brewer PB, Ruzicka K, Blilou I, Rouquie D, Benkova E, Scheres B, Friml J: **Polar PIN localization directs auxin flow in plants**. *Science* 2006, **312**:883.

38. Marhavy P, Duclercq J, Weller B, Feraru E, Bielach A, Offringa R, Friml J, Schwechheimer C, Murphy A, Benkova E: **Cytokinin controls polarity of PIN1-dependent auxin transport during lateral root organogenesis**. *Curr Biol* 2014, **24**:1031-1037.

39. Pedmale UV, Liscum E: **Regulation of phototropic signaling in *Arabidopsis* via phosphorylation state changes in the phototropin 1-interacting protein NPH3**. *J Biol Chem* 2007, **282**:19992-20001.

40. Demarsy E, Schepens I, Okajima K, Hersch M, Bergmann S, Christie J, Shimazaki K, Tokutomi S, Fankhauser C: **Phytochrome kinase substrate 4 is phosphorylated by the phototropin 1 photoreceptor**. *EMBO J* 2012, **31**:3457-3467.

41. Inoue S, Kinoshita T, Matsumoto M, Nakayama KI, Doi M, Shimazaki K: **Blue light-induced autophosphorylation of phototropin is a primary step for signaling**. *Proc Natl Acad Sci USA* 2008, **105**:5626-5631.

42. Liscum E, Briggs WR: **Mutations in the NPH1 locus of *Arabidopsis* disrupt the perception of phototropic stimuli**. *Plant Cell* 1995, **7**:473-485.

43. Haga K, Sakai T: **PIN auxin efflux carriers are necessary for pulse-induced but not continuous light-induced phototropism in *Arabidopsis***. *Plant Physiol* 2012, **160**:763-776.

44. Sakamoto K, Briggs WR: **Cellular and subcellular localization of phototropin 1**. *Plant Cell* 2002, **14**:1723-1735.

45. Titapiwatanakun B, Blakeslee JJ, Bandyopadhyay A, Yang H, Mravec J, Sauer M, Cheng Y, Adamec J, Nagashima A, Geisler M *et al.*: **ABCB19/PGP19 stabilises PIN1 in membrane microdomains in *Arabidopsis***. *Plant J* 2009, **57**:27-44.

46. Henrichs S, Wang B, Fukao Y, Zhu J, Charrier L, Bailly A, Oehring SC, Linnert M, Weiwad M, Endler A *et al.*: **Regulation of ABCB1/PGP1-catalysed auxin transport by linker phosphorylation**. *EMBO J* 2012, **31**:2965-2980.

47. Wang B, Henrichs S, Geisler M: **The AGC kinase PINOID, blocks interactive ABCB/PIN auxin transport**. *Plant Signal Behav* 2012, **7**:1515-1517.

48. Blakeslee JJ, Bandyopadhyay A, Lee OR, Mravec J, Titapiwatanakun B, Sauer M, Makam SN, Cheng Y, Bouchard R, Adamec J *et al.*: **Interactions among PIN-FORMED and P-glycoprotein auxin transporters in *Arabidopsis***. *Plant Cell* 2007, **19**:131-147.

49. Kaiserli E, Sullivan S, Jones MA, Feeney KA, Christie JM: **Domain swapping to assess the mechanistic basis of *Arabidopsis* phototropin 1 receptor kinase activation and endocytosis by blue light**. *Plant Cell* 2009, **21**:3226-3244.

50. Kong SG, Suzuki T, Tamura K, Mochizuki N, Hara-Nishimura I, Nagatani A: **Blue light-induced association of phototropin 2 with the Golgi apparatus**. *Plant J* 2006, **45**:994-1005.

51. Roberts D, Pedmale UV, Morrow J, Sachdev S, Lechner E, Tang X, Zheng N, Hannink M, Genschik P, Liscum E: **Modulation of phototropic responsiveness in *Arabidopsis* through ubiquitination of phototropin 1 by the CUL3-Ring E3 ubiquitin ligase CRL3(NPH3)**. *Plant Cell* 2011, **23**:3627-3640.

52. Furutani M, Kajiwara T, Kato T, Treml BS, Stockum C, Torres-Ruiz RA, Tasaka M: **The gene MACCHI-BOU 4/ENHANCER OF PINOID encodes a NPH3-like protein and reveals similarities between organogenesis and phototropism at the molecular level**. *Development* 2007, **134**:3849-3859.

3.3 Draft Publication 3 A phospholipid-binding K-rich motif and phosphorylation control plasma membrane localization and polarity of D6 PROTEIN KINASE (in preparation)

Inês C. R. Barbosa[1], Melina Zourelidou[1], Ingo Heilman[2] and Claus Schwechheimer[1]

3.3.1 Summary

The third publication of this thesis is an as-yet unpublished manuscript summarizing the results from an advanced study on the control of D6PK membrane association. We had previously shown that D6PK localization is strictly required for the maintenance of PIN phosphorylation and PIN-mediated auxin transport growth (Barbosa et al, 2014; Zourelidou et al, 2014). We also identified some commonalities and differences in the targeting and constitutive recycling of D6PK compared to the PINs. However, the exact mechanism by which D6PK is anchored to the plasma membrane and how its polarity is controlled remained to be investigated.

In this paper, I identify biochemical mechanisms through which D6PK is anchored to and restricted to its polar domain at the plasma membrane. In lipid binding assays, I show that D6PK binds to polyacidic phospholipids *in vitro*, i.e. PA (phosphatidic acid) and PIPs (phosphoinositides). In root epidermis, pharmacologic inhibition of different steps of PA, PI(3)P, and PI(4)P biosynthesis led to D6PK internalization, while inhibition of $PI(4,5)P_2$ hydrolysis led to the loss of D6PK polarity. Using a series of D6PK deletion variants, I show that the D6PK middle domain is required and sufficient for plasma membrane localization. Within this domain, an amino acid stretch comprising six lysine residues, that we called the K-rich motif, is required for PA and PIP binding *in vitro* and when mutated results in an almost complete internalization of D6PK into soluble and endomembrane compartments *in vivo*. These mutations did not affect the kinase activity *in vitro* but impaired the ability of the kinase to complement a *d6pk d6pkl1* mutant and PIN3 phosphorylation defects *in vivo*. I further characterized two serines adjacent to the K-rich motif of D6PK that had previously been identified as phosphorylation sites in D6PKL2. Non-phosphorylatable mutants loose D6PK polarity, while phosphomimic mutations into aspartic acids result in a significant internalization of D6PK. Moreover, the non-phosphorylatable D6PK is resistant to BFA- and phosphatase inhibitor-induced D6PK internalization, suggesting that phosphorylation at these two serines is required for D6PK polarity control, D6PK recycling and its phosphorylation-induced internalization. Although these mutant kinases are biochemically active kinases, the non-phosphorylatable, apolar and non-recycling D6PK variant cannot complement *d6pk d6pkl1* defects (e.g. PIN3 phosphorylation and tropisms), while the partially internalized phosphomimic D6PK can.

Thus, the D6PK K-rich motif is required for the plasma membrane localization and function of D6PK, while the nearby serines are likely phosphorylation targets controlling D6PK recycling, polarity, and function. Based on my data, we present a model in the concluding figure

of thispaper, which will be substantiated by a few additional studies as discussed in the Discussion section of this thesis.

3.3.2 Contributions

For this publication draft, I designed and performed all experiments and data analysis. The manuscript and figure concept was developed, written, and prepared by myself with input from Claus Schwechheimer[1]. Melina Zourelidou[1] assisted with the kinase experiments and Ingo Heilmann[2] obtained co-authorship because he provided an unpublished mutant material. Mutant and reporter lines were generated with the technical assistance of Jutta Elgner[1], who is acknowledged in the manuscript draft.

[1]Plant Systems Biology, Center of Life and Food Sciences Weihenstephan, Technische Universität München, 85354 Freising, Germany

[2]Department of Cellular Biochemistry, Martin-Luther-University Halle-Wittenberg, 06120 Halle (Saale), Germany

A phospholipid-binding K-rich motif and phosphorylation control plasma membrane localization and polarity of D6 PROTEIN KINASE

Inês C. R. Barbosa[1], Melina Zourelidou[1], Ingo Heilman[2] and Claus Schwechheimer[1]

Abstract

The polar transport of the phytohormone auxin is essential to the spatio-temporal control of plant development. Major players for polar auxin transport are the auxin efflux carriers PIN-FORMED proteins, as they are polarly localized in the cells and thereby regulate the direction of the cell-to-cell auxin transport. Recent work showed that the AGCVIII kinases D6 PROTEIN KINASE and paralogs are critical regulators of polar auxin transport in plants. D6PK directly phosphorylates PIN proteins and is required to the activation of PIN-mediated auxin efflux in *Xenopus* oocytes and *in planta*. D6PK is polarly localized at the plasma membrane, colocalizes with its PIN substrate, and its localization is strictly required to maintain PIN phosphorylation levels and auxin transport-dependent growth. The mechanisms controlling D6PK localization are as yet enigmatic. Here, we found that D6PK directly binds polyacidic phospholipids *in vitro* and that phospholipid composition critically determines its localization *in vivo*. We identified a polybasic motif within the middle domain, the K-rich motif, required for D6PK phospholipid binding *in vitro* and membrane association and localization *in vivo*. Importantly, the K-rich motif was also required for proper PIN3 phosphorylation and tropism responses. Futhermore, we show that putative phosphorylation events near the K-rich motif, at S310 and S311, are required for D6PK membrane association, recycling and polarity control. Hence, we propose that D6PK is anchored to the plasma membrane by ionic interactions between its K-rich motif and polyacidic phospholipids and that this interaction is regulated by phosphorylation to promote D6PK recycling and steady-state polarity maintenance. Our work identifies key molecular mechanisms involved in D6PK membrane anchoring and polarity control that rely on phospholipid composition, phosphorylation, and recycling.

[1]Plant Systems Biology, Center of Life and Food Sciences Weihenstephan, Technische Universität München, 85354 Freising, Germany

[2]Department of Cellular Biochemistry, Martin-Luther-University Halle-Wittenberg, 06120 Halle (Saale), Germany

Introduction

Cell polarity, or the asymmetric distribution of cellular components along a particular axis, is a fundamental property of seemingly all organisms. In multi-cellular organisms, cell polarity is crucial for proper signaling, cell fate determination, physiology, growth, and morphogenesis. Although there are substantial differences in morphology and function among different organisms, the underlying cellular mechanisms required for cell polarity establishment and maintenance, such as cytoskeleton reorganization or polar vesicle trafficking, as well as the molecular components involved, such as small GTPases like yeast and mammalian CDC42 (CELL DIVISION CONTROL PROTEIN 42) or PIPs (phosphoinositides), are surprisingly conserved (Thompson, 2013; Yang, 2008).

In plants, the polar distribution of the phytohormone auxin provides an attractive biological system to study cell polarity (Yang, 2008). Auxin distribution within the plant is controlled at the spatial and temporal level by local auxin metabolism as well as by cell-to-cell auxin transport across cells and tissues (Vanneste & Friml, 2009). This results in the formation of local auxin maxima and minima that trigger different responses such as cell division, cell elongation or cell differentiation. Ultimately, seemingly all organ development as well as all dynamic tropic growth in plants rely on differential auxin distribution patterns and auxin-induced cellular responses (Teale et al, 2006). Critical players in polar auxin transport are the PIN (PIN-FORMED) auxin efflux carriers, which are polarly localized in the plasma membrane of many cells. Tissue-specific PIN polarities are sufficient to explain auxin distribution gradients across organs, such as root and shoot meristems (Grieneisen et al, 2007; Jönsson et al, 2006). Moreover, gravity and light stimulus-dependent changes in PIN polarity correlate with observed auxin redistribution patterns that are required for directional growth (Ding et al, 2011; Kleine-Vehn et al, 2010; Rakusová et al, 2011). PIN polarity and PIN-dependent auxin transport require phosphorylation by protein kinases, most prominently the D6PK (D6 PROTEIN KINASE) and PID (PINOID) AGCVIII kinases, which directly phosphorylate PINs and control their polarity (PID) or activity (PID and D6PK) (Friml et al, 2004; Zourelidou et al, 2014). D6PK and PID are peripheral plasma membrane-localized proteins and D6PK, just like its PIN substrates but in contrast to PID, is polarly localized at the basal plasma membrane of many cells (Dhonukshe et al, 2010; Zourelidou et al, 2009). Importantly, in the absence of AGCVIII kinase-mediated phosphorylation PIN-mediated auxin efflux is strongly compromised *in planta* and when tested in *Xenopus* oocytes (Willige et al, 2013; Zourelidou et al, 2014). Hence, AGCVIII kinase-mediated PIN phosphorylation is determinant for the direction and activity of PIN-mediated auxin transport.

Although D6PK and PINs are polarly targeted to the plasma membrane, their trafficking to the polar domain is mediated by different pathways (Barbosa et al, 2014). PIN plasma membrane abundance and polarity control has been intensively studied and PINs have emerged as model cargoes for polar transport in plants (Kania et al, 2014). As they are integral membrane proteins, establishment and maintenance of PIN polarity requires membrane trafficking. Though, it is still unclear whether the targeting of *de novo* synthesized PINs is polar

or apolar (retracted Dhonukshe et al, 2008; Kania et al, 2014), it is well established that constitutive recycling, mediated by clathrin-dependent endocytosis and GNOM-dependent exocytosis, in combination with reduced lateral diffusion in the plasma membrane are required to maintain PIN polarity (Feraru et al, 2011; Kleine-Vehn et al, 2011). Hence, PIN polarity is not static but involves highly regulated and dynamic membrane trafficking events.

Much less is known about the mechanisms controlling the abundance and polarity of D6PK at the plasma membrane. As a peripheral membrane protein, it is expected that the mechanisms determining its plasma membrane and polar localization differ from those of the PINs. Indeed, we have previously shown that the D6PK polarity domain does not always follow that of the PINs and that D6PK recycling also differs from that of PINs. D6PK undergoes GNOM-dependent but clathrin-independent constitutive recycling and its trafficking kinetics are much faster than that of the PINs. Importantly, manipulation of D6PK plasma membrane abundance critically determines PIN phosphorylation and auxin transport-dependent growth (Barbosa et al, 2014; Zourelidou et al, 2014). However, the molecular mechanisms anchoring D6PK to the plasma membrane and the determinants of its polarity remain to be identified.

Peripheral membrane proteins can be anchored to membranes by diverse mechanisms such as protein-protein or protein-lipid interactions or by immersion into the lipid bilayer with the help of hydrophobic residues or lipid modifications (Cho & Stahelin, 2005). Often recruitment of peripheral proteins to membranes requires more than one anchoring mechanism, which is thought to confer stability and specificity to the protein targeting (Carlton & Cullen, 2005). For example, small GTPases are commonly anchored to membranes through lipid modifications, such as myristoylation and S-acylation, and ionic interactions between polybasic motifs and acidic phospholipids that determine final organelle targeting (Di Paolo & De Camilli, 2006; Heo et al, 2006). As a consequence, targeting and removal of peripheral proteins to membranes can be mediated by substantially different mechanisms, (e.g. membrane trafficking, lipid metabolism, posttranslational modifications) which are in all cases highly dynamic processes.

The very low abundant phospholipids (<1% of total phospholipids) belonging to the PIPs (phosphoinositides) are important players in the recruitment of peripheral proteins to membranes. PIPs are phosphorylated derivatives of PI (phosphatidylinositol) and different cell membranes have specific PIP composition, which is tightly regulated by local PIP-kinases and phosphatases and determines organelle identity, trafficking, function, and signaling (Behnia & Munro, 2005). A differential PIP composition within the plasma membrane was also shown to be essential for the determination of polar domains. For example, the local accumulation of $PI(4,5)P_2$ defines the bud scar in *Saccharomyces cerevisae* and the leading pseudopods of *Dictyostelium discoideum*; whereas mutually exclusive domains of $PI(4,5)P_2$ and $PI(3,4,5)P_3$ confer apical and baso-lateral identity, respectively, in mammalian and *Drosophila* epithelia (Orlando & Guo, 2009). In plants, enrichment of $PI(4,5)P_2$ at the apical plasma membrane of root hairs and pollen tubes is required for the proper polar growth of these cell types (Kost, 2008). Peripheral membrane proteins bind PIPs through PIP species-specific binding domains

(e.g. PI(3)P-binding FYVE-domain) or through less specific ionic interactions between stretches of polybasic residues (e.g. lysine) and the negatively charged headgroups of PIPs. Since D6PK is a peripheral membrane protein and polarly localized, direct or indirect binding to plasma membrane PIPs could determine its membrane anchoring as well as polarity.

Here, we determined the molecular mechanisms that control plasma membrane anchoring and polarity control of D6PK in *Arabidopsis*. We show that D6PK is able to bind phospholipids with polyacidic headgroups and that the phospholipid composition critically determines its plasma membrane recruitment and polarity. We identified a K (lysine)-rich motif within the D6PK middle domain that is required for D6PK phospholipid binding, plasma membrane localization, and auxin transport-dependent growth. Moreover, we show that phosphorylation of adjacent serines critically determines D6PK affinity for the plasma membrane as well as its polarity. Thus, we establish a set of molecular landmarks for D6PK plasma membrane recruitment and polarity control that are crucial for proper PIN-mediated auxin transport.

Materials and Methods

Biological material

The following previously published *Arabidopsis thaliana* mutants and transgenic lines were used in this study: single (*d6pk0*), double (*d6pk01*), and triple (*d6pk012*) mutants of the alleles *d6pk*-1 (SALK_061847; *d6pk0*), *d6pkl1*- 1 (SALK_056618; *d6pk1*) and *d6pkl2*-2 or (SALK_086127; *d6pk2*) (Zourelidou et al, 2009); *pip5k1* (SALK_146728) and *pip5k2* (SALK_012487) (Ischebeck et al, 2013); 35S:YFP:D6PK and 35S:YFP:D6PKinactive in the wild-type Columbia-0 background and D6PK:YFP:D6PK in the *d6pk012* triple mutant background (Willige et al, 2013; Zourelidou et al, 2009).

Cloning procedures

The deletions of D6PK domains were generated by PCR amplification of Gateway-compatible PCR fragments from a vector (pDONR201) containing the *D6PK* coding sequence, pDONR-D6PK (Zourelidou et al, 2009) with the primers: IB3/IB2 for ΔN (109 to 499 amino acids of D6PK), IB1/IB4 for N (1 to 108), IB1/IB5 for ΔC (1 to 446), IB6/IB2 for C (447 to 499), IB7/IB8 for MID (255 to 335) (Table 1). The PCR fragments were then inserted into the entry vector pDONR201. The ΔMID (1 to 334 and 356 to 499) deletion was obtained by SacI digestion and religation of a pEXTAG-YFP:D6PK clone, that had been previously mutagenized with the primers IB9 and IB10 that introduced SacI sites adjacent to middle domain.

Mutations in the D6PK K-rich motif and of the serines 310 and 311 were obtained by PCR-directed mutagenesis in pDONR-D6PK. For the D6PK-3KA mutant, the lysines K315, K317 and K318 were replaced by alanines. For the D6PK-6KA mutant the lysines K312, K314 and K320 were mutated in the D6PK-3KA construct using the primer IB62. D6PK S310 and S311 mutations were introduced with the primer IB72 for the alanine substitutions (D6PK-SSAA) and with the primer IB73 for the aspartic acid substitutions (D6PK-SSDD).

Table 1 List of primers used for cloning of D6PK domain deletions and mutagenesis.
F, forward; R, reverse; In bold is the Gateway compatible sequence, underlined is the introduced STOP codon in the *Deletion primers* and introduced mutations in the *Mutation primers*; [Phos] indicates 5' phosphorylation for PCR-directed mutagenesis.

Primer	Name	F/R	Sequence
Deletion primers			
IB 1	YFP:D6 full GW	F	GGGG**ACAAGTTTGTACAAAAAAGCAGGCT**TCATGATGGCTTCAAAAACTCCAGAAG
IB 2	YFP:D6 full GW	R	GGGG**ACCACTTTGTACAAGAAAGCTGGGT**CTCAGAAGAAATCAAACTCAAGATAATT
IB 3	YFP:D6 -N' GW	F	GGGG**ACAAGTTTGTACAAAAAAGCAGGCT**TCTTTAGGCTCTTGAAGAGGTTAGGAT
IB 4	YFP:N' GW	R	GGGG**ACCACTTTGTACAAGAAAGCTGGGT**CCTAATGATTCAAACCCAAACCACCAT
IB 5	YFP:D6 -C' GW	R	GGGG**ACCACTTTGTACAAGAAAGCTGGGT**CCTAAAAGAAAGGATGTTGCTTTATCTCTGT
IB 6	YFP:C GW	F	GGGG**ACAAGTTTGTACAAAAAAGCAGGCT**TCGAAGGAGTGAATTGGGCTCTGGTT
IB 7	YFP:MID	F	GGGG**ACAAGTTTGTACAAAAAAGCAGGCT**TCCTCTCCCTGAGATGTACTGTGA
IB 8	YFP:MID	R	GGGG**ACCACTTTGTACAAGAAAGCTGGGT**CCTAAACGAGTTCTGGTAACGGAGTTA
IB 9	D6-MID SacI_1	F	[Phos]GATTTTGA***G***CTCTCCCTGAGA
IB 10	D6-MID SacI_2	F	[Phos]CCGTTACCAGA***G***CTCGTTGCA
Mutation primers			
IB 70	3KA	F	[Phos]TCATCGAAATCCAAGGCAGACGCGGCACCGAAAACCGAAAA
IB 62	6KA	F	[Phos]TTCTTCTCATCGGCATCCGCGGCAGACGCGGCACCGGCAACCGAAAACGGGAA
IB 72	SSAA	F	[Phos]GGTCCTCGGTTCTTCGCAGCGAAATCCAAGAAAGACA
IB 73	SSDD	F	[Phos]GGTCCTCGGTTCTTCGACGATAAATCCAAGAAAGA

The resulting pDONR-D6PK entry clones containing deletions and mutations were introduced into the destination vectors pDEST15 to obtain GST (GLUTATHIONE-S-TRANSFERASE) N-terminal fusions for recombinant expression in bacteria; and into pEXTAG-YFP-GW to obtain expression of YFP N-terminal fusions from 35S CaMV promoter in plants. D6PK mutant variants were subsequently excised as XhoI/NotI fragments and inserted into a pGREEN0229 containing the D6PK promoter to yield D6PK mutant variants expressed from the *D6PK* promoter (Zourelidou et al, 2014). All pEXTAG-YFP-GW constructs were transformed into wild-type Col-0 and all the pGREEN0229 constructs were transformed into *d6pk01* by Agrobacterium-mediated transformation and using floral dip (Clough & Bent, 1998).

Inhibitor treatments and confocal microscopy

Unless otherwise stated, seedlings were grown in continuous light (110 µmol m^{-2} s^{-1}) at 21 ºC for 5-7 days on ½ MS [2.15 g/l Murashige and Skoog salts, 0.5 g/l 2-(N-morpholino)ethanesulfonic acid, 8 g/l agar, pH 5.8]. The following chemicals and inhibitors were used: Wortmannin (Applichem); LY294002 (Sigma); U73343 (Sigma); U73122 (Sigma); R59022 (Sigma); Propanolol (Sigma); 1- and 2-butanol (Sigma); Brefeldin A (Life Technologies); 1-NAA (Sigma); Calyculin A (Millipore) and Staurosporine (Millipore). All inhibitors were dissolved in DMSO and controlled by mock-treatments performed in parallel. Inhibitor treatments were performed as previously described: Wortmannin (Jaillais et al, 2006), LY294002 (Aggarwal et al, 2013), U73343 and U73122 (Andreeva et al, 2010; Zhao et al, 2010); R59022, propranolol and 1-butanol (Li & Xue, 2007; Potocky et al, 2014); BFA and 1-NAA (Barbosa et al, 2014) and Calyculin A (Urano et al, 2012). FM4-64 (2 µM, Life

Techologies) staining was performed as described in the respective figure legends. All images were taken with an Olympus FV1000 confocal microscope with high sensitivity GaAsP detectors (Olympus, Hamburg, Germany), using identical acquisition settings between samples.

Phospholipid binding assays

For lipid-binding assays, proteins were recombinantly expressed in *Escherichia coli* BL21 cultures transformed with pDEST15 plasmids (for the GST-fusion proteins) and with pGEX 6P1(GE Healthcare, for GST alone), and purified using glutathinone sepharose 4B beads (GE Healthcare). Liposome assays were performed as described before (Schapire et al, 2008) with some modifications: 100 µg total lipids (PS/PC = 1:1 and PS/PC/PA = 1:1:1 [w:w]; PS [Phosphatidylserine, Sigma] and PC [Phosphatidylcholine, Sigma]; PA, [Phosphatidic acid, Echelon]) were used for 2 µg recombinant protein sample. Phospholipids (PS and PC in chlorophorm, PA in methanol:chlorophorm:H_2O, [1:1:0.1]) were mixed and dried as a thin layer under a stream of nitrogen. Dried lipids were resuspended in Buffer A (50 mM HEPES [pH 6.8], 100 mM NaCl , 4 mM EGTA) by vortexing for 20 minutes. Large multilamellar vesicles were disrupted into small unilamellar vesicles (SUVs) in a sonication bath. SUVs were collected by 20,000 *g* centrifugation and resuspended in Buffer A. Proteins were incubated by shaking with liposomes for 15 minutes at 27°C. Liposomes and bound proteins were collected by 20,000 *g* centrifugation and washed 3 times. Bound fractions were boiled in 2x Laemmli buffer.

Lipid overlay assays using PIP-strips (Echelon) were performed following manufacturer's instructions. Briefly, membranes were blocked overnight in a blocking buffer at 4°C, with 4% BSA either in TBS-T (0.1% Tween) or PBS-T (0.1% Tween). PIP-Strip membranes (Echelon) were incubated with purified proteins (0.5 µg/mL), then incubated with anti-GST (1:2000, GE Healthcare) and anti-goat peroxidase conjugate (1:8000, Sigma-Aldrich). Incubations were done using blocking buffer, at room temperature, and for 1 h. Membranes were washed three times between incubations steps with either TBS-T or PBS-T for 10 min. Bound proteins were detected with Pierce ECL Plus Western Blotting Substrate (Thermo Scientific) in a Fujifilm LAS 4000 mini (Fuji, Japan).

Kinase assays

In vitro kinase assays were performed with purified recombinant kinases using GST:PIN1 cytosolic loop as a substrate (Zourelidou et al, 2009). Equal protein amounts (approximately 0.5 µg) were incubated for 60 min at 28°C in a buffer (25 mM Tris-HCl [pH 7.5], 5 mM $MgCl_2$, 0.2 mM EDTA, 50 µM ATP, 1x Complete protease inhibitor cocktail [Roche]) supplemented with 10 µCi [γ-^{32}P]ATP (370 MBq specific activity 185 TBq; [Hartmann Analytic]). Reactions were stopped by adding 5x Laemmli buffer, boiled, and then separated in two SDS-PAGE gels, one stained with Coomassie Brilliant Blue for the loading control and the other exposed to X-ray film for autoradiography.

Negative gravitropism and phototropism responses

Seedlings were grown for 2.5 days on 1/2 MS in the dark, agravitropically growing seedlings were straightened under green safe light 2 hrs prior to the experiments. For phototropism response experiments, etiolated seedlings were transferred to a FloraLED chamber (CLF Plant Climatics, Wertingen, Germany) and illuminated for 4 h with 5 µmol m^{-2} s^{-1} unilateral blue light. For the hypocotyl negative gravitropism response experiments, plates were reoriented by 90º and kept in the dark for additional 20 h. Plates were scanned and bending angles were quantified using Image J.

Immunoblots

For the detection of YFP tagged D6PK and its variants, roots of 7 day-old seedlings were homogenized with PEB (protein extraction buffer; 50 mM Tris-HCl [pH 7.5], 150 mM NaCl, 0.1 mM MG132, 0.1 mM PMSF, 1% [v/v] Protease inhibitor cocktail [Sigma], and PhosStop phosphatase inhibitor cocktail [Roche]), unless otherwise stated. Subcellular fractionation was performed by ultra-centrifugation at 100,000 *g* of pre-cleared total extracts (supernatant of 10,000 *g*, S10), obtaining soluble (supernatant, S100) and membrane (pellet, P100) fractions. P100 fractions were resuspended in same volume as S100 with PEB. Samples were denatured with 1x Laemmli buffer and heated at 42ºC for 15 min. For immunoblotting, the equivalent of 10 µg of total of protein was separated in 10% SDS-PAGE and transferred to nitrocellulose membranes (GE Healthcare) by semi-dry blotting. Immunoblots were detected with primary antibodies (rabbit α-GFP [1:3000, Life Technologies] and rabbit α-UGP [1:2000, Agrisera]) and secondary antibody (goat α-rabbit HRP [1:2000, Sigma]). Chemiluminescence detection was performed with a Fujifilm LAS 4000 mini (Fuji, Japan), total band intensities and band intensity profiles were quantified using the Fujifilm Multi Gauge v3.0 software as specified in the respective figure legends.

For phosphatase treatments, soluble and membrane protein extracts were prepared by homogenizing roots expressing YFP:D6PK and YFP:D6PKin in PEB without PhosStop followed by subcellular fractionation. Phosphatase treatments were performed using the equivalent of 30 µg of total protein of either soluble (S100) or membrane (P100) fractions, incubated with 350 U of λ phosphatase (λPPase) and the manufacturers buffer (1x) (New England Biolabs) for 15 min at room temperature. Heat inactivated (98°C, 5 min) λPPase was used as a negative control, and only the commercial buffer (1x) was added to the samples as a mock. The dephosphorylation reaction was stopped by the addition of 1x Laemmli buffer.

For PIN3 immunoblots, protein extraction, quantification and profile analysis was performed as previously described (Barbosa et al, 2014; Willige et al, 2013) using 4 day-old dark-grown seedlings.

Results

Phospholipid binding of D6PK and phospholipid-dependent D6PK localization in vivo

D6PK colocalizes with members of the PIN auxin-efflux facilitator family at the basal plasma membrane of many cells. The plasma membrane association of D6PK is essential for PIN phosphorylation, PIN activation, and auxin transport-dependent growth (Barbosa & Schwechheimer, 2014; Zourelidou et al, 2014). D6PK is a membrane-associated protein but the molecular determinants of this membrane association are unknown. To examine whether D6PK binds phospholipids, we performed *in vitro* lipid overlay experiments with recombinant D6PK and strips with a set of common plasma membrane lipids. In these experiments, D6PK was able to bind PA and the following PIPs: PI(3)P, PI(4)P and PI(5)P, $PI(3,4)P_2$, $PI(3,5)P_2$, $PI(4,5)P_2$, $PI(3,4,5)P_3$ **(Figure 3.3.1A)**. D6PK binding was strongest for PI(3)P when using Tris-buffered solutions and for PA when using phosphate-buffered solutions of comparable ionic strength (188 mM and 181 mM, respectively). Both experiments indicated a preference of D6PK for phospholipids containing polyacidic head groups, whereas no binding to phospholipids with neutral (PC and PE) or monoacidic (PI and PS) head groups was observed. We could, subsequently, confirm this binding preference in a lipid bilayer context where D6PK was bound to liposomes containing a mix of the polyacidic PA and neutral PS and PC, but not to liposomes containing only PS and PC **(Figure 3.3.1B)**.

To address whether phospholipid composition determines the intracellular distribution of D6PK *in vivo*, we examined D6PK localization following treatments with PIPs and PA biosynthesis inhibitors. PIPs biosynthesis starts from phosphatidylinositol (PI) and involves several phosphorylation and dephosphorylation steps by PIP-kinases and phosphatases; PA, on the other side, is produced either from $PI(4,5)P_2$ by phosphoinositide phospholipase C (PI-PLC) or from PC and PE by phospholipase D (PLD) (Meijer & Munnik, 2003) **(Figure 3.3.1C)**. Interestingly, Wortmannin (WM) and LY294002, inhibitors of PI3-kinase (WM and LY294002) and of PI4-kinase (WM) led to the internalization and depletion of D6PK from the plasma membrane already after 30 min (Baggiolini et al, 1987; Vlahos et al, 1994) **(Figure 3.3.1C** and **D)**. Surprisingly, this was not accompanied by an increase of soluble D6PK, as monitored by subcellular fractionation of root extracts **(Figure 3.3.1E)**. Strikingly, treatments with U73122 (+), an inhibitor of PI-PLC-mediated hydrolysis of $PI(4,5)P_2$, but not treatments with its inactive analog U73343 (-) led to a depolarization of D6PK from basal to apolar and appearance in endosomes (Bleasdale et al, 1990) **(Figure 3.3.1C** and **D)**. This effect was extremely fast and already detectable within 5 min of treatment (data not shown). These findings indicated that PI(3)P, PI(4)P or its derivatives were essential for D6PK plasma membrane association, whereas $PI(4,5)P_2$ or its derivatives critically determined D6PK basal polarity.

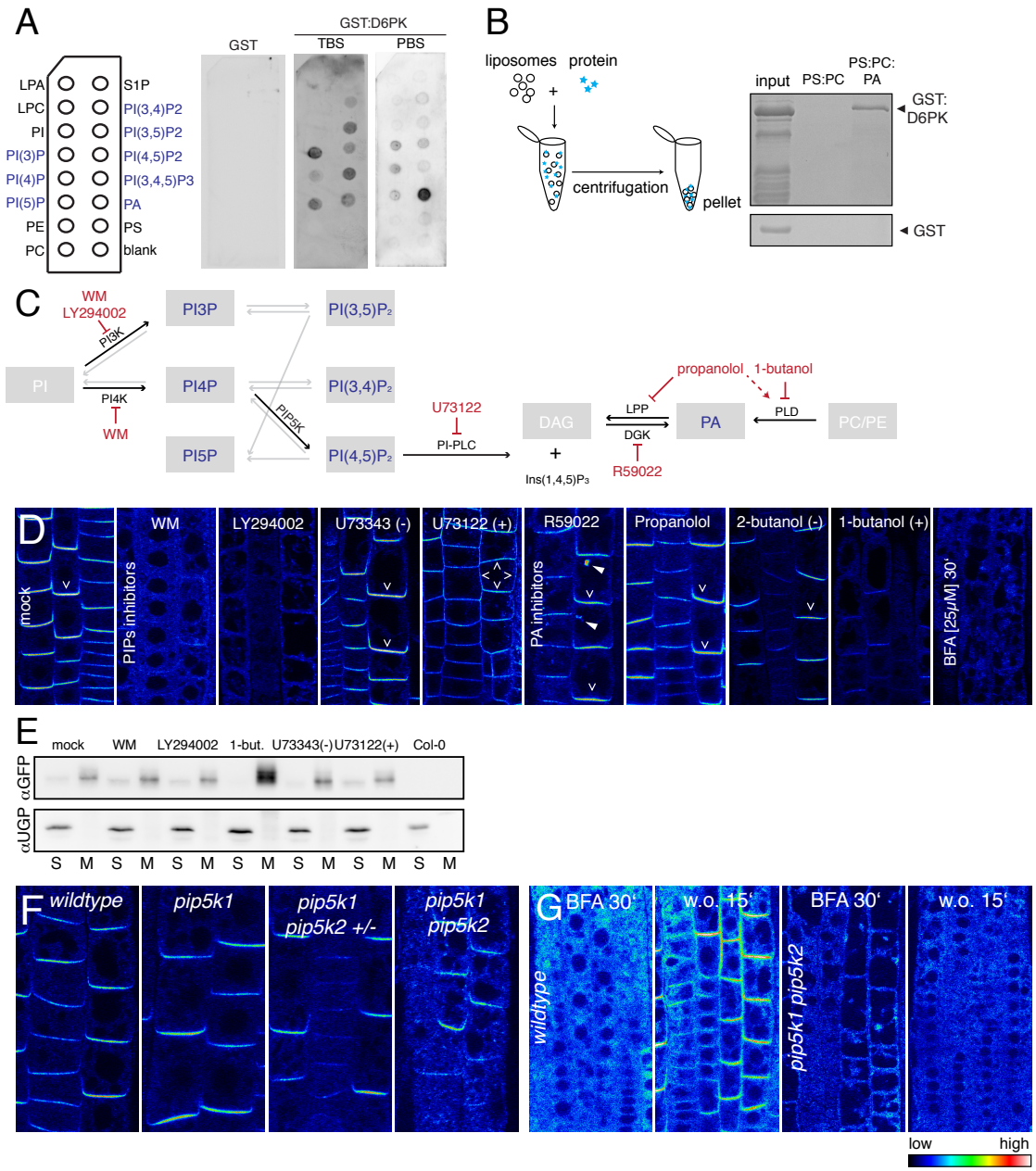

Figure 3.3.1 D6PK binds phospholipids *in vitro* and *in vivo* phospholipid composition determines its localization.

(A) and **(B)** Phospholipid binding assays with recombinantly expressed and purified GST and GST:D6PK and PIP-strip membranes (A) and liposome containing PC:PS and PC:PS:PA (B). **(C)** Schematic representation of PIP and PA biosynthesis and respective inhibitors in red. The black arrows mark biosynthetic steps and enzymes analyzed in our study (Aggarwal et al, 2013; Heilmann, 2009; Meijer & Munnik, 2003). **(D)** Representative confocal images of root epidermis cells from 5 day-old seedlings expressing D6PK:YFP:D6PK and treated with various inhibitors as indicated. All treatments were performed for 30 minutes in liquid media: mock [0.1% DMSO], WM [33 μM], LY294002 [200 μM)], U73343 (-) inactive and U73122 (+) active analogs [5 μM], R59022 [50 μM], Propanolol [50 μM], 2-butanol (-) inactive and 1-butanol (+) active analogs [0.8 %]. BFA treatment (25 μM, 30 minutes) is shown as control for signal intensity of internalized D6PK, known not to affect D6PK abundance. All experiments were repeated three times with similar results. **(E)** Immunoblots of protein extracts after subcellular fractionation by ultra-centrifugation from roots of 7 day-old 35S:YFP:D6PK seedlings treated in the same way as in (D), effects of the inhibitors on 35S:YFP:D6PK localization were similar in these conditions (data not shown). S, soluble supernatant; M, membrane

(Figure 3.3.1 continued) pellet. αGFP was used to detect YFP:D6PK, αUGP was used as a control for the soluble fraction. **(F)** and **(G)** Localization of D6PK:YFP:D6PK in *pip5k1 pip5k2* mutants in untreated (F); after BFA treatment [25 μM] for 30 min (BFA 30') and after same BFA treatment followed by 15 min washout (w.o. 15') (G). The analysis was performed in root epidermis of 7 day-old D6PK:YFP:D6PK *pip5k1/pip5k1 PIP5K2/pip5k2* seedlings (n=30), followed by genotyping, with similar results for at least 6 seedlings per genotype. The semiquantitive color-coded heatmap for signal intensities in (D), (F), and (G) is provided. LPA, lysophosphatidic acid; LPC, lysophosphatidylcholine; PI, phosphatidylinositol; PI(x)P, phosphatidylinositol mono-/bi-/tri-phosphates or phosphoinositides; PE, phosphatidylethanolamine; PC, phosphatidylcholine; S1P, sphingosine-1-phosphate; PA, phosphatidic acid; PS, phosphatidylserine; PI3K, PI 3-kinases; PI4K, PI 4-kinases; PI5K, PI 5-kinases; PIP5K, PI(4)P 5-Kinases; WM, Wortmannin; PI-PLC, PI(4,5)P_2-phospholipase C; Ins(1,4,5)P_3, inositol 1,4,5-triphosphate; LPP, lipid phosphate phosphatase; DAG, diacylglycerol; DGK, DAG Kinase; PLD, phospholipase D.

We also modulated PA abundance with R59022, an inhibitor of DAG kinase (DGK) and PI-PLC dependent-PA synthesis (de Chaffoy de Courcelles et al, 1985) **(Figure 3.3.1C)**. While this treatment did not result in the reduction or depolarization of plasma membrane-associated D6PK, it led to the accumulation of D6PK in large endosomal compartments **(Figure 3.3.1D)**. At the same time, inhibition of PLD-dependent PA production by 1-butanol treatment did not affect D6PK polarity but resulted in the partial internalization of D6PK (Potocky et al, 2014) **(Figure 3.3.1D)**. This was, however again, not accompanied by a solubilization of D6PK **(Figure 3.3.1E)**. Conversely, anticipated increases in PA abundance by propanolol treatment had no obvious effect on D6PK localization (Potocky et al, 2014) **(Figure 3.3.1D)**. Taken together, these results suggest that intracellular PA levels contribute to D6PK localization, but in a differential manner depending on whether they are derived from PI-PLC or PLD pathways.

In summary, D6PK was able to bind the polyacidic phospholipids PIPs and PA *in vitro*. Pharmacologic interference with PIP and PA metabolism *in vivo* led to either D6PK internalization to endosomes or depolarization, but never to its complete solubilization. These findings suggest that the relative distribution of polyacidic PIPs and PA determine the specificity of D6PK for plasma membrane or endomembranes, and, in the case of the interference with PI(4,5)P_2, the restriction of D6PK to the basal plasma membrane domain.

PIP5K1 and PIP5K2 are required for proper targeting and recycling of D6PK

The *in vitro* binding assays and the inhibitor analysis suggested that PI(4,5)P_2 may control D6PK polarity in the root epidermis. This finding was intriguing because PI(4,5)P_2 is known to accumulate in apical-basal domains of root epidermal cells (Ischebeck et al, 2013; Tejos et al, 2014). Among the 11 isoforms of PIP5Ks (PI(4)P 5-kinases), PIP5K1 and PIP5K2 preferentially localize to apical-basal domains in the root epidermis (Ischebeck et al, 2013; Tejos et al, 2014). When we introduced YFP:D6PK (D6PK) into the *pip5k1 pip5k2* mutant, we noted the presence of D6PK in intracellular vesicles in the double mutant but not in the *pip5k* single mutants **(Figure 3.3.1F)**. To dissect whether D6PK recycling was affected in these mutants, we tested the response to the recycling inhibitor BFA. While the internalization of D6PK following BFA-treatment was comparable between the wild type and the *pip5k1 pip5k2* mutant, the retargeting of YFP:D6PK to the plasma membrane following a 15 min BFA wash was compromised in *pip5k1 pip5k2* where retargeting to the basal plasma membrane could only

be observed after one hour **(Figure 3.3.1G** and not shown). This suggested that the targeting of YFP:D6PK to the plasma membrane is PI(4,5)P_2-dependent.

The D6PK middle domain is required and sufficient for D6PK plasma membrane anchoring

AGCVIII protein kinases, including D6PK, contain a kinase domain that is interrupted in the sub-domains VII and VIII by a 36 - 90 amino acid insertion or middle domain (MID) and flanked by a long N-terminus and a short C-terminus **(Figure 3.3.2A)** (Galván-Ampudia & Offringa, 2007). To identify the membrane-anchoring domain of D6PK, we analyzed the *in vivo* localization of D6PK deletion variants of the N-terminus (ΔN), the middle domain (ΔMID), and the C-terminus (ΔC); as well as the respective single domains as YFP-fusions. Interestingly, the plasma membrane association was lost in the deletion variants of any of the three domains that accumulated in the cytosol, but subcellular fractionation analysis showed that all three variants still retained endomembrane association **(Figure 3.3.2B)**. In the case of ΔMID, endosomal localization was visible in confocal images, but these were not detectable for ΔN and ΔC, prossibly due to their weak expression **(Figure 3.3.2B**; open arrows). Conversely, when examined in isolation, the N- and C-termini did not show an intrinsic ability either to localize to the plasma membrane or to associate to endomembranes. In turn, the MID domain was sufficient not only for plasma membrane association but also, at least partially, for D6PK polarity **(Figure 3.3.2B**; note the MID signals at the basal and lateral domains). To identify the nature of endosomal D6PK deletion variants and possible recycling of MID domain, we performed BFA-treatments. While none of the deletions accumulated as clear as D6PK in the BFA compartment, the MID domain was not or only partially internalized as it was still detected at the plasma membrane after 90 minutes of BFA treatment **(Figure 3.3.2C** and **Supplementary Figure 3.3.1)**. In summary, we found that D6PK plasma membrane localization required all three domains outside of the kinase domain but only the MID domain, though having different recycling kinetics than D6PK, was sufficient to recapitulate D6PK plasma membrane association and polarity.

To determine which domain could confer kinase substrate-specificity and whether these deletions were active kinases, we performed *in vitro* kinase assays using the PIN1 cytosolic loop as a phosphorylation substrate. Here, we found that ΔN and ΔMID lost the ability to transphosphorylate PIN1, but retained their kinase activity as revealed by their autophosphorylation, which was interestingly increased compared to D6PK. In turn, ΔC yielded no detectable auto- or trans-phosphorylation activities **(Figure 3.3.2D)**. Thus, these results indicated that the N-terminus and the MID domain might participate in the recognition of PIN substrates by D6PK, whereas the C-terminus may be involved in the control of D6PK kinase activity.

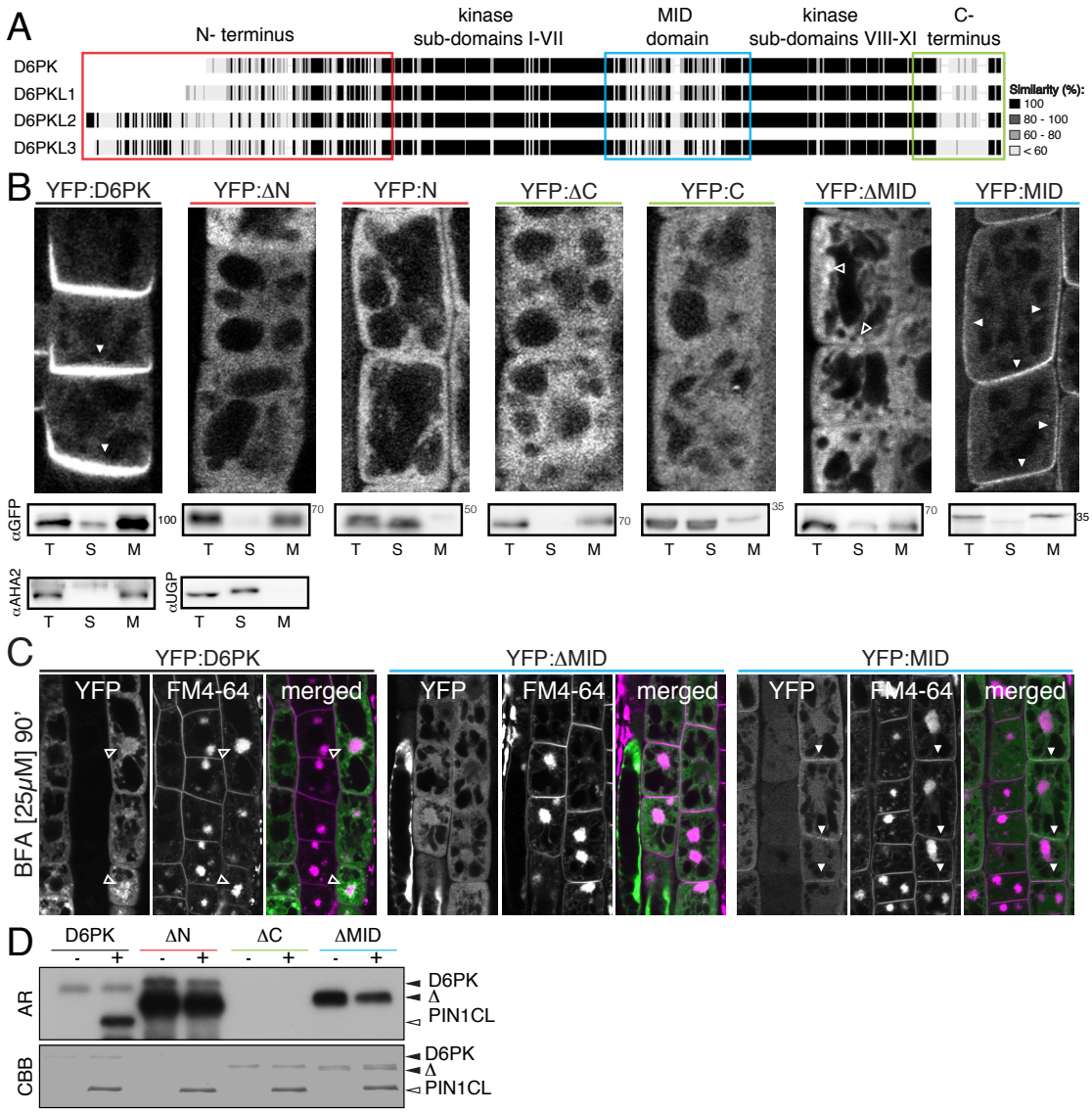

Figure 3.3.2 The middle domain of D6PK is required and sufficient for D6PK plasma membrane localization. **(A)** Alignment of protein sequences of D6PK and D6PKL-1 to D6PKL-3 with amino acid similarities coded in gray-scale and depiction ofapproximate position of analyzed domains. **(B)** Representative confocal images of root meristem epidermis from 7 day-old seedlings (upper) and αGFP immunoblots of protein extracts after subcellular fractionation by ultracentrifugation of root extracts from 7 day-old seedlings (lower panels) of 35S:YFP:D6PK and its deletion variants. T, total fraction (supernatant at 10,000 *g*, S10); S, soluble fraction (S100); and M membrane fraction (P100). Representative membrane plasma membrane H^+-ATPase (αAHA2), and soluble UDP-glucose pyrophosphorylase (αUGP) controls. **(C)** Confocal images 35S:YFP:D6PK (YFP:D6PK) and the 35S:YFP:D6PK deletion variants YFP:ΔMID and YFP:MID, treated with BFA [25 *μ*M] and FM4-64 [2 *μ*M] in liquid media for 90 min. **(D)** Representative autoradiographs (AR) and Coomassie Brilliant Blue (CBB)-stained loading control from *in vitro* kinase assays with recombinant GST:D6PK (D6PK), GST:D6PK-deletions (ΔN, ΔC and ΔMID) with and without the GST:PIN1 cytosolic loop (PIN1 CL).

The MID domain harbors a K-rich motif required for phospholipid binding and D6PK plasma membrane association

Since the middle domain was sufficient to target D6PK to the basal plasma membrane and D6PK plasma membrane targeting was seemingly controlled by phospholipid binding, we searched for possible motifs that could confer D6PK binding to negatively charged phospholipids. Our attention was drawn to a positively charged motif comprised of six lysines (K) that was conserved among the 4 D6PK homologues, which we designated the K-rich motif **(Figure 3.3.3A)**. In line with a functional role of this motif, we found that phospholipid binding was partially or fully compromised when three (3KA) or six (6KA) lysines were replaced by uncharged alanines in D6PK **(Figure 3.3.3B)**. Importantly, these mutations did not affect the D6PK auto- or trans-phosphorylation activities in *in vitro* kinase assays **(Figure 3.3.3C)**.

In parallel, we also observed that these 3KA and 6KA mutations impaired the plasma membrane association of YFP:D6PK and led to an accumulation of the proteins in the cytosol as well as in endosomes. The internalization ranged from partial to complete, for the 3KA and 6KA variants, respectively, either expressed from the constitutive 35S CaMV promoter or the *D6PK* promoter **(Figure 3.3.3D and E)**. Curiously, the 6KA protein expressed from the strong constitutive 35S CaMV promoter was apparently more internalized than when expressed from the *D6PK* promoter. This suggested that higher 6KA protein dosage leads to more internalization. This observation contrasted the fact that, when expressed from the *D6PK* promoter, the stronger 6KA expressing lines had substantially more plasma membrane localized *D6PK* than weaker lines. Since *D6PK* promoter most likely confers endogenous D6PK protein levels, it is reasonable to assume that the internalization of 6KA mutants decreased with increasing abundance of the protein. This scenario would match the observation from the *in vitro* binding assays that lysine mutations reduced but did not completely abolish the affinity of D6PK for phospholipids. Subcellular fractionation using the 35S CaMv expressing lines showed that the membrane association of D6PK was unaffected in the 3KA variant but was reduced from ~80% to only 40% in 6KA, suggesting that besides contributing to plasma membrane association, the K-rich motif contribute to the D6PK membrane binding *per se* **(Figure 3.3.3F)**. Taken together, these results showed that the K-rich motif within the middle domain was required for D6PK phospholipid binding *in vitro* and conferred the ability to D6PK to be recruited to the basal plasma membrane and to membranes in general.

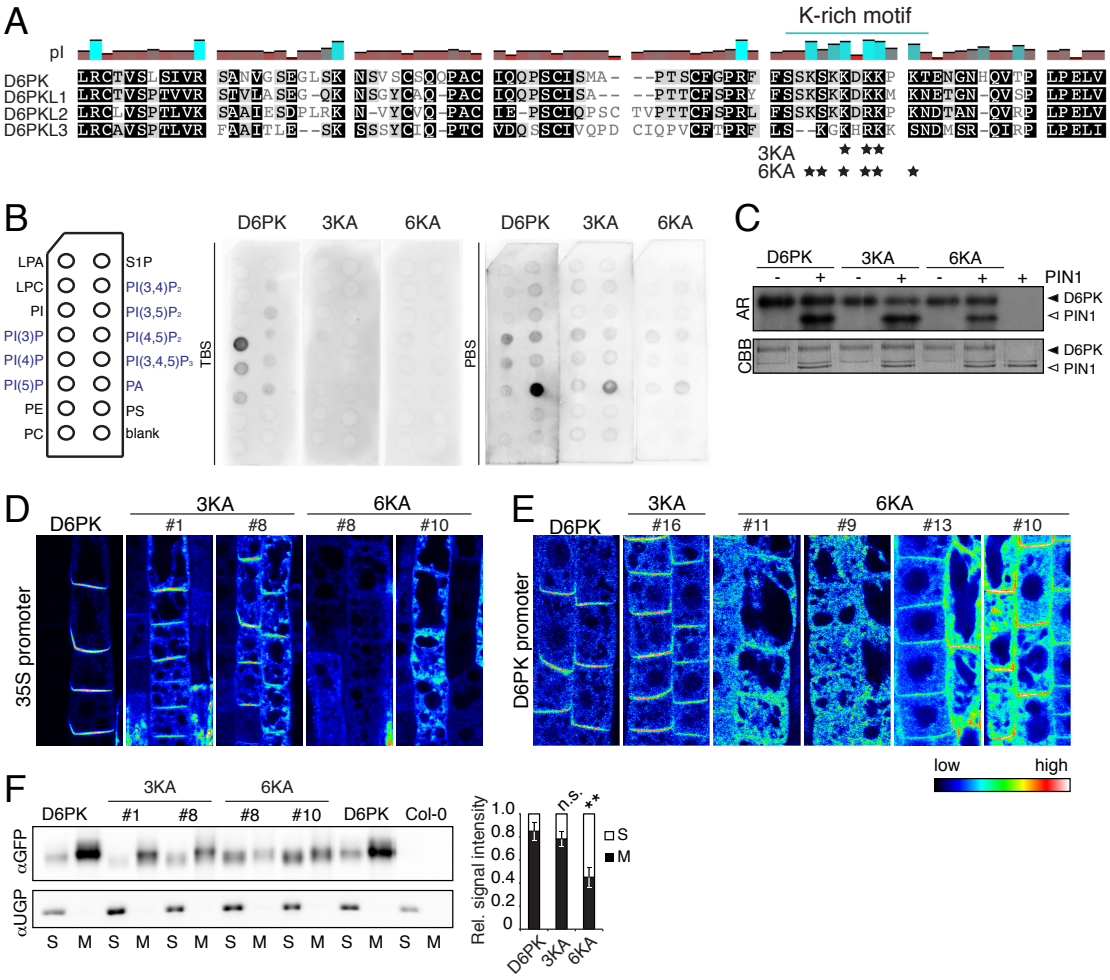

Figure 3.3.3 The K-rich motif within the middle domain is required for D6PK phospholipid binding, membrane association, and plasma membrane localization.

(A) Alignment of the middle domain protein sequences of D6PK (a.a. 255 to 335 in D6PK) and D6PKL1 – D6PKL3 with the amino acid similarities coded in gray-scale and the mean isoelectric point (pI) from basic (blue) to acidic (red) at each position. The stars depict lysine-to-alanine substitutions in 3KA and 6KA in the K-rich motif. **(B)** Representative PIP-strip lipid overlay assay with GST:D6PK (D6PK) and GST:D6PK-3KA (3KA) and GST:D6PK-6KA (6KA). **(C)** Representative autoradiographs (AR) and respective CBB (Coomassie Brilliant Blue)-stained loading control gels from *in vitro* kinase assays with recombinant D6PK, 3KA, and 6KA with and without the GST:PIN1 cytosolic loop (PIN1 CL). **(D)** and **(E)** Confocal images of YFP:D6PK, YFP:D6PK-3KA (3KA), and YFP:D6PK-6KA (6KA) in root meristem epidermis of 7 day-old seedlings, expressed from the 35S CaMv (D) and the *D6PK* (E) promoters. Numbers refer to the identity of independent T1 transgenic lines. **(F)** Representative immunoblot with αGFP after subcellular fractionation of root extracts from 35S:YFP:D6PK, 3KA and 6KA seedlings. Densitometric quantification of the relative signal intensities of S and M fractions was performed using three biological replicates and by pooling two transgenic lines for 3KA and 6KA.

The K-rich motif is required for D6PK function in a plasma membrane localization-dependent manner

D6PK abundance at the plasma membrane is critical for PIN phosphorylation and auxin-transport dependent growth (Barbosa et al, 2014). The *d6pk d6pkl1* (*d6pk01*) mutants are impaired in auxin transport- and PIN-dependent growth responses, including negative gravitropism and phototropism of the hypocotyl (Willige et al, 2013). To test the functionality of the mislocalized 3KA and 6KA D6PK protein variants in these responses, we introduced a D6PKp:YFP:D6PK transgene with these mutations into *d6pk01* double mutants. While the wild-type and 3KA mutated versions efficiently complemented *d6pk01* tropism defects in negative gravitropism and phototropism assays, the 6KA mutant lines varied from no to almost full complementation **(Figure 3.3.4A** and **B)**. The complementation efficiency of the individual 6KA lines correlated with the expression level and plasma membrane abundance of the proteins: strongly expressing lines with plasma membrane localized 6KA (or 3KA) complemented the mutant, whereas low expressing lines with only internalized 6KA did not complement **(Figure 3.3.4A, B** and **Figure 3.3.4E)**. These findings indicated that the kinases with the lysine mutations were functional, as also suggested by the *in vitro* kinase assays, but only when present at the plasma membrane.

Overexpression of *D6PK* leads to defective hypocotyl growth in dark grown seedlings. This growth defect likely results from misregulated auxin transport as a consequence of increased D6PK abundance at the plasma membrane and ectopic expression. This phenotype can be suppressed with the auxin transport inhibitor NPA and also with mild BFA treatments that are sufficient to displace D6PK but not the PINs from the plasma membrane (Barbosa et al, 2014; Zourelidou et al, 2009). Interestingly, the observed defects in hypocotyl bending, apical hook formation, and cell shape of the *D6PK* overexpression lines, were milder when the partially internalized 3KA was overexpressed and almost completely absent when the completely internalized 6KA was overexpressed **(Figure 3.3.4C, D** and **Figure 3.3.4D)**. Thus, ectopic function of D6PK in auxin-transport dependent growth strictly required an intact K-rich motif and the presence of D6PK at the plasma membrane.

PIN3 is a major PIN protein in hypocotyl tropisms and a direct target of D6PK phosphorylation. PIN3 phosphorylation is strongly reduced in higher order *d6pk* mutants, such as *d6pk01* and *d6pk012* (Willige et al, 2013), and also in conditions interfering with *D6PK* localization such as BFA-treatment or $gnom^{B/E}$ mutations (Barbosa et al, 2014). When we examined the PIN3 phosphorylation levels in the D6PKp:YFP:D6PK lines with 3KA and 6KA mutations, we detected a clear correlation between the ability to complement the tropism defects of *d6pk01* **(Figure 3.3.4A** and **B)** and PIN3 phosphorylation levels **(Figure 3.3.4E-G)**. We thus concluded that the K-rich motif critically determined the ability of D6PK to maintain PIN phosphorylation levels and consequently auxin transport-dependent growth. Importantly, our results indicate that K-rich contribution to this is through the control of D6PK abundance at the plasma membrane and not through the control of D6PK kinase activity.

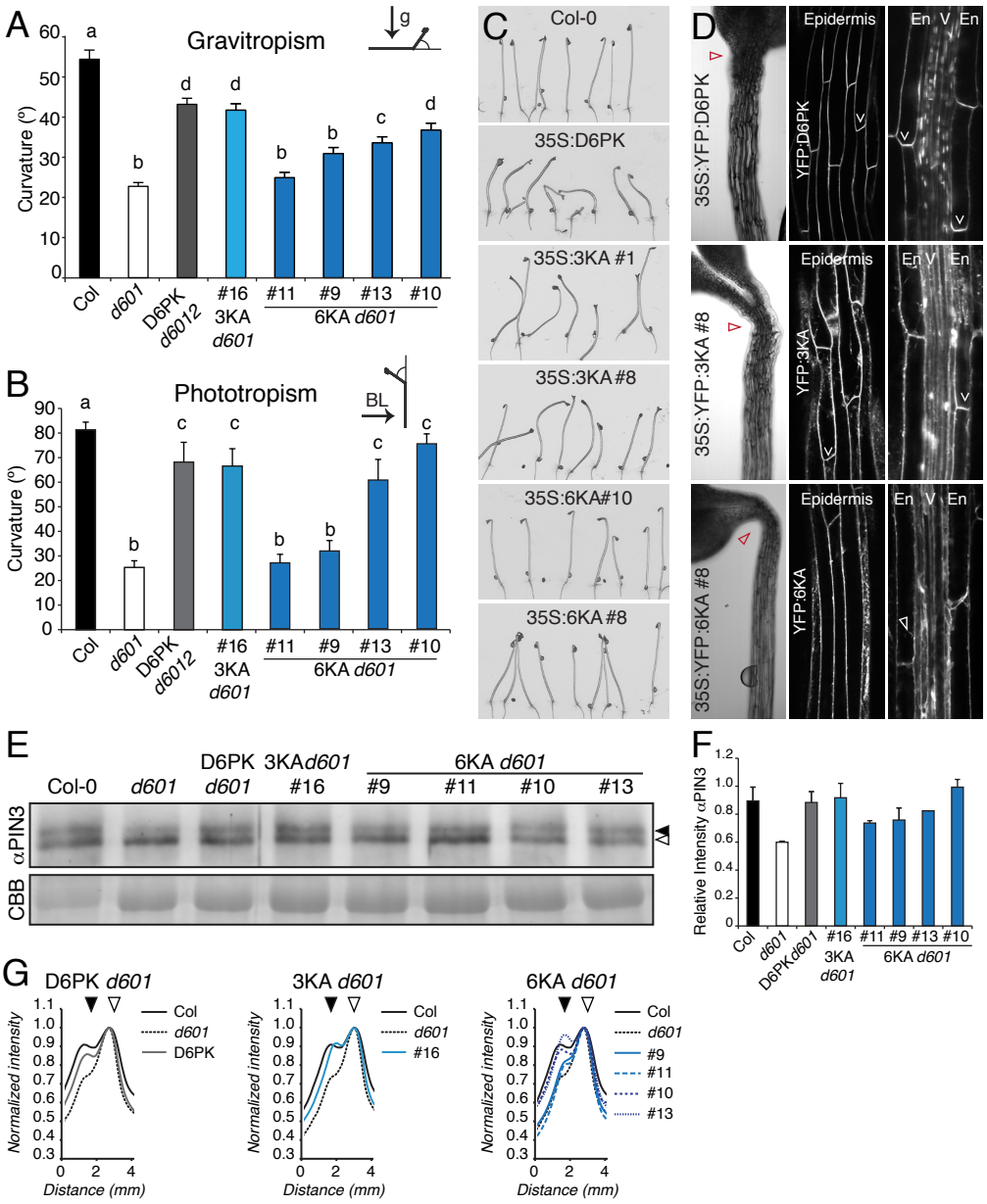

Figure 3.3.4 K-rich motif is required for proper D6PK function in hypocotyl tropic responses and PIN3 phosphorylation in a plasma membrane abundance-dependent manner.

(A) and **(B)** Complementation of tropism defects of *d6pk* mutant phenotypes in independent transgenic lines with D6PKp:YFP:D6PK in *d6pk012* and D6PKp:YFP:D6PK carrying 3KA or 6KA mutations in *d6pk01* (T3 hemizygous generation). Negative gravitropic hypocotyl bending after reorientation by 90º for 20 hrs (A) and hypocotyl phototropic response after 4 hrs of 5 µmol m^{-2} s^{-1} blue light (B) of 3 day-old etiolated seedlings; shown is the average and standard error from 3 biological replicates of one representative experiment; n > 30 seedlings. Pairwise Student's t-test, different letters mark statiscally significant differences ($p < 0.05$), same letter represent non-statiscally significant differences. **(C)** Representative photographs of 3 day-old etiolated seedlings overexpressing D6PK, 3KA and 6KA. Two independent T1 transgenic lines are shown. **(D)** Representative confocal pictures of 3 day-old etiolated seedlings of 35S:YFP:D6PK and 35S:YFP:D6PK carrying 3KA (YFP:3KA) and 6KA (YFP:6KA) mutations: hypocotyl and apical hook overview (left pannel, bright field); hypocotyl epidermis surface view (middle, YFP channel) and mid hypocotyl view, depicting endodermis (En) and vasculature (V) tissues (right, YFP channel). **(E)** and **(F)** Representative immunoblots of membrane protein extracts from 4 day-old etiolated seedlings with αPIN3 and CBB loading control (E) and respective densitometric profiles comparing the relative intensities of the upper band, i.e. phosphorylated PIN3 (closed arrow) and the lower band, i.e. unphosphorylated PIN3 (open arrow) of the different proteins and complementation lines to Col-0 and *d6pk01*. Each profile was normalized to and aligned to the maximum value of the lower band (F). **(G)** Mean and standard deviation of the relative upper to lower band intensities of αPIN3 signals from two biological replicates.

D6PK is phosphorylated by other kinases at the plasma membrane

AGC kinases from other organisms and also several plant AGCVIII kinases (e.g. *Arabidopsis* phot1 and tomato ADI3) are themselves phosphorylation targets and phosphorylation impacts on their function and localization (Ek-Ramos et al, 2010; Kaiserli et al, 2009; Pearce et al, 2010). As we were interested in identifying mechanisms controlling D6PK activity and localization, we noticed with interest that the electrophoretic mobility of D6PK in SDS-PAGE was altered after treatment with BFA (Barbosa et al, 2014) as well as in the lysine mutant variants **(Figure 3.3.3F)**, suggesting that D6PK is post-translationally modified. To identify whether the observed D6PK mobility changes could be a result of phosphorylation, we performed λ phosphatase treatments on root extracts of 35S:YFP:D6PK seedlings. We found that both, membrane and soluble D6PK fractions, were sensitive to these phosphatase treatments, resulting in the appearance of faster migrating bands, which were absent in samples treated with the mock and inactive phosphatase **(Figure 3.3.5A** and **B**, red arrow). In addition, although the inactive kinase dead version of D6PK (*D6PKin*) showed faster mobility than D6PK in the mock control, *D6PKin* was still sensitive to the phosphatase treatment and run with a similar mobility as phosphatase-treated wild-type D6PK. Careful analysis of the D6PK migration profiles during a BFA-time course experiment, showed that BFA induced an almost complete disappearance of the phosphatase-sensitive forms of D6PK and the appearance of the presumably de-phosphorylated fast migrating form of D6PK **(Figure 3.3.5C)**. Taken together, these results suggested that D6PK is highly phosphorylated by other protein kinases, and to some extent by itself, and, as predicted based on its SDS-PAGE mobility after BFA treatment this phosphorylation seemingly occurs only when D6PK is present at the plasma membrane.

Putative phosphorylation sites near the K-rich motif are crucial for D6PK plasma membrane abundance, polarity, and recycling

D6PK is constitutively targeted to and removed from the plasma membrane and auxin treatment promotes its internalization (Barbosa et al, 2014). It is conceivable that the plasma membrane association through the K-rich motif is regulated and mediates these changes on D6PK localization. Interestingly, a global phosphoproteomic study had identified phosphorylation at two conserved serines in D6PKL2 corresponding to S310 and S311 in D6PK (Durek et al, 2010; Heazlewood et al, 2008) **(Figure 3.3.6A)**. Since these two serines are directly adjacent to the K-rich motif, we predicted that this phosphorylation could regulate the function of D6PK and possibly of the K-rich motif. To address this, we replaced these two serines by either uncharged alanines (SSAA, phosphomutant) or by negatively charged aspartic acid (SSDD, phosphomimic) to mimic the negative charges introduced by the serine phosphorylation. Importantly, neither of these mutations affected the *in vitro* kinase activity of D6PK **(Figure 3.3.6B)**. Interestingly, SSAA mutation on D6PKp:YFP:D6PK led to a less internalized and also less polarized D6PK localization in the root epidermis, as determined by the ratios of cytosolic to membrane (internalization index) and of lateral to basal (polarity index) average pixel intensities, respectively. In turn, the SSDD mutated lines displayed no change in polarity but an increased internalization index **(Figure 3.3.6C – E)**. In subcellular fractionation with overexpressing

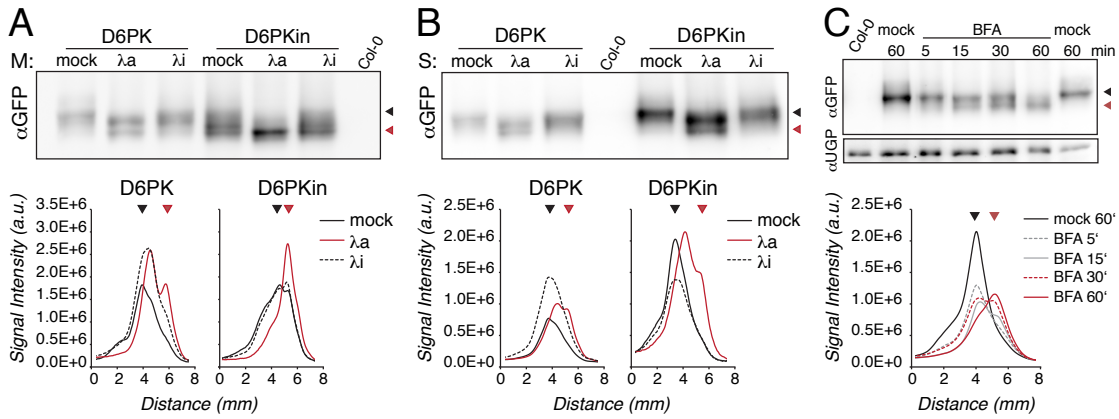

Figure 3.3.5 D6PK is phosphorylated by other kinases in a localization-dependent manner.
(A) and **(B)** Immunoblots with α-GFP and respective densitometric profiles of membrane (A) and soluble (B) fractions from root protein extracts of 7 day-old 35S:YFP:D6PK (D6PK) and inactive 35S:YFP:D6PK (D6PKin) seedlings. The fractions were split into three treatments: mock, active lambda phosphatase (λa) and heat-inactivated lambda phosphatase (λi). No normalization or alignment of the profiles was performed. Both D6PK and D6PKin protein mobilities were affected by λa treatment. Note the appearance of a new intensity peak with faster mobility in λa samples (red arrow) relative to an intensity peak with slower mobility that is typical in the mock and λi samples (black arrow). D6PKin mock and λi samples showed two peaks of equal intensity, but predominantly one faster peak after λa treatment (A). Shown is one representative of three biological replicates. **(C)** D6PK SDS-PAGE mobility changes after BFA treatment [25 *μ*M] from membrane fractions of root extracts of 7 day-old seedlings monitored by αGFP immunoblot and respective densitometric profiles. Note the progressive shift from a slow migrating form to a faster migrating form. Shown is one representative of three biological replicates.

lines of these constructs, we detected a significant increase in soluble SSDD protein, suggestive for a reduced affinity to membranes, whereas SSAA fractionated similar to the wild-type D6PK protein **(Figure 3.3.6F** and **G)**. In these immunoblots, we observed two unexpected results. On the one side SSAA protein migration was seemingly unaltered in comparison to the wild-type; and on the other side the presumably phosphomimic SSDD migrated faster **(Figure 3.3.6H)**, similarly to the non-phosphorylated forms of D6PK **(Figure 3.3.5)**. Although protein SDS-PAGE mobility can be a good indicator of the phosphorylation status of a given protein, this is not a precise predictive feature, i.e. phosphorylation is not always accompanied by SDS-PAGE mobility changes, since these do not only rely on mass but seem to depend on the charge of the surrounding residues (Peck, 2006). Therefore, these results indicated that the integrity of S310 and S311 was required for proper D6PK membrane targeting and polarity control, probably through phosphorylation, but that the loss of phosphorylation by SSAA mutations did not impact on D6PK in SDS-PAGE mobility. The unexpected faster migration of the phosphomimic SSDD could be maybe explained by the depletion of the protein from the plasma membrane, which possibly affects its protein-protein interaction environment and leads to reduced total phosphorylation levels, similar to what is observed for internalized D6PK after BFA treatment **(Figure 3.3.5)**.

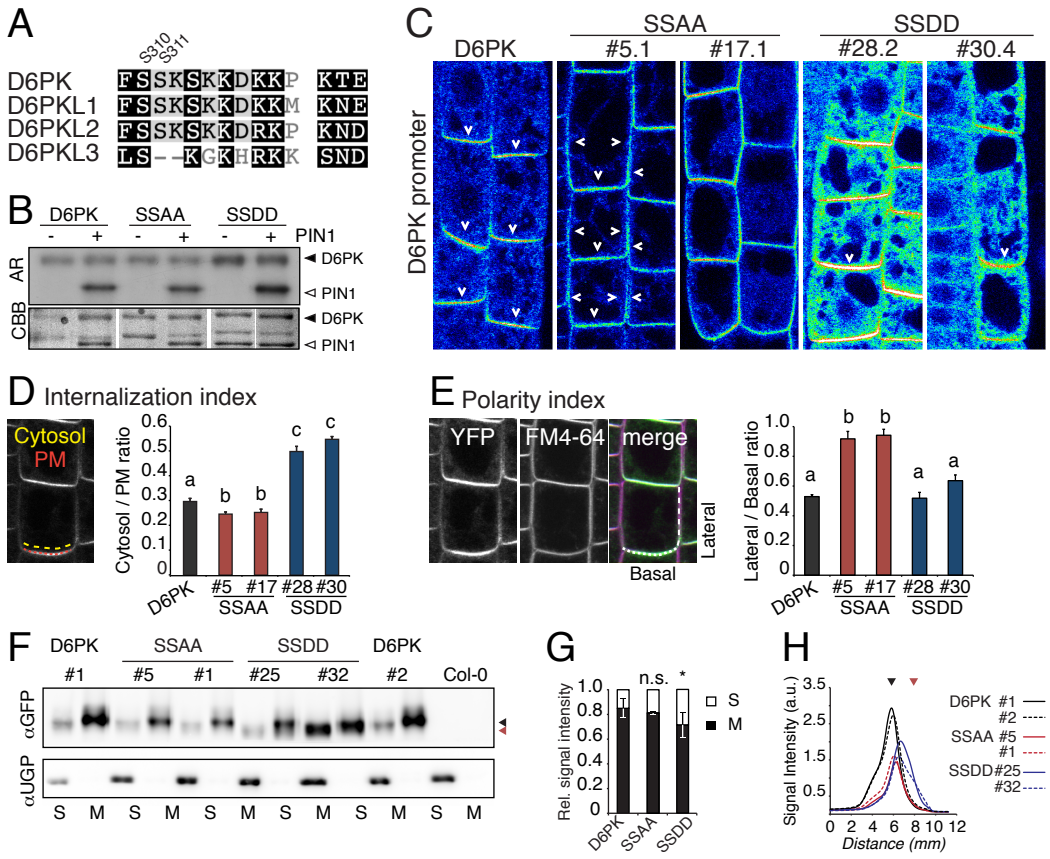

Figure 3.3.6 Serines 310 and 311 are required for the polarity and membrane association of D6PK.
(A) Alignment protein sequences of the K-rich motif and adjacent S310 and S311 phosphorylation targets of D6PK and D6PKL1 – D6PKL3 (a.a. 309 to 322 in D6PK) with amino acid similarities coded in gray-scale as in Figure 3.3.3. (B) Representative autoradiograph (AR) and Coomassie Brilliant Blue (CBB) of *in vitro* kinase assay with GST:D6PK, GST:D6PK-SSAA and -SSDD, with or without the PIN1 cytosolic loop substrate. Experiment was repeated twice with similar results. (C) Confocal images of root meristem epidermis cells of 5 day-old D6PKp:YFP:D6PK and D6PKp:YFP:D6PK-SSAA (SSAA) and -SSDD (SSDD) seedlings showing independent T1 transgenic lines. (D) Quantification of the respective internalization index, as the ratio of average gray values of cytosol (line above the plasma membrane, yellow) to plasma membrane (red line). (E) Quantification of the polarity index, as the ratio of lateral to basal plasma membrane average gray values in the YFP channel, normalized to the same ratio in the FM4-64 channel of the same picture. Pairwise Student's t-test, different letters mark statiscally significant differences ($p < 0.05$), same letter represent non-statiscally significant differences. (F) Representative αGFP immunoblot of subcellular fractionation of root extracts from 7 day-old seedlings of independent 35S:YFP:D6PK and 35S:YFP:D6PK-SSAA (SSAA) and -SSDD (SSDD) T1 transgenic lines. S, soluble; M membrane fraction. (G) Densitometric quantification of the relative signal intensities of S and M fractions of 3 biological replicates, pooling the transgenic lines from respective phenotypes. (H) Densitometric profiles of M fractions from blot in (F), note that both SSAA lines have the same mobility as D6PK, as judged by the maximum peak position (black arrowhead), whereas both SSDD lines have relatively more protein with faster mobility than D6PK or SSAA, as judged by the broader distribution of the profiles towards the end of the gel (red arrowhead). Note that possible drifts in SDS-PAGE are controlled by the mobility (see profiles) of two D6PK samples in the first and last lane of the blot.

Given that phosphorylation at S310 and S311 could underlie the control of D6PK localization, we were interested to see whether SSAA and SSDD mutants were impaired in the BFA- and auxin-induced internalization of D6PK. Upon BFA treatment, both D6PK and SSDD were completely detached from the plasma membrane and appeared in the BFA-compartments. In contrast, SSAA remained at the plasma membrane although the FM4-64-labelled BFA compartments were clearly formed also in these cells **(Figure 3.3.7A)**. This implied that phosphorylation at S310 and S311 was required for the constitutive internalization of D6PK, which can be observed when inhibiting D6PK targeting by BFA. However, auxin treatments that we had previously shown to promote D6PK internalization had similar effects on the localization of SSAA and SSDD mutants **(Figure 3.3.7B)**, indicating that auxin-induced D6PK internalization is independent of these two serines and likely their phosphorylation status.

In summary, this analysis revealed that mutations in the putative phosphorylation sites impair D6PK plasma membrane association and polarity. These results are in agreement with the presumed role of S310 and S311 phosphorylation as a surface charge switches in the proximity to the K-rich motif, triggering D6PK internalization. Interestingly, loss of phosphorylation in SSAA led to a more stable membrane association (reduced cytosol/PM ratio and loss of BFA-sensitivity) and a loss of polarity. We, thus, propose that S310 and S311 phosphorylation-mediated internalization is required for D6PK recycling and polarity maintenance. Since SSAA and SSDD, like D6PK, display auxin-dependent internalization, the promotive effects of auxin on D6PK internalization are likely dependent on other mechanisms.

S310 and S311 are likely phosphorylation targets of D6PK

So far, our analysis supported a possible role of phosphorylation at positions S310 and S311in D6PK plasma membrane polar targeting and recycling. To further test whether these sites are indeed phosphorylation targets, we reasoned that treatments with kinase- and phosphatase-inhibitors could lead to similar defects on D6PK localization *in vivo* as in the phosphosite mutations, and that SSAA and SSDD should be either insensitive or hypersensitive to these treatments. Interestingly, we found that treatment with Staurosporine, a broad-spectrum kinase inhibitor (Omura et al, 1995), led to the depolarization of D6PK **(Figure 3.3.7C)** and thereby strongly resembled the SSAA localization. However, while the already depolarized SSAA remained unchanged, Staurosporine treatment led also to the depolarization of SSDD as in the case of D6PK **(Figure 3.3.7C)**. This result indicated that Staurosporine-induced D6PK depolarization was independent of the S310 and S311 phosphorylation status and thus mechanistically different from the depolarization observed in SSAA. This was not surprising since Staurosporine is a broad-spectrum kinase inhibitor (Walker et al, 2000). Interestingly the Staurosporine-induced apolar D6PK remained BFA-sensitive (data not shown) whereas SSAA was BFA-insensitive. In turn, treatment with the Ser-/Thr-phosphatase inhibitor Calyculin A led to an almost complete internalization of D6PK but had no effect on SSAA localization, indicating that phosphorylation at S310 and S311 was likely involved in Calyculin A-induced D6PK internalization (Ishihara et al, 1989). However, the already partially internalized SSDD

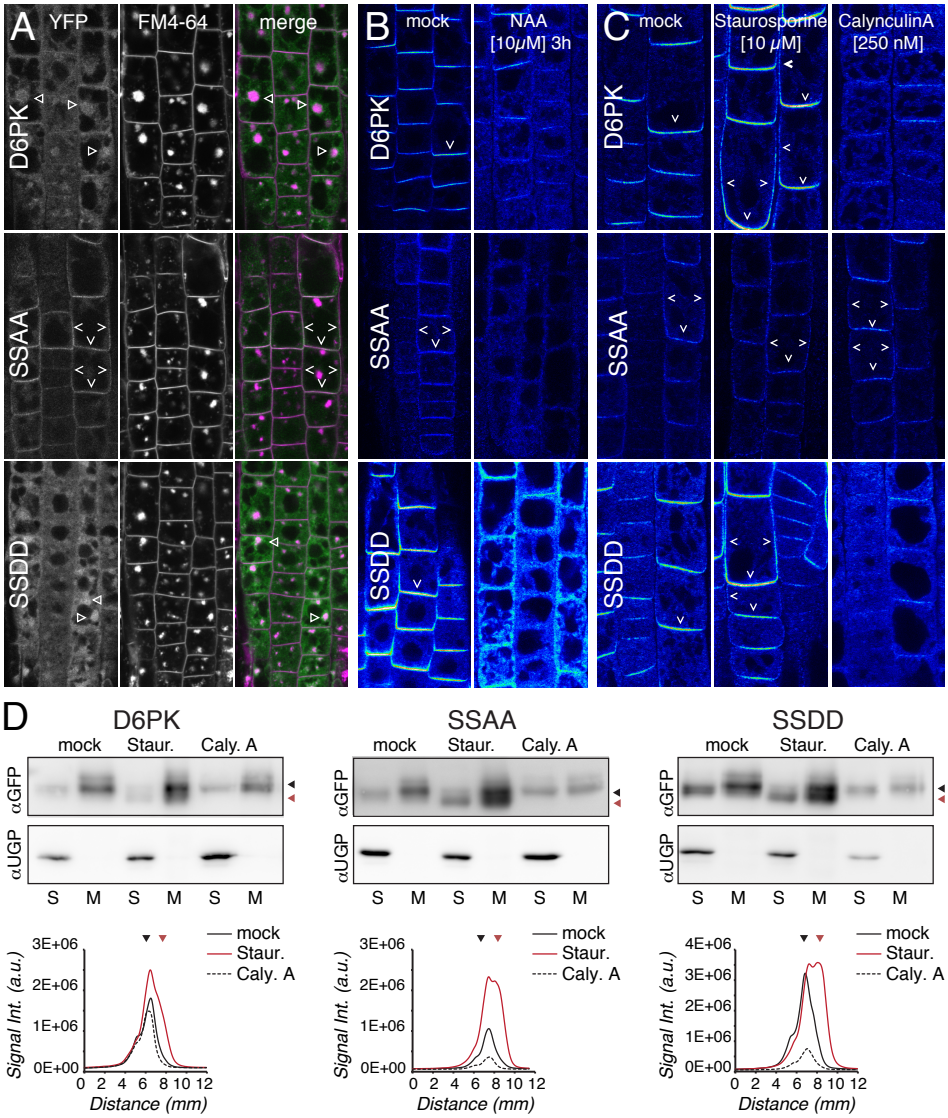

Figure 3.3.7 S310 and S311 are required for D6PK recycling, phosphatase inhibitor-induced internalization and kinase inhibitor-induced SDS-PAGE mobility changes.

(A) to **(C)** Confocal images of root meristem epidermis cells of 5 day-old seedlings showing localization of D6PKp:YFP:D6PK and D6PKp:YFP:D6PK-SSAA (SSAA) and -SSDD (SSDD) in response to 90 min treatments with BFA [25 μM] and FM4-64 [2μM]. Note the colocalization of D6PK and SSDD with FM4-64 labeled BFA compartment (triangle) and the unaffected apolar plasma membrane localization of SSAA (open arrows) (A). Treatment with synthetic auxin 1-NAA [10μM] and mock for 3 h. Note the reduction of plasma membrane signal and increase of cytosolic signals for all genotypes after 1-NAA treatment for all D6PK variants (B). Treatments with mock, Staurosporine [10 μM] and Calyculin A [250 nM] for 90 min. Note the Calyculin A-induced internalization of D6PK and SSDD that does not take place for SSAA, and the Staurosporine-induced lateralization of D6PK and SSDD (C). **(D)** Representative immunoblots and densitometric profiles of protein extracts after subcellular fractionation (M fraction) from roots of 7 day-old seedlings treated with mock, Staurosporine and Calyculin A as in (C), expressing either 35S:YFP:D6PK and 35S:YFP:D6PK-SSAA (SSAA) and -SSDD (SSDD). Note the Staurosporine-induced faster mobility for all D6PK variants, and the stronger effect of Staurosporine on SSAA and SSDD than on D6PK. Shown is one of two biological replicates.

was further internalized after Calyculin A treatment, indicating that phosphorylation changes on additional sites of D6PK or other unrelated proteins contributed to the full response of D6PK to Calyculin A **(Figure 3.3.7C)**.

We also monitored the effects of the Staurosporine and Calyculin A treatments on protein mobility and subcellular fractionation **(Figure 3.3.7D)**. Here, we found that Staurosporine treatment did not lead to changes in D6PK subcellular fractionation but to a faster D6PK mobility suggestive of decreased phosphorylation, as observed after the lambda phosphatase treatment **(Figure 3.3.5)**. Interestingly, SSAA and SSDD displayed a more dramatic mobility change, indicating a more effective de-phosphorylation by Staurosporine treatment **(Figure 3.3.7D)**. On the other side, Calyculin A had no obvious effects on the mobility or subcellular fractionation of D6PK, indicating that Calyculin A-induced internalized D6PK was likely still membrane associated and did not become further phosphorylated or de-phosphorylated. Taken together, these results supported the notion that the cellular phosphorylation state impacted on D6PK localization. Staurosporine-induced changes on D6PK localization seemed independent from S310 and S311, but these sites seemingly contributed to the Staurosporine-induced D6PK mobility changes. Finally, Calyculin A-induced internalization of D6PK required phosphorylation at S310 and S311 (but possibly also other sites), in line with the proposed role for a phosphorylation charge-switch at these sites modulating D6PK plasma membrane localization.

S310 and S311 are required for D6PK in vivo function

In order to understand the biological relevance of these two putative phosphosites, we tested the ability of SSAA and SSDD mutated versions of D6PK:YFP:D6PK to complement *d6pk01* mutant and of 35S:YFP:D6PK to induce *D6PK* overexpression phenotypes **(Figure 3.3.8A – C)**. Although the apolarly distributed SSAA protein was still an active kinase *in vitro* **(Figure 3.3.6)** and induced typical *D6PK* phenotypes when overexpressed **(Figure 3.3.8C)**, it was not able to complement the gravitropism and phototropism defects of *d6pk01* in any of the lines analyzed **(Figure 3.3.8A** and **B)**. In contrast, the SSDD could complement *d6pk01* phenotypes to the same extent as the wild-type D6PK, and could also induce typical overexpression *D6PK* phenotypes **(Figure 3.3.8A – C)**. In each case, the observed complementation efficiency of *d6pk01* phenotypes correlated with PIN3 phosphorylation levels: SSAA transgenics had similar PIN3 phosphorylation levels as *d6pk01*, whereas SSDD transgenics had similar PIN3 phosphorylation levels as the wildtype **(Figure 3.3.8D – F)**. The fact that SSAA behaved like D6PK when overexpressed but not when expressed from a D6PK promoter fragment was puzzling. It could be envisioned that, since SSAA mutation does not impair the kinase activity, overexpression is sufficient to trigger ectopical D6PK-induced developmental defects despite of the polarity and recycling defects of the SSAA. But, endogenous expression levels of SSAA might be limiting to overcome these defects and thus insufficient to complement of *d6pk01*. Regardless of the reason behind this discrepancy, it can still be concluded that S310 and S311 play an important role for D6PK function in the control of auxin transport, with an important role in the control of D6PK polarity and recycling.

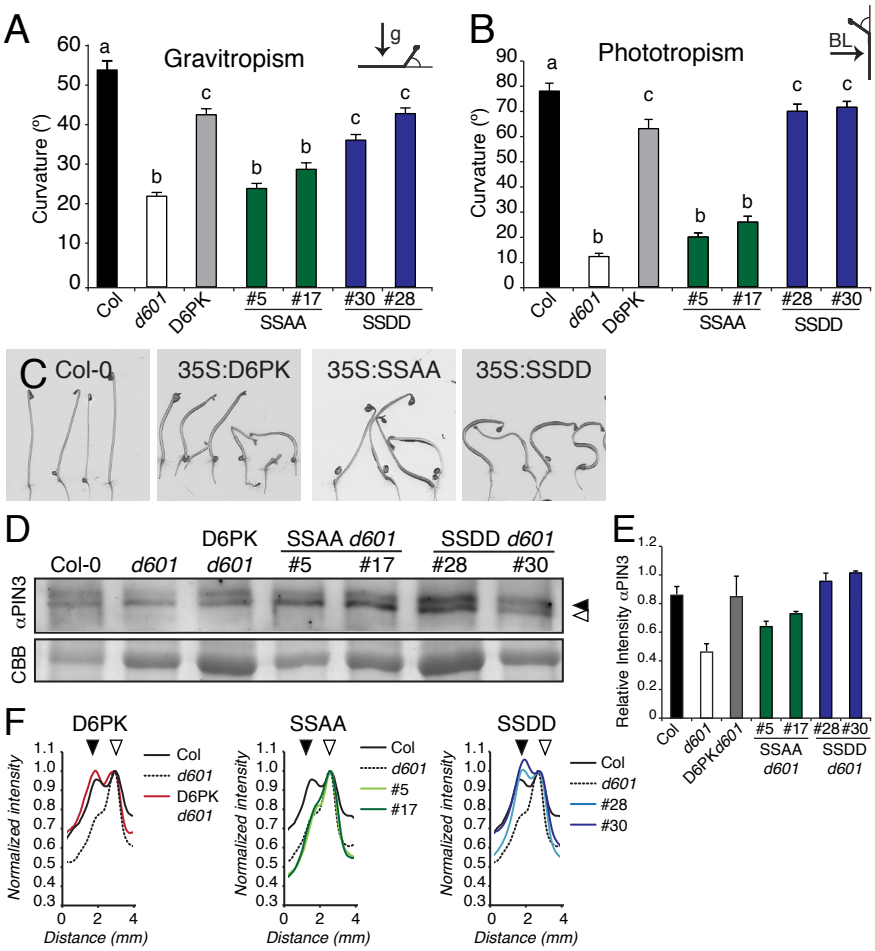

Figure 3.3.8 S310 and S311 are required for D6PK function, likely through phosphorylation.

(A) and **(B)** Complementation of tropism defects of *d6pk* mutant phenotypes in independent transgenic lines with D6PKp:YFP:D6PK in *d6pk012* and D6PKp:YFP:D6PK carrying SSAA or SSDD mutations in *d6pk01* (T3 hemizygous generation). Negative gravitropic hypocotyl bending after reorientation by 90º for 20 hrs (A) and hypocotyl phototropic response after 4 hrs of 5 µmol m^{-2} s^{-1} blue light (B) of 3 day-old etiolated seedlings. Average and standard error of representative experiments from 3 biological replicates; n > 30 seedlings; Pairwise Student's t-test, different letters mark statiscally significant differences ($p < 0.05$), same letter represent non-statiscally significant differences. **(C)** Representative photographs of 3 day-old etiolated wild-type seedlings and seedlings overexpressing D6PK, SSAA, and SSDD. **(D)** and **(E)** Representative immunoblots of membrane protein extracts from 4 day-old etiolated seedlings with αPIN3 and CBB loading control (D) and respective densitometric profiles comparing relative intensities of the upper band, i.e. phosphorylated PIN3 (closed arrow), with that of the lower band, i.e. unphosphorylated PIN3 (open arrow) of the different proteins and complementation lines to Col-0 and *d6pk01*. Each profile was normalized to and aligned to the maximum value of the lower band (E). **(F)** Mean and standard deviation of relative upper to lower band intensities of αPIN3 from two biological replicates.

Discussion

Establishing and maintaining cell polarity is essential for most biological processes. Polar auxin transport is critically determined by the polarized distribution of the PIN auxin efflux carriers and the presence of regulatory kinases such as D6PK (Wisniewska et al, 200; Barbosa & Schwechheimer, 2014). Here, we identified molecular components determining D6PK anchoring and polarity maintenance at the plasma membrane: a phospholipid-binding K-rich motif and nearby phosphorylation sites. Based on these findings, we propose a model according to which plasma membrane-specific and polarly distributed phospholipids recruit D6PK, via the K-rich motif, and phosphorylation determines the affinity of D6PK to the plasma membrane, its recycling kinetics, and its polar distribution **(Figure 3.3.9)**.

D6PK could bind to polyacidic PIPs and PA *in vitro* and this binding was dependent on a K-rich motif in the middle domain of the protein. *In vivo* manipulation of PIP and PA metabolism with chemical inhibitors as well as genetic interference with $PIP(4,5)P_2$ synthesis led to the internalization of D6PK and impaired its polar plasma membrane distribution. At the same time, mutations at the K-rich motif led to decreased D6PK plasma membrane association and increased abundance of the protein in the cellular soluble fraction. These findings strongly support the notion that D6PK is recruited to the plasma membrane by unspecific ionic interactions between its K-rich motif and polyacidic phospholipids. The fact that D6PK with a deletion of the middle domain, which includes the K-rich motif, still retained membrane association and that none of the inhibitor treatments promoted a complete D6PK solubilization suggests that additional mechanisms control D6PK membrane anchoring. This would not be surprising since so-called co-incidence detection mechanisms have already been implicated in the recruitment of many peripheral membrane proteins. In co-incidence detection, the low affinity recruitment to membranes, e.g. through ionic interactions, is reinforced by a second interaction, e.g. lipid modification or protein interaction, and this is thought to determine stability and specificity of the protein-lipid interaction (Carlton & Cullen, 2005; Hammond & Balla, 2015). For example, specific recruitment of AP-2 (ADAPTOR PROTEIN2) to plasma membrane endocytosis sites requires both the binding of AP-2 to $PI(4,5)P_2$ as well as to endocytosis motif-containing cargos, while TGN (trans-Golgi network) recruitment of FAPP1 (FOUR PHOSPHATE ADAPTOR PROTEIN1) requires both PI(4)P and ARF1 (ADP RIBOSYLATION FACTOR-GTPase 1) binding (Carlton & Cullen, 2005). Thus, it is easily conceivable that other mechanisms besides phospholipid binding operate in the specific recruitment of D6PK to its polar domain at the plasma membrane.

The D6PK variants with mutations in the K-rich motif were unable to fully complement *d6pk01* or mimic *D6PK* overexpression phenotypes. This is in agreement with previously described observations that manipulation of D6PK localization, by BFA treatment or GNOM loss-of-function mutation, impairs its function in PIN phosphorylation and auxin transport-dependent growth (Barbosa et al, 2014; Zourelidou et al, 2014). Notably, increased internalization of D6PK-6KA transgenic lines was inversely correlated with the ability to complement the tropism and PIN3 defects of *d6pk01*.

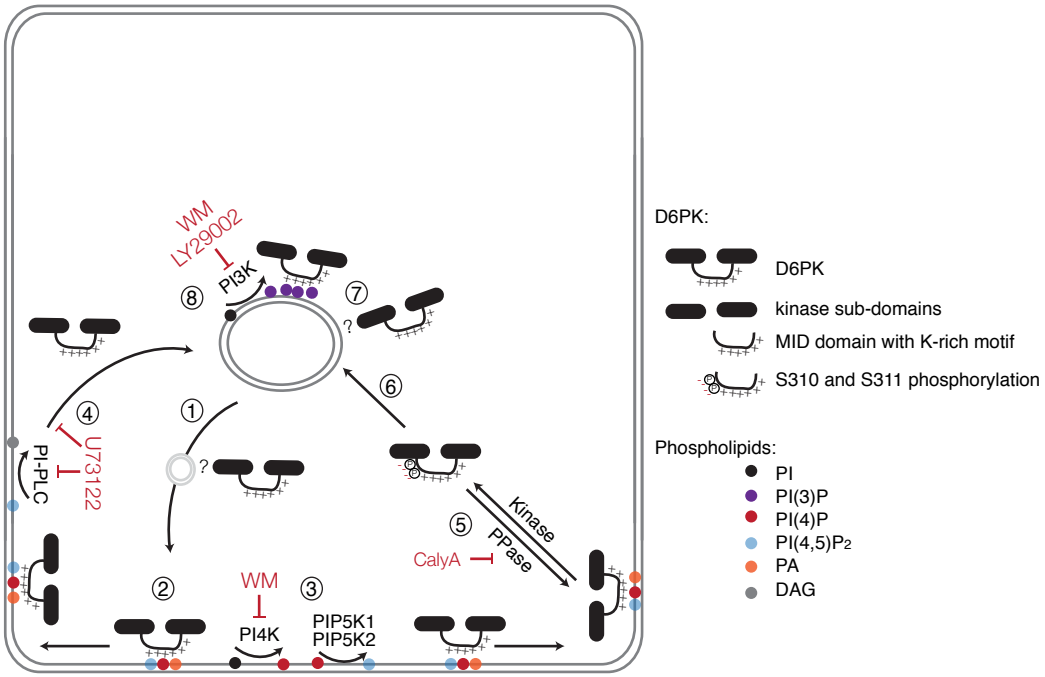

Figure 3.3.9 Working model for D6PK plasma membrane anchoring and polarity control.
D6PK localization is controlled by the steady state action of diverse components determining the phospholipid composition of membranes and the D6PK phosphorylation status. Inhibitor treatments impair this equilibrium. **(1)** Targeting of D6PK to the plasma membrane is dependent on the trafficking regulator GNOM and can be blocked by BFA, suggesting that this targeting can be mediated by vesicle-mediated transport (Barbosa et al, 2014). **(2)** At the plasma membrane, D6PK binds to polyacidic phospholipids such as PA, PI(4)P, and $PI(4,5)P_2$, through its polybasic K-rich motif. **(3)** Impairment of PI(4)P biosynthesis by Wortmannin (WM) treatment or of $PI(4,5)P_2$ by PIP5Ks loss-of-function leads to the displacement D6PK from the plasma membrane to endosomes, where it likely binds other phospholipids. **(4)** Treatment with the inhibitor U73122 leads to a quick depolarization of D6PK, implying that the D6PK polarity domain is restricted by the action of PI-PLC enzymes. **(5)** Phosphatase-inhibitor treatments lead to the internalization of D6PK in a S310 and S311-dependent manner, suggesting that S310 and S311 phosphorylation can serve as a charge-switch to displace D6PK from the plasma membrane. The fact that SSAA mutants are insensitive to BFA and apolar, also suggests that S310 and S311 phosphorylation-mediated internalization is required for D6PK recycling-kinetics and polarity control. **(6)** Internalized D6PK (e.g. after BFA treatment or with 6KA mutation) is relatively less phosphorylated than plasma membrane localized D6PK, suggesting that phosphorylation occurs at the plasma membrane and that internalized D6PK is rapidly dephosphorylated. **(7)** Internalized D6PK binds to endosomes but this binding can be independent of the K-rich and middle domain, as suggested by the endomembrane association of ΔMID and D6PK-6KA mutants. **(8)** Finally, the inhibition of the biosynthesis of endosomal localized PI(3)P by WM or LY294002 also determines D6PK plasma membrane abundance, possibly through an effect on the trafficking of endosomal-localized D6PK or other indirect effects.

Thus, D6PK plasma membrane abundance and activity on PINs requires the K-rich motif. The fact that different 6KA lines have differential complementation efficiency, which is suggestive for a D6PK abundance threshold, can be further explored in the future for other D6PK- and PIN-dependent auxin transport processes.

In *Arabidopsis*, D6PK belongs to the AGC1 subgroup of the 23-member AGCVIII kinase family, which includes also the well-studied plasma membrane-associated PID, WAGs, and phots (phototropins)**(Figure 3.3.10)**. Alignment of AGCVIII kinases reveals that the K-rich motif is conserved at the C-terminus of the middle domain of 14 AGCVIII kinases, including the four D6PKs (marked with a blue star in **Figure 3.3.10**). The presence of at least one of the two highly conserved K or R (arginine) residues at the positions corresponding to D6PK K315 and K317, at least two more additional K or R residues located N-terminally from K315; and one K or R residue located C-terminally of K317 appear to be striking features of this group of kinases. The respective stretches of basic amino acids could contribute to similar membrane ionic interactions as shown here for the K-rich motif of D6PK. From these 14 kinases, only a few have been characterized at the molecular level as yet and the *in vivo* localization was determined for even fewer, rendering this prediction still rather preliminary at the present stage. Among the characterized examples are the phot blue light receptors. In line with the prediction that proteins with a polybasic stretch interact with the plasma membrane, phot1 and phot2 were shown to be plasma membrane localized and to be partially internalized to endosomes (phot1) and to the Golgi (phot2) after blue light irradiation (Kaiserli et al, 2009; Kong et al, 2006; Wan et al, 2008). In turn, UCN (UNICORN) and UCNL (UNICORN-LIKE), which are involved in planar growth development, have the above-mentioned conserved basic stretch but UCN is localized to the nucleus and cytosol. This however, was proposed to rely in a nuclear localizing signal sequence (Enugutti et al, 2012).

The non-conservation of the K-rich motif in PID, WAG1, and WAG2 is interesting since PID and WAGs are plasma membrane-associated but, as opposed to D6PK, not polarly localized (Dhonukshe et al, 2010). Nonetheless, the PID middle domain was reported to be required and sufficient for plasma membrane localization when the protein was expressed in yeast, but the underlying mechanisms were not further studied (Zegzouti et al, 2006). Interestingly the K-rich motif of the AGC1.3 tomato orthologue, ADI3, which localizes at the plasma membrane and to the nucleus, was shown to function as a nuclear localization signal (NLS) required for the translocation of ADI3 to the nucleus upon pathogen attack (Ek-Ramos et al, 2010; Ek-Ramos et al, 2014). Dual-targeting function of protein polybasic motifs, i.e. targeting to the nucleus or the plasma membrane, has previously been described. Here, the specific molecular context near the polybasic motif, e.g. presence of hydrophobic residues as well as the phosphorylation status, seem critical for the targeting to one or the other part of the cell (Heo et al, 2006; Maures et al, 2011). In the case of D6PK, there is at present no indication for a localization of the protein to the nucleus or a biological role in this compartment. However, our findings, together with the studies on ADI3, indicate that specific features in the polybasic-motif of AGCVIII kinases might lead to either plasma membrane or nuclear targeting. Finally, serines at D6PK position S310 and S311 occur only in D6PK, D6PKL1 and D6PKL2, while few other members of the AGC1 clade, including D6PKL3, have only one serine at the position corresponding to D6PK S310.

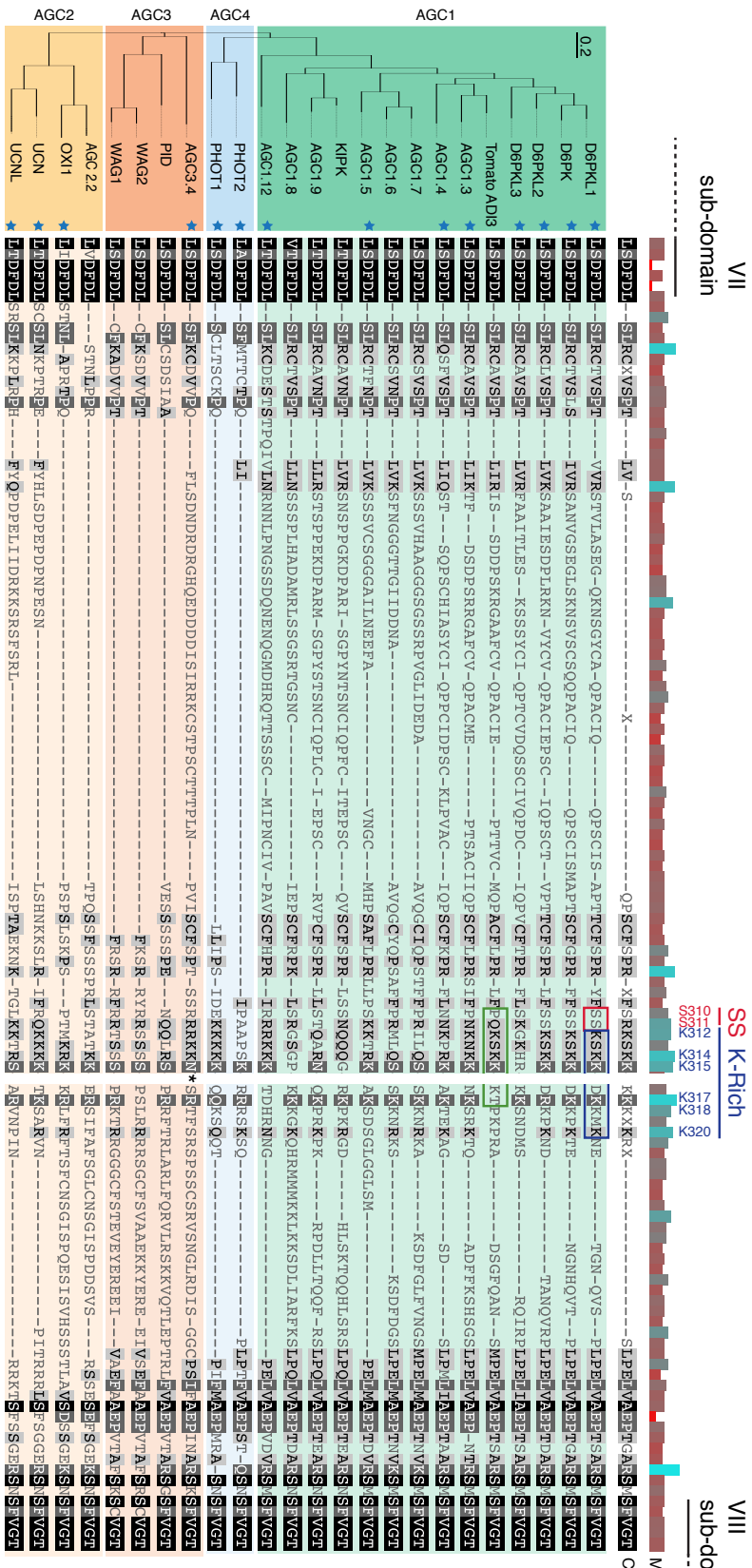
VII
sub-domain
SS
K-Rich
S310
S311
K312
K314
K315
K317
K318
K320
VIII
sub-domain
Mean pI
Consensus
AGC1
AGC2
AGC3
AGC4
0.2
D6PKL1
D6PK
D6PKL2
D6PKL3
Tomato AD3
AGC1.3
AGC1.4
AGC1.7
AGC1.6
AGC1.5
KIPK
AGC1.9
AGC1.8
AGC1.12
PHOT2
PHOT1
AGC3.4
PID
WAG2
WAG1
AGC 2.2
OXI1
UCN
UCNL
AGC3.4 deleted sequence
VVTTTIHENAAGTSDSVKSNDVS

In summary, the analyses on the AGCVIII kinases middle domain (D6PK, ADI3 and PID) clearly indicate that the middle domain has a targeting function for these kinases and could serve as a landmark of AGCVIII kinase localization and regulation in plants.

Both, PIPs and PA, qualify as plasma membrane components for the recruitment and polarity control of D6PK. Pharmacological manipulation of almost all steps of PIP and PA metabolism had an impact on D6PK localization in our experiments, indicating that probably more than one of these phospholipid species or their precursors engage in D6PK binding. PA localization is not well understood in plants. PA is produced by stimulus-dependent activation of PLD or PI-PLC, for which differential localization has been reported at least in other organisms (e.g. PLDs occur at multiple compartments, mitochondria, Golgi, endosomes and plasma membrane; while PI-PLC occurs mostly at the plasma membrane) (Nishioka et al, 2010; Jenkins & Frohman, 2005). To our knowledge, only one PA biosensor has been tested so far in plants, but its localization is only known in pollen tubes. There it localizes in the subapical plasma membrane (Potocky et al, 2014), thus colocalizing with its producing enzyme PI-PLC (Helling et al, 2006; Zhao et al, 2012). Interestingly, PI-PLC substrate PI(4,5)P_2 localization is complementary and excluded from the PI-PLC and PA-rich subapical membrane, indicating PI-PLC controls PI(4,5)P_2 and PA localization(Kost, 2008). As discussed below, PI(4,5)P_2 is polarly localized in many cells throughout plant development, including the root epidermis, which could indicate that PI-PLCs, and thus PA, are also polarly localized in these cells.

PIP distribution is spatially regulated and confers membrane identity and domain organization (Behnia & Munro, 2005; Comer & Parent, 2007; van den Bogaart et al, 2011). Also in plants, different PIP species are known to be differentially distributed: PI(4)P as well as PI(4,5)P_2 reside in the plasma membrane and PI(3)P in late endosomes and the tonoplast (Simon et al, 2014; Vermeer et al, 2006; Vermeer et al, 2009). The cellular distribution of PI(5)P or PI(3,5)P_2 is still unknown in plants and finally, neither PI(3,4)P_2 nor PI(3,4,5)P_3 have yet been detected in plants (Heilmann, 2009; Munnik & Nielsen, 2011). In our experiments, treatments with WM and LY294002 that should result in the depletion of PI(3)P (both) and PI(4)P (only WM) caused D6PK internalization but did not affect its membrane association. Since PI(3)P is not present at the plasma membrane, the effects of WM and LY294002 on D6PK localization are most likely caused by PI(4)P depletion at the plasma

Figure 3.3.10 (previous page) AGCVIII kinases phylogenetic tree and protein alignment of their middle domain.

Phylogenetic tree and protein alignment of the middle domain using the 23 *Arabidopsis* AGCVIII kinases and the tomato AGCVIII kinase ADI3. Full length protein sequences were used for the alignment and the phylogeny (Cost matrix: Blosum62, gap open penalty: 12, gap extension penalty: 3). For clearer representation of the K-rich motif, 23 amino acids from AGC3.4 were deleted, since they interrupted the aligned K-rich of all 23 other kinases. Blue stars mark kinases with a conserved basic motif at the position corresponding to the D6PK K-rich motif. The D6PK K-rich motif is highlighted in blue. D6PK S310 and S311 are indicated in red; the ADI3 nucleus localization sequence is indicated in green (Ek-Ramos et al, 2014).

membrane and/or could be the result of indirect effects, e.g. on membrane trafficking. In both cases, the effects observed were within a rather short time and thus we therefore would like to argue that the effects are rather direct than indirect.

Interestingly, the U73122-mediated inhibition of $PI(4,5)P_2$ hydrolysis led to a quick depolarization of D6PK. This strikingly resembled the U73122-induced depolarization of a pollen tube tip-localized $PI(4,5)P_2$ biosensor, which was supposedly the result of the inhibition of subapical and lateral localized PI-PLCs (Helling et al, 2006; Zhao et al, 2012). Since the $PI(4,5)P_2$ biosensor has apico-basal polarity in root epidermis cells (Ischebeck et al, 2013; Tejos et al, 2014), it is tempting to speculate (and feasible to test) that U73122 treatment would also block lateral PI-PLC function in the root epidermis and lead to the depolarization of apico-basally distributed $PI(4,5)P_2$, thus recruiting basal D6PK to the lateral and apical domains. In support of $PI(4,5)P_2$ as a plasma membrane recruiting factor for D6PK, we show that PIP5K1 and PIP5K2 are required for proper D6PK plasma membrane targeting in root epidermis cells. Moreover, another member of this protein family, the root hair-specific PIP5K3, was recently shown to be required for the localization of D6PK at the tips of initiating root hairs (Stanislas et al, under revision). Since PIPs are established polarity landmarks in other organisms (Comer & Parent, 2007), our findings further support the known role of plant $PI(4,5)P_2$ as polarity landmark in plants (Kost, 2008) and identify D6PK as one of its *in vivo* cognate polar partners.

Our study also indicates that phosphorylation at two serines (S310 and S311), adjacent to the K-rich motif, may be crucial for D6PK plasma membrane association and D6PK polarity. The phosphorylation of residues adjacent to polybasic motifs may act as a charge-switch mechanism that disrupts protein-lipid ionic interactions. These charge switches have been proposed to release proteins from membranes, such as MARCKS (MYRISTOYLATED ALANINE-RICH PROTEIN KINASE C SUBSTRATE) and K-Ras (K-RAS GTPases) by PKC (PROTEIN KINASE C)-phosphorylation and BKI1 (BRI1 KINASE INHIBITOR1) by BRI1 (BRASSINOSTEROID INSENSITIVE1)-dependent phosphorylation (Bivona et al, 2006; Jaillais et al, 2011; McLaughlin & Aderem, 1995). Our analyses of D6PK phosphorylation suggest that D6PK is phosphorylated at the plasma membrane, possibly at many sites, and dephosphorylated when internalized. In line with this, phosphatase-inhibitor treatments led to a complete internalization of D6PK. Remarkably, D6PK variants with alanine replacement mutations at D6PK S310 and S311 remained at the plasma membrane after phosphatase-inhibitor treatments, while the relatively more internalized S310 and S311 phosphomimic variants were further internalized. Importantly, auxin-induced internalization of D6PK seemed to be independent of S310 and S311. Together, these findings are supportive for a role of S310 and S311 phosphorylation in phosphorylation-induced D6PK internalization but suggest at the same time that other phosphorylation target residues also contribute to the complete phosphatase inhibitor-induced internalization. Thus, D6PK may associate and dissociate to and from the plasma membrane in a phosphorylation-dependent manner.

D6PK is rapidly removed from the plasma membrane by an unknown and, possibly, vesicle trafficking-independent mechanism (Barbosa et al, 2014). While, recycling is required for the

polarity maintenance of PINs, the role of D6PK recycling is still unclear. Interestingly, D6PK SSAA mutations led to a loss of BFA-induced internalization and of D6PK polarity, suggesting that D6PK SSAA remained stably associated with the plasma membrane and may have lost its basal polarity due to impaired recycling rendering the protein more susceptible to lateral diffusion. The polarity of many plasma membrane-localized proteins requires constitutive recycling and polar redelivery to prevent lateral diffusion in the plasma membrane (Marco et al, 2007). The polarity of plasma membrane peripheral proteins also requires recycling, which can be mediated by slower endocytosis and/or faster dissociation, followed by polar targeting, as observed in *Saccharomyces cerevisiae* Cdc42, *Schizosaccharomyces pombe* POM1, *Caenorhabditis elegans* PAR (PARTITIONING-DEFECTIVE) proteins and plant ROP-GTPases (Goehring, 2014; Hachet et al, 2011; Kost, 2008; Slaughter et al, 2009). In many cases, like for POM1 and PAR proteins, it is known that phosphorylation triggers membrane dissociation and maintains protein polarity. In fission yeast, a tip-localized phosphatase dephosphorylates POM1 at a polybasic motif, thereby allowing POM1 phospholipid binding and membrane association. Away from the tip, the phosphatase is not present and POM1 autophosphorylation at multiple sites accumulates and de-stabilizes ionic protein-lipid interactions, leading to its membrane dissociation. Thus, the POM1 phosphorylation status generates a POM1 plasma membrane gradient from the tip to the center of the cell (Hachet et al, 2011). In the case of PAR proteins, reciprocal phosphorylation by PAR complex-kinases on the anterior versus posterior PAR complex subunits leads to reciprocal internalization and thus mutual exclusion of anterior versus posterior complexes (Hoege & Hyman, 2013). In this context, our findings that D6PK-SSAA is resistant to BFA- and phosphatase inhibitor-induced internalization and, at the same time, apolarly distributed in the plasma membrane, strongly suggest that D6PK constitutive recycling is required for polarity maintenance and that S310 and S311 phosphorylation might mediate this process by inducing D6PK internalization. This hypothesis is worth of future investigations, as it would bring a biological function for the observed fast recycling kinetics of D6PK in the control of its polarity maintenance.

The functional analysis of the S310 and S311 mutants indicated that the D6PK-SSDD phosphomimic variant, although significantly internalized, could efficiently complement the PIN3 phosphorylation and tropism defects of *d6pk01* mutants and mimic *D6PK* overexpression phenotypes. This indicates that either SSDD-induced internalization of D6PK is below the threshold where D6PK plasma membrane abundance becomes limiting for its function; and/or that SSDD has gain-of-function properties that compensate its internalization. In this regard, it is important to mention that the SSDD transgenics, as judged by confocal microscopy, accumulated apparently more protein than their wild-type counterparts and that we cannot exclude that SSDD internalization is compensated by a feedback mechanism leading to elevated protein levels.

Transgenic plants expressing the plasma membrane but apolarly localized D6PK mutant variants with alanine replacement mutations of S310 and S311, D6PK-SSAA, mimicked *D6PK* overexpression phenotypes. However, these variants did not complement *d6pk01* mutant

phenotypes when expressed from a D6PK promoter fragment. This could be explained by a similar feedback mechanism as suggested for SSDD, which would lead to reduced protein levels – also suggested by the confocal imaging analysis – and consequently limiting D6PK function. Alternatively, it could be envisioned that the non-polar localization of SSAA results in reduced colocalization with PIN proteins and, thus, a reduced ability to phosphorylate and activate PINs. Future dissection of these effects on localization and the underlying feedback mechanisms (e.g. by apolarly targeted or membrane-stabilized D6PK versions) could yield a better understanding of whether not only plasma membrane abundance but also polarity is required for D6PK function.

In summary, our observations strongly support that D6PK abundance at the plasma membrane determines PIN phosphorylation and auxin transport. With the present study, we propose a model for D6PK plasma membrane anchoring and polarity maintenance where both, plasma membrane phospholipid composition and D6PK surface charge at the K-rich motif of the middle domain critically determine D6PK plasma membrane steady-state levels **(Figure 3.3.9)**. This model provides a basis for the involvement of phospholipid- and phosphorylation-mediated regulation of auxin transport intensity, and possibly directionality, by D6PK plasma membrane abundance and distribution. It also contributes to the short-list of polar peripheral membrane proteins in plants that has been analyzed at the molecular level as yet. In the case of D6PK, polarity control seems to rely on similar molecular components, such as PIP composition, and mechanistic principles, such as phosphorylation-dependent recycling, as has been described for polarity counterparts from yeast and animal systems. Since other plant AGCVIII kinases share similar sequence motifs with D6PK, it may well be that these principles also apply to the localization and functional control of these plant-specific kinases.

Acknowledgments

We thank Nadine Gerstenberg and Alkistis Bassukas (Technische Universität München, Germany) for their help during experiments as part of their student internships; and Jutta Elgner (Technische Universität München, Germany) for technical support. This work was supported by a fellowship from the Fundação para a Ciência e Tecnologia (FCT) to I.C.R.B. (SFRH/BD/73187/2010) and a grant from the Deutsche Forschungsgemeinschaft (SCHW751/12-1) to C.S.

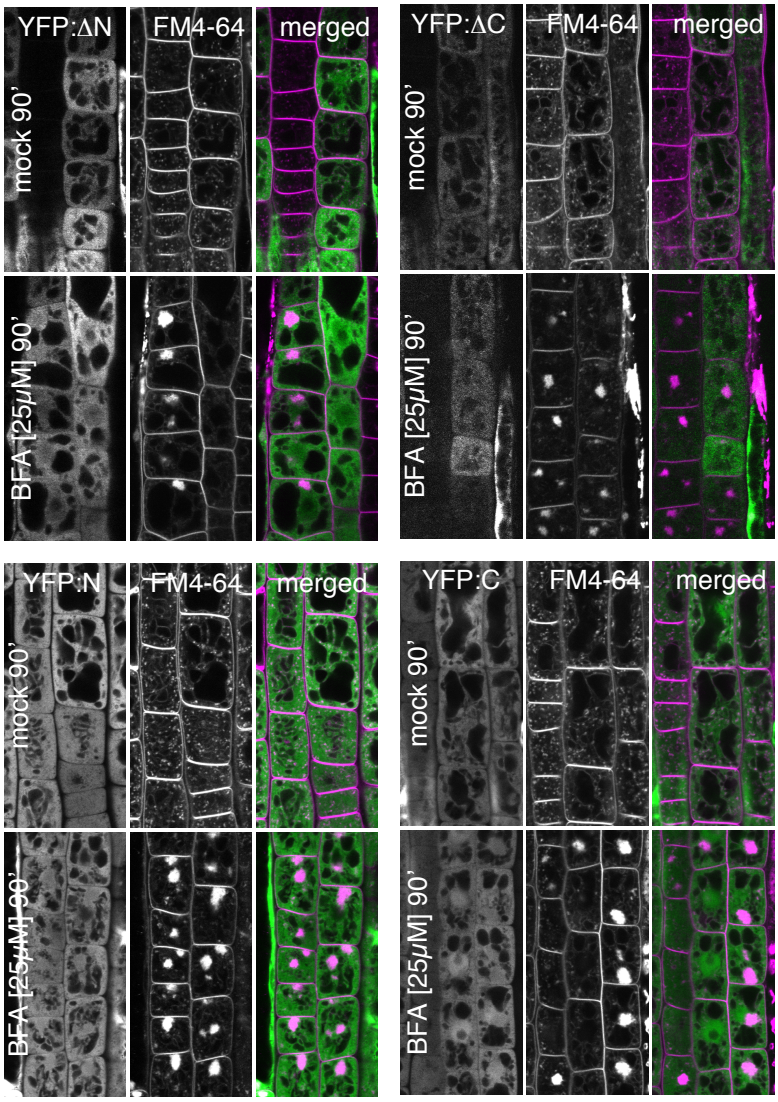

Supplementary Figure 3.3.1 Deletions of D6PK do not localize to the BFA-compartments.

Confocal images of root epidermis cells from 7 day-old seedlings expressing 35S:YFP:D6PK-deletions (YFP:ΔN, YFP:N, YFP:ΔC and YFP:C) treated for 90 minutes with mock and FM4-64 [2 μM] (upper pannels) or with BFA [25 μM] and FM4-64 [2 μM] (lower pannels).

4 Discussion and conclusions

4.1 Emerging picture of D6PK trafficking and polarity control

In this thesis, I identified diverse mechanisms involved in the control of D6PK trafficking and polarity. It emerges from my studies that the regulatory mechanisms and components of D6PK cell trafficking share features that are found in previously studied integral membrane proteins as well as in peripheral membrane proteins from plants or other eukaryotic organisms. On the one hand, the D6PK internalization dynamics after different inhibitor treatments resemble that of a protein membrane-dissociation mechanism: it is extremely fast, complete and, in the case of BFA-treatments, quickly reversed after BFA-washout; it is also independent of clathrin-mediated endocytosis and presumably requires phosphorylation at S310 and S311 of D6PK. In addition, mutations in its polybasic K-rich motif significantly impair D6PK membrane association, indicating that D6PK-membrane anchoring are mediated by ionic interactions. On the other hand, D6PK trafficking resembles the vesicle-mediated trafficking of integral membrane proteins: plasma membrane targeting requires the function of the membrane trafficking regulators, here specifically the ARF-GEF GNOM, and D6PK remained membrane-associated after internalization following pharmacologic and genetic interference treatments.

In the following sections, I will discuss how the trafficking of D6PK differs from that of its PIN substrates, which are well-studied polarity models in plants. I will also provide some examples from the published literature on the trafficking of other eukaryotic peripheral membrane proteins, with which D6PK shares trafficking and regulatory features. Together, this should help to support the model of D6PK trafficking and polarity control proposed here.

4.1.1 Comparison between D6PK and PIN proteins, models for polar trafficking in plants

GNOM regulates PIN polarity and D6PK plasma membrane targeting

I could show that D6PK, as the PINs, undergoes constitutive and GNOM-dependent recycling between the plasma membrane and endosomes **(Figure 4.1.1A)**. Although this process is apparently similar to that shown for the PINs, there are important differences between the recycling of D6PK and PINs. First, apparently, only a fraction of the PIN proteins undergoes recycling, as judged by the fact that even prolonged BFA treatments (12 h) never lead to a complete depletion of PIN proteins from the plasma membrane, but rather to defects in polarity; in turn, D6PK is always completely internalized

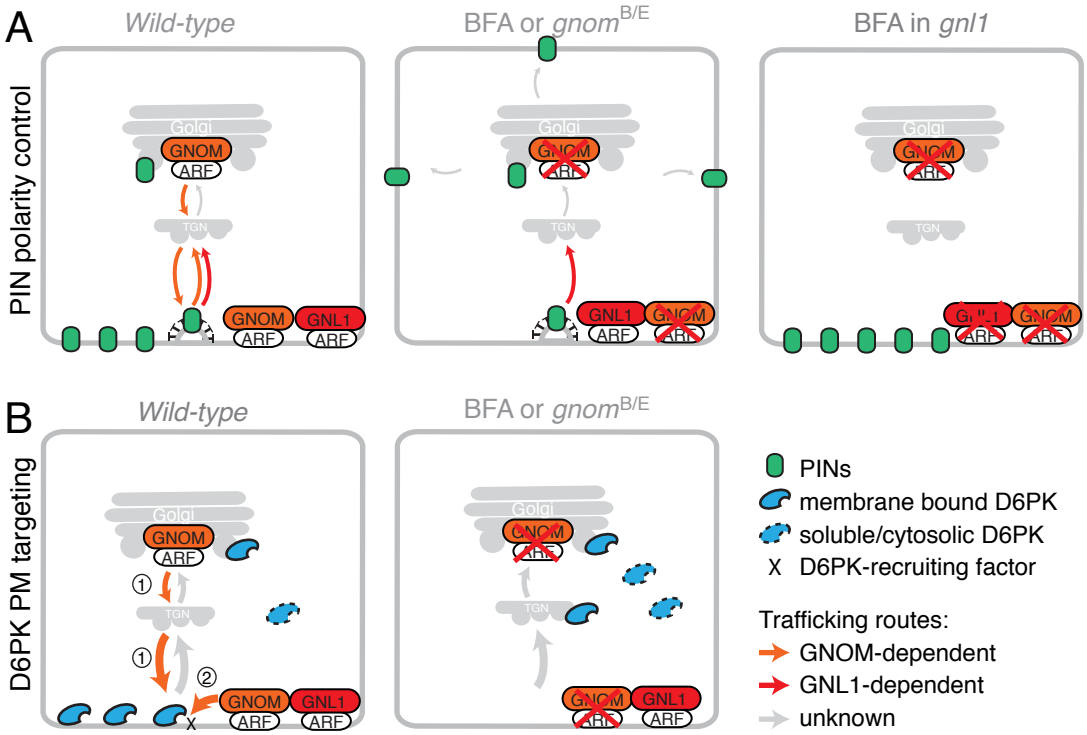

Figure 4.1.1 Models for GNOM function in D6PK and PIN trafficking.
(A) Current understanding of the mode of action of GNOM in PIN trafficking. GNOM resides at the Golgi, where it presumably controls PIN exocytosis, and at the plasma membrane, where it controls PIN endocytosis together with GNL1. After BFA treatment or in *gnom*$^{B/E}$ mutants, PIN exocytosis is blocked but PIN endocytosis is still functional due to the presence of GNL1. As a consequence, PINs accumulate over time in endosomal BFA compartments and eventually are retargeted to the plasma membrane by alternative apolar or apical pathways. In *gnl1,* BFA treatment efficiently blocks PIN exo- and endocytosis, thus PINs remain at the plasma membrane. **(B)** In the case of D6PK trafficking, GNOM could have two possible roles. Either it is involved in the vesicle-meditated Golgi to plasma membrane trafficking of D6PK or in that of an unknown D6PK-recruiting factor (1). Alternatively, GNOM may control the recruitment of D6PK or of an unknown D6PK-recruiting factor directly at the plasma membrane via ARF-GTPase activation of plasma membrane effectors (2). Impaired GNOM function by BFA or *gnom*$^{B/E}$ mutants would result in both cases in the observed internalization of D6PK into the intracellular space where D6PK is both, soluble and endomembranes-associated.

upon BFA treatment and remains internalized also after prolonged treatment (12 h, data not shown), indicating that the entire D6PK plasma membrane protein pool undergoes recycling. Second, the kinetics of GNOM-dependent recycling are very different between the two proteins: D6PK is rapidly internalized following BFA treatment (5 min) and fully recovers its polar localization shortly after a washout treatment (15 min) whereas PINs appear in intracellular BFA compartments comparatively late (30 min) and their retargeting to the plasma membrane takes considerably longer (more than 60 min in our experimental conditions). Third, D6PK is partially internalized in the *gnom*$^{B/E}$ partial loss-of-function mutants but, whenever present at the

plasma membrane, is polarly localized. In turn, PINs remain plasma membrane-localized in *gnom*$^{B/E}$ but have only occasionally polarity defects. This indicates that D6PK but not PINs strictly requires GNOM for plasma membrane targeting and that PINs, but probably not D6PK, require GNOM for polarity control (Barbosa et al, 2014; Ikeda et al, 2009; Kleine-Vehn et al, 2008).

The ARF-GEF GNOM is localized at the plasma membrane and at the Golgi where it presumably controls the activation of ARF-GTPases and their downstream effectors controlling vesicle coating and budding (D'Souza-Schorey & Chavrier, 2006; Donaldson & Jackson, 2000). BFA traps an ARF-GEF/ARF-GDP transient complex and blocks the GDP to GTP exchange (Peyroche et al, 1999). BFA binding requires a conserved methionine in the Sec7 domain of ARF-GEFs, which, when mutated to a leucine, impairs BFA-binding without affecting GEF function (Geldner et al, 2003; Mossessova et al, 2003). The effects of BFA on D6PK and PIN localization are suppressed in transgenic lines expressing a BFA-insensitive GNOM^{M696L} variant, hence it can be deduced that GNOM requires normal ARF-GEF-mediated ARF-GTPase activation for the targeting of both proteins. Since PINs are integral membrane proteins, it can be easily conceived that GNOM is required for budding and coating of PIN-carrying vesicles. Golgi-localized GNOM would control, likely indirectly, the sorting and exocytosis of internalized PINs at the TGN (Naramoto et al, 2014). Plasma membrane-localized GNOM would control PIN endocytosis, but due to the presence of the BFA-insensitive GNL1, endocytosis of PINs can still occur in the presence of BFA. PIN endocytosis can only be blocked by BFA in a *gnl1* mutant or when GNL1 is mutated into a BFA-sensitive ARF-GEF (Irani et al, 2012; Naramoto et al, 2010; Richter et al, 2007) **(Figure 4.1.1A)**.

Since D6PK is a peripheral membrane protein, which may not necessarily require vesicle-mediated trafficking for its association to the plasma membrane, GNOM could control D6PK localization both in the Golgi and at the plasma membrane **(Figure 4.1.1B)**. On the one hand, D6PK might undergo, as the PINs, GNOM-dependent vesicle trafficking from the Golgi/TGN to the plasma membrane. In this case, it must be assumed that this GNOM-dependent vesicle trafficking of D6PK to the plasma membrane must be extremely fast to counteract the fast dissociation (~5 min) of D6PK from the plasma membrane. This hypothesis, though not impossible, seems not sufficient to explain BFA-induced D6PK mislocalization. Although internalized D6PK is mostly membrane-associated after BFA-treatment, D6PK does not completely colocalize with BFA compartments but also appears in the cytosol where it may be soluble or may be attached to vesicles that are not (or not yet) part of BFA compartments (Barbosa et al, 2014; Robinson et al, 2008). On the other hand, it could be envisioned that GNOM-dependent ARF-GTPase activation at the plasma membrane leads to the recruitment of D6PK itself or of a recruiting factor to the plasma membrane. In this case, BFA would cause an impairment of D6PK recruitment to the plasma membrane and lead to its quick accumulation in the intracellular space, due to the fast dissociation rate from the plasma membrane. This scenario would fit the observed fast kinetics of D6PK dissociation after BFA treatment and its reassociation after BFA-washout treatments. This scenario would also be in line with the fast

dissociation (~5 min) of ARF-GTPases and their effectors from membranes, e.g. COPI and clathrin vesicle coats, after BFA treatment (D'Souza-Schorey & Chavrier, 2006; Donaldson et al, 1990; Klausner et al, 1992; Presley et al, 2002; Ritzenthaler et al, 2002).

Two assumptions would have to be made to support this latter scenario: First, that internalized D6PK would quickly associate to endomembrane compartments, since D6PK remains in the membrane fraction after BFA treatment; and second that GNL1, though redundant with GNOM in many aspects and also present at the plasma membrane, would have no function on the plasma membrane recruitment of D6PK, since BFA cannot block its function but can block D6PK recruitment to the plasma membrane **(Figure 4.1.1B)**.

At present, none of the two scenarios can undoubtedly be excluded or supported. Future identification of the responsible ARF-GTPase and the downstream effectors involved in the targeting of D6PK to the plasma membrane should help to clarify the exact mechanism of D6PK plasma membrane targeting. This might be a difficult task since the *Arabidopsis* genome encodes 21 ARF-GTPases (Vernoud et al, 2003). To overcome this redundancy, inducible and localized expression of GDP/GTP-locked versions of ARF-GTPase 1 were used to dissect the function of the six-membered ARF-GTPase 1 group in root hair initiation (Xu & Scheres, 2005). In turn, many of the known ARF-GTPases effectors could qualify as D6PK-recruiting factors such as coating complexes (e.g. clathrin, COPI), lipid modifying enzymes (e.g. PIP 5-kinases, PLD) or tethering factors (e.g. exocyst)(Donaldson & Jackson, 2011).

PIP 5-kinases are currently the most intriguing regulators from this list since I showed that PIP5K1 and PIP5K2 are required for proper D6PK delivery to the plasma membrane and that U73122-induced $PI(4,5)P_2$ accumulation leads to depolarized D6PK (Barbosa et al, in preparation). Curiously, a link between an ARF-GTPase and $PI(4,5)P_2$ production has previously been proposed in tobacco pollen tubes representing a promising precedence for such a regulatory mechanism also in plants (Kost et al, 1999).

In conclusion, the ARF-GEF protein GNOM controls D6PK and PIN localization and its function is crucial for auxin-dependent growth. The requirements of D6PK and PIN on GNOM are substantially different and indicate that GNOM-dependent trafficking of these proteins requires different molecular and trafficking processes. The identification of the downstream effectors of GNOM is an imperative task for future research since it is required to understand its diverse roles in protein trafficking and polar auxin transport.

Auxin feedbacks on PIN endocytosis and D6PK plasma membrane abundance

As reported for the PINs, I observed that exogenous application of auxin impacted on D6PK localization in root cells. Here again, the effects of auxin on D6PK differ greatly from the effects of auxin on PINs. While PIN short-term auxin treatments (≤ 2 h) inhibit clathrin-mediated endocytosis of PIN proteins, D6PK is transiently internalized and retargeted to the plasma membrane in the first 30 min of auxin treatment **(Figure 4.1.2A)** (Barbosa et al, 2014; Robert et al, 2010). In turn, longer auxin treatments (> 2 h) that promote PIN internalization, vacuolar targeting, and degradation, lead to the internalization of D6PK **(Figure 4.1.2B)** (Abas et al, 2006; Barbosa et al, 2014; Baster et al, 2013; Benjamins & Scheres, 2008; Paciorek et al, 2005).

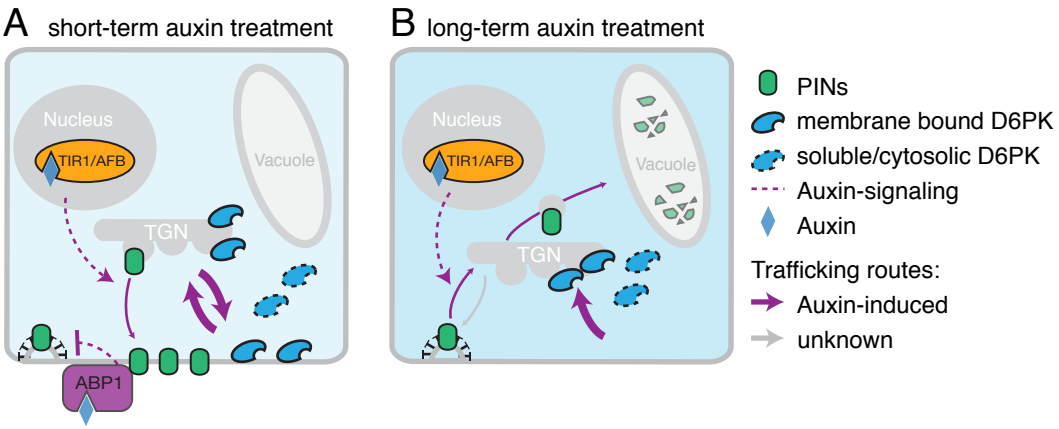

Figure 4.1.2 Effects of exogenous auxin application on D6PK and PIN trafficking.
(A) Short-term auxin application (≤ 2 h) leads to an increase in PIN abundance at the plasma membrane, by both, $SCF^{TIR1/AFB}$ activation of *PIN* transcription and ABP1-mediated inhibition of PIN endocytosis. The same treatment leads to a D6PK transient *disequilibrium*, which may be the result of an initial internalization from the plasma membrane followed by a retargeting to the plasma membrane, via an unknown mechanism. **(B)** Long-term auxin application (> 2 h) leads to reduced PIN abundance as a consequence of $SCF^{TIR1/AFB}$-promoted targeting of PINs for vacuolar degradation and to D6PK internalization via an as yet unknown mechanism.

PIN abundance and trafficking responses to these exogenous treatments correlated well with the effects of gravity-induced endogenous auxin redistribution effects on PIN2 kinetics (Baster et al, 2013). These findings support the notion that these auxin treatments have a physiological relevance, at least in the root gravitropism response. D6PK is likely not essential for PIN2-mediated root gravitropism, as judged by the mild root gravitropism phenotypes of the *d6pk* mutants and the fact that the two proteins do not colocalize at the epidermis where PIN2 is apical and D6PK is basal. For this reason, another physiologic system than root gravitropism has to be explored to monitor simultaneously D6PKs and PINs localization kinetics after redistribution of endogenous auxin. These could for example be phototropic or gravitropic

responses of etiolated seedlings, where D6PK and PIN3 localization in the hypocotyl could be monitored before and after asymmetric auxin redistribution in the bending zone.

The mechanism by which D6PK is internalized in response to auxin is still unclear. While phosphorylation at D6PK S310 and S311 seemingly triggers D6PK membrane dissociation and is strictly required for BFA-induced D6PK internalization, it is not required for auxin-induced D6PK internalization. In this context, knowledge about the stimuli-dependent internalization obtained for other AGCVIII kinases may provide some inspiration. phot1 and phot2 are internalized upon blue light exposure and ADI3, a putative orthologue of *Arabidopsis* AGC1.3 from tomato, is internalized upon pathogen attack. In both cases, internalization occurs upon phosphorylation at the conserved activation loop of these kinases (Ek-Ramos et al, 2014; Kaiserli et al, 2009; Kong et al, 2006). Since we observed, in the context of a different study, an auxin-induced increase in the phosphorylation of the D6PK activation loop (unpublished data), it would be interesting to test whether this phosphorylation is required and sufficient to induce D6PK internalization, as it is in the case of the phots and ADI3.

Additionally, treatments with two synthetic auxins with differential affinities to ABP1 and $SCF^{TIR1/AFB}$ signaling modules could be used to dissect at least the signaling core involved in auxin-induced D6PK internalization: 5-FIAA (5-Fluoroindole-3-acetic acid) promotes $SCF^{TIR1/AFB}$ transcriptional changes but not ABP1-dependent inhibition of PIN endocytosis and, inversely, PEO-IAA (α-(phenylethyl-2-oxo)-indole-3-acetic acid) has no (and even an antagonistic) effect on $SCF^{TIR1/AFB}$ signaling but promotes ABP1-dependent inhibition of endocytosis (Ma & Robert, 2014; Rigal et al, 2014).

Hence, our findings indicate that auxin feeds back on its own transport not only via the control of PIN abundance and trafficking but also via the control of the D6PK localization. Dissection of the here reported effects of auxin on D6PK localization are of pivotal importance for understanding auxin-dependent development, since our work firmly shows that the presence of D6PK is required for PIN activation and auxin transport-mediated growth. Due to this interdependence of D6PK and PINs for active auxin transport, I believe that both processes can no longer be studied independently.

PI(4,5)P_2 as an anchor and polarity landmark for D6PK at the plasma membrane

In the present thesis, it also became apparent that the ability of D6PK to bind phospholipids could mediate its anchoring to the plasma membrane. In particular, I provide support for PI(4,5)P_2 as an important phospholipid for D6PK plasma membrane-anchoring and polarity control. PI(4,5)P_2 has also been implicated in PIN polarity control, but again its role in controlling D6PK and PIN localization seems to differ between these two protein classes **(Figure 4.1.3)**.

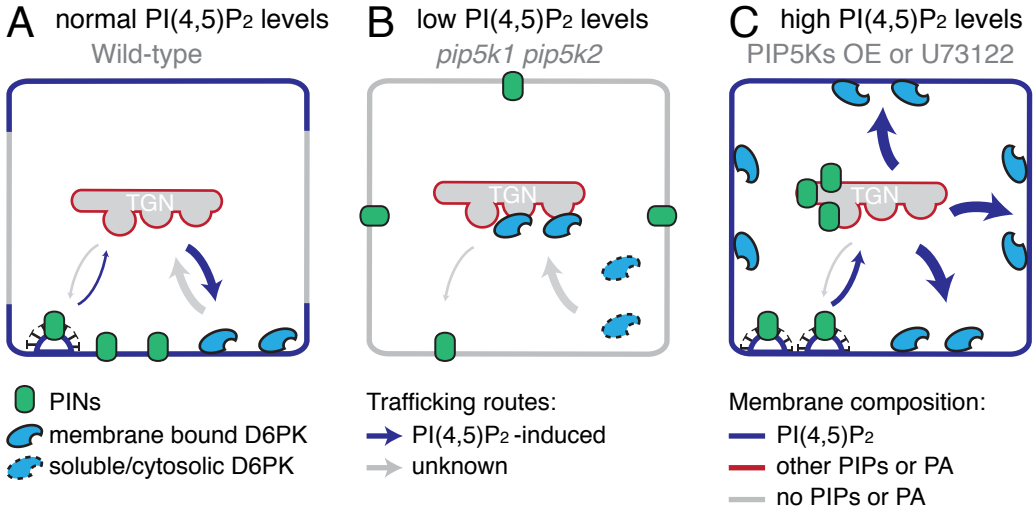

Figure 4.1.3 Effects of PI(4,5)P_2 plasma membrane composition on D6PK and PINs.
(A) In wild-type roots, PI(4,5)P_2 is bipolarly localized to the apical and basal plasma membrane. PI(4,5)P_2 is involved in clathrin-mediated endocytosis, thereby possibly controlling PIN trafficking, and in the recruitment of cytosolic PI(4,5)P_2-binding proteins, possibly including D6PK. **(B)** In *pip5k1 pi5k2* mutants, PI(4,5)P_2 levels are reduced leading to reduced PIN endocytosis and thus PIN polarity defects, as well as to reduced D6PK recruitment to the plasma membrane. In this case, D6PK might be recruited to endomembranes composed other polyacidic phospholipids such as other PIPs or PA, for which D6PK has normally a reduced affinity compared to PI(4,5)P_2. **(C)** High levels of PI(4,5)P_2 induced by *PIP5K1* or *PIP5K2* overexpression (PIP5Ks OE) lead to increased PIN endocytosis and intracellular accumulation of PINs. High levels of PI(4,5)P_2 induced by U73122-inhibition of PI-PLC leads to quick depolarization of D6PK, presumably because PI(4,5)P_2 also becomes apolar and recruits D6PK to lateral and apical plasma membrane domains.

In *pip5k1 pip5k2* mutants with reduced PI(4,5)P_2 levels, PINs have reduced clathrin-mediated endocytosis and polarity defects, e.g. PIN2 is shifted from the basal to the apical plasma membrane in root cortex cells and from the basal to the apical plasma membrane in embryonic procambial cells **(Figure 4.1.3B)**(Ischebeck et al, 2013; Tejos et al, 2014). In contrast, neither D6PK polarity nor BFA-induced internalization were affected in *pip5k1 pip5k2* mutants. However, D6PK was partially internalized and could be detected in the cytosol and in endosomal compartments, which correlated with a slower retargeting to the plasma membrane upon BFA treatment **(Figure 4.1.3B)**(Barbosa et al, in preparation). In contrast, accumulation of PI(4,5)P_2 via inhibition of PI-PLC by U73122 led to a quick depolarization of D6PK, while

accumulation of $PI(4,5)P_2$ via *PIP5K* overexpression promoted PIN internalization **(Figure 4.1.3C)** (Barbosa et al, in preparation; Ischebeck et al, 2013).

$PI(4,5)P_2$ is a plasma membrane-localized PIP that is typically involved in the polarity control in many eukaryotic cells. For instance, the spatial segregation of $PI(3,4,5)P_3$ from $PI(4,5)P_2$ domains at the plasma membrane is a highly conserved polarity pattern. In chemotactic cells of *Dictyostelium discoideum* as well as in mammalian neutrophils, leading versus retracting pseudopods are enriched in $PI(3,4,5)P_3$ and $PI(4,5)P_2$, respectively. Or in *Drosophilla* and mammalian epithelia, basolateral versus apical domains are composed of $PI(3,4,5)P_3$ and $PI(4,5)P_2$, respectively (Comer & Parent, 2007). Yeast and plants do not produce $PI(3,4,5)P_3$, but instead their polarized cells are enriched in $PI(4,5)P_2$. Local accumulation of $PI(4,5)P_2$ has been described in many processes of yeast polar growth, e.g. during invasive growth or during pheromone-induced anisotropy (Arkowitz & Bassilana, 2014; Garrenton et al, 2010; Guillas et al, 2013). In plants, $PI(4,5)P_2$ accumulates in the tips of pollen tubes and root hairs but it is also polar in many cells throughout plant development (Ischebeck et al, 2010; Tejos et al, 2014).

Additionally, $PI(4,5)P_2$ is required for proper clathrin-mediated endocytosis, since many of its components directly bind to $PI(4,5)P_2$ (e.g. AP-2, Dynamin) and since dynamic rounds of $PI(4,5)P_2$ synthesis and hydrolysis are crucial for the different steps of vesicle initiation, maturation, and fission (Balla, 2013; Sun et al, 2007). There is sparse, but convergent evidence for a similar role of $PI(4,5)P_2$ in plant cell endocytosis (Helling et al, 2006; Ischebeck et al, 2010; Zhao et al, 2010). For instance, the *pip5k1 pip5k2* mutants displayed defective clathrin vesicle dynamics at the plasma membrane and reduced PIN endocytosis rates (Ischebeck et al, 2013). Based on these endocytosis defects and the above-mentioned PIN polarity defects in *pip5k* mutants and overexpressors, it was proposed that $PI(4,5)P_2$ controls PIN polarity by regulating their clathrin-mediated endocytosis, since this is a known mechanism for PIN polarity maintenance (Ischebeck et al, 2013; Kitakura et al, 2011).

In the control of D6PK polarity, the role of $PI(4,5)P_2$ has to be different from that proposed for the PINs, since D6PK does not undergo clathrin-mediated endocytosis but has itself the ability to bind $PI(4,5)P_2$. It could be envisioned that $PI(4,5)P_2$ directly recruits D6PK to the plasma membrane. This hypothesis is very attractive, since $PI(4,5)P_2$ is enriched at the apical and basal domains of root epidermis cells where D6PK is basal (Ischebeck et al, 2013; Tejos et al, 2014). In this scenario, reduced $PI(4,5)P_2$ levels could explain D6PK partial internalization in *pip5k1 pip5k2* mutants **(Figure 4.1.3B)**. In turn, predicted $PI(4,5)P_2$ accumulation and lateralization after U73122 treatment could explain the observed D6PK depolarization **(Figure 4.1.3C)**. With regard to the latter, this would be similar to the reported U73122-induced depolarization of the tip-localized $PI(4,5)P_2$ biosensors in pollen tubes (Helling et al, 2006).

To test this hypothesis, it should first be confirmed that *pip5k1 pip5k2* have reduced $PI(4,5)P_2$ levels at the plasma membrane *in vivo*, as $PI(4,5)P_2$ levels have so far only been analyzed in total plant extracts. Furthermore, it should be confirmed that U73122 leads to a depolarization of $PI(4,5)P_2$ in the root epidermis, as it does in pollen tubes. To do so, the

recently developed high avidity PI(4,5)P_2 biosensors (Simon et al, 2014), should be tested in the *pip5k1 pip5k2* mutant and following U73122 treatment where they should ideally show similar responses as D6PK. Alternatively, rapamycin-inducible systems that allow recruiting phospholipid biosynthesis enzymes to the plasma membrane could be used to manipulate its phospholipid composition *in vivo* and monitor D6PK localization (Suh et al, 2006). Inducible plasma membrane PI(4,5)P_2 depletion, e.g. by PI-PLC recruitment, should lead to D6PK internalization while inducible PI(4,5)P_2 increase, e.g. by PIP5K recruitment, should lead to stabilization and potentially loss of D6PK polarity at the plasma membrane.

Another attractive hypothesis to test would be whether the previously described BFA- and auxin-induced internalization of D6PK is mediated by phospholipid composition changes, i.e. whether these treatments also induce PI(4,5)P_2 biosensor internalization. As mentioned before, PIP kinases are downstream effectors of ARF-GTPase (Di Paolo & De Camilli, 2006). So, BFA-induced D6PK internalization could be a direct consequence of the inhibition of a plasma membrane ARF-GTPase and the block of PI(4,5)P_2 production. In turn, auxin treatments lead to the transcriptional regulation of *PIP5K1* and *PIPK2* expression and as well to changes in the relative abundance of PI(4,5)P_2 and its precursor PI(4)P (Tejos et al, 2014).

In summary, my comparative analysis of D6PK and PIN trafficking, in search for mechanisms of D6PK-polarity control, clearly shows that the two proteins have substantially different plasma membrane residence times, polarity control mechanisms and membrane anchoring requirements. D6PK polarity apparently undergoes a much more dynamic control of its polarity than the PINs. This observations fit to the expectation that phosphorylation is typically a transient signal, with strong and thus tightly controlled effects on PIN activity. The presence and absence of D6PK at the plasma membrane seems then to constitute an effective mechanism to fine tune auxin transport and plant growth.

Importantly, all mechanisms that I analyzed here, that were previously believed to only affect PIN polarity, affected also D6PK localization in one way or another. In light of our group's findings that PIN-mediated auxin transport requires D6PK membrane localization, this indicates that previous interpretations of the auxin transport phenotypes of mutants like *gnom*$^{B/E}$ or *pip5k1 pipk2*, and possibly others, must be reevaluated. These studies attributed the observed phenotypes to the typically very low frequency PIN polarity defects, but as presented here, these phenotypes could just as well also be attributed to D6PK internalization and consequently reduced PIN-phosphorylation and activity. This prediction was actually confirmed in the *gnom*$^{B/E}$ mutant, where D6PK internalization correlates with reduced PIN3 phosphorylation and with tropism defects (Barbosa et al, 2014). Since PIN localization at the plasma membrane is not sufficient to predict active auxin transport, future similar studies cannot advance such conclusions anymore without the knowledge of the PIN activation status. As shown here, PIN activation status can be predicted based on the presence of PIN regulatory kinases (D6PK, PID, and probably others) at the plasma membrane or it can be directly assessed by for example *in situ* immunostaining using PIN phosphosite-specific antibodies (Zourelidou et al, 2014).

4.1.2 Comparison of D6PK to other polar peripheral membrane proteins from plants and non-plant species

D6PK is a new polarity marker in plants

In plants, several polarly localized plasma membrane proteins with distinct functions and polar domains have been identified **(Table 2)**. The ability of plant cells to define polar domains with diverse functions might be of crucial importance for adaption to changes in the environment (Kania et al, 2014). A survey of the known polarly distributed proteins in plants indicates that the polar distribution at the plasma membrane occurs in proteins that employ a diverse set of membrane attachment modes such as direct membrane integration, lipid modifications or protein-protein interactions and that also rely on diverse mechanisms for their polarity control **(Table 2)**. Unfortunately, there is still a rather limited understanding of the polarity control of these proteins with the notable exception of the intensively studied PINs.

Since the differences on the control of D6PK and PIN polarity have already been discussed above, the D6PK polarity control will be compared to other non-PIN polarity markers from plants and other organisms in this section. Specifically, two interesting examples will be discussed because they can provide some insight into possible mechanisms for D6PK polarity control: the RHO-GTPases and polarity regulators – ROPs (in plants) and CDC42 (in yeast and mammals), which are peripheral proteins and undergo dynamic vesicle-dependent and vesicle-independent targeting to the plasma membrane, and the PAR proteins (in animals) and POM1 (in fission yeast), which are also polarity regulators and peripheral proteins but whose dynamic polarity is mediated by phosphorylation in combination with positive and negative feedback mechanisms.

RHO-GTPases as polarity regulators: yeast CDC42 and plant ROPs

How cell polarity is established and maintained is an obvious and recurrent question in the study of cell biology. The currently best-studied example for a master polarity regulator is CDC42, a member of the highly conserved RHO-GTPase family, which is involved in polarity establishment in yeast and mammals (Thompson, 2013). In yeast, the local activation of CDC42 instructs localized endo- and exocytosis, consequently leading to symmetry breaking and cell wall as well as cytoskeleton remodeling, and ultimately polarized outgrowth (Iden & Collard, 2008). Similarly, ROPs (RHO-LIKE PROTIENS OF PLANTS) control the polar growth of pollen tubes and root hairs in plants. In these cells, tip-localized active ROPs control cytoskeleton and vesicle trafficking that are required for tip growth (Yang & Lavagi, 2012).

Table 2 Selected list of polarly localized proteins in plants.
As integral membrane proteins: PINs, NIP5;1 (NOD26-LIKE INTRINSIC PROTEINS 5;1); BOR1 (REQUIRES HIGH BORON 1) and ITR1 (IRON-REGULATED TRANSPORTER 1). And as peripheral membrane proteins: D6PK; BRX (BREVIS RADIX); BASL (BREAK OF ASYMMETRY IN STOMATAL LINEAGE); ROPs; PI-PLC and PIP5Ks. Col, columela; Epi, epidermis; En, endodermis; LRC, lateral root cap. Refer to List of Abbreviations for other components not spelled out here.

Protein	Function	Type	Polar domain	Mechanisms of polarity control	References
PINs	Polar auxin efflux	Integral	Apical, basal and apolar depending on the tissue	Recycling (GNOM); endocytosis (Clathrin); phosphorylation (PID/WAGs and PP6); plasma membrane composition ($PI(4,5)P_2$ and sterols); reduced lateral diffusion (cell wall, CESA3)	(Feraru et al, 2011; Kitakura et al, 2011; Kleine-Vehn & Friml, 2008; Luschnig & Vert, 2014; Willemsen et al, 2003)
NIP5;1	Boric acid channel	Integral	Distal side of Epi, LRC	Unknown	(Takano et al, 2010)
BOR1	Boric acid exporter	Integral	Proximal side of Col, Epi and LRC, En	Phosphorylation-dependent polar sorting (low Boron, unknown kinase)	(Takano et al, 2010)
ITR1	Iron transporter	Integral	Outer side of Epi	Zn, Mn and Co availability; recycling (FYVE1)	(Barberon et al, 2014)
D6PK	PIN phosphorylation and activation	Peripheral, Polybasic region	Basal (rootward) in most cells	$PI(4,5)P_2$ composition and phosphorylation at S310 and S311	(Barbosa et al, in preparation)
BRX	Auxin and brassinosteroid signaling (?)	Peripheral Unknown	Basal in vascular cells	Unknown	(Scacchi et al, 2009)
BASL	Scaffold protein in stomata development	Peripheral, MAPK-docking domain	Distal to asymmetric cell division in stomata	Phosphorylation (MAPK3/6)	(Dong et al, 2009; Zhang et al, 2015)
ROPs	Polarity, trafficking and cytoskeleton regulators	Peripheral, Prenylation, S-acylation and Polybasic region	Pollen tubes and root hairs tips and diverse polarity in other cell types	Activation (F-actin and Rho-GEF) and de-activation (RhoGAP, RhoGDI) cycles	(Kost, 2008; Lavy & Yalovsky, 2006; Yang & Lavagi, 2012)
PI-PLC3	$PI(4,5)P_2$ hydrolysis	Peripheral, EF and C2 domains	Lateral membrane of pollen tubes	Unknown	(Helling et al, 2006)
PIP5Ks	$PI(4,5)P_2$ synthesis	Peripheral Unknown	Apical-basal in roots and in tips of pollen tube and root hairs	Unknown	(Ischebeck et al, 2013; Tejos et al, 2014; Zhao et al, 2010)

In yeast interphase cells, the geranylgeranyl-modified and membrane-anchored CDC42 is uniformly distributed at the plasma membrane. During cell division, CDC42 polarizes spontaneously or following internal cues such as the bud scar that remains from previous cell divisions. This spontaneous polarization is thought to occur through positive feedback mechanisms through GEF-dependent CDC42 activation, CDC42 self-recruitment, and actin-dependent CDC42 polarization (Altschuler et al, 2008; Martin & Arkowitz, 2014; Thompson, 2013). Established CDC42 polarity is not static but, due to membrane lateral diffusion,

requires a dynamic maintenance by recycling. This is achieved through CDC42 polar exocytosis and dynamic CDC42 internalization. CDC42 internalization is mediated by fast RDI (RHO-GDP DISSOCIATION INHIBITORS)-dependent CDC42 membrane dissociation, which binds GDP-bound CDC42 and traps it in the cytosol, as well as by the slower actin-dependent endocytosis (Marco et al, 2007; Slaughter et al, 2009).

The polarity of plant ROPs, which are also lipid-modified by prenylation or S-acylation, is dynamically controlled by positive and negative feedbacks (Craddock et al, 2012; Yang & Lavagi, 2012). Polarly localized active ROPs instruct vesicle and F-actin-mediated exocytosis to the plasma membrane. ROP-mediated polar exocytosis delivers both activating ROP-GEFs but also inactivating ROP-GAPs and RDI dissociation factors. ROP-GEFs provide a positive feedback regulation required for local ROP-enrichment. ROP-GAPs and RDIs provide a negative feedback thought to be required for the restriction of active ROPs to the right polar domain (Craddock et al, 2012; Yang, 2008; Yang & Lavagi, 2012).

In summary, these two types of RHO-GTPases provide examples for how polarity establishment and maintenance of peripheral membrane proteins requires a mix of local recruitment, vesicle trafficking, and dissociation events. In this context, it would be interesting to explore how these polarity principles apply to D6PK steady state polarity. For instance, one could determine whether D6PK polarity relies on positive or negative feedback mechanisms, e.g. whether the PIN phosphorylation status feeds back on D6PK localization. Also, it would be interesting to determine the kinetics and relative contribution of the different targeting and retargeting modules that contribute to D6PK polarity, namely the vesicle-mediated transport, e.g. GNOM-dependent Golgi-to-plasma membrane trafficking, and the association/dissociation cycles, e.g. PIP-binding and presumably S310 and S311 phosphorylation-mediated internalization. This could be achieved using quantitative imaging approaches such as photoactivatable and inducible D6PK variants. These experiments would provide a quantitative and dynamic framework that could be modeled and explored to understand the minimal requirements for D6PK polarity establishment and maintenance at the plasma membrane.

In addition, since RHO-GTPases are themselves polarity organizers that are highly conserved in many organisms and polarized cells, it would not be surprising if D6PK polarity relied on such proteins. Interestingly, the specific recruitment of membrane proteins often relies on the interaction of proteins with phospholipids and small GTPases such as ROPs or ARF-GTPase (Di Paolo & De Camilli, 2006). *Arabidopsis* encodes 11 ROPs that have specific but also overlapping expression domains and localization but also seem to participate in the establishment of mutually exclusive domains, e.g. ROP2 and ROP6 regulate lobes and indents formation of pavement cells, respectively (Craddock et al, 2012; Yang & Lavagi, 2012). Particularly interesting in this context is the role of auxin as an internal organizing cue to the establishment these mutually exclusive polar domains (Xu et al, 2014; Xu et al, 2011a; Xu et al, 2011b). As suggested above for ARF-GTPases, the expression of dominant GDP/GTP-locked ROP-variants in combination with differential auxin treatments would allow dissecting the possible roles of a ROP-auxin module in the control of D6PK polarity.

Phosphorylation as a polarity switch: PAR proteins and POM1

Phosphorylation is a reversible protein modification that can interfere with protein conformation, activity, charge, and protein interactions. Because of these characteristics, phosphorylation provides an ideal mechanism for the maintenance of dynamic polarized states of peripheral membrane proteins, as discussed in the following examples. In the context of my thesis, I identified two likely phosphorylation sites in D6PK that, when substituted by non-phosphorylatable or phosphomimic amino acids, significantly disturbed D6PK localization and polarity. These phosphorylation sites emerge presently as the most interesting candidate sites for D6PK polarity maintenance.

PAR proteins are polarity regulators in animal cells that are absent from plants and yeast (Geldner, 2009; Goehring, 2014; Macara, 2004). In animals, PARs are responsible for the determination of mutually exclusive polar domains such as the anterior versus posterior domains of *Caenorhabditis elegans* zygotes or the apical versus basolateral domains of *Drosophila melanogaster* and mammalian epithelia (Hoege & Hyman, 2013; Thompson, 2013). PARs act in conserved core modules with additional players that are specific for each species. The anterior module in *C. elegans* zygotes and the apical module in epithelia consist of the scaffold proteins PAR-3 and PAR-6 (PDZ [PSD95/Dlg/ZO1] domain-containing proteins) and of the kinase aPKC-3 (ATYPICAL PROTEIN KINASE C). The posterior module of *C. elegans* zygotes and basolateral module in epithelia consist of the serine/threonine kinase PAR-1 and of the RING finger protein PAR-2. At the boundaries of the two domains, reciprocal phosphorylations between the PAR-kinases of each complex (aPKC and PAR-1) and components of the opposite complex, lead to the internalization of PAR components and thus exclusion of each module from the opposite domain. It is not clear how phosphorylation disturbs the membrane anchoring of PAR components but it is thought that induced conformation or charge changes are involved (Goehring, 2014; Hoege & Hyman, 2013). Alternative models suggest that cytoplasmic proteins, such as the 14-3-3 domain-containing protein PAR-5, bind the phosphorylated serine or threonine residues and thereby displace PAR components from the membrane and sequester them in the cytosol (Goehring, 2014).

An interesting feature of PAR proteins is their mobility. They are very mobile in the membrane and actively exchanged between the cytosol and the membrane (Goehring, 2014). Positive and negative feedbacks have been proposed that control the enrichment and depletion of PARs at the right domains. In contrast to CDC42, PAR proteins are not transported in vesicles but transported passively by flows along the anterior-posterior axis, which are induced by the translocation of a cortical actomyosin network (Goehring, 2014).

POM1, a member of the DIRK protein kinase family, is another interesting polar peripheral protein, which coordinates bipolar growth and cell division in fission yeast (Hachet et al, 2011). POM1 is recruited to the polar ends of the plasma membrane by microtubule transported and tip-localized landmark proteins. POM1 forms a gradient from the tip towards the middle of the cells that serves as a sensor for cell size and cell division control. The molecular mechanism underlying this gradient formation was recently unraveled (Hachet et al, 2011). It was found

that tip-recruited phosphorylated POM1 becomes dephosphorylated by tip-enriched phosphatases. POM1 then attaches to the membrane by ionic interaction between a polybasic motif and negatively charged phospholipids. As it moves laterally in the membrane, i.e. away from the tip, its colocalization with phosphatases diminishes and POM1 autophosphorylation at multiple sites accumulates. Phosphorylation near the polybasic motif disturbs POM1 protein-lipid ionic interaction and eventually leads to its internalization. Thus, phosphorylation constitutes a membrane dissociation mechanism but also an intrinsic sensor for POM1 position in the cell, where the phosphorylation level correlates with POM1 position.

The PAR and POM1 examples show that the protein phosphorylation status is a common theme in polar organization of peripheral plasma membrane proteins that can act in different modes. In the case of D6PK, interference with its phosphorylation status by inhibitor treatments or mutations at two putative phosphorylation sites affected its membrane association/dissociation kinetics as well as its polarity. Based on these examples, it can be easily conceived that phosphorylation affects D6PK conformation, protein-protein or protein-PIP interactions or surface charge. In the draft for Publication 3 (Barbosa et al, in preparation) and in the following sections, I discuss the possibility that D6PK phosphorylation-imposed charges neutralize the K-rich motif and displace D6PK from the plasma membrane. The data presented in the draft for Publication 3 also suggest that these phosphorylation events could explain D6PK dynamic plasma membrane association/dissociation and polarity control in a manner that is similar to that described for POM1. The dissection of these phosphorylation events, for example with the experiments suggested in 5.2.2, is imperative and can be mechanistically insightful for the understanding of D6PK and general polarity control in plants.

4.2 D6PK membrane anchoring via phospholipid binding

As described in the manuscript draft for Publication 3, a deletion- and mutagenesis-analysis of D6PK has allowed me to propose a molecular mechanism for the plasma membrane attachment of D6PK. I showed that D6PK is able to bind polyacidic phospholipids through a K-rich motif within the D6PK middle domain. Conversely, phospholipid composition determined its localization *in vivo* and putative phosphorylation nearby the K-rich motif determined its plasma membrane association and polarity. These findings led to the hypothetical model that D6PK plasma membrane anchoring is mediated by direct ionic interactions with phospholipids, while polarity is determined by both, phospholipid composition and phosphorylation-dependent trafficking and recycling. In the following sections, I will discuss to what extent the current data support this model and suggest experiments that could be performed in the future to further substantiate it.

4.2.1 The K-rich motif determines ionic interaction of D6PK with polyacidic phospholipids

Peripheral membrane proteins can be attached to membranes by diverse and often multiple mechanisms, such as protein-protein interactions, protein-lipid interactions or lipid-modifications (Carlton & Cullen, 2005; Heo et al, 2006; Cho & Stahelin, 2005; Sorek et al, 2009). In the draft for **Publication 3**, I provide several lines of evidence that the K-rich motif of the D6PK middle domain mediates D6PK-phospholipid interaction and anchoring to the plasma membrane.

First, I found that D6PK directly binds negatively charged phospholipids in lipid overlay experiments. However, the binding specificity *in vitro* does not always reflect the one *in vivo* (Kavran et al, 1998). Therefore, it is advisable to confirm the binding specificity of D6PK to the different phospholipids using complementary approaches such as liposome binding assays that have the advantage of being performed with lipids in a bilayer context. D6PK binding to PA- and not to PS-/PC-containing liposomes could already be confirmed using recombinant D6PK. The same result should be obtained for the PIP species and ideally, performed using D6PK from plant extracts, e.g. after YFP:D6PK-immunoprecipitation in the presence of biotinylated liposomes for pull-down assays (Knodler & Mayinger, 2005).

Second, pharmacologic and genetic interference with the synthesis and catabolism of polyacidic phospholipids interfered with D6PK localization *in vivo*. Pharmacologic treatments are not free from off-target effects. In particular, some of these treatments are not well established in plants and their effects are often only inferred from the effects known in animal or yeast cells. Since there are newly developed PIP- and PA-sensors available for plants, it would be important to repeat all treatments with these sensors and assess drug effectiveness and specificity in the cells examined here (Potocky et al, 2014; Simon et al, 2014).

Third, the middle domain was required and sufficient for D6PK membrane anchoring. Though this was a very clear result, it is unclear why the deletions that retain the middle domain but lack the N- or C-terminus did not associate with the plasma membrane. Also, the fact that the middle domain-deletion protein is still associated to membranes, albeit not plasma membrane, suggests that D6PK has additional mechanisms for membrane anchoring. This is not an unlikely scenario since polybasic interactions are of low affinity and often enhanced by an additional anchoring mechanism such as N-terminal myristoylation or C-terminal farnesylation (Heo et al, 2006). It would be interesting to determine, e.g. by mass spectrometry, whether such lipid modifications occur in D6PK and how they or other modifications act together with the K-rich motif to determine D6PK polar localization.

Finally, neutral alanine substitutions at the K-rich motif interfered with D6PK phospholipid binding *in vitro* as well as membrane association and localization *in vivo*. These two observations are strongly indicative for the K-rich motif being the surface for ionic lipid interaction, however the available data are just correlative, i.e. *in vitro* binding affinity correlates with *in vivo* localization. Ideally, *in vivo* support for K-rich motif-mediated phospholipid binding should be obtained. For example, as already suggested, by liposome pull-down assays with YFP:D6PK

versus YFP:D6PK-6KA, by comparing YFP:D6PK versus YFP:D6PK-6KA sensitivity to pharmacologic or genetic interference with phospholipid metabolism, or by substituting the lysines of the K-rich motif by negatively charged residues, which should lead to membrane repulsion (Schmick et al, 2014).

4.2.2 Phosphorylation at S310 and S311 controls D6PK plasma membrane affinity

In the draft for **Publication 3**, I also explore the possibility that D6PK phospholipid binding is regulated by phosphorylation at S310 and S311, which are located next to the K-rich motif and could neutralize the protein's net charge and release D6PK from the plasma membrane. The phosphorylation-dependent release of proteins from membranes commonly occurs in proteins where polybasic motifs mediate membrane anchoring, such as K-RAS and MARCKS, which are interestingly both phosphorylated by the AGC kinase PKC (Bivona et al, 2006; Thelen et al, 1991). In the case of MARCKS, PKC-dependent phosphorylation at three phosphorylation sites reduces the positive net charge of a 13-lysine stretch and reduces its plasma membrane localization and binding to acidic liposomes (Kim et al, 1994; Thelen et al, 1991). For K-RAS, PKC-dependent phosphorylation at a single serine is sufficient to internalize its eight lysine-motif to release the protein to the cytosol and to endomembranes (Bivona et al, 2006).

At present, the following lines of evidence support a role for S310 and S311 and their phosphorylation in the control of D6PK localization:

First, treatments with the phosphatase-inhibitor Calyculin A led to D6PK internalization in a S310 and S311-dependent manner. This is perhaps the strongest evidence since the action of Calyculin A on D6PK-internalization can be specifically reversed by mutations in the candidate phosphosite. However, ideally these specific phosphorylation events should be determined for D6PK, as for now only D6PKL2 was detected as being phosphorylated at these sites. Mass spectrometry can provide such a result, but also other alternative tools can be used to determine the phosphorylation events, and these may even be more insightful or versatile. These include the use of phosphosite-specific antibodies that allow detecting these events by immunoblotting *in vitro* or by immunostaining *in vivo*; or the determination of the kinetics of phosphorylation following different treatments with e.g. BFA or auxin. Alternatively, phosphate-binding chemicals, e.g. Phos-Tag, may improve the resolution of D6PK phosphorylation and may be used to detect S310 and S311-specific isoforms in immunoblots, and allow comparing YFP:D6PK and its phosphosite-mutant variants also in different conditions.

Second, phosphomimic mutations of S310 and S311 with negatively charged aspartic acids near the K-rich motif interfered with D6PK membrane association and localization *in vivo*. This result supports, in a manner independent from that obtained with the K-rich motif mutations, the importance of the net charge near or at the K-rich motif for D6PK plasma membrane anchoring. Although the addition of negative charges by the two aspartic acids significantly altered the subcellular localization of D6PK, its effect on D6PK membrane association were relatively modest: D6PK detected in the soluble fraction increased from 17% for YFP:D6PK to

30% for YFP:D6PK-SSDD, compared to 60% for YFP:D6PK-6KA. This suggests that internalized D6PK-SDD may still be attached to endomembranes. Interestingly, internalized K-RAS after phosphorylation or when carrying phosphomimic mutations is also still associated with endomembranes (Bivona et al, 2006). Such a differential recruitment of polybasic domains to different cellular membranes was reported to be a function of its charge, with the most positively charged motif being preferentially associated with $PI(4,5)P_2$ and $PI(3,4,5)P_3$ at the plasma membrane and the less positively charged protein being associated with the less electronegative PS-rich endomembranes (Yeung et al, 2008). These phenomena may be transferable to D6PK and may then also explain the still strong membrane association of YFP:D6PK-SSDD. To support this hypothesis, the ratio between plasma membrane and endomembrane-associated D6PK could be determined for YFP:D6PK and its mutant variants. Alternatively, it could be envisioned that mutations of YFP:D6PK-SSDD lead to shorter residence times of D6PK at the plasma membrane, due to higher dissociation rates. Such behaviors could be accessed with photoconvertible fluorophores or with FRAP (fluorescence recovery after photobleaching) experiments.

Third, the replacement of S310 and S311 by alanines correlated with a more stable plasma membrane association of D6PK. YFP:D6PK-SSAA appears resistant to BFA- and Calyculin A-induced D6PK internalization and YFP:D6PK-SSAA is generally less polar than its wild type counterpart. Besides supporting the role of phosphorylation in D6PK phospholipid binding, this result indicates that D6PK internalization after BFA-treatment is not a default but a regulated process that requires S310 and S311 and that D6PK internalization is required for D6PK polarity establishment. To confirm that YFP:D6PK-SSAA is more stably associated with the plasma membrane, its residence time could be measured with photoconvertible fluorophores. The YFP:D6PK-SSAA line might also provide an interesting tool to determine how GNOM acts in D6PK localization. Specifically, it would be interesting to check the localization of YFP:D6PK-SSAA in $gnom^{B/E}$ mutants. In $gnom^{B/E}$ mutants, D6PK accumulates intracellularly in the same way as D6PK does in the wild type after BFA treatment. This could either be a result of impaired *de novo* targeting of D6PK or of defective D6PK recycling. If GNOM was involved in *de novo* targeting of D6PK then YFP:D6PK-SSAA should be trapped intracellularly, similarly to YFP:D6PK in $gnom^{B/E}$. In turn, if GNOM was involved in the recycling of D6PK, because YFP:D6PK-SSAA cannot be internalized, YFP:D6PK-SSAA should remain at the plasma membrane in $gnom^{B/E}$.

In parallel, it still needs to be clarified whether the observed differential protein abundance in YFP:D6PK-SSDD and YFP:D6PK-SSAA, when compared to YFP:D6PK, is a result of altered feedback D6PK-dependent mechanisms that may act on *D6PK* transcription, D6PK translation or its protein turnover.

Finally, it would be interesting to clarify the identity of the protein kinase that is responsible for S310 and S311 phosphorylation. At present, it seems unlikely that D6PK itself phosphorylates these sites since plants overexpressing inactive D6PK (35S:YFP:D6PKin) have

neither defective localization nor altered BFA responses, unless this phosphorylation occurs inter-molecularly between endogenous D6PK and inactive D6PK (Barbosa et al, 2014).

In summary, the data on D6PK binding to phospholipids through the K-rich motif and regulatory phosphorylation at S310 and S311 reported here support these mechanisms as good candidates to explain the observed D6PK-membrane association kinetics and D6PK polarity control. They offer a preliminary matrix for future dissection and can also provide inspiration for the identification of D6PK upstream regulators.

4.3 D6PK plasma membrane abundance is rate-limiting for PIN-mediated auxin transport

In **Publication 1** and the draft for **Publication 3**, D6PK abundance at the plasma membrane was shown to critically determine PIN phosphorylation and auxin transport-dependent growth using diverse chemical treatments and genetic conditions.

These observations together with other work from our group that showed that D6PK activates PIN-mediated auxin transport (Willige et al, 2013; Zourelidou et al, 2014) have led me to propose a model according to which the presence of D6PK at the plasma membrane critically determines PIN phosphorylation, promotes auxin efflux activity, and ultimately auxin transport-dependent growth, e.g. during tropic responses **(Figure 4.3.1)**.

I have been able to generate at least three scenarios where the abundance of D6PK (and other D6PKs) at the plasma membrane correlates with PIN phosphorylation and auxin transport-dependent growth. First, titration of D6PK from the plasma membrane by low dosage BFA-treatments affected tropisms and PIN3 phosphorylation, and this effect could be suppressed by YFP:D6PK overexpression (Barbosa et al, 2014). Second, *d6pk* single and *d6pk01* double mutants were hypersensitive to BFA-induced tropism defects (Barbosa et al, 2014). Third, transgenic lines expressing YFP:D6PK with lysine mutations (YFP:D6PK-6KA) were less efficient in complementing *d6pk* mutants when the mutations resulted in decreased plasma membrane association (Barbosa et al, in preparation). To further substantiate this correlation between D6PK plasma membrane abundance and actual auxin transport rates, the D6PK mutant variants could be tested for PIN-activation in auxin transport experiments in oocytes, provided that they have the same localization defects in these cells. Conversely, complementation lines of these mutant variants in *d6pk01* mutants could be tested in established auxin transport experiments *in planta*, i.e. in inflorescence stems and hypocotyls of etiolated seedlings (Willige et al, 2013; Zourelidou et al, 2014). Alternatively, further characterization of the complementation efficiency of these D6PK mutants in other D6PK-dependent phenotypes might reveal differential D6PK-plasma membrane abundance requirements such as cotyledon formation defects, lateral root formation defects, or stem branching defects. In their combination, the experiments outlined here will lead to a better understanding of the plasma membrane-attachment and the polarity control of D6PK *in planta*.

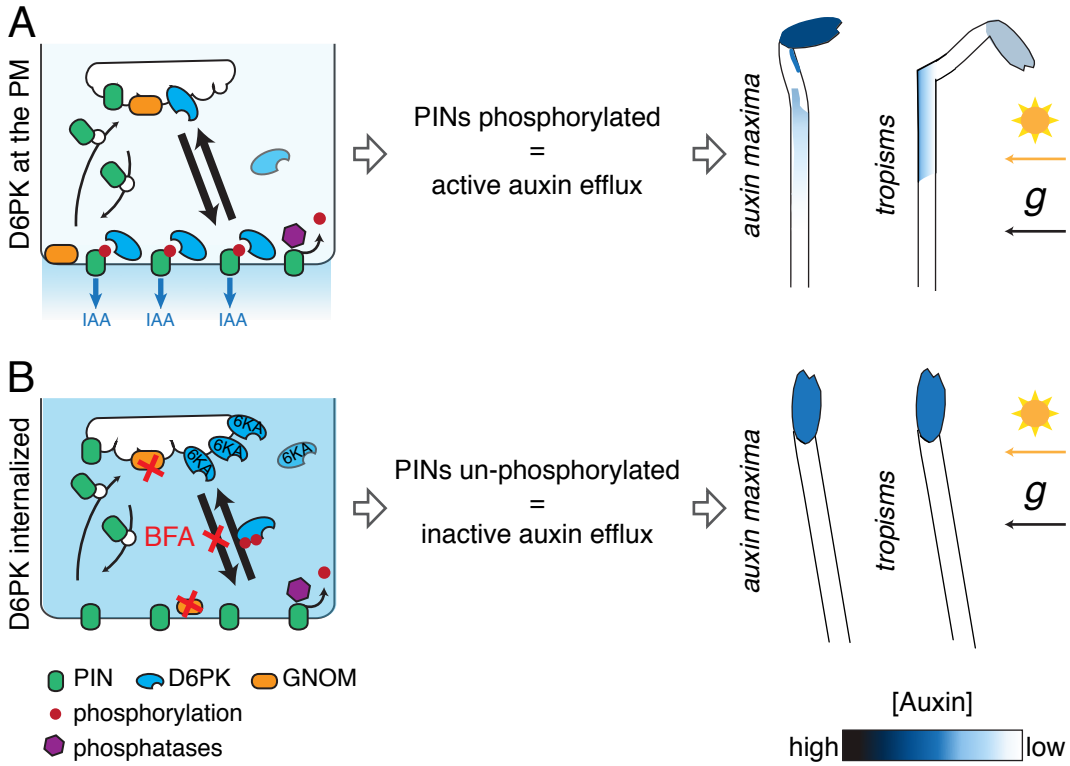

Figure 4.3.1 Working model for D6PK trafficking and D6PK control of PIN-mediated auxin transport.
(A) Dynamic trafficking, recruitment, and recycling maintain steady state D6PK levels at the plasma membrane required for PIN phosphorylation and activation of their auxin efflux capacity. Active PIN-mediated polar auxin transport at the cellular level is translated into proper auxin distribution at the organ level required, for example, for apical hook formation and tropic responses to light and gravity (*g*) stimuli in etiolated seedlings. **(B)** Failure in the trafficking, recruitment or recycling of D6PK to the plasma membrane lead to mistargeting of D6PK to internal membranes and the cytosol. Under these conditions, PIN phosphorylation is reduced by the action of counteracting phosphatases, leading to inactive auxin transport. Impaired cell-to-cell polar auxin transport leads to defective auxin distribution that impairs for example apical hook formation or tropism responses in a similar manner as observed in *d6pk* mutants.

4.4 Concluding remarks

In summary, this thesis presents the dissection of the cellular behavior of D6PK and clearly shows the interdependence of PIN and D6PK (and possibly other related protein kinase) at the plasma membrane for the maintenance of auxin transport at the cellular level, which is then translated into morphological changes at the organ level. The fact that not only D6PK but also other AGCVIII kinases, such as PID, can directly regulate auxin efflux, but have substantially different trafficking requirements and plasma membrane distributions, clearly demonstrates that much more work is needed to understand polar auxin transport and that currently established models are too simplistic. I hope this work lays a good and inspiring basis for the future dissection of these complex and dynamic molecular switches that control some of the most fascinating aspects of plant development.

5 Reference List

Abas L, Benjamins R, Malenica N, Paciorek T, Wisniewska J, Moulinier-Anzola JC, Sieberer T, Friml J, Luschnig C (2006) Intracellular trafficking and proteolysis of the Arabidopsis auxin-efflux facilitator PIN2 are involved in root gravitropism. *Nat Cell Biol* **8:** 249-256

Abel S, Theologis A (2010) Odyssey of auxin. *Cold Spring Harb Perspect Biol* **2:** a004572

Adamowski M, Friml J (2015) PIN-dependent auxin transport: action, regulation, and evolution. *Plant Cell* **27:** 20-32

Aggarwal C, Labuz J, Gabrys H (2013) Phosphoinositides play differential roles in regulating phototropin1- and phototropin2-mediated chloroplast movements in Arabidopsis. *PLoS One* **8:** e55393

Altschuler SJ, Angenent SB, Wang Y, Wu LF (2008) On the spontaneous emergence of cell polarity. *Nature* **454:** 886-889

Anders N, Jürgens G (2008) Large ARF guanine nucleotide exchange factors in membrane trafficking. *Cellular and Molecular Life Sciences* **65:** 3433-3445

Andreeva Z, Barton D, Armour WJ, Li MY, Liao LF, McKellar HL, Pethybridge KA, Marc J (2010) Inhibition of phospholipase C disrupts cytoskeletal organization and gravitropic growth in Arabidopsis roots. *Planta* **232:** 1263-1279

Arkowitz RA, Bassilana M (2014) Rho GTPase-phosphatidylinositol phosphate interplay in fungal cell polarity. *Biochemical Society transactions* **42:** 206-211

Baggiolini M, Dewald B, Schnyder J, Ruch W, Cooper PH, Payne TG (1987) Inhibition of the phagocytosis-induced respiratory burst by the fungal metabolite wortmannin and some analogues. *Experimental cell research* **169:** 408-418

Balla T (2013) Phosphoinositides: tiny lipids with giant impact on cell regulation. *Physiological reviews* **93:** 1019-1137

Ballesteros I, Dominguez T, Sauer M, Paredes P, Duprat A, Rojo E, Sanmartin M, Sanchez-Serrano JJ (2013) Specialized functions of the PP2A subfamily II catalytic subunits PP2A-C3 and PP2A-C4 in the distribution of auxin fluxes and development in Arabidopsis. *Plant J* **73:** 862-872

Barberon M, Dubeaux G, Kolb C, Isono E, Zelazny E, Vert G (2014) Polarization of IRON-REGULATED TRANSPORTER 1 (IRT1) to the plant-soil interface plays crucial role in metal homeostasis. *Proceedings of the National Academy of Sciences* **111:** 8293-8298

Barbosa ICR, Schwechheimer C (2014) Dynamic control of auxin transport-dependent growth by AGCVIII protein kinases. *Curr Opin Plant Biol* **22C:** 108-115

Barbosa ICR, Zourelidou M, Heilmann I, Schwechheimer C (in preparation) A phospholipid-binding K-rich motif and phosphorylation control plasma membrane localization and polarity of D6 PROTEIN KINASE.

Barbosa ICR, Zourelidou M, Willige BC, Weller B, Schwechheimer C (2014) D6 PROTEIN KINASE Activates Auxin Transport-Dependent Growth and PIN-FORMED Phosphorylation at the Plasma Membrane. *Dev Cell* **29:** 674-685

Bargmann BO, Vanneste S, Krouk G, Nawy T, Efroni I, Shani E, Choe G, Friml J, Bergmann DC, Estelle M, Birnbaum KD (2013) A map of cell type-specific auxin responses. *Mol Syst Biol* **9:** 688

Baster P, Robert S, Kleine-Vehn J, Vanneste S, Kania U, Grunewald W, De Rybel B, Beeckman T, Friml J (2013) SCFTIR1/AFB-auxin signalling regulates PIN vacuolar trafficking and auxin fluxes during root gravitropism. *EMBO J* **32:** 260-274

Beck M, Zhou J, Faulkner C, MacLean D, Robatzek S (2012) Spatio-temporal cellular dynamics of the Arabidopsis flagellin receptor reveal activation status-dependent endosomal sorting. *Plant Cell* **24:** 4205-4219

Behnia R, Munro S (2005) Organelle identity and the signposts for membrane traffic. *Nature* **438:** 597-604

Benjamins R, Scheres B (2008) Auxin: the looping star in plant development. *Annual Review of Plant Biology* **59:** 443-465

Benkova E, Michniewicz M, Sauer M, Teichmann T, Seifertová D, Jürgens G, Friml J (2003) Local, Efflux-Dependent Auxin gradients as a common module for plant organ formation. *Cell* **115:** 591-602

Bennett SRM, Alvarez J, Bossinger G, Smyth DR (1995) Morphogenesis in pinoid mutants of Arabidopsis thaliana. *The Plant Journal* **8:** 505-520

Bivona TG, Quatela SE, Bodemann BO, Ahearn IM, Soskis MJ, Mor A, Miura J, Wiener HH, Wright L, Saba SG, Yim D, Fein A, Perez de Castro I, Li C, Thompson CB, Cox AD, Philips MR (2006) PKC regulates a farnesyl-electrostatic switch on K-Ras that promotes its association with Bcl-XL on mitochondria and induces apoptosis. *Mol Cell* **21:** 481-493

Bleasdale JE, Thakur NR, Gremban RS, Bundy GL, Fitzpatrick FA, Smith RJ, Bunting S (1990) Selective inhibition of receptor-coupled phospholipase C-dependent processes in human platelets and polymorphonuclear neutrophils. *The Journal of pharmacology and experimental therapeutics* **255:** 756-768

Blilou I, Xu J, Wildwater M, Willemsen V, Paponov I, Friml J, Heidstra R, Aida M, Palme K, Scheres B (2005) The PIN auxin efflux facilitator network controls growth and patterning in Arabidopsis roots. *Nature* **433:** 39-44

Boysen-Jensen P (1911) La transmission de l'initiation phototropique dans l'Avena. *Oversigt over det Kongelige Danske Videnskabernes Selskabs* **3:** 1 – 29

Brunoud G, Wells DM, Oliva M, Larrieu A, Mirabet V, Burrow AH, Beeckman T, Kepinski S, Traas J, Bennett MJ, Vernoux T (2012) A novel sensor to map auxin response and distribution at high spatio-temporal resolution. *Nature* **482:** 103-106

Busch M, Mayer U, Jurgens G (1996) Molecular analysis of the Arabidopsis pattern formation of gene GNOM: gene structure and intragenic complementation. *Molecular & general genetics : MGG* **250:** 681-691

Calderon Villalobos LI, Lee S, De Oliveira C, Ivetac A, Brandt W, Armitage L, Sheard LB, Tan X, Parry G, Mao H, Zheng N, Napier R, Kepinski S, Estelle M (2012) A combinatorial TIR1/AFB-Aux/IAA co-receptor system for differential sensing of auxin. *Nat Chem Biol* **8:** 477-485

Carlton JG, Cullen PJ (2005) Coincidence detection in phosphoinositide signaling. *Trends Cell Biol* **15:** 540-547

Chen X, Naramoto S, Robert Sp, Tejos R, Löfke C, Lin D, Yang Z, Friml J (2012) ABP1 and ROP6 GTPase signaling regulate clathrin-mediated endocytosis in Arabidopsis roots. *Current Biology* **22:** 1326-1332

Cho W, Stahelin RV (2005) Membrane-protein interactions in cell signaling and membrane trafficking. *Annual review of biophysics and biomolecular structure* **34:** 119-151

Christie JM, Yang H, Richter GL, Sullivan S, Thomson CE, Lin J, Titapiwatanakun B, Ennis M, Kaiserli E, Lee OR, Adamec J, Peer WA, Murphy AS (2011) phot1 inhibition of ABCB19 primes lateral auxin fluxes in the shoot apex required for phototropism. PLoS Biol **9**: e1001076

Christensen SK, Dagenais N, Chory J, Weigel D (2000) Regulation of auxin response by the protein kinase PINOID. *Cell* **100:** 469-478

Clough SJ, Bent AF (1998) Floral dip: a simplified method for Agrobacterium-mediated transformation of Arabidopsis thaliana. *Plant J* **16:** 735-743

Comer FI, Parent CA (2007) Phosphoinositides specify polarity during epithelial organ development. *Cell* **128:** 239-240

Craddock C, Lavagi I, Yang Z (2012) New insights into Rho signaling from plant ROP/Rac GTPases. *Trends Cell Biol* **22:** 492-501

D'Souza-Schorey C, Chavrier P (2006) ARF proteins: roles in membrane traffic and beyond. *Nat Rev Mol Cell Biol* **7:** 347-358

Dai M, Zhang C, Kania U, Chen F, Xue Q, McCray T, Li G, Qin G, Wakeley M, Terzaghi W, Wan J, Zhao Y, Xu J, Friml J, Deng XW, Wang H (2012) A PP6-type phosphatase holoenzyme directly regulates PIN phosphorylation and auxin efflux in Arabidopsis. *Plant Cell* **24:** 2497-2514

Darwin C, Darwin F (1880) *The power of movement in plants*, London: John Murray Publishers.

de Chaffoy de Courcelles DC, Roevens P, Van Belle H (1985) R 59 022, a diacylglycerol kinase inhibitor. Its effect on diacylglycerol and thrombin-induced C kinase activation in the intact platelet. *J Biol Chem* **260:** 15762-15770

Dharmasiri N, Dharmasiri S, Estelle M (2005) The F-box protein TIR1 is an auxin receptor. *Nature* **435:** 441-445

Dhonukshe P (2011) PIN polarity regulation by AGC-3 kinases and ARF-GEF: A recurrent theme with context dependent modifications for plant development and response. *Plant Signaling & Behavior* **6:** 1333-1337

Dhonukshe P, Aniento F, Hwang I, Robinson DG, Mravec J, Stierhof Y-D, Friml J (2007) Clathrin-mediated constitutive endocytosis of PIN auxin efflux carriers in Arabidopsis. *Current Biology* **17:** 520-527

Dhonukshe P, Huang F, Galvan-Ampudia CS, Mähönen AP, Kleine-Vehn J, Xu J, Quint A, Prasad K, Friml J, Scheres B, Offringa R (2010) Plasma membrane-bound AGC3 kinases phosphorylate PIN auxin carriers at TPRXS(N/S) motifs to direct apical PIN recycling. *Development* **137:** 3245-3255

Dhonukshe P, Tanaka H, Goh T, Ebine K, Mahonen AP, Prasad K, Blilou I, Geldner N, Xu J, Uemura T, Chory J, Ueda T, Nakano A, Scheres B, Friml J (2008) Generation of cell polarity in plants links endocytosis, auxin distribution and cell fate decisions. *Nature* **456:** 962-966

Di Paolo G, De Camilli P (2006) Phosphoinositides in cell regulation and membrane dynamics. *Nature* **443:** 651-657

Ding Z, Galvan-Ampudia CS, Demarsy E, Langowski L, Kleine-Vehn J, Fan Y, Morita MT, Tasaka M, Fankhauser C, Offringa R, Friml J (2011) Light-mediated polarization of the PIN3 auxin transporter for the phototropic response in Arabidopsis. *Nat Cell Biol* **13:** 447-452

Donaldson JG, Jackson CL (2000) Regulators and effectors of the ARF GTPases. *Current Opinion in Cell Biology* **12:** 475-482

Donaldson JG, Jackson CL (2011) ARF family G proteins and their regulators: roles in membrane transport, development and disease. *Nat Rev Mol Cell Biol* **12:** 362-375

Donaldson JG, Lippincott-Schwartz J, Bloom GS, Kreis TE, Klausner RD (1990) Dissociation of a 110-kD peripheral membrane protein from the Golgi apparatus is an early event in brefeldin A action. *J Cell Biol* **111:** 2295-2306

Dong J, MacAlister CA, Bergmann DC (2009) BASL controls asymmetric cell division in Arabidopsis. *Cell* **137:** 1320-1330

Durek P, Schmidt R, Heazlewood JL, Jones A, MacLean D, Nagel A, Kersten B, Schulze WX (2010) PhosPhAt: the Arabidopsis thaliana phosphorylation site database. An update. *Nucleic Acids Res* **38:** D828-834

Ek-Ramos MaJ, Avila J, Cheng C, Martin GB, Devarenne TP (2010) The T-loop extension of the tomato protein kinase AvrPto-dependent Pto-interacting protein 3 (Adi3) directs nuclear localization for suppression of plant Cell Death. *Journal of Biological Chemistry* **285:** 17584-17594

Ek-Ramos MJ, Avila J, Nelson Dittrich AC, Su D, Gray JW, Devarenne TP (2014) The Tomato Cell Death Suppressor Adi3 Is Restricted to the Endosomal System in Response to the *Pseudomonas syringae* Effector Protein AvrPto. *PLoS ONE* **9:** e110807

Enders TA, Oh S, Yang Z, Montgomery BL, Strader LC (2015) Genome Sequencing of Arabidopsis abp1-5 Reveals Second-Site Mutations That May Affect Phenotypes. *Plant Cell*

Enugutti B, Kirchhelle C, Oelschner M, Torres Ruiz RA, Schliebner I, Leister D, Schneitz K (2012) Regulation of planar growth by the Arabidopsis AGC protein kinase UNICORN. *Proc Natl Acad Sci U S A* **109:** 15060-15065

Feraru E, Feraru MI, Kleine-Vehn Jr, Martiniére A, Mouille Gg, Vanneste S, Vernhettes S, Runions J, Friml J (2011) PIN polarity maintenance by the cell wall in Arabidopsis. *Current Biology* **21:** 338-343

Fitting H (1907) Die Leitung troptisticher Reize im parallelotropen Pflanzenteilen. *Jahrbucher fur Wissenschaftliche Botanik* **44:** 177 – 253

Friml J, Wisniewska J, Benkova E, Mendgen K, Palme K (2002) Lateral relocation of auxin efflux regulator PIN3 mediates tropism in Arabidopsis. *Nature* **415:** 806-809

Friml J, Vieten A, Sauer M, Weijers D, Schwarz H, Hamann T, Offringa R, Jurgens G (2003) Efflux-dependent auxin gradients establish the apical-basal axis of Arabidopsis. *Nature* **426:** 147-153

Friml J, Yang X, Michniewicz M, Weijers D, Quint A, Tietz O, Benjamins R, Ouwerkerk PBF, Ljung K, Sandberg G, Hooykaas PJJ, Palme K, Offringa R (2004) A PINOID-dependent binary switch in apical-basal PIN polar targeting directs auxin efflux. *Science* **306:** 862-865

Galván-Ampudia CS, Offringa R (2007) Plant evolution: AGC kinases tell the auxin tale. *Trends in Plant Science* **12:** 541-547

Gälweiler L, Guan C, Müller A, Wisman E, Mendgen K, Yephremov A, Palme K (1998) Regulation of polar auxin transport by AtPIN1 in Arabidopsis vascular tissue. *Science* **282:** 2226-2230

Gao Y, Zhang Y, Zhang D, Dai X, Estelle M, Zhao Y (2015) Auxin binding protein 1 (ABP1) is not required for either auxin signaling or Arabidopsis development. *Proc Natl Acad Sci U S A* **112:** 2275-2280

Garrenton LS, Stefan CJ, McMurray MA, Emr SD, Thorner J (2010) Pheromone-induced anisotropy in yeast plasma membrane phosphatidylinositol-4,5-bisphosphate distribution is required for MAPK signaling. *Proc Natl Acad Sci U S A* **107:** 11805-11810

Geldner N (2009) Cell polarity in plants - a PARspective on PINs. *Current Opinion in Plant Biology* **12:** 42-48

Geldner N, Anders N, Wolters H, Keicher J, Kornberger W, Muller P, Delbarre A, Ueda T, Nakano A, Jürgens G (2003) The Arabidopsis GNOM ARF-GEF mediates endosomal recycling, auxin transport, and auxin-dependent plant growth. *Cell* **112:** 219-230

Geldner N, Richter S, Vieten A, Marquardt S, Torres-Ruiz RA, Mayer U, Jürgens G (2004) Partial loss-of-function alleles reveal a role for GNOM in auxin transport-related, post-embryonic development of Arabidopsis. *Development* **131:** 389-400

Goehring NW (2014) PAR polarity: from complexity to design principles. *Experimental cell research* **328:** 258-266

Goldsmith MHM (1977) The Polar Transport of Auxin. *Annual Review of Plant Physiology* **28:** 439-478

Gray WM, Kepinski S, Rouse D, Leyser O, Estelle M (2001) Auxin regulates SCF(TIR1)-dependent degradation of AUX/IAA proteins. *Nature* **414:** 271-276

Grieneisen VA, Xu J, Maree AFM, Hogeweg P, Scheres B (2007) Auxin transport is sufficient to generate a maximum and gradient guiding root growth. *Nature* **449:** 1008-1013

Grones P, Chen X, Simon S, Kaufmann WA, De Rycke R, Nodzynski T, Zazimalova E, Friml J (2015) Auxin-binding pocket of ABP1 is crucial for its gain-of-function cellular and developmental roles. *J Exp Bot*

Grunewald W, Friml J (2010) The march of the PINs: developmental plasticity by dynamic polar targeting in plant cells. *Embo J* **29:** 2700-2714

Guillas I, Vernay A, Vitagliano JJ, Arkowitz RA (2013) Phosphatidylinositol 4,5-bisphosphate is required for invasive growth in *Saccharomyces cerevisiae*. *J Cell Sci* **126:** 3602-3614

Hachet O, Berthelot-Grosjean M, Kokkoris K, Vincenzetti V, Moosbrugger J, Martin SG (2011) A phosphorylation cycle shapes gradients of the DYRK family kinase Pom1 at the plasma membrane. *Cell* **145:** 1116-1128

Hammond GR, Balla T (2015) Polyphosphoinositide binding domains: Key to inositol lipid biology. *Biochim Biophys Acta* **1851:** 746-758

Havens KA, Guseman JM, Jang SS, Pierre-Jerome E, Bolten N, Klavins E, Nemhauser JL (2012) A synthetic approach reveals extensive tunability of auxin signaling. *Plant Physiol* **160:** 135-142

Heazlewood JL, Durek P, Hummel J, Selbig J, Weckwerth W, Walther D, Schulze WX (2008) PhosPhAt: a database of phosphorylation sites in Arabidopsis thaliana and a plant-specific phosphorylation site predictor. *Nucleic Acids Res* **36:** D1015-1021

Heilmann I (2009) Using genetic tools to understand plant phosphoinositide signalling. *Trends Plant Sci* **14:** 171-179

Heisler MG, Ohno C, Das P, Sieber P, Reddy GV, Long JA, Meyerowitz EM (2005) Patterns of auxin transport and gene expression during primordium development revealed by live imaging of the Arabidopsis inflorescence meristem. *Current Biology* **15:** 1899-1911

Helling D, Possart A, Cottier S, Klahre U, Kost B (2006) Pollen tube tip growth depends on plasma membrane polarization mediated by tobacco PLC3 activity and endocytic membrane recycling. *Plant Cell* **18:** 3519-3534

Hellens R, Edwards EA, Leyland N, Bean S, Mullineaux P (2000) pGreen: a versatile and flexible binary Ti vector for Agrobacterium-mediated plant transformation. *Plant Molecular Biology* **42:** 819-832

Heo WD, Inoue T, Park WS, Kim ML, Park BO, Wandless TJ, Meyer T (2006) PI(3,4,5)P3 and PI(4,5)P2 Lipids target proteins with polybasic clusters to the plasma Membrane. *Science* **314:** 1458-1461

Hoege C, Hyman AA (2013) Principles of PAR polarity in *Caenorhabditis elegans* embryos. *Nat Rev Mol Cell Biol* **14:** 315-322

Hofmann NR (2014) The importance of being absent: auxin minima are required for axillary meristem formation. *Plant Cell* **26:** 1836

Holland JJ, Roberts D, Liscum E (2009) Understanding phototropism: from Darwin to today. *J Exp Bot* **60:** 1969-1978

Huang F, Kemel Zago M, Abas L, van Marion A, Galvan-Ampudia CS, Offringa R (2010) Phosphorylation of conserved PIN motifs directs Arabidopsis PIN1 polarity and auxin transport. *Plant Cell* **22:** 1129-1142

Iden S, Collard JG (2008) Crosstalk between small GTPases and polarity proteins in cell polarization. *Nat Rev Mol Cell Biol* **9:** 846-859

Ikeda Y, Men S, Fischer U, Stepanova AN, Alonso JM, Ljung K, Grebe M (2009) Local auxin biosynthesis modulates gradient-directed planar polarity in Arabidopsis. *Nat Cell Biol* **11:** 731-738

Irani NG, Di Rubbo S, Mylle E, Van den Begin J, Schneider-Pizoń J, Hniliková J, Šíša M, Buyst D, Vilarrasa-Blasi J, Szatmári A-M, Van Damme D, Mishev K, Codreanu M-C, Kohout L, Strnad M, Caño-Delgado AI, Friml J, Madder A, Russinova E (2012)

Fluorescent castasterone reveals BRI1 signaling from the plasma membrane. *Nat Chem Biol* **8**: 583-589

Ischebeck T, Seiler S, Heilmann I (2010) At the poles across kingdoms: phosphoinositides and polar tip growth. *Protoplasma* **240:** 13-31

Ischebeck T, Werner S, Krishnamoorthy P, Lerche J, Meijon M, Stenzel I, Lofke C, Wiessner T, Im YJ, Perera IY, Iven T, Feussner I, Busch W, Boss WF, Teichmann T, Hause B, Persson S, Heilmann I (2013) Phosphatidylinositol 4,5-bisphosphate influences PIN polarization by controlling clathrin-mediated membrane trafficking in Arabidopsis. *Plant Cell* **25:** 4894-4911

Ishihara H, Martin BL, Brautigan DL, Karaki H, Ozaki H, Kato Y, Fusetani N, Watabe S, Hashimoto K, Uemura D, et al. (1989) Calyculin A and okadaic acid: inhibitors of protein phosphatase activity. *Biochem Biophys Res Commun* **159:** 871-877

Jaillais Y, Fobis-Loisy I, Miege C, Rollin C, Gaude T (2006) AtSNX1 defines an endosome for auxin-carrier trafficking in Arabidopsis. *Nature* **443:** 106-109

Jaillais Y, Hothorn M, Belkhadir Y, Dabi T, Nimchuk ZL, Meyerowitz EM, Chory J (2011) Tyrosine phosphorylation controls brassinosteroid receptor activation by triggering membrane release of its kinase inhibitor. *Genes Dev* **25:** 232-237

Jenkins GM, Frohman MA (2005) Phospholipase D: a lipid centric review. *Cellular and molecular life sciences : CMLS* **62:** 2305-2316

Jönsson H, Heisler MG, Shapiro BE, Meyerowitz EM, Mjolsness E (2006) An auxin-driven polarized transport model for phyllotaxis. *Proc Natl Acad Sci U S A* **103:** 1633-1638

Jurado S, Abraham Z, Manzano C, Lopez-Torrejon G, Pacios LF, Del Pozo JC (2010) The Arabidopsis cell cycle F-box protein SKP2A binds to auxin. *Plant Cell* **22:** 3891-3904

Kaiserli E, Sullivan S, Jones MA, Feeney KA, Christie JM (2009) Domain swapping to assess the mechanistic basis of Arabidopsis phototropin 1 receptor kinase activation and endocytosis by blue light. *Plant Cell* **21:** 3226-3244

Kania U, Fendrych M, Friml J (2014) Polar delivery in plants; commonalities and differences to animal epithelial cells. *Open biology* **4:** 140017

Kavran JM, Klein DE, Lee A, Falasca M, Isakoff SJ, Skolnik EY, Lemmon MA (1998) Specificity and promiscuity in phosphoinositide binding by pleckstrin homology domains. *J Biol Chem* **273:** 30497-30508

Kepinski S, Leyser O (2005) The Arabidopsis F-box protein TIR1 is an auxin receptor. *Nature* **435:** 446-451

Kim J, Blackshear PJ, Johnson JD, McLaughlin S (1994) Phosphorylation reverses the membrane association of peptides that correspond to the basic domains of MARCKS and neuromodulin. *Biophys J* **67:** 227-237

Kitakura S, Vanneste S, Robert S, Löfke C, Teichmann T, Tanaka H, Friml J (2011) Clathrin mediates endocytosis and polar distribution of PIN auxin transporters in Arabidopsis. *Plant Cell* **23**:1920-1931.

Klausner RD, Donaldson JG, Lippincott-Schwartz J (1992) Brefeldin A: insights into the control of membrane traffic and organelle structure. *J Cell Biol* **116:** 1071-1080

Kleine-Vehn J, Dhonukshe P, Sauer M, Brewer PB, Wisniewska J, Paciorek T, Benková E, Friml J (2008) ARF GEF-Dependent transcytosis and polar delivery of PIN auxin carriers in Arabidopsis. *Current Biology* **18:** 526-531

Kleine-Vehn J, Friml J (2008) Polar targeting and endocytic recycling in auxin-dependent plant development. *Annual Review of Cell and Developmental Biology* **24:** 447-473

Kleine-Vehn J, Huang F, Naramoto S, Zhang J, Michniewicz M, Offringa R, Friml J (2009) PIN auxin efflux carrier polarity is regulated by PINOID kinase-mediated recruitment into GNOM-independent trafficking in Arabidopsis. *Plant Cell* **21:** 3839-3849

Kleine-Vehn J, Wabnik K, Martiniere A, Langowski L, Willig K, Naramoto S, Leitner J, Tanaka H, Jakobs S, Robert S, Luschnig C, Govaerts W, W Hell S, Runions J, Friml J (2011) Recycling, clustering, and endocytosis jointly maintain PIN auxin carrier polarity at the plasma membrane. *Mol Syst Biol* **7**

Kleine-Vehn Jr, Ding Z, Jones AR, Tasaka M, Morita MT, Friml J (2010) Gravity-induced PIN transcytosis for polarization of auxin fluxes in gravity-sensing root cells. *Proceedings of the National Academy of Sciences* **107:** 22344-22349

Knodler A, Mayinger P (2005) Analysis of phosphoinositide-binding proteins using liposomes as an affinity matrix. *BioTechniques* **38:** 858, 860, 862

Kogl F H-SA (1931) Mitteilung uber pflanzliche wachstumsstoffe. Uber die vhemie des euchsstoffs. *Proceedings Koninklijke Nederlandse Akademie van Wetenschappen* **34:** 1411–1416

Kong S-G, Suzuki T, Tamura K, Mochizuki N, Hara-Nishimura I, Nagatani A (2006) Blue light-induced association of phototropin 2 with the Golgi apparatus. *The Plant Journal* **45:** 994-1005

Korasick DA, Westfall CS, Lee SG, Nanao MH, Dumas R, Hagen G, Guilfoyle TJ, Jez JM, Strader LC (2014) Molecular basis for AUXIN RESPONSE FACTOR protein interaction and the control of auxin response repression. *Proc Natl Acad Sci U S A* **111:** 5427-5432

Kost B (2008) Spatial control of Rho (Rac-Rop) signaling in tip-growing plant cells. *Trends Cell Biol* **18:** 119-127

Kost B, Lemichez E, Spielhofer P, Hong Y, Tolias K, Carpenter C, Chua NH (1999) Rac homologues and compartmentalized phosphatidylinositol 4, 5-bisphosphate act in a common pathway to regulate polar pollen tube growth. *J Cell Biol* **145:** 317-330

Krahn MP, Klopfenstein DR, Fischer N, Wodarz A (2010) Membrane targeting of Bazooka/PAR-3 is mediated by direct binding to phosphoinositide lipids. *Curr Biol* **20:** 636-642

Krecek P, Skupa P, Libus J, Naramoto S, Tejos R, Friml J, Zazimalova E (2009) The PIN-FORMED (PIN) protein family of auxin transporters. *Genome biology* **10:** 249

Lavy M, Yalovsky S (2006) Association of Arabidopsis type-II ROPs with the plasma membrane requires a conserved C-terminal sequence motif and a proximal polybasic domain. *Plant J* **46:** 934-947

Le J, Liu XG, Yang KZ, Chen XL, Zou JJ, Wang HZ, Wang M, Vanneste S, Morita M, Tasaka M, Ding ZJ, Friml J, Beeckman T, Sack F (2014) Auxin transport and activity regulate stomatal patterning and development. *Nature communications* **5:** 3090

Li G, Xue H-W (2007) Arabidopsis PLDζ2 Regulates Vesicle Trafficking and Is Required for Auxin Response. *Plant Cell* **19:** 281-295

Li H, Lin D, Dhonukshe P, Nagawa S, Chen D, Friml J, Scheres B, Guo H, Yang Z (2011) Phosphorylation switch modulates the interdigitated pattern of PIN1 localization and cell expansion in Arabidopsis leaf epidermis. *Cell Res* **21:** 970-978

Li L, Shi X, Guo X, Li H, Xu C (2014) Ionic protein-lipid interaction at the plasma membrane: what can the charge do? *Trends Biochem Sci* **39:** 130-140

Liu CM (2015) Auxin Binding Protein 1 (ABP1): a matter of fact. *J Integr Plant Biol* **57:** 234-235

Luschnig C, Vert G (2014) The dynamics of plant plasma membrane proteins: PINs and beyond. *Development* **141:** 2924-2938

Ma Q, Robert S (2014) Auxin biology revealed by small molecules. *Physiologia plantarum* **151:** 25-42

Macara IG (2004) Par proteins: partners in polarization. *Curr Biol* **14:** R160-162

Marco E, Wedlich-Soldner R, Li R, Altschuler SJ, Wu LF (2007) Endocytosis optimizes the dynamic localization of membrane proteins that regulate cortical polarity. *Cell* **129:** 411-422

Martin SG, Arkowitz RA (2014) Cell polarization in budding and fission yeasts. *FEMS microbiology reviews* **38:** 228-253

Maures TJ, Su H-W, Argetsinger LS, Grinstein S, Carter-Su C (2011) Phosphorylation controls a dual-function polybasic nuclear localization sequence in the adapter protein SH2β1 to regulate its cellular function and distribution. *Journal of Cell Science* **124:** 1542-1552

Mayer U, Buttner G, Jürgens G (1993) Apical-basal pattern formation in the Arabidopsis embryo: studies on the role of the gnom gene. *Development* **117:** 149-162

McCaffrey LM, Macara IG (2009) Widely conserved signaling pathways in the establishment of cell polarity. *Cold Spring Harb Perspect Biol* **1:** a001370

McLaughlin S, Aderem A (1995) The myristoyl-electrostatic switch: a modulator of reversible protein-membrane interactions. *Trends Biochem Sci* **20:** 272-276

Meijer HJG, Munnik T (2003) Phospholipid-based signaling in plants. *Annual Review of Plant Biology* **54:** 265-306

Michniewicz M, Zago MK, Abas L, Weijers D, Schweighofer A, Meskiene I, Heisler MG, Ohno C, Zhang J, Huang F, Schwab R, Weigel D, Meyerowitz EM, Luschnig C, Offringa R, Friml J (2007) Antagonistic regulation of PIN phosphorylation by PP2A and PINOID directs auxin flux. *Cell* **130:** 1044-1056

Moore I (2002) Gravitropism: lateral thinking in auxin transport. *Curr Biol* **12:** R452-454

Mossessova E, Corpina RA, Goldberg J (2003) Crystal structure of ARF1*Sec7 complexed with Brefeldin A and its implications for the guanine nucleotide exchange mechanism. *Mol Cell* **12:** 1403-1411

Muller A, Guan C, Galweiler L, Tanzler P, Huijser P, Marchant A, Parry G, Bennett M, Wisman E, Palme K (1998) AtPIN2 defines a locus of Arabidopsis for root gravitropism control. *EMBO J* **17:** 6903-6911

Munnik T, Nielsen E (2011) Green light for polyphosphoinositide signals in plants. *Cur Op Plant Bio* **14:** 489-497

Naramoto S, Kleine-Vehn Jr, Robert Sp, Fujimoto M, Dainobu T, Paciorek T, Ueda T, Nakano A, Van Montagu MCE, Fukuda H, Friml J (2010) ADP-ribosylation factor machinery mediates endocytosis in plant cells. *Proc Natl Acad Sci U S A* **107:**21890–21895

Naramoto S, Otegui MS, Kutsuna N, de Rycke R, Dainobu T, Karampelias M, Fujimoto M, Feraru E, Miki D, Fukuda H, Nakano A, Friml J (2014) Insights into the Localization and Function of the Membrane Trafficking Regulator GNOM ARF-GEF at the Golgi Apparatus in Arabidopsis. *Plant Cell* **26:** 3062-3076

Nielsen ME, Feechan A, Bohlenius H, Ueda T, Thordal-Christensen H (2012) Arabidopsis ARF-GTP exchange factor, GNOM, mediates transport required for innate immunity and focal accumulation of syntaxin PEN1. *Proc Natl Acad Sci U S A* **109:** 11443-11448

Nishioka T, Frohman MA, Matsuda M, Kiyokawa E (2010) Heterogeneity of phosphatidic acid levels and distribution at the plasma membrane in living cells as visualized by a Foster resonance energy transfer (FRET) biosensor. *J Biol Chem* **285:** 35979-35987

Offringa R, Huang F (2013) Phosphorylation-dependent trafficking of plasma membrane proteins in animal and plant cells. *Journal of Integrative Plant Biology* **55:** 789-808

Omura S, Sasaki Y, Iwai Y, Takeshima H (1995) Staurosporine, a potentially important gift from a microorganism. *The Journal of antibiotics* **48:** 535-548

Orlando K, Guo W (2009) Membrane organization and dynamics in cell polarity. *Cold Spring Harb Perspect Biol* **1:** a001321

Paál A (1918) Über phototropische Reizleitung. *Jahrbucher fur Wissenschaftliche Botanik* **58:** 406 – 456

Paciorek T, Zazimalova E, Ruthardt N, Petrasek J, Stierhof YD, Kleine-Vehn J, Morris DA, Emans N, Jurgens G, Geldner N, Friml J (2005) Auxin inhibits endocytosis and promotes its own efflux from cells. *Nature* **435:** 1251-1256

Pearce LR, Komander D, Alessi DR (2010) The nuts and bolts of AGC protein kinases. *Nat Rev Mol Cell Biol* **11:** 9-22

Peck SC (2006) Analysis of protein phosphorylation: methods and strategies for studying kinases and substrates. *Plant J* **45:** 512-522

Petersson SV, Johansson AI, Kowalczyk M, Makoveychuk A, Wang JY, Moritz T, Grebe M, Benfey PN, Sandberg Gr, Ljung K (2009) An auxin gradient and maximum in the Arabidopsis root apex shown by high-resolution cell-specific analysis of IAA distribution and synthesis. *Plant Cell* **21:** 1659-1668

Petrasek J, Friml J (2009) Auxin transport routes in plant development. *Development* **136:** 2675-2688

Peyroche A, Antonny B, Robineau S, Acker J, Cherfils J, Jackson CL (1999) Brefeldin A acts to stabilize an abortive ARF-GDP-Sec7 domain protein complex: involvement of specific residues of the Sec7 domain. *Mol Cell* **3:** 275-285

Potocky M, Pleskot R, Pejchar P, Vitale N, Kost B, Zarsky V (2014) Live-cell imaging of phosphatidic acid dynamics in pollen tubes visualized by Spo20p-derived biosensor. *The New phytologist* **203:** 483-494

Presley JF, Ward TH, Pfeifer AC, Siggia ED, Phair RD, Lippincott-Schwartz J (2002) Dissection of COPI and Arf1 dynamics in vivo and role in Golgi membrane transport. *Nature* **417:** 187-193

Rademacher EH, Offringa R (2012) Evolutionary adaptations of plant AGC kinases: from light signaling to cell polarity regulation. *Frontiers in Plant Science* **3**

Rakusova H, Fendrych M, Friml J (2015) Intracellular trafficking and PIN-mediated cell polarity during tropic responses in plants. *Curr Opin Plant Biol* **23:** 116-123

Rakusová H, Gallego-Bartolomé J, Vanstraelen M, Robert HS, Alabadí D, Blázquez MA, Benková E, Friml J (2011) Polarization of PIN3-dependent auxin transport for hypocotyl gravitropic response in Arabidopsis thaliana. *The Plant Journal* **67:** 817-826

Raven JA (1975) Transport of indoleacetic acid in plant cells in relation to pH and electrical portential gradients, and its significance for polar IAA transport. *New Phytologist* **74:** 163-172

Rentel MC, Lecourieux D, Ouaked F, Usher SL, Petersen L, Okamoto H, Knight H, Peck SC, Grierson CS, Hirt H, Knight MR (2004) OXI1 kinase is necessary for oxidative burst-mediated signalling in Arabidopsis. *Nature* **427:** 858-861

Richter S, Geldner N, Schrader J, Wolters H, Stierhof Y-D, Rios G, Koncz C, Robinson DG, Jürgens G (2007) Functional diversification of closely related ARF-GEFs in protein secretion and recycling. *Nature* **448:** 488-492

Rigal A, Ma Q, Robert S (2014) Unraveling plant hormone signaling through the use of small molecules. *Front Plant Sci* **5:** 373

Ritzenthaler C, Nebenfuhr A, Movafeghi A, Stussi-Garaud C, Behnia L, Pimpl P, Staehelin LA, Robinson DG (2002) Reevaluation of the effects of brefeldin A on plant cells using tobacco bright yellow 2 cells expressing Golgi-targeted green fluorescent protein and COPI antisera. *Plant Cell* **14:** 237-261

Robert HS, Crhak Khaitova L, Mroue S, Benkova E (2015) The importance of localized auxin production for morphogenesis of reproductive organs and embryos in Arabidopsis. *J Exp Bot*

Robert HS, Friml J (2009) Auxin and other signals on the move in plants. *Nat Chem Biol* **5:** 325-332

Robert S, Kleine-Vehn J, Barbez E, Sauer M, Paciorek T, Baster P, Vanneste S, Zhang J, Simon S, Covanova M, Hayashi K, Dhonukshe P, Yang Z, Bednarek SY, Jones AM, Luschnig C, Aniento F, Zazimalova E, Friml J (2010) ABP1 mediates auxin inhibition of clathrin-dependent endocytosis in Arabidopsis. *Cell* **143:** 111-121

Robinson DG, Jiang LW, Schumacher K (2008) The endosomal system of plants: charting new and familiar territories. *Plant Physiology* **147:** 1482-1492

Rubery PH, Sheldrake AR (1973) Effect of pH and surface charge on cell uptake of auxin. *Nature: New biology* **244:** 285-288

Rubery PH, Sheldrake AR (1974) Carrier-mediated auxin transport. *Planta* **118:** 101-121

Sabatini S, Beis D, Wolkenfelt H, Murfett J, Guilfoyle T, Malamy J, Benfey P, Leyser O, Bechtold N, Weisbeek P, Scheres B (1999) An auxin-dependent distal organizer of pattern and polarity in the Arabidopsis root. *Cell* **99:** 463-472

Sachs T (1969) Polarity and the Induction of Organized Vascular Tissues. *Annals of Botany* **33:** 263-275

Sachs T (1981) The control of the patterned differentiation of vascular tissues. In *Advances in Botanical Research*, Woolhouse HW (ed), Vol. Volume 9, pp 151-262. Academic Press

Santiago-Tirado FH, Bretscher A (2011) Membrane-trafficking sorting hubs: cooperation between PI4P and small GTPases at the trans-Golgi network. *Trends in Cell Biology* **21:** 515-525

Scacchi E, Osmont KS, Beuchat J, Salinas P, Navarrete-Gómez M, Trigueros M, Ferrándiz C, Hardtke CS (2009) Dynamic, auxin-responsive plasma membrane-to-nucleus movement of Arabidopsis BRX. *Development* **136:** 2059-2067

Schapire AL, Voigt B, Jasik J, Rosado A, Lopez-Cobollo R, Menzel D, Salinas J, Mancuso S, Valpuesta V, Baluska F, Botella MA (2008) Arabidopsis synaptotagmin 1 is required for the maintenance of plasma membrane integrity and cell viability. *Plant Cell* **20:** 3374-3388

Schmick M, Vartak N, Papke B, Kovacevic M, Truxius DC, Rossmannek L, Bastiaens PI (2014) KRas localizes to the plasma membrane by spatial cycles of solubilization, trapping and vesicular transport. *Cell* **157:** 459-471

Shevell DE, Leu WM, Gillmor CS, Xia G, Feldmann KA, Chua NH (1994) EMB30 is essential for normal cell division, cell expansion, and cell adhesion in Arabidopsis and encodes a protein that has similarity to Sec7. *Cell* **77:** 1051-1062

Simon ML, Platre MP, Assil S, van Wijk R, Chen WY, Chory J, Dreux M, Munnik T, Jaillais Y (2014) A multi-colour/multi-affinity marker set to visualize phosphoinositide dynamics in Arabidopsis. *Plant J* **77:** 322-337

Slaughter BD, Das A, Schwartz JW, Rubinstein B, Li R (2009) Dual modes of cdc42 recycling fine-tune polarized morphogenesis. *Dev Cell* **17:** 823-835

Sorefan K, Girin T, Liljegren SJ, Ljung K, Robles P, Galvan-Ampudia CS, Offringa R, Friml J, Yanofsky MF, Ostergaard L (2009) A regulated auxin minimum is required for seed dispersal in Arabidopsis. *Nature* **459:** 583-586

Sorek N, Bloch D, Yalovsky S (2009) Protein lipid modifications in signaling and subcellular targeting. *Current Opinion in Plant Biology* **12:** 714-720

Stanislas T, Hüser A, Barbosa ICR, Kiefer CS, Brackmann K, Pietra S, Gustavsson A, Zourelidou M, Schwechheimer C, Grebe M D6 PROTEIN KINASE is a lipid domain-dependent mediator of Arabidopsis planar polarity. *Nature Plants* (under revision[accepted September 2015])

Steinmann T, Geldner N, Grebe M, Mangold S, Jackson CL, Paris S, Gälweiler L, Palme K, Jürgens G (1999) Coordinated Polar Localization of Auxin Efflux Carrier PIN1 by GNOM ARF GEF. *Science* **286:** 316-318

Suh BC, Inoue T, Meyer T, Hille B (2006) Rapid chemically induced changes of PtdIns(4,5)P2 gate KCNQ ion channels. *Science* **314:** 1454-1457

Sun Y, Carroll S, Kaksonen M, Toshima JY, Drubin DG (2007) PtdIns(4,5)P_2 turnover is required for multiple stages during clathrin- and actin-dependent endocytic internalization. *J Cell Biol* **177:** 355-367

Takano J, Tanaka M, Toyoda A, Miwa K, Kasai K, Fuji K, Onouchi H, Naito S, Fujiwara T (2010) Polar localization and degradation of Arabidopsis boron transporters through distinct trafficking pathways. *Proc Natl Acad Sci U S A* **107:** 5220-5225

Tan X, Calderon-Villalobos LI, Sharon M, Zheng C, Robinson CV, Estelle M, Zheng N (2007) Mechanism of auxin perception by the TIR1 ubiquitin ligase. *Nature* **446:** 640-645

Tanaka H, Dhonukshe P, Brewer PB, Friml J (2006) Spatiotemporal asymmetric auxin distribution: a means to coordinate plant development. *Cel Mol Life Scie* **63:** 2738-2754

Teale WD, Paponov IA, Palme K (2006) Auxin in action: signalling, transport and the control of plant growth and development. *Nat Rev Mol Cell Biol* **7:** 847-859

Tejos R, Sauer M, Vanneste S, Palacios-Gomez M, Li H, Heilmann M, van Wijk R, Vermeer JE, Heilmann I, Munnik T, Friml J (2014) Bipolar plasma membrane distribution of phosphoinositides and their requirement for auxin-mediated cell polarity and patterning in Arabidopsis. *Plant Cell* **26:** 2114-2128

Thelen M, Rosen A, Nairn AC, Aderem A (1991) Regulation by phosphorylation of reversible association of a myristoylated protein kinase C substrate with the plasma membrane. *Nature* **351:** 320-322

Thimann KV, Went F (1934) On the chemical nature of the root-forming hormone. *Proceedings Koninklijke Nederlandse Akademie van Wetenschappen* **37:** 456 – 459

Thole JM, Nielsen E (2008) Phosphoinositides in plants: novel functions in membrane trafficking. *Cur Op Plant Bio* **11:** 620-631

Thompson BJ (2013) Cell polarity: models and mechanisms from yeast, worms and flies. *Development* **140:** 13-21

Ulmasov T, Murfett J, Hagen G, Guilfoyle TJ (1997) Aux/IAA proteins repress expression of reporter genes containing natural and highly active synthetic auxin response elements. *Plant Cell* **9:** 1963-1971

Urano D, Phan N, Jones JC, Yang J, Huang J, Grigston J, Philip Taylor J, Jones AM (2012) Endocytosis of the seven-transmembrane RGS1 protein activates G-protein-coupled signalling in Arabidopsis. *Nat Cell Biol* **14:** 1079-1088

van den Bogaart G, Meyenberg K, Risselada HJ, Amin H, Willig KI, Hubrich BE, Dier M, Hell SW, Grubmuller H, Diederichsen U, Jahn R (2011) Membrane protein sequestering by ionic protein-lipid interactions. *Nature* **479:** 552-555

Vanneste S, Friml J (2009) Auxin: A Trigger for Change in Plant Development. *Cell* **136:** 1005-1016

Vermeer JE, van Leeuwen W, Tobena-Santamaria R, Laxalt AM, Jones DR, Divecha N, Gadella TW, Jr., Munnik T (2006) Visualization of PtdIns3P dynamics in living plant cells. *Plant J* **47:** 687-700

Vermeer JEM, Thole JM, Goedhart J, Nielsen E, Munnik T, Gadella Jr TWJ (2009) Imaging phosphatidylinositol 4-phosphate dynamics in living plant cells. *Plant J* **57:** 356-372

Vernoud V, Horton AC, Yang Z, Nielsen E (2003) Analysis of the small GTPase gene superfamily of Arabidopsis. *Plant Physiol* **131:** 1191-1208

Vernoux T, Brunoud G, Farcot E, Morin V, Van den Daele H, Legrand J, Oliva M, Das P, Larrieu A, Wells D, Guedon Y, Armitage L, Picard F, Guyomarc'h S, Cellier C, Parry G, Koumproglou R, Doonan JH, Estelle M, Godin C, Kepinski S, Bennett M, De Veylder L, Traas J (2011) The auxin signalling network translates dynamic input into robust patterning at the shoot apex. *Mol Syst Biol* **7**

Vlahos CJ, Matter WF, Hui KY, Brown RF (1994) A specific inhibitor of phosphatidylinositol 3-kinase, 2-(4-morpholinyl)-8-phenyl-4H-1-benzopyran-4-one (LY294002). *J Biol Chem* **269:** 5241-5248

Walker EH, Pacold ME, Perisic O, Stephens L, Hawkins PT, Wymann MP, Williams RL (2000) Structural determinants of phosphoinositide 3-kinase inhibition by wortmannin, LY294002, quercetin, myricetin, and Staurosporine. *Mol Cell* **6:** 909-919

Wan Y-L, Eisinger W, Ehrhardt D, Kubitscheck U, Baluska F, Briggs W (2008) The subcellular localization and blue-light-induced movement of phototropin 1-GFP in etiolated seedlings of Arabidopsis thaliana. *Mol Plant* **1:** 103-117

Wang R, Estelle M (2014) Diversity and specificity: auxin perception and signaling through the TIR1/AFB pathway. *Curr Opin Plant Biol* **21C:** 51-58

Whippo CW, Hangarter RP (2006) Phototropism: bending towards enlightenment. *Plant Cell* **18:** 1110-1119

Whippo CW, Hangarter RP (2009) The "sensational" power of movement in plants: A Darwinian system for studying the evolution of behavior. *American journal of botany* **96:** 2115-2127

Willemsen V, Friml J, Grebe M, van den Toorn A, Palme K, Scheres B (2003) Cell Polarity and PIN protein positioning in Arabidopsis require STEROL METHYLTRANSFERASE1 function. *Plant Cell* **15:** 612-625

Willige BC, Ahlers S, Zourelidou M, Barbosa ICR, Demarsy E, Trevisan M, Davis PA, Roelfsema MRG, Hangarter R, Fankhauser C, Schwechheimer C (2013) D6PK AGCVIII kinases are required for auxin transport and phototropic hypocotyl bending in Arabidopsis. *Plant Cell* **25:** 1674-1688

Wisniewska J, Xu J, Seifertova D, Brewer PB, Ruzicka K, Blilou I, Rouquie D, Benkova E, Scheres B, Friml J (2006) Polar PIN localization directs auxin flow in plants. *Science* **312:** 883

Wolters H, Anders N, Geldner N, Gavidia R, Jurgens G (2011) Coordination of apical and basal embryo development revealed by tissue-specific GNOM functions. *Development* **138:** 117-126

Xu J, Scheres B (2005) Dissection of Arabidopsis ADP-RIBOSYLATION FACTOR 1 function in epidermal cell polarity. *Plant Cell* **17:** 525-536

Xu T, Dai N, Chen J, Nagawa S, Cao M, Li H, Zhou Z, Chen X, De Rycke R, Rakusova H, Wang W, Jones AM, Friml J, Patterson SE, Bleecker AB, Yang Z (2014) Cell surface ABP1-TMK auxin-sensing complex activates ROP GTPase signaling. *Science* **343:** 1025-1028

Xu T, Nagawa S, Yang Z (2011a) Uniform auxin triggers the Rho GTPase-dependent formation of interdigitation patterns in pavement cells. *Small GTPases* **2:** 227-232

Xu T, Wen M, Nagawa S, Fu Y, Chen J-G, Wu M-J, Perrot-Rechenmann C, Friml J, Jones AM, Yang Z (2011b) Cell surface- and Rho GTPase-based auxin signaling controls cellular interdigitation in Arabidopsis. *Cell* **143:** 99-110

Yang Z (2008) Cell polarity signaling in Arabidopsis. *Ann Rev Cell Dev Bio* **24:** 551-575

Yang Z, Lavagi I (2012) Spatial control of plasma membrane domains: ROP GTPase-based symmetry breaking. *Curr Opin Plant Biol* **15:** 601-607

Yeung T, Gilbert GE, Shi J, Silvius J, Kapus A, Grinstein S (2008) Membrane phosphatidylserine regulates surface charge and protein localization. *Science* **319:** 210-213

Zadnikova P, Petrasek J, Marhavy P, Raz V, Vandenbussche F, Ding Z, Schwarzerova K, Morita MT, Tasaka M, Hejatko J, Van Der Straeten D, Friml J, Benkova E (2010) Role of PINmediated auxin efflux in apical hook development of Arabidopsis thaliana. *Development* **137:** 607-617

Zazimalova E, Murphy AS, Yang H, Hoyerova K, Hosek P (2010) Auxin transporters: why so many? *Cold Spring Harb Perspect Biol* **2:** :a001552

Zegzouti H, Li W, Lorenz TC, Xie M, Payne CT, Smith K, Glenny S, Payne GS, Christensen SK (2006) Structural and Functional Insights into the Regulation of Arabidopsis AGC VIIIa Kinases. *J Biol Chem* **281:** 35520-35530

Zhang J, Nodzynski T, Pencik A, Rolcik J, Friml J (2010) PIN phosphorylation is sufficient to mediate PIN polarity and direct auxin transport. *Proc Natl Acad Sci U S A* **107:** 918-922

Zhang Y, Wang P, Shao W, Zhu JK, Dong J (2015) The BASL polarity protein controls a MAPK signaling feedback loop in asymmetric cell division. *Dev Cell* **33:** 136-149

Zhao Y, Yan A, Feijó JA, Furutani M, Takenawa T, Hwang I, Fu Y, Yang Z (2012) Phosphoinositides regulate clathrin-dependent endocytosis at the tip of pollen tubes in Arabidopsis and tobacco. *Plant Cell* **22:** 4031-4044

Zourelidou M, Absmanner B, Weller B, Barbosa ICR, Willige BC, Fastner A, Streit V, Port S, Colcombet J, van Bentem S, Hirt H, Kuster B, Schulze W, Hammes U, Schwechheimer C (2014) Auxin efflux by PIN-FORMED proteins is activated by two different protein kinases, D6 PROTEIN KINASE and PINOID. *Elife, **2014; 3:** e02860*

Zourelidou M, Müller I, Willige BC, Nill C, Jikumaru Y, Li H, Schwechheimer C (2009) The polarly localized D6 PROTEIN KINASE is required for efficient auxin transport in Arabidopsis thaliana. *Development* **136:** 627-636

Appendix

List of plant materials

Table 3 List of publised *Arabidopsis* transgenic lines and mutants used in this thesis.
All transgenics and mutants were generated in *Arabidopsis thaliana* (L.) Heynh. var. Columbia (Col-0).

Name	Locus	Reference
Mutants		
d6pk0; SALK_061847	AT5G55910	(Zourelidou et al, 2009)
d6pk1; SALK_056618	AT4G26610	(Zourelidou et al, 2009)
d6pk2; SALK_086127	AT5G47750	(Zourelidou et al, 2009)
gnom$^{B/E}$; *B4049* and *emb30-1*	AT1G13980	(Geldner et al, 2004)
pid; SALK_049736	AT2G34650	(Dhonukshe et al, 2010)
pin3-3	AT1G70940	(Friml et al, 2002)
pin4-101; GABI_593F01	AT2G01420	(Willige et al, 2013)
pin7-102; SALK_062056	AT1G23080	(Willige et al, 2013)
pip5k1; SALK_146728	AT1G21980	(Ischebeck et al, 2013)
pip5k2; SALK_012487	AT1G21980	(Ischebeck et al, 2013)
Transgenics		
35S:YFP:D6PK		(Zourelidou et al, 2009)
35S:YFP:D6PK inactive		(Barbosa et al, 2014)
D6PK:YFP:D6PK		(Willige et al, 2013)
DR5:GUS		(Sabatini et al, 1999)
DII-VENUS		(Brunoud et al, 2012)
mDII-VENUS		(Brunoud et al, 2012)
GN^{wt}		(Geldner et al, 2003)
GN^{M696L}		(Geldner et al, 2003)
INTAM:HUB		(Kitakura et al, 2011)
PIN1:PIN1:GFP		(Benkova et al, 2003)
PIN2:PIN2:GFP		(Abas et al, 2006)
PIN3:PIN3:GFP		(Zadnikova et al, 2010)
35S:CLC:mKO		(Naramoto et al, 2010)

Primer list and genotyping

Table 4 List of genotyping primers used in this thesis.
Nr, refers to laboratory stock number; RP, Right-Border primer for T-DNA genotyping.

Nr	Name	Sequence	T-DNA
Genotyping SALK mutants			
IB31	LBb1-3 T-DNA	ATTTTGCCGATTTCGGAAC	
IB25	D6 genotyping F	TGATGGCTTCAAAAACTCCAGAAGGATC	RP
IB26	D6 genotyping R	ACTCTGATCAGATCTTACAC	
IB37	D6 intron specific F	AGACAACCCGGGAAACGCTTC	
IB27	D6L1 genotyping F	CATTTCCATGGAAGAAGGTGATGAGCT	
IB28	D6L1 genotyping R	ACTCCAGAACCATACTTCGAGGCCAT	RP
IB29	D6L2 genotyping F	CTTCGCCTTTGATGATCTCTG	
IB30	D6L2 genotyping R	AGTGACCGAGAGTAGCTGCAGC	RP
IB13	PID genotyping F	CAGTCGGGAAACTCAACTGTC	
IB14	PID genotyping R	ATTTTGCGATGAAAGTTGTGG	RP
Genotyping Transgenic lines			
IB19	YFP:D6PK (YFP specific) F	ATGGTGAGCAAGGGCGAGGA	
IB16	GNOM (gene specific) F	CCTGAAAACACAACTGGTTCGTGA	
IB17	$GNOM^{M696L}$ (pBAR specific) R	ATCTGAATTAAGCTTGAGCTCTAGA	
IB18	$GNOM^{wt}$ (pBAR specific) R	AGCGTGAAGCTGAATTCGTCGA	
Genotyping $gnom^{B/E}$ trans-heterozygous of alleles *emb30-1* and *B4049*			
IB56	*emb30-1* genot PCR F	TTCAAGTTCTCAATGAGTTTGCTGG	
IB57	*emb30-1* genot 1st PCR R	CTCACTTGTAAGGTCACGAACCAGTT	
IB58	*emb30-1* genot 2nd PCR R	CATTGTTGCAGATGGAGTGAAAGAG	
IB69	$gnom^{BE}$ sequencing	CTGGATGGTTAAGTGTGACAA	

Genotyping of SALK T-DNA mutant plants was performed by PCR, using wildtype specific (genotyping F/R) and T-DNA specifc (RP/LB1-3) primer combinations (Table 4).

Genotyping of transgenic plants was performed by PCR using a gene-specific and a transgene specific primer (for YFP:D6PK, YFP-specific primer was used; for GNOM transgenics a pBAR specific primer was used).

Trans-heterozygous plants of $gnom^{B/E}$ were first genotyped for the allele *emb30-1* by a first PCR amplification (IB56/IB57), followed by a second PCR (IB56/IB58) using the first PCR fragment diluted (1:100) as a template, and after purification, the PCR fragment was digested with the enzyme HinfI. Wildtype plants yield fragments of sizes: 193, 65, 47, 32, 20bp; *emb30-1* heterozygous plants yielded 193, 97, 65, 47, 32, 20bp; and *emb30-1* homozygous plants yielded 193, 97, 47, 20bp, which were resolved in 1.5% agarose gels. To genotype the *B4049* allele, purified PCR fragments (IB56/IB57) were sequenced with primer IB69.

List of plasmids generated

The following plasmids were used in this thesis: pDONR201 (Invitrogen); pExtag-YFP-GW (a gift from J. Parker, Cologne, Germany); pDEST15 (Invitrogen); pGREEN0029 (Hellens et al, 2000) and p35SGW-MYC (LifeTechnologies, Carlsbad, CA). Cloning procedures are described in Materials and Methods of Publication 3 and obtained the plasmids are listed below.

Table 5 List of plasmids generated in this thesis.
Nr, refers to laboratory stock number; binary, expression in *E. coli* and *A. tumefasciens*; Transgenic plants, indicates the genetic background where plasmids were transformed.

Nr	Name	Vector	Expression system	Transgenic plants
P4	pDONR:D6PKΔN	pDONR201	*E. coli*	
P5	pDONR:N	pDONR201	*E. coli*	
P8	pDONR:MID	pDONR201	*E. coli*	
P6	pDONR:D6PKΔC	pDONR201	*E. coli*	
P7	pDONR:C	pDONR201	*E. coli*	
P9	35S:YFP:D6PKΔN	pEXTAG-YFP-GW	binary	Col-0
P10	35S:YFP:N	pEXTAG-YFP-GW	binary	Col-0
P14	35S:YFP:D6PKΔMID	pEXTAG-YFP-GW	binary	Col-0
P13	35S:YFP:MID	pEXTAG-YFP-GW	binary	Col-0
P11	35S:YFP:D6PKΔC	pEXTAG-YFP-GW	binary	Col-0
P12	35S:YFP:C	pEXTAG-YFP-GW	binary	Col-0
P27	GST:D6PKΔN	pDEST15	*E. coli*	
P29	GST:D6PKΔMID	pDEST15	*E. coli*	
P28	GST:D6PKΔC	pDEST15	*E. coli*	
P55	pDONR:D6PK-3KA	pDONR201	*E. coli*	
P59	pDONR:D6PK-6KA	pDONR201	*E. coli*	
P65	pDONR:D6PK-SSAA	pDONR201	*E. coli*	
P57	GST:D6PK-3KA	pDEST15	*E. coli*	
P61	GST:D6PK-6KA	pDEST15	*E. coli*	
P70	GST:D6PK-SSAA	pDEST15	*E. coli*	
P71	GST:D6PK-SSDD	pDEST15	*E. coli*	
P56	35S:YFP:D6PK-3KA	pEXTAG-YFP-GW	binary	Col-0
P60	35S:YFP:D6PK-6KA	pEXTAG-YFP-GW	binary	Col-0
P66	35S:YFP:D6PK-SSAA	pEXTAG-YFP-GW	binary	Col-0
P68	35S:YFP:D6PK-SSDD	pEXTAG-YFP-GW	binary	Col-0
P58	D6PK:YFP:D6PK-3KA	pGREEN0229	binary	*d6pk01*
P62	D6PK:YFP:D6PK-6KA	pGREEN0229	binary	*d6pk01*
P67	D6PK:YFP:D6PK-SSAA	pGREEN0229	binary	*d6pk01*
P69	D6PK:YFP:D6PK-SSDD	pGREEN0229	binary	*d6pk01*
P15	35S:PID	p35SGW-MYC	binary	Col-0

.

Curriculum Vitae

Curriculum Vitae

Persönliche Daten

Name:	Inês Catarina Ramos Barbosa
Geburtsdatum:	07.11.1985
Geburtsort:	Lissabon, Portugal
Familienstand:	ledig
Adresse:	Sommerstr. 25, 81543 München
E-Mail:	ines.barbosa@wzw.tum.de

Studium und Beruf

Sept. 2010 – heute	**Promotionsstudium** Technische Universität München (TUM) Lehrstuhl für Systembiologie der Pflanzen Titel: *Trafficking and polarity control of the D6PK protein kinase of* Arabidopsis thaliana. Betreuer: Prof. Dr. Claus Schwechheimer
Jul. 2011 – Jun. 2015	**Externe Doktorandin** Stipendium Fundação para a Ciência e Tecnologia, Portugal
Sept. 2009 – Aug. 2010	**Wissenschaftliche Mitarbeiterin** Instituto Gulbenkian de Ciência, Oeiras, Portugal Titel: *Functional characterization of the mRNA splicing-regulators SR PROTEINS in* Arabidopsis thaliana Betreuerin: Dr. Paula Duque
Sept. 2007 – Dez. 2008	**M.Sc. Ökologie und Umweltmanagement** Lehrstuhl für Grünlandlehre, TUM, und Faculdade de Ciências da Universidade de Lisboa (FCUL) Portugal Titel: *Reconstruction of Alpine meadows ^{13}C discrimination during the last century using the horns of* Capra ibex. Betreuer: Prof. Dr. Hans Schnyder (TUM) und Dr. Cristina Máguas (FCUL)
Sept. 2006 – Feb. 2007	**Austauschstudentin ERASMUS** Faculdade de Biologia, Universitat Barcelona, Spain
Sept. 2003 – Jul. 2007	**Diplomstudium Biologie** Faculdade de Ciências da Universidade de Lisboa (FCUL), Portugal
Sept. 2000 – Jul. 2003	**Abitur Naturwissenschaften** Escola Secundária Leal da Câmara, Rio de Mouro, Sintra, Portugal

Publikationsliste

Stanislas T, Hüser A, Barbosa ICR, Kiefer CS, Brackmann K, Pietra S, Gustavsson A, Zourelidou M, Schwechheimer C, Grebe M D6 PROTEIN KINASE is a lipid domain-dependent mediator of Arabidopsis planar polarity. *Nature Plants* (under revision [accepted September 2015])

Barbosa ICR, Schwechheimer C (2014) Dynamic control of auxin transport-dependent growth by AGCVIII protein kinases. *Curr Opin Plant Biol* 22: 108-115

Barbosa ICR, Zourelidou M, Willige BC, Weller B, Schwechheimer C (2014) D6 PROTEIN KINASE activates auxin transport-dependent growth and PIN-FORMED phosphorylation at the plasma membrane. *Dev Cell* 29: 674-685.

Zourelidou M, Absmanner B, Weller B, Barbosa ICR, Willige BC, Fastner A, Streit V, Port S, Colcombet J, van Bentem S, Hirt H, Kuster B, Schulze W, Hammes U, Schwechheimer C (2014) Auxin efflux by PIN-FORMED proteins is activated by two different protein kinases, D6 PROTEIN KINASE and PINOID. *Elife,* 2014; 3: e02860.

Willige BC, Ahlers S, Zourelidou M, Barbosa ICR, Demarsy E, Trevisan M, Davis PA, Roelfsema MRG, Hangarter R, Fankhauser C, Schwechheimer C (2013) D6PK AGCVIII kinases are required for auxin transport and phototropic hypocotyl bending in Arabidopsis. *Plant Cell*, 25:1674-1688.

Barbosa ICR, Kley M, Schäufele R, Auerswald K, Schröder W, Filli F, Hertwig S, Schnyder H (2009) Analysing the isotopic life history of the alpine ungulates *Capra ibex* and *Rupicapra rupicapra rupicapra* through their horns. *Rapid Comm Mass Spectrometry* 23: 2347-2356.

Barbosa ICR, Köhler IH, Auerswald K, Lüps P, Schnyder H (2010) Last-century changes of alpine grassland water-use efficiency: a reconstruction through carbon isotope analysis of a time-series of *Capra ibex* horns. *Global Change Biology* 16: 1171-1180.

Konferenzen

Sept. 2014	Teilnahme an der 9. TNAM (Tri-National Arabidopsis Meeting) mit dem Poster „Deciphering the polar targeting of the auxin transport regulator D6PK" *Heidelberg, Deutschland*
Aug. 2014	Teilnahme an ENPER (European Network for Endomembrane Research) 2014 mit dem Poster „Deciphering the polar targeting of the auxin transport regulator D6PK" *Lecce, Italien*
Aug. 2013	Teilnahme an ENPER 2013 mit dem Vortrag „Dynamic polar targeting of the AGCVIII kinase D6PK: implications for PIN phosphorylation and auxin transport" *Gent, Belgien*
Sept. 2012	Teilnahme an der 8. TNAM mit dem Poster „Polarity control of the D6 protein kinase from *Arabidopsis thaliana*" *Lausanne, Schweiz*
Feb. 2012	Teilnahme an der 25. Tagung Molekularbiologie der Pflanzen 2012 mit dem Vortrag „Regulation of the cellular polarity of an AGCVIII kinase: D6PK" *Dabringhausen, Deutschland*
Sept. 2011	Teilnahme an ENPER 2011 mit dem Vortrag „Regulation of the cellular polarity of the AGC VIII kinase D6PK" *Assissi, Italien*

Lehrtätigkeiten

2013 bis 2015	Konzeption und Mitbetreuung zweier Forschungspraktika und zweier Masterarbeiten.
Sept. 2014	Seminarvortrag im Rahmen der Vorlesungsreihe Pflanzenbiotechnologie „D6PK phosphorylation of PIN proteins: a molecular switch for polar auxin transport in plants"

Acknowledgements

After these years of hard work, I look back and appreciate that I was never alone, but always accompanied and supported by many people that I wish to thank here. All contributed to the *making of* and the *enjoying of* this doctoral project.

I would like first to thank my supervisor Prof. Dr. Claus Schwechheimer for entrusting me this exciting project, giving me guidance and inspiration to carry out my experiments and great support for my personal development in the diverse tasks that surge during a PhD. Also thanks to the D6PK group: Melina, Benny, Björn, Lana, Hiro and Siv, for sharing their enthusiasm with me, supporting me with any help I needed, for great discussions, and for a great teamwork. Without them, much of this thesis would have seemed an unreachable and, for sure, much less exciting task. Special thanks to the technical assistance from Jutta, without her, a lot of the work here would have been difficult to achieve.

Then, I also have to thank all current and previous colleagues from the lab Plant Systems Biology for all the technical (liters of buffers, liquid nitrogen, and heavy kitchen duties) and emotional (sometimes you can only get it from someone who understands what a PhD is about!) support they gave me, patience and for sharing with me their enthusiasm, knowledge and problems, which made this experience very rich in all senses. Special thanks to my train-partners Quirin and Manolis, for making this routine duty a pleasure and always a wonderful time of friendship. To Nina for her smile and support in many instances. To Björn, for great discussions, mentoring and for so many things he taught me. To Melina, for her care and enthusiasm. To Anthi, Maike, Kamila and Conny for the good mood in the lab and help with anything I needed. To René, for the entertaining and fruitful discussions (not only scientific). Also thanks to Erika for introducing me to the wonders of confocal imaging and for productive discussions. To Nina, Eleni, Benny, Lana and Uli for the joyful moments in Freising. Finally, thanks to Julia for great tips and guidance in the final steps of writing this thesis.

Thanks also to Prasad Vadepalli for sharing his never-ending enthusiasm, after long confocal sessions, and also for helping me out with problems and reading my drafts. Thanks to the people of the SFB 924 student initiative for the exciting and fruitful teamwork, exchange and good times in the retreats.

I thank the Portuguese Fundação para a Ciência e Tecnologia for granting me the scholarship that supported this work.

I must also thank the Sommer9, specially Martin and Sébastian for the opportunity to write my thesis there and everyone for the great work and friendly atmosphere; and Janin for very important tips in Word.

Also, special thanks to Prof. Schneitz for taking the task to examine my thesis, and to Prof. Schnyder – who was my MSc. thesis supervisor and taught me a lot about what it takes to do science – to lead my examiners' committee.

Finally, I want to thank my parents, my brother, my family, and friends in Portugal that even far away, always gave me the strongest support and believe. Special thanks to Cristina for the last minute, round-the-clock, full support in the writing of this thesis. Last but not least, thanks to Martin for sharing this experience with me with unconditional support, understanding, care, love and motivation. Without him, this would have been impossible.